Universidad del País Vasco Euskal Herriko Unibertsitatea

IMPLICATION OF CERAMIDE 1-PHOSPHATE IN OBESITY-ASSOCIATED PROCESSES. ROLE OF PEMT

Doctoral Thesis

"International Doctor Mention"

Marta Ordoñez Zaragoza Noviembre 2015

Index

INDEX

Abstract **7**

Abbreviations **11**

Introduction **21**

1. Obesity 23
1.1. Obesity and the metabolic síndrome – an epidemic on the rise 23
1.2. Adipose tissue, a major player in metabolism 24
1.2.1. Adipose tissue function 25
1.2.2. Adipose tissue composition 25
1.2.2.1. Immune cells in obesity 26
1.2.2.2. Adipocytes in obesity 29
1.3. Adipocyte differentiation process 30
1.3.1. Transcriptional regulation of adipocyte differentiation 32
1.3.2. Role of phosphatidylethanolamine methyltransferase (PEMT) in adipogenesis 34
1.4. Obesity-associated inflammation 35
1.4.1. Initiation and development of adipose tissue inflammation 35
1.4.2. Macrophage polarization in obesity 37
1.5. Molecular biology in obesity 38
1.5.1. Mitogen-activated protein kinase (MAPK) pathway 39
1.5.2. Phosphatidylinositol 3-kinase (PI3K)/protein kinase B (PKB) pathway 41
1.5.3. JAK/STAT/SOCS pathway 42
2. Sphingolipids 43
2.1. Metabolism of sphingolipids 44
2.2. Bioactive sphingolipids 46
2.2.1. Ceramides 47
2.2.2. Sphingosine 48
2.2.3. Sphingosine 1-phosphate 48
2.2.4. Ceramide 1-phosphate and ceramide kinase 49
2.2.5. Putative receptor of C1P 51
3. Sphingolipids and obesity 51
3.1. Bioactive sphingolipids in obesity 51
3.1.1. Ceramides in obesity 51
3.1.2. Possible role of C1P in obesity 52
3.1.2.1. C1P and the control of inflammation 52
3.1.2.2. C1P and cell migration 53
4. References 54

Objectives **65**

Materials and Methods **69**

1. Materials 71
1.1. Reagents 71
1.2. Cell lines 74

1.2.1. J774A.1 cell line 74
1.2.2. 3T3-L1 cell line 75
2. Animal handling and diets 75
3. Methods 76
3.1. Delivery of C1P to cells in culture 76
3.2. Determination of cell migration. Boyden chamber assay 76
3.3. Cell viability assay (MTS-Formazan method) 78
3.4. Western blotting 79
3.5. Gelatin zymography 80
3.6. Measurement of actin polymerization by flow cytometry 81
3.7. Quantitative Enzyme-Linked Immunoabsorbent assay (ELISA) 81
3.7.1. Determination of IL-1β concentration in J774A.1 cell culture medium 81
3.7.2. Determination of MCP-1, TNF-α, IL-4, IL-10, RANTES, Leptin, VEGF and IL-1α concentration in white adipose tissue 83
3.7.2.1. Determiantion of MCP-1, TNF-α and IL-10 concentration in white adipose tissue 83
3.7.2.2. Determination of RANTES, IL-1α, IL-4 and Leptin concentration in white adipose tissue 84
3.7.3. Determination of cytokine release in 3T3-L1 differentiated cells 85
3.7.3.1. Determination of Leptin, IL-4 and VEGF concentration in 3T3-L1 differentiated cells 85
3.7.3.2. Determination of MCP-1, IL-10, TNF-α and IL-6 concentration in 3T3-L1 differentiated cells 85
3.8. 3T3-L1 preadipocytes differentiation protocol 85
3.9. Oil Red staining protocol 86
3.10. Triacylglycerol assay kit 86
3.11. Semi -quantitative detection of inflammation-related cytokines 87
3.12. Small interfering RNA (siRNA) transfection protocol 89
3.12.1. siRNA transfection protocol for IL-1β release experiments in J774A.1 macrophages 90
3.12.2. siRNA transfection protocol for migration experiments in J774A.1 macrophages 91
3.12.3. siRNA transfection protocol for gelatin zymography experiments in J774A.1 macrophages 92
3.12.4. siRNA trasnfection protocol for Western blot analysis in J774A.1 macrophages 93
3.12.5. siRNA transfection protocol for flow cytometry analysis in J774A.1 macrophages 93
3.12.6. siRNA transfection (by electroporation) protocol for adipogenesis asssays in 3T3-L1 cells 94
3.13. PEMT plasmid overexpression for migration assays in J774A.1 macrophages 95
3.14. PEMT plasmid overexpression for Western blot analysis in J774A.1 macrophages 96
3.15. Determination of Cerk activity using NBD-Ceramide as the enzyme substrate in cell homogenates 96
3.16. RT-PCR for M1 and M2 macrophage markers in white adipose tissue 97
3.16.1. RNA isolation from tissue by tryzol 97

3.16.2. DNAse I treatment of RNA for RT-PCR and q-PCR protocols 98
3.16.3. q-PCR 98
3.17. M1 macrophage phenotype detection by immunofluorescence staining of white adipose tissue 100
4. Statistical analyses 100
References 101

Chapter 1: Matrix metalloproteinases -2 and -9 (MMP-2 and MMP-9) are implicated in C1P-induced macrophage migration 103

1. Introduction 105
1.1. Extracellular matrix (ECM) 105
1.2. Matrix metalloproteinases (MMPs) 106
1.2.1. Biological roles of MMPs 107
1.2.2. MMPs in obesity 108
1.3. Macrophage migration 108
1.3.1. C1P and cell migration 110
2. Results 111
2.1. C1P induces MMP-2 and MMP-9 protein expression and activity in J774A.1 macrophages 111
2.2. PI3K and ERK kinases are implicated in C1P-induced MMP-2 and MMP-9 activation 114
2.3. MMP-2 and MMP-9 gelatinases are implicated in C1P-induced macrophage migration 116
2.4. Actin polymerization is implicated in C1P-induced macrophage Migration 118
2.5. Paxillin is involved in C1P-induced actin polymerization in J774A.1 cells 125
2.6. C1P induces IL-1β release in J774A.1 cells 126
2.7. ERK and PI3K are implicated in C1P-induced IL-1β release 127
2.8. Lack of toxicity of the inhibitors used in this work 129
3. Discussion 131
4. References 136

Chapter 2: Implication of C1P and CERK in adipogenesis 141

1. Introduction **143**
1.1. Adipogenesis in obesity 143
1.1.1. 3T3-L1 cell differentiation process 143
1.1.2. Transcriptional control of adipocyte outcome 144
1.1.3. MAPK signaling pathway in adipogenesis 146
1.2. Sphingolipids in obesity 146
2. Results **147**
2.1. Adipogenic induction medium (AIM) induces 3T3-L1 cell differentiation 147
2.2. CERK activity is required during 3T3-L1 cell differentiation process 149
2.3. Exogenous Ceramide 1-phosphate decreases adipogenesis in 3T3-L1 cells 152
2.4. Ceramide 1-phosphate induces sustained ERK phosphorylation

under AIM conditions 158
2.5. Ceramide 1-phosphate prevents adipogenic differentiation through ERK pathway 161
2.6. C1P suppresses adipocyte differentiation in a Gi protein-coupled protein receptor (GPCR)- dependent manner 163
2.7. Lack of toxicity of the inhibitors and agonist used in this work 166
3. Discussion 168
4. References 174

Chapter 3: Phosphatidylethanolamine methyltransferase (PEMT) is implicated in obesity-associated inflammation and cell migration 179

1. **Introduction** 181
1.1. Obesity-associated inflammation 181
1.1.1. Macrophage infiltration into white adipose tissue (WAT) 182
1.1.2. Macrophage polarization 182
1.1.2.1. Classically activated M1 “pro-inflammatory” macrophages 182
1.1.2.2. Alternativelly activated M2 “anti-inflammatory” Macrophages 183
1.2. Phosphatydilylethanolamine N-methyltransferase (PEMT) 184
1.2.1. Physiological functions of PEMT 185
2. **Results** 186
2.1. C1P decreases PEMT expression in 3T3-L1 differentiated cells 186
2.2. Deficiency of PEMT protects mice from obesity-induced multi-cytokine release in white adipose tissue 187
2.3. Quantification of IL-1α, RANTES, MCP-1, IL-4, TNF-α, Leptin and IL-10 levels in WAT after HFD-feeding 188
2.4. Deficiency of PEMT alters the phenotype of adipose tissue Macrophages 190
2.5. PEMT overexpression induces J774A.1 macrophage migration in a time-dependent manner 195
2.6. PEMT overexpression induces ERK, Akt and mTOR phosphorylation in J774A.1 macrophages 196
2.7. The PI3K/Akt/mTOR pathway is implicated in PEMT overexpression-induced macrophage migration 197
2.8. Lack of toxicity of the inhibitors used in this work 201
3. Discussion 202
4. References 206

Conclusions 213

Appendix 217

Abstract

ABSTRACT

Obesity is the most common metabolic disease in developed nations and has become a global epidemic in recent years. Therefore, understanding the molecular mechanisms that regulate obesity-associated processes, such as cell migration, adipogenesis and inflammation, can be a crucial step for developing novel therapeutic strategies to control obesity and obesity-related pathologies. It is well known that sphingolipid content in tissue undergoes dramatic alterations in metabolic diseases suggesting that these lipids might mediate the pathology associated with metabolic disease. In this thesis, we demonstrate that ceramide 1-phosphate (C1P) enhances macrophage migration, an action that requires the activation of matrix metalloproteinase-2 and -9. We also provide evidence suggesting that adipogenesis of cultured mouse 3T3-L1 preadipocytes is associated with an increase in ceramide kinase (CERK) protein expression and activity. In addition, we demonstrate that exogenous C1P inhibits adipocyte differentiation of 3T3-L1 cells, as confirmed by a reduction in triglyceride accumulation and a reduction in the expression of adipocyte specific genes. This action of C1P implicates the activation of extracellular signal-regulated kinases (ERK1/2). We have also found that the lack of phosphatidylethanolamine methyl transferase (PEMT), the enzyme responsible for phosphatidylcholine biosynthesis in liver and whose expression is blocked by C1P, attenuates obesity-associated inflammation. This occurs by decreasing both, the number of classically activated M1 “pro-inflammatory” macrophages and pro-inflammatory cytokine levels in adipose tissue. Moreover, we also demonstrate that PEMT overexpression induces macrophage migration, an action that requires the activation of PI3K/Akt/mTOR pathway. These findings may help to develop new therapeutic strategies for the treatment of obesity and obesity-related diseases.

Abbreviations

ABBREVIATIONS

AA	Arachidonic acid
ABTS	2,2´- Azino-bis(3-ethylbenzothiazoline-6-sulfonic acid
AdipoR1	Adiponectin Receptor 1
AIM	Adipogenic Induction Medium
AP-1	Activator Protein 1
aP-2	Adipocyte protein 2
APC	Antigen Presenting Cell
AT	Adipose Tissue
ATM	Adipose Tissue Macrophage
ATP	Adenosine Triphosphate
BAT	Brown Adipose Tissue
BCA	Bicinchonic Acid
BSA	Bobine serum albumin
c-AMP	Cyclic Adenosine Monophosphate
C1P	Ceramide 1-phosphate
C1PP	Ceramide 1-phosphate Phosphatase
CCL2 (MCP-1)	Chemokine Ligand 2
CD	Cluster of differentiation
CDase	Ceramidase
cDNA	Complementary Deoxyribonucleic Acid
CDP	5´cytidine diphosphate

C/EBPbeta	CCAAT/enhancer binding protein beta
Cer	Ceramide
CERK	Ceramide Kinase
CERS	Ceramide Synthase
CERT	Ceramide Transport Protein
CLS	Crown-like Structures
CNS	Central Nervous System
CREB	cAMP response element binding protein
CT	CTP:phosphocholine cytidylyltransferase
CTP	Cytidine 5´-triphosphate
CXCL14	Chemokine (C-X-C motif) ligand 14
DAG	Diacylglycerol
DES	Desaturase
dhCer	Dihydroceramide
DEPC	Diethylpyrocarbonate
DMEM	Dulbecco´s modified Eagle´s medium
DNA	Deoxyribonucleic Acid
DNAse	Deoxyribonuclease
dNTP	Deoxynucleotide triphosphate
DTT	Dithiothreitol
ECM	Extracellular matrix
EDTA	Ethylenediaminetetraacetic Acid
ELISA	Enzyme-linked Immunosorbet Assay

ERK	Extracellular signal-regulated Kinase
F-actin	Filamentous actin
FBS	Fetal Bovine Serum
FFA	Free Fatty Acid
FITC	Fluorescein isothiocyanate
GABA	γ-Aminobutyric acid
G-actin	Globular actin
GAPDH	Glyceraldehide 3-phosphate Dehydrogenase
GC	Glucocorticoid
GM	Growth Medium
GPCR	Gi Protein-coupled Receptor
GLUT	Glucose Transporter
HEPES	4-(2-hydroxyethyl)-1-piperazineethanesulfonic Acid
HFD	High Fat Diet
HRP	Horseradish Peroxidase
IBMX	3-isobutyl-1-methylxanthine
IGF	Insulin Growth Factor
IL	Interleukin
INF	Interferon
iNOS	Inducible Nitric Oxide Synthase
IR	Insulin Resistance
JAK	Janus Kinase
JNK	c-Jun N-terminal Kinase

KLFs	Kruppel-like Factors
LAP	Liver activated protein
LCB	Long Chain Bases
LepR	Leptin Receptor
LIP	Liver inhibitory protein
LPS	Lipopolisaccharide
Mac1	Macrophage antigen 1
MAPK	Mitogen-activated Protein Kinase
MCE	Mitotic Clonal Expansion
MCP-1 (CCL2)	Monocyte Chemoattractant Protein 1
MEK	Mitogen-activated Kinase
MCH	Major Histocompatibility Complex
M-CSF	Macrophage colony- stimulating factor
MIF	Macrophage migration Inhibitory Factor
MIP-2	Macrophage Inhibitory Protein 2
MMP	Matrix metalloproteinase
mRNA	Messenger Ribonucleic Acid
MSCs	Mesenchymal stem cells
MT-MMP	Membrane-type matrix metalloproteinase
mTOR	Mammalian Target of Rapamycin
MTS	3-(4,5-dimethylthiazol-2-yl)-5-(3-carboxymethoxyphenyl)-2-(4-sulfophenyl)-2H-tetrazolium
NBD	7-nitrobenz-2-oxa-1,3-diazol-4-yl

NCS	Newborn Calf Serum
NFκB	Nueclear-factor kappa-light-chain-enhancer of activated B cells
NHR	Nuclear Hormone Receptor
NKT	Natural Killer T cell
NO	Nitric Oxide
NPY	Neuropeptide Y
OptiMEM	Modification of Eagle´s Minimal Essential Medium
PA	Phosphatidic acid
PAGE	Poliacrilamide Gel Electrophoresis
PAI-1	Plasminogen Activator Inhibitor-1
PBS	Phosphate- buffered Saline
PC	Phosphatidylcholine
PCR	Polymerase Chain Reaction
PE	Phosphatidylethanolamine
PE	Phycoerythrin
PEMT	Phosphatidylethanolamine N-methyltransferase
PG	Proteoglicans
PGE2	Prostaglandin E2
PH	Plekstrin Homology
PIC	Protease Inhibitor Cockail
PIP	Phosphatidylinositol 3-phosphate
PIP2	Phosphatidylinositol 3,4-biphosphate
PIP3	Phosphatidylinositol 3,4,5-triphosphate

PI3K	Phosphoinositide 3-kinase
PKB/Akt	Protein Kinase B
PKC	Protein Kinase C
PLA	Phospholipase A
PLD	Phospholipase D
PMA	Phorbol 12-myristate 13-acetate
PMS	Phenazine Methosulfate
POMC	Proopiomelanocortin
PPARγ	Peroxisome Proliferator-activated Receptor γ
Ptx	Pertussis Toxin
qPCR	Quantitative Polymerase Chain Reaction
RANTES	Regulated on Activation Normal T Cell Expressed and Secreted
RISCs	RNA-induced silencing complexes
RNA	Ribonucleic Acid
ROS	Reactive oxygen species
RT-PCR	Reverse Transcription-Polymerase Chain Reaction
RXR	Retinoid X Receptor
S1P	Sphingosine 1-phosphate
SDS	Sodium Dodecyl Sulfate
SEM	Standard Error of the Mean
siRNA	Small Interfering Ribonucleic Acid
SM	Sphyngomyelin

SMase	Sphingomyelinase
SMS	Sphingomyelin Synthase
SOCS	Suppressors of cytokine signaling
Spa	Sphinganine
Sph	Sphingosine
SphK	Sphingosine Kinase
SPP	Sphingosine Phosphatase
SPT	Serine Palmitoyltransferase
Src	Proto-oncogene tyrosine-protein kinase
SREBP-1c	Sterol Regulatory Element-Binding Protein 1c
STAT	Signal Transducer and Activator of Transcription
T2DM	Type 2 diabetes mellitus
TBS	Tris-buffered Saline
TG	Triglycerides
TGF	Transforming growth factor
Th	Helper T lymphocyte
TIMP	Tissue Inhibitor Metalloproteinase
TLR	Toll-like Receptor
TMB	3,3´,5,5´-Tetramethylbenzidine
TNFα	Tumor Necrosis Factor α
Treg	T regulatory lymphocytes
TYK2	Tyrosine Kinase 2
TZDs	Thiazolidinediones

VEGF	Vascular Endothelial Growth Factor
WAT	White Adipose Tissue
WHO	World Health Organization

Introduction

1. INTRODUCTION

Homeostasis is the ability of a system or living organism to adjust its internal environment to maintain a stable equilibrium. Many diseases are a result of homeostatic imbalance or an inability of the body to restore a functional and stable internal environment. In particular, when energy homeostasis is disrupted due to an imbalance between food intake and food expenditure, adipose tissue suffers morphological changes and consequently, it exerts inflammatory effects that are linked to the most important health problems associated with obesity, including cardiovascular disease and type 2 diabetes mellitus. The endocrine impact of adipose tissue on energy homeostasis and inflammation highlights the critical health implications of obesity and the importance of effective prevention and management strategies in clinical practice.

1. OBESITY

1.1. Obesity and the metabolic syndrome – an epidemic on the rise

In western societies, chronic diseases such as diabetes, obesity, atherosclerosis and cancer are responsible for most deaths. In particular, over the past twenty years there has been a rapid increase in the prevalence of obesity due to consumption of a high-fat diet (HFD), sedentary lifestyle and genetic predisposition. Nowadays, obesity is considered the pandemic of the 21st century and its accelerated expansion, together with complications associated to the disease, comprise a major public health concern worldwide [1]. According to World Health Organization (WHO), 1.4 billion people are currently overweight and 312 million are classified as obese [2, 3] and these numbers are estimated to increase.

Obesity is one of the most frequent physiological disorders and is associated with a wide variety of conditions [4] including hypertension [5], dyslipidemia [6], type II diabetes (T2D) [7-9], non-alcoholic fatty liver disease [10, 11], cardiovascular diseases, including atherosclerosis [12-15], insulin resistance (IR) [7], and certain forms of

cancers [16, 17], giving rise to substantially increased cardiovascular and cerebrovascular morbidity and mortality. Thus, due to the immense array of health complications related to obesity (Figure 1.1.2), it is critical to understand the underlying mechanisms associated with the obese state.

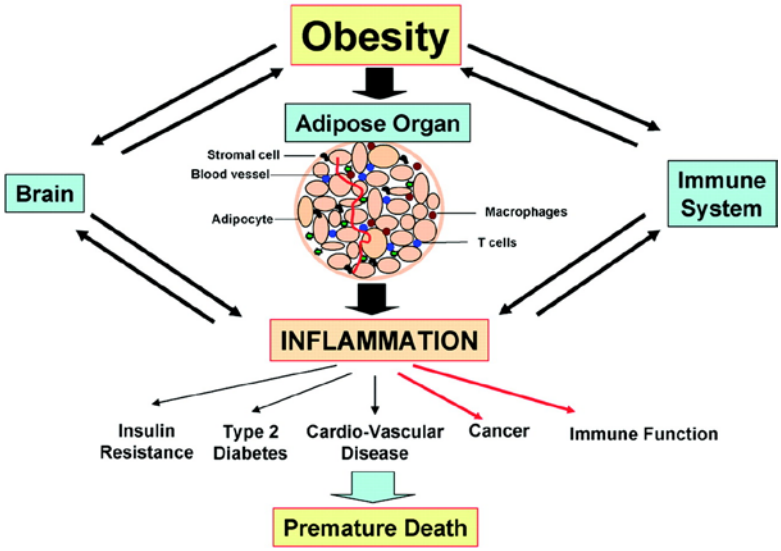

Figure 1.1.2. Obesity related health complications. Adipose-immune interactions during obesity. Obesity-related inflammation is responsible for secondary disease states of obesity, leading to premature death. Figure taken from [18].

From a biomedical perspective, obesity is the result of an energy imbalance wherein energy intake exceeds energy expenditure over time. This energy excess leads to fat accumulation, which is associated with local and systemic chronic state of low-grade adipose tissue inflammation. This inflammation is characterized by an increase of immune cell infiltration into obese adipose tissue [19, 20] and increased production and subsequent secretion of pro-inflammatory factors into the circulatory system. Obesity-induced inflammation exerts profound effects on metabolic pathways, leading to the development of certain diseases [21-24].

1.2. Adipose tissue, a major player in metabolism

There are two different adipose tissue depots within the body: the brown adipose tissue (BAT) and the white adipose tissue (WAT), both of which differ in a few significant properties. White adipocytes contain single, large lipid droplets that appear to comprise the majority of cell volume while the cytoplasm and nucleus are found at the cell

periphery. In contrast, brown adipocytes are characterized by multilocular lipid droplets and high mitochondrial content.

In humans, WAT is the most common adipose tissue in adults, whereas BAT is mainly an infancy-associated fat that is specialized in thermoregulation. Although WAT is the main source of energy and its main function is to control energy balance by triacylglycerol storage and mobilization, it also plays a pivotal role as endocrine and paracrine organ. WAT mediates numerous physiological and pathological processes by secreting factors that control glucose and lipid metabolism, appetite, immunological responses, inflammatory responses, angiogenesis, blood pressure regulation and reproductive function [25, 26].

Based on the location, the adipose tissue can be classified as subcutaneous adipose tissue, underneath the dermis, or visceral adipose tissue, which resides in the cavities of the body. It has been shown that visceral and subcutaneous adipose tissue show distinct gene expression patterns. Furthermore, visceral adipose tissue displays a greater risk for triggering metabolic complications than subcutaneous adipose tissue [27].

1.2.1. Adipose tissue function

In the past, the role of adipose tissue (AT) in the development of obesity and its consequences was considered to be a passive one. Nowadays, AT is considered an active endocrine organ involved in numerous metabolic, hormonal, and immune processes, which products and reactions are able to act not only locally but also influence other organs and thus, it plays a crucial role in the whole body homeostasis.

1.2.2. Adipose tissue composition

From the histological point of view, AT is characterized by a marked cellular heterogeneity. Among its cellular components, we can find adipocytes, preadipocytes, fibroblasts, endothelial cells and multipotent stem cells, which are able to differentiate into several cell types. Overall, fat tissue is composed of approximately one-third of mature adipocytes, a main cellular component, surrounded by supporting connective tissue that is highly vascularized and innervated. The remaining two-thirds are a combination of small mesenchymal stem cells (MSCs), T regulatory cells, endothelial

precursor cells, macrophages and preadipocytes in various stages of development (figure 1.2.2.1) [28].

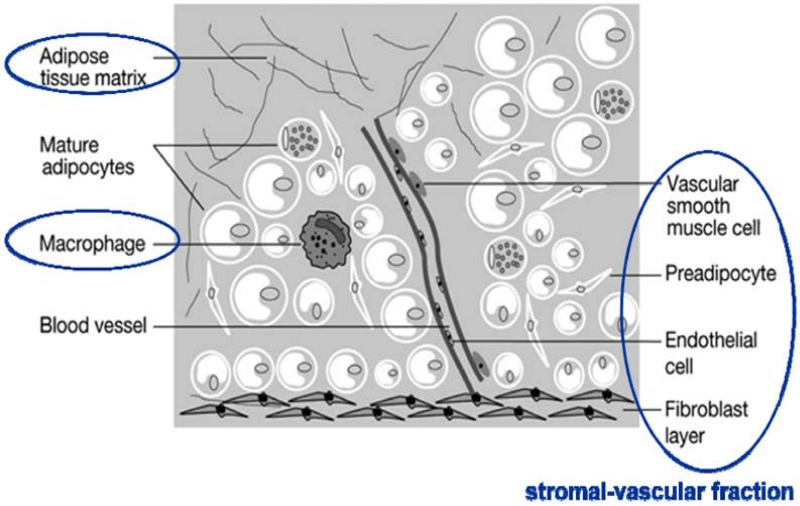

Figure 1.2.2.1. Adipose tissue composition. Adipose tissue is composed of mature adipocytes, preadipocytes, macrophages, adipose tissue matrix and a stroma-vascular cell fraction. Picture taken from [29].

1.2.2.1. Immune cells in obesity

The maintenance of the metabolic homeostasis requires balanced immune response and an integrated network of multiple cell types. AT-resident immune cells include almost the full spectrum of immune cell types, which play important roles in the tissue housekeeping, removal of detritus and apoptotic cells, and the tissue homeostasis maintenance under non-obese conditions [30]. However, fat accumulation leads to substantial changes in the amount and function of immune cells causing an increment in the number and activity of some of them, most notably macrophages, mast cells, neutrophils, and T- and B lymphocytes, while simultaneously reducing others including eosinophils and several subsets of T lymphocytes (T helper 2 (Th2), Treg, and NKT cells) [31]. This imbalance lies at the very core of the development of obesity-related local and systemic inflammation (Figure 1.2.2.1.1).

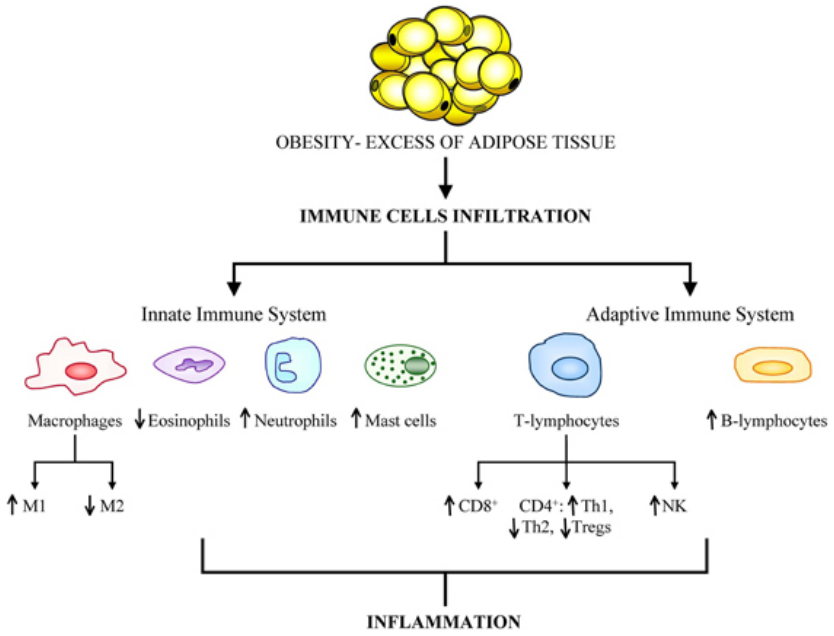

Figure 1.2.2.1.1. Immune cell types in obese adipose tissue. Figure taken from [32].

- *Role of adaptative immune cells in obesity:*

Adaptative immune system is composed of various specialized cells that are able to recognize and eliminate pathogens efficiently. In addition, adaptative immunity develops memory cells for each pathogen in order to respond in a faster and stronger manner if the pathogen which has been erased, enters the organism again.

Lymphocytes are central to all adaptive immune response. They originate from stem cells in the bone marrow and mature either in the bone marrow (B lymphocytes) or in the thymus (T lymphocytes), after exiting the bone marrow [33]. B lymphocytes are responsible for the promotion of humoral immunity by producing specific antibodies for malignant antigens, but they can also act as antigen-presenting cells (APCs) via major histocompatibility complex I (MHCI) and major histocompatibility complex II (MHCII) molecules. T lymphocytes are further divided into functional subsets: cytotoxic T cells, which generate cell-mediated immune responses, and helper T lymphocytes (Th cells), which regulate immune system, controlling the quality and strength of all immune responses.

Recent studies have shown that T cells in adipose tissue play a role in the regulation of adipose tissue macrophage (ATM) numbers and activation state. In general, among T lymphocytes, it appears that $CD8^+$ T cells are involved in the recruitment and activation of ATMs and promote a pro-inflammatory cascade associated with insulin resistance

[34, 35]. $CD4^+$ T helper 1 (T_H1) cells as well, produce pro-inflammatory cytokines associated with insulin resistance [36]. On the contrary, T_H2 cells and $CD4^+$ regulatory T (Treg) cells produce anti-inflammatory cytokines.

Also, it has been described that in obesity, B cells accumulate in the visceral fat of obese mice after 3 weeks of feeding on high fat diet (HFD) [37]. Feeding B-cell-deficient mice on HFD or treating wild-type HFD-fed mice with B-cell-depleting anti-CD20 antibody protected them from insulin resistance and glucose intolerance. This data suggest an important role of B cells in the maintenance of the obese phenotype.

- *Role of innate immune cells in obesity:*

The innate immune system responds to pathogens or damage-derived stimuli in a non-specific manner. The innate immune cells include Natural Killer cells, mast cells, eosinophils, basophils, macrophages, neutrophils and dendritic cells. These phagocytic cells (macrophages, neutrophils and dendritic cells) are responsible of the most important responses of the innate immune system, which are the production of chemokines, activation of the complement cascade and activation of adaptative immune cells by antigen presentation.

Nevertheless, concerning tissue homeostasis, the most important ones are macrophages due to their multiple functions in innate immunity and their capacity to activate the adaptive immune system. The surface of the macrophages is equipped with many receptors, which interact with stimuli leading to activation of macrophage functions, such as phagocytosis, adhesion, chemotaxis, secretion of different molecules and antigen processing and presentation. All these macrophage functions must be tightly regulated since they can be harmful for the organism. Furthermore, there are many illnesses related to macrophage dysregulation, most of them due to the chronic inflammation produced by macrophages.

It has been shown that adipose tissue functions are regulated by these phagocytic cells [22, 38, 39] and the progressive infiltration of macrophages into adipose tissue leads to a pro-inflammatory response [19, 20]. In fact, metabolic dysfunction in obese individuals has been correlated with the presence of histological features in inflamed adipose tissue called crown-like structures (CLS), which represent an accumulation of macrophages around dead adipocytes [40, 41].

Most of the ATMs come from sources outside of the body fat, mainly from systemic circulation. However, it seems that a small fraction of ATMs can originate from local preadipocytes, since activated preadipocytes exert several antigenic characteristics similar to macrophages, including the expression of macrophage antigens F4/80, Mac1, CD80, CD86 and CD45, and phagocytosis.

Other innate immune cells have also been suggested to participate in obesity. Mast cells are present in a higher numbers in the adipose tissue of obese mice and humans compared with their counterparts. Moreover, mast cells have been suggested to contribute to glucose intolerance in adipose tissue and muscle [42]. On the other hand, eosinophils in visceral adipose tissue (VAT) produce IL-4 and IL-13, cytokines that promote differentiation of ATM into a class of macrophages with a marked inflammatory phenotype. It has been shown that mice genetically deficient for eosinophils display increased adiposity and insulin resistance when placed on a HFD [43].

1.2.2.2. Adipocytes in obesity

Adipocytes, also known as fat cells or lipocytes, are the main constituent of white adipose tissue. They are characterized by a large internal fat droplet, which engrosses the cell so that the cytoplasm is condensed into a thin layer surrounding the lipid droplet while the nucleus is set aside in the outer edge of the cell. Although their primary function is to control energy balance by storing triacylglycerol at times of energy excess and mobilizing it during energy deprivation, they also mediate numerous physiological and pathological processes by releasing a variety of proteins termed adipokines, which exert numerous metabolic and vascular effects [44]. Notably, obesity alters the production of adipokines such as adiponectin and leptin.

Adiponectin: Adiponectin, also known as adipoQ or adipocyte complement-related protein, is a 30kDa polypeptide released exclusively from adipocytes of WAT. In contrast to leptin, adiponectin levels decrease with obesity and are elevated during starvation. This hormone modulates a number of metabolic processes, including glucose regulation and fatty acid oxidation [45]. In particular, this adipokine enhances insulin sensitivity in muscle, adipose tissue and liver. In muscles it binds to Adiponectin Receptor 1 (AdipoR1) and promotes glucose uptake and free fatty acids (FFA)

oxidation [46]. Apart from the metabolic effects, adiponectin attenuates the inflammation and insulin resistance [47]. It is believed that this inverse correlation between obesity, insulin resistance and adiponectin is crucial to trigger their related pathogenesis [47].

Leptin: Leptin (from Greek λεπτός *leptos*, "thin"), is the first adipocytokine (Greek adipo-, fat; cytos-, cell; and -kinos, movement) identified. This 16kDa polypeptide, once secreted from adipocytes and released into the blood, acts on many tissues and induces effects on muscles, bones, pancreatic beta cells, immune cells and also several other tissues and organs. However, the most important effect is believed to be on the Central Nervous System (CNS) [48]. Leptin regulates energy homeostasis by controlling satiety and body weight. This action is primarily mediated by three leptin-sensitive neurons (brain neurons that express Leptin receptor, LepR) found within the arcuate nucleus of the hypothalamus: neuropeptide Y (NPY), γ-aminobutyric acid (GABA), and proopiomelanocortin (POMC) neurons [49]. In obese individuals, leptin secretion is increased in order to reduce food intake. Once secreted, this adipokine comes across the blood-brain-barrier inhibiting NPY and GABA neurons [50, 51], whilst simultaneously stimulating POMC neurons in the hypothalamus [52, 53]. In this way, energy expenditure is increased not only by the signal to the brain, but also directly via leptin receptors on peripheral targets and influences food intake through a direct effect on the hypothalamus.

Alongside its role in energy homeostasis, leptin is able to modulate the immune system due to its structural similarity to cytokines and also due to the fact that class I cytokine receptors are found on immune cells, such as monocytes, lymphocytes, and neutrophils [54]. Therefore, it is believed that the chronic inflammatory state observed in obesity is attributed to the elevated leptin levels through upregulation of phagocytosis by macrophages, promotion of T-helper 1 cell responses, and mediating the release of further pro-inflammatory cytokines such as TNF-α and IL-6 [54].

1.3. Adipocyte differentiation process

Cellular differentiation is a process in which cells derived mitotically from a common ancestor become different from one another, both in their function and in their morphology. In particular, adipocytes have a remarkable capacity to differentiate and

adapt to the nutritional status of the body. During the development of obesity, adipocytes continue storing lipids giving rise to an increase in both adipocyte cell number by proliferation and differentiation of preadipocytes (hyperplasia), and enlargement of adipocyte volume due to increased lipogenesis of fat cells (hypertrophy) [55, 56].

In order to achieve a successful transformation into mature adipocytes, preadipocytes undergo important changes in morphology and gene expression during the differentiation process (also known as adipogenesis), which is commonly divided into 2 stages: the first stage is named “determination phase”, while the second stage is referred to as “terminal differentiation”. The determination phase leads undifferentiated cells to enter the adipogenic differentiation program becoming pre-adipocytes. Subsequently, growth-arrested preadipocytes re-enter cell cycle and undergo several rounds of cell division, known as the mitotic clonal expansion (MCE), which contributes to the hyperplasia of adipocytes. Following the MCE, preadipocytes enter a unique growth arrested stage, G_D (D for differentiation), considered to be a point of no return for commitment to terminal differentiation. During terminal differentiation 3T3-L1 cells transform from a fibroblastic morphology and become mature adipocytes, with round shape and lipid filled vacuoles, and with their biochemical characteristics [57]. They also acquire the machinery that is necessary for lipid transport and synthesis, insulin action and the secretion of adipocyte-specific proteins [58].

Another important step in adipogenesis is extracellular matrix (ECM) remodeling [59, 60]. ECM not only functions to provide mechanical support for a fat pad, but also regulates the physiological and pathological events of adipose tissue remodeling through a variety of signaling pathways [61]. In order to decrease the effect of mechanical stress and to function properly, adipocytes surround themselves with a dynamic ECM. During the process of adipogenesis, the ECM emerges from fibrillar to a laminar structure as cells transfer from determination stage to differentiation stage. During differentiation, the fibronectin-rich matrix of preadipocyte needs to be converted into the typical basement membrane of a mature adipocyte, which includes laminin, nidogen/entacin and type- IV and –VI collagens (figure 1.3.1.). Two main systems involved in ECM remodeling are the plasminogen/plasmin cascade as well as the matrix metalloproteinases and tissue inhibitor of matrix metalloproteinases (MMP/TIMP). During adipogenesis plasmin is activated and degrades the fibronectin-rich preadipocyte

stromal matrix [62]. The matrix metalloproteinases and their inhibitors have diverse effects on adipogenesis. Whereas several MMPs such as MMP2, MMP9 and MT1-MMP promote adipogenesis, others like MMP3, MMP11and MMP19 have the inverse effect.

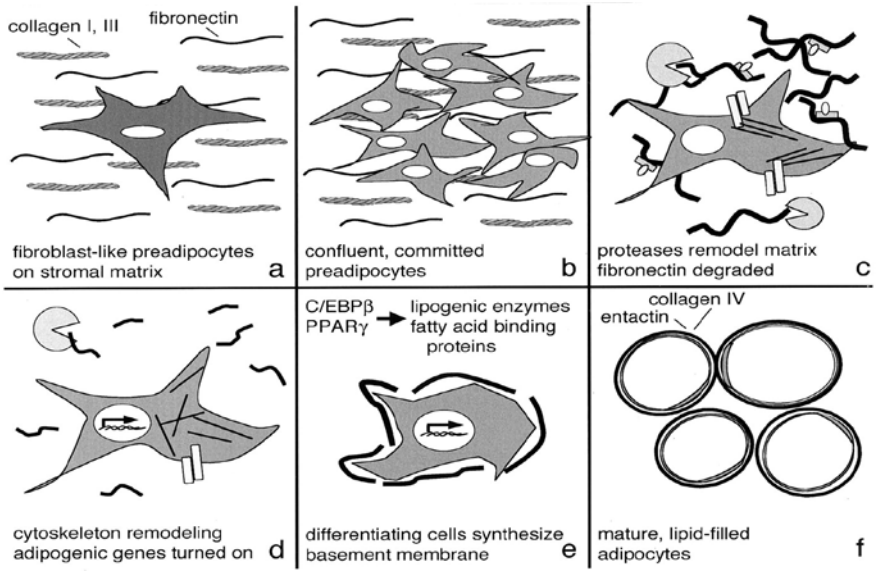

Figure 1.3.1: Summary of adipocyte differentiation. a: Preadipocytes growth in stromal ECM rich in fibronectin and fibrillar collagens. **b:** Once confluent, the cells are committed to differentiate. **c:** Proteases then extensively remodel the ECM; notably fibronectin is degraded. **d:** The cytoskeleton is also remodeled and transcription factors initiate changes in gene expression **e:** The mature adipocytes produce lipogenic proteins and deposit basement membrane. **f:** At the end of differentiation, the adipocytes are round and filled with lipid. Figure taken from [59].

1.3.1. Transcriptional regulation of adipocyte differentiation

The differentiation of preadipocytes into adipocytes is a multi-step process which is tightly regulated by an elaborate network of adipogenic transcription factors that coordinate expression of hundreds of proteins responsible for establishing the mature fat-cell phenotype. The current model for adipocyte differentiation (figure 1.3.1.1) suggests that during the entire differentiation process there are several essential molecular interactions that occur among members of the CCAAT-enhancer-binding proteins (C/EBPs) and the peroxisome proliferator-activated receptor (PPAR) families. The adipogenic cascade can be divided into at least two waves of transcription factors that drive the adipogenic program. The first wave is initiated by adipogenic stimuli that activate several early adipogenic factors including C/EBPβ/δ, Kruppel-like factors (KLFs), cAMP response element binding protein (CREB), early growth response 2

(Krox20), and sterol regulatory element-binding protein 1c (SREBP-1c). These transcription factors in turn induce expression of the second wave of transcription factors, of which PPARγ and C/EBPα are the most important. These key adipogenic factors then induce expression of the gene program that leads to the mature adipocyte phenotype [26, 63, 64].

PPARγ: The peroxisome proliferator-activated receptor (PPAR) belongs to a family with three members, α, δ and γ forms, and is a member of the nuclear hormone receptor (NHR) superfamily. PPARs must heterodimerize with another nuclear hormone receptor (the retinoid X receptor, or RXR) prior to bind DNA and be transcriptionally active. From the PPAR family, it is PPARγ which is relevant for adipogenesis since no factor has been discovered that promotes adipogenesis in the absence of PPARγ. Multiple FFA and their derivates, as well as certain eicosanoids, act as low affinity ligands for PPARγ, but an endogenous PPARγ ligand has not been identified. Nevertheless, PPARγ can be activated by synthetic compounds called thiazolidinediones (TZDs) [65], which are used clinically as antidiabetic agents. PPARγ is the dominant isoform found in fat cells [66] and it is the responsible for activating most of the genes involved in fatty acid binding, storage and metabolism, and gluconeogenesis. The action of PPARγ is mediated through two protein isoforms: PPARγ-1 and PPARγ-2. PPARγ-1 is constitutively expressed whereas PPARγ-2 expression is restricted to adipose tissue. Both isoforms are strongly induced during preadipocyte differentiation in vitro and both are highly expressed in adipose tissue in animals. PPARγ-1 is induced earlier than PPARγ-2 and is maintained at high levels during adipocyte differentiation.

C/EBP: C/EBPs (CCAAT/Enhancer Binding Protein) family of transcription factors belongs to the basic-leucine zipper class of transcription factors. Six isoforms (α, β, γ, δ, ε and ζ) have been described. In adipocytes, three members of the family are implicated as positive regulators of adipogenesis; C/EBPα, C/EBPβ and C/EBPδ [67]. C/EBPα acts as a promoter for many adipocyte genes such as GLUT4, Leptin and aP2 and it has been linked to different features of adipogenesis such as growth arrest, insulin sensitivity and promoting the expression of PPARγ. C/EBPβ and C/EBPδ are expressed early after induction of adipogenesis. Ectopic expression of C/EBPβ, but not C/EBPδ alone, has

proven to be sufficient to induce differentiation *in vitro* [68]. C/EBPs can be regulated at many levels, including transcription, as measured by mRNA levels in cells. Indeed, cAMP, a well-known inducer of adipogenesis *in vitro*, can enhances the expression of both C/EBPα and C/EBPβ. Post-translational regulation of C/EBPs, particularly changes in phosphorylation, can modify the activity of C/EBP proteins as well. Finally, the activity of C/EBPs can be modulated by the presence of other family members; C/EBPζ, for example, cannot bind DNA itself but does dimerize with other C/EBPs, thus acting as a natural dominant-negative inhibitor of C/EBP activity.

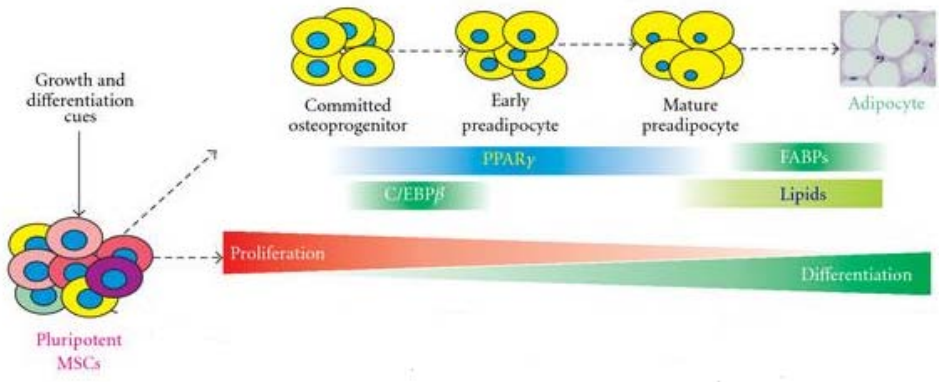

Figure 1.3.1.1 Adipogenic differentiation pathways. The lineage-specific differentiation is a multiple-stage and well-coordinated process regulated by master regulators, such as PPARγ and C/EBPβ. Taken from [69].

1.3.2. Role of phosphatidylethanolamine methyltransferase (PEMT) in adipogenesis

Phosphatidylcholine (PC), which is required to maintain membrane integrity and normal very low density lipoprotein secretion, is the major membrane phospholipid in mammalian cells. The main pathway for biosynthesis of PC in all eukaryotic cells is the CDP-choline pathway (also known as Kennedy pathway), catalyzed by CTP:phosphocholine cytidylyltransferase (CT). There is an alternative pathway for PC biosynthesis where phosphatidylethanolamine methiltransferase (PEMT), a small integral membrane enzyme (~22 kDa), catalyzes the synthesis of PC by the sequential methylation of phosphatidylethanolamine (PE). PEMT is quantitatively important in liver and 30% of PC made in the liver is via PEMT reaction, whereas most of the remaining biosynthetic-derived PC in liver originates via CDP-choline pathway [70].

Although PEMT is highly expressed in the liver, PEMT expression was also detected during the differentiation of 3T3-L1 cells into adipocytes and mouse white adipose tissue (WAT) [71]. Moreover, PEMT provides impressive protection against diet-induced obesity and insulin resistance [72]. When *Pemt*$^{-/-}$ mice were fed with a high fat diet, oxygen consumption was increased and weight gain was prevented. In these mice, triglyceride (TG) storage was shifted from adipose to liver (for storage) and muscle (for oxidation). The most likely explanation for these observations is that PEMT deficiency decreases the availability of choline. Therefore, PEMT is an important regulator of whole body energy metabolism.

1.4. Obesity-associated inflammation

Inflammation is a coordinated response to any harmful stimuli, and its main goal is to bring the system back to a normal baseline. In response to injury, irritation, or infection, the body initiates a network of signals. The inflammatory response triggered by obesity involves many components of the classical inflammatory response to pathogens and includes systemic increase in circulating inflammatory cytokines and acute phase proteins (e.g., C-reactive protein), recruitment of immune cells to inflamed tissues and generation of reparative tissue response. However, the nature of obesity-induced inflammation is unique compared with other inflammatory paradigms in several key aspects.

The chronic nature of obesity produces a low-grade activation of the innate immune system that affects steady-state measures of metabolic homeostasis over time. Therefore, obesity was shown to be associated with a slightly different type of inflammation referred to as chronic low-grade sterile inflammation or metainflammation and characterized by only a modest increase in circulating pro-inflammatory factors and the absence of clinical signs of inflammation [73].

1.4.1. Initiation and development of adipose tissue inflammation

During obesity, excessive body fat accumulation, mostly due to an imbalance between energy intake and expenditure, leads to a marked expansion of visceral adipose tissue with alterations on adipocytes themselves (hypertrophy and hyperplasia), their supporting matrix, and immune cell infiltrates. Together, these changes lead to a myriad of effects, including hypoxia, adipocyte cell death, enhanced chemokine secretion, and

dysregulation in fatty acid fluxes. Those mechanisms will induce obesity-associated inflammation, which plays a pivotal role in the development of obesity-related complications.

Adipocyte death: Macrophages, as "professional" phagocytes, are able to remove numerous molecules, ranging from small lipids, to colonies of pathogens or to dead cells [74]. The necrosis of adipocytes, driven by hypertrophy and accelerated by obesity, is one of the phagocytic stimulus that regulates the infiltration of adipose tissue macrophages (ATMs) [40]. Indeed, macrophages have been shown to aggregate, forming crown-like structures (CLSs) surrounding necrotic adipocytes in advanced obesity [40, 75-77].

Chemotactic regulation: Chemokines are small pro-inflammatory molecules that promote macrophage mobilization from bone marrow into tissues. There is a considerable evidence for the pathophysiological role of macrophage- and/or hypertrophic adipocyte-derived chemotactic MCP-1 /CCR2 pathways in the regulation of monocyte accumulation in obese AT [78]. In particular, increased expression levels of monocyte chemoattractant protein-1 (MCP-1), CXCL14 (chemokine C-X-C motif ligand 14), macrophage inflammatory protein -1α (MIP-1α), monocyte chemoattractant protein -2 (MCP-2), monocyte chemoattractant protein-3 (MCP-3) and regulated on activation normal T cell expressed and secreted (RANTES) can be observed in AT of mice with genetic or diet-induced obesity [20, 79].

Hypoxia: Adipocyte hypertrophy creates areas of local AT microhypoxia at the earliest stages of expansion, which suggest that AT is poorly oxygenated in obese state [80]. Because of this lack of oxygen, many adipokines that are related to inflammation, such as macrophage migration inhibitory factor (MIF), interleukin 6 (IL-6), vascular endothelial growth factor (VEGF), leptin and the matrix metalloproteinases MMP2 and MMP9, are increased.

Fatty acid flux: FFAs, stored in the form of triglycerides in AT, are released from hypertrophic adipocytes through lipolysis during fasting. Some of these FFAs are shunted to the liver and stored in lipid droplets, while some of them are oxidized in other organs. However, FFAs can also serve as ligands for TLR4 complex [81], thereby activating the classical inflammatory response in the context of increased local extracellular lipid concentrations, which ultimately drives ATM accumulation [82, 83].

While these four mechanisms of macrophage recruitment and infiltration into AT may act independently, the metabolic and inflammatory pathways are tightly interconnected. In this way, unlike adipocytes, which uniquely secrete adipokines such as leptin and adiponectin [84-86], macrophages are a major source of pro-inflammatory cytokines which can function in a paracrine and endocrine fashion to cause decreased insulin sensitivity. Activation of these tissue macrophages leads to the release of a variety of chemokines, which in turn recruit additional macrophages, setting up a feed-forward process that further increases ATM content and propagates the chronic inflammatory state.

1.4.2. Macrophage polarization in obesity

Although the adipocyte is the key player orchestrating local changes in the microenvironment, much evidence also points toward a pivotal role for macrophages in such remodeling events. Two main sub-populations of macrophages have been described: the first are referred to as “classically activated” or M1 macrophages. These are induced by the type II class interferon, also known as interferon γ (INFγ), and secrete pro-inflammatory cytokines such as IL-1β, MCP-1, IL-6, TNFα and leptin. M1 macrophages also produce high quantities of reactive oxygen species (ROS) such as nitric oxide (NO) through inducible nitric oxide synthase (iNOS) activity in response to invading pathogens which in turn induces oxidative stress. The second group of macrophages was first described as “alternatively activated” or M2 macrophages. Alternatively activated macrophages have been divided into three groups due to differences in the method of activation: M2a, M2b and M2c macrophages. These different sub-groups are involved in wound healing and immunoregulation. Wound healing M2a macrophages are primarily induced by IL-4 and/or IL-13. These types of macrophages produce anti-inflammatory cytokines such as IL-10, arginase and IL-1 receptor antagonist [87]. M2b macrophages are regulatory macrophages that produce high yields of IL-10 to block the pro-inflammatory action of IL-12, thus dampening inflammation. M2b are induced through the combined action of TLR and another immune complex or stimuli. The third group of M2 macrophages are M2c macrophages, which are induced by IL-10 and express high levels of the cell surface marker mannose receptor (CD206) that has been implicated in tissue remodeling [88]. Both, M1 and M2 macrophages express different cell surface markers. Triple-positive

cells (F4/80+CD11b+CD11c+) are associated with M1-polarization state, while double-positive cells (F4/80+CD11b+CD11c-) indicate M2 macrophages.

In obesity, ATMs undergo a phenotypic switch from anti-inflammatory status (M2) in the adipose tissue of lean individuals to a pro-inflammatory (M1) status in adipose tissues of obese subjects [89, 90], which results in the development of tissue inflammation and systemic insulin resistance (figure 1.4.2.1). Therefore, in an obese state, where adiposity is increased, adipocytes increase in size and suffer hypertrophy and hypoxia, which leads to a release of some pro-inflammatory cytokines such as MCP-1. This cytokine makes M1 macrophages to migrate into the adipose tissue [91]. Once macrophages are recruited in the adipose tissue, they release pro-inflammatory cytokines and surround the necrotic or dead adipocytes in order to remove them and, thus, reshaping the adipose tissue.

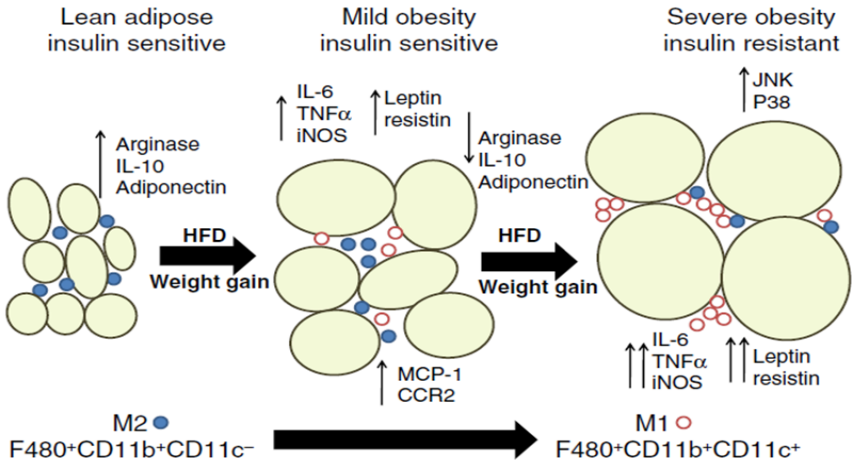

Figure 1.4.2.1: Macrophage polarization state in obesity. Figure taken from [92].

1.5. Molecular biology in obesity

During the process of going from lean to obese, adipose tissue undergoes important changes, giving rise to chronic inflammation. This obesity-associated inflammation might be important from the obesity-cancer link [93]. Furthermore, the increased risk of obesity-related cancers could be mediated in part by different obesity-related cancer risk factors such as increased blood levels of insulin, IGF-1, cytokines IL-1, IL-6, TNF-α and leptin, and downregulation of the expression of anti-inflammatory factors like adiponectin, among others.

A unifying characteristic of all these inflammatory factors is that they could initially activate phosphoinositide 3-kinase (PI3K/Akt), mitogen-activated protein kinase (MAPK) and signal transducer and activator of transcription 3 (STAT3) pathways (Figure 1.5.1), which are important signaling pathways in obesity and obesity-associated disorders [94-98].

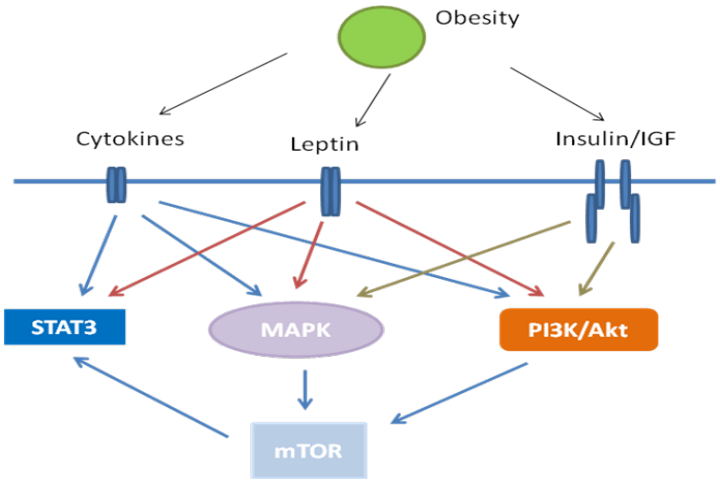

Figure 1.5.1. Multiple signal pathways in obesity-associated cancer. Multiple cancer risk factors in obesity are increased including insulin/IGF-1, cytokines and leptin. These factors activate PI3K/Akt, MAPK and STAT3 pathways via their receptors. Both PI3K/Akt and MAPK activate mTOR. Activated mTOR can activate STAT3. Taken from [98].

1.5.1. Mitogen-activated protein kinase (MAPK) pathway

Mitogen-activated protein (MAP) kinases are serine/threonine-specific protein kinases that respond to extracellular stimuli (mitogens, osmotic stress, head shock and pro-inflammatory cytokines) and can regulate many cellular activities. These include gene expression, cell differentiation and migration, mitosis, proliferation, cell survival and, the wound healing process in tissues.

MAP kinase cascades are activated by several growth factors but also by inflammatory cytokines. The signal is propagated by sequential phosphorylation and activation of the sequential kinases, eventually leading to the phosphorylation of target regulatory proteins. At present, four different mammalian MAPK cascades have been identified and named according to their MAPK components: extracellular signal-regulated kinase 1 and 2 (ERK1/2), c-Jun N-terminal kinase (JNK), p38, and ERK5.

The ERK1/2 cascade was the first MAPK pathway elucidated and is considered a prototype of these kinase cascades [99]. In most cases, the activation of the membrane receptors is transmitted by several mechanisms to the small GTPase Ras, which is activated mainly at the plasma membrane. The extracellular signal-Regulated Kinases (ERK) 1/2 (also known as p44 and p42 MAP kinase, respectively) recruit the MAP3K, also known as Raf. Thereafter, the signal is transmitted to the MAPKKs, called MEK1 and MEK2 (MEK1/2) and finally these two transmit their signal to ERK1 and ERK2 (ERK1/2) (Figure 1.5.1). When ERK1/2 is activated it can phosphorylate hundreds of substrates in many cellular locations, and these are responsible for the induction of ERK1/2-dependent cellular processes.

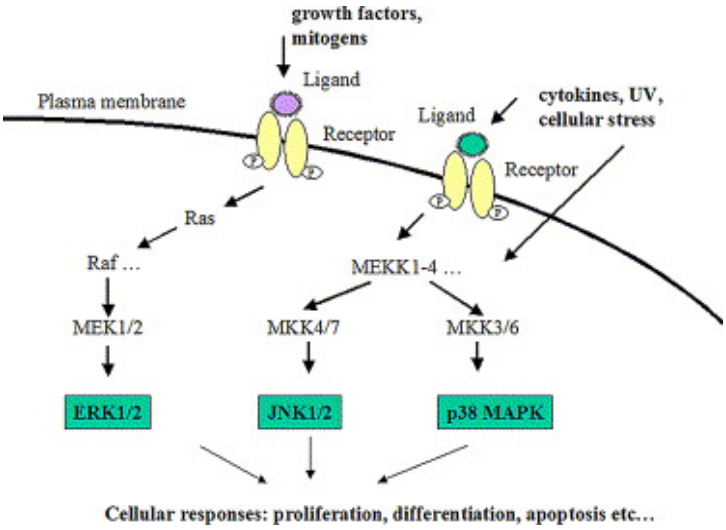

Figure 1.5.1.1. MAPK signal transduction pathway. The major classic MAPK pathway is the Ras-Raf-Mek-ERK1/2 pathway, in which Ras phosphorylates Raf, Raf phosphorylates MEK and MEK phosphorylates ERK1/2. Other pathways include p38 MAPK pathway and the JNK pathway in which MKK-4 or 7 phosphorylates JNK and MKK-3or 6 phosphorylates the p38 MAPK. Figure taken from [95].

It is known that the ERK pathway is involved in adipocyte differentiation and obesity displaying both positive and negative effects [95, 100, 101]. Besides, activated ERK1/2 can activate STAT3, mTOR and other kinases and transcriptional factors, resulting in carcinogenesis and metastasis [102, 103].

1.5.2. Phosphatidylinositol 3-kinase (PI3K)/protein kinase B (PKB, also known as Akt) pathway

Phosphatidylinositol 3-kinases (PI3Ks) are a family of enzymes involved in cellular functions such as cell growth, proliferation, differentiation, motility, survival and intracellular trafficking.

PI3K is able to phosphorylate certain membrane-bound lipids known as phosphoinositides. The three steps that grant Akt recruitment into the cell membrane are: Phosphatidylinositol 3-phosphate (PIP), Phosphatidylinositol (3,4)-biphosphate (PIP_2), Phosphatidylinositol (3,4,5)-triphosphate (PIP_3). Once Akt1 is attracted to the membrane through PIP_3, its kinase activity is promoted. This kinase can further activate other kinases such as Mammalian Target of Rapamycin (mTOR), which activates specific transcription factors (Figure 1.5.2.1).

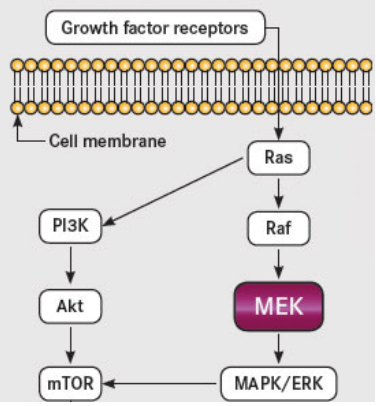

Figure 1.5.2.1. MAPK and PI3K/Akt signaling pathways

In obesity, insulin, insulin-like growth factor, leptin, TNF-α and IL-6 levels are increased whereas adiponectin levels are reduced. These obesity-induced factors have been shown to increase the PI3K/Akt pathway activity, which, in turn, regulates downstream targets leading to increased cell survival. Inhibition of this pathway could be helpful in the prevention of obesity-associated colon cancer (Figure 1.5.2.2) [104].

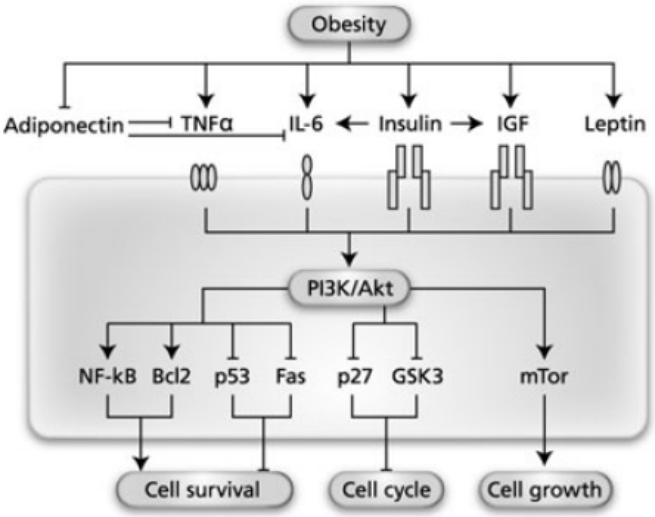

Figure 1.5.2.2 Links between obesity, PI3K/Akt and cancer. Several factors, altered in obesity, increase the activity of the PI3K/Akt signal pathway. The PI3K/Akt signal pathway in turn activates signals for cell survival, cell growth and cell cycle leading to carcinogenesis. Picture taken from [104].

1.5.3. JAK/STAT/SOCS pathway

The Janus Kinase (JAK)-signaling pathway can be activated by a variety of cytokines, hormones and growth factors to regulate numerous developmental and homeostatic processes, including hematopoiesis, immune cell development, stem cell maintenance and organism growth. However, chronic activation of JAK-STAT underlies various diseases such as cancer and obesity [105, 106].

Four members of the JAK family have been identified to date, namely JAK 1, 2, 3 and TYK2. Upon binding of the ligand to its receptor, two or more receptor-associated JAKs are recruited close to the receptor and thereby cause its oligomerization, which leads to their autophosphorylation. Once phosphorylated, activated JAKs phosphorylate signature tyrosine residues in the cytoplasmic region of receptors to create docking sites for STATs.

The suppressor of cytokine signaling (SOCS) molecules are induced by several inflammatory cytokines and act as a negative feedback signal by inhibiting JAK and STAT activation and phosphorylation. SOCS protein family includes eight members (SOCS1-7 and CIS), which possess a SH2 domain, and a SOCS-box domain controlling

the degradation of interacting proteins. At the molecular level, the SOCS proteins interact with the tyrosine kinases JAKs or directly with the receptor of some cytokines, thus blocking the tyrosine phosphorylation of the transcription factor STAT. Several cellular studies have demonstrated that SOCS negatively regulate signaling pathways of some hormones including leptin and insulin. In this regard, SOCS3 is induced by leptin and insulin and is involved in a negative feedback loop of the JAK/STAT signaling pathway.

In obesity, circulating levels of leptin and IL-6 are increased. These molecules are able to activate the JAK-STAT3 signaling pathway (Figure 1.5.3.1). While Leptin (Lep) acts predominantly in the central nervous system, IL-6 has been reported to act in peripheral organs. Activation of the JAK-STAT3 signaling pathway induced by Leptin and IL-6 leads to an increase in the expression of the negative regulator SOCS3. SOCS3 in turn not only blocks leptin and IL-6 signaling but also impairs insulin (INS) action leading to obesity and insulin resistance.

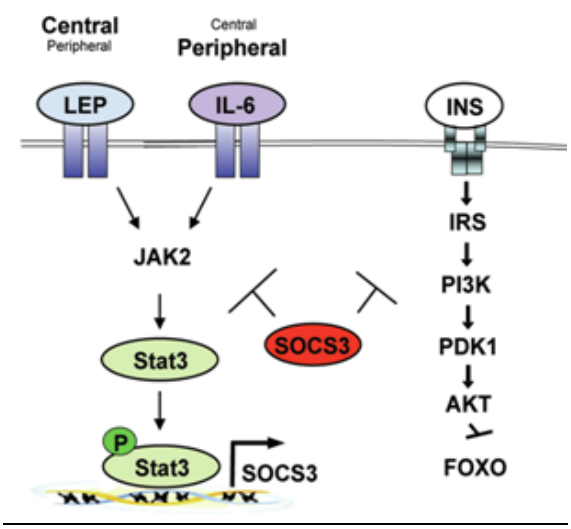

Figure 1.5.3.1. Chronic JAK/STAT/SOCS3 signaling in obesity. Obesity increases circulating levels of leptin and IL-6 that in turn chronically activate intracellular JAK-STAT3 signaling**.** Picture taken from [97].

2. SPHINGOLIPIDS

Sphingolipids have been considered for many years as simple structural components of cells. Nevertheless, in the past few decades they have emerged as potent bioactive lipids

able to regulate many essential cell functions. In particular, Ceramide (Cer), Sphingosine (Sph), Sphingosine 1-phosphate (S1P) and Ceramide 1-phosphate (C1P), were discovered to act as bioactive molecules, playing very divergent roles, from regulation of signal transduction pathways, through direction of protein sorting to the mediation of cell-to-cell interactions and recognition.

Sphingolipids can be defined by the presence of a backbone called a sphingoid base (Figure 2.1.). Sphingoids, also known as Long Chain Bases (LCB), are long-chain aliphatic amines, containing two or three hydroxyl groups, and often a distinctive trans-double bond in position 4. The most regular type of sphingoid bases in animal tissues and humans are Sphingosine (Sph) and its saturated analogue dihydrosphingosine or Sphinganine (Spa). There are some patterns which define the association between specific components of these sphingoid bases, but the potential number of combinations gives an idea of the complexity that these lipids can reach.

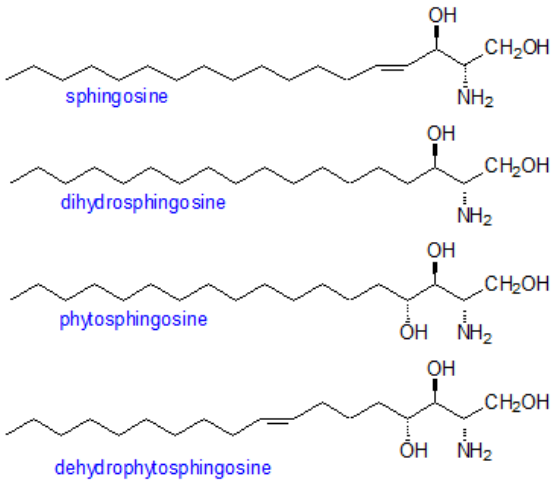

Figure 2.1 Structure of four different sphingoid bases. Taken from AOCS Lipid Library

2.1. Metabolism of sphingolipids

Ceramide (Cer) is the central core in sphingolipid metabolism. Apart from being essential part of the cell membrane structure it is also an important signaling molecule capable of regulating cell proliferation, differentiation, adhesion, migration and apoptosis. There is a great variety of ceramides with differences in the length of their

fatty acids and in the number of unsaturations. Furthermore, each organism or tissue can synthesize different ceramide species.

Cer can be generated by at least three major mechanisms: the *de novo* pathway, through hydrolysis of complex lipids, especially sphingomyelin, and through the salvage pathway (Figure 2.1.1.).

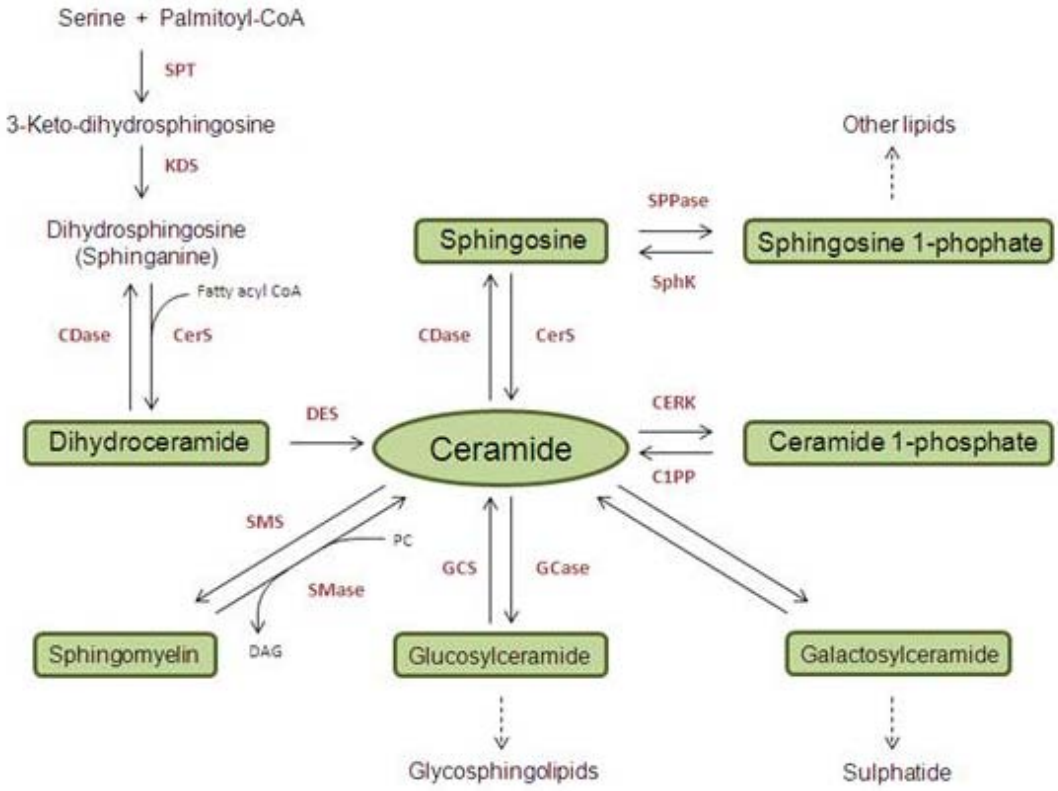

Figure 2.1.1. General metabolism of sphingolipids

A. The *de novo* synthesis pathway:

This anabolic pathway takes place in the endoplasmic reticulum and starts with the condensation of serine and palmitoyl-CoA catalayzed by Serine Palmitoyl Transferase (SPT) to generate the transient intermediate 3-ketodihydrosphingosine, which undergoes rapid reduction to dyhidrosphingosine, also known as Sphinganine, through the action of 3-keto-sphingosine reductase. Upon the N-acylation by ceramide synthase (CerS), sphinganine is then transformed into dihydroceramide (dhCer). The last step of this pathway is catalyzed by a desaturase (DES) through introduction of a trans-4,5 double bond in the dihydroceramide molecule to generate ceramide (Figure 2.1.1.).

B. Sphingomyelin hydrolysis:

The second major mechanism for Ceramide formation occurs through the hydrolysis of complex lipids, especially sphingomyelin (SM). In this hydrolytic pathway, which takes place in the plasma membrane, lysosomes or mitochondria SM is cleaved by one of several sphingomyelinases (SMases) releasing phosphocholine and Cer. The opposite reaction is catalyzed by SM synthase (SMS) which is an important enzyme due to its capacity of controlling ceramide and sphingomielin levels in cells. Specifically, SMS catalyzes the transfer of phosphocholine from Phosphatidylcholine (PC) to Cer, thereby releasing Diacylglycerol (DAG) and lowering the levels of ceramide to produce SM.

C. The salvage pathway.

The third most important mechanism for generating ceramide is the sphingosine salvage pathway, in which Sph produced from the metabolism of complex sphingolipids, is recycled to form Cer through the action of Ceramide Synthase (CerS).

Once formed, ceramides can undergo further processing to generate more complex sphingolipids, such as glycosylceramides or complex glycosphingolipids, which in turn, upon their breakdown by specific glucosidases and galactosidases, can once again generate Cer. Ceramides can also be metabolized by Ceramidases (CDases), which remove the amide-linked fatty acid to give rise to Sph, and thus Sph can be available either for recycling into Cer or phosphorylation by one of the two Sph kinase enzymes (SphK). The product for this reaction, Sphingosine 1-phosphate (S1P), can lose the phosphate group through the action of Sphingosine Phosphatases (SPPases) or be metabolized by S1P lyase for further conversion into other lipids. Finally, Cer can undergo phosphorylation by the action of Ceramide Kinase (CERK) to generate Ceramide 1-phophate (C1P), and this last molecule can be transformed back into Cer by the action of Ceramide 1-phosphate Phosphatase (C1PP) (Figure 2.1.1.).

2.2. Bioactive sphingolipids

Bioactive sphingolipids can be activated by different types of agonists and once their production is increased, sphingolipid species can regulate several downstream targets

and thus, mediate their diverse effects on cells. It has been described that internal levels of various sphingolipids differ according to a common pattern. The concentration of Cer is one order of magnitude above Sph and S1P, but it is also known that a small change in Cer can drastically increase levels in Sph or S1P. This balance between Cer/S1P species is known as the "sphingolipid rheostat" [107].

2.2.1. Ceramides

Ceramides (Cer) consist of a sphingosine backbone covalently linked to a fatty acid via an amide bond (Figure 2.2.1.1.). Unlike the sphingoid precursors, ceramides are not soluble in water and are located in membrane compartments, including the plasma membrane, where they participate in raft formation.

It has been reported that ceramides are able to induce cell cycle arrest and promote apoptosis [108, 109]. Besides, ceramides also play an important role in the regulation of autophagy, cell differentiation, survival, and inflammatory response [110-118]. Cer can function through direct activation of protein phosphatases PP1A and PP2A, which can perform critical responses, such as cell apoptosis through inactivation of the anti-apoptotic targets Akt and Bcl2, and activating pro-apoptotic proteins Bad and Bax [119]. It has also been shown that Cer can regulate the activity of many members of the protein kinase C (PKC) family of proteins. For instance it activates PKCξ, which has been described as a regulator of gene expression through nuclear factor-κ B (NFκB). Another binding target for Cer is the cellular protease cathepsin D, which may regulate the actions of lysosomally generated ceramides [120].

The process of ceramide production appears to be an important research area that could help to elucidate the subsequent bioactive sphingolipids derived from this molecule and their cellular functions. Cer and its downstream metabolites have been suggested to play a decisive role in a number of pathological states, including obesity, cancer, neurodegeneration, diabetes, microbial pathogenesis, and inflammation.

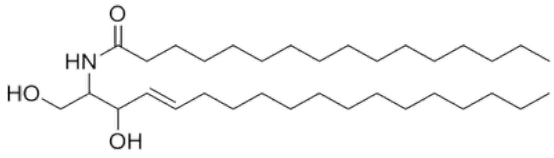

Figure 2.2.1.1. C-16 Ceramide

2.2.2. Sphingosine

Sphingosine (Sph) is an 18-carbon amino alcohol with an unsaturated hydrocarbon chain (Figure 2.2.2.1). Sph has been connected with cellular processes such as inducing cell cycle arrest and apoptosis by modulation of protein kinases and other signalling pathways. It has roles in regulating the actin cytoskeleton and endocytosis and has been shown to inhibit PKC [121]. Kinase targets for sphingoid bases have been found in yeast, indicating functions in regulating endocytosis, cell cycle arrest and protein synthesis [119].

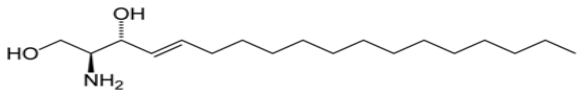

Figure 2.2.2.1. Sphingosine

2.2.3. Sphingosine 1-phosphate

Phosphorylation of sphingosine by Sphingosine Kinases 1 and 2 (SphK1 and SphK2) produces sphingosine 1-phosphate (S1P) [120, 122] (Figure 2.2.3.1.), which can regulate a variety of cellular functions including cell growth and survival, differentiation, and angiogenesis [123-126]. S1P can be produced intracellularly, and it is also present in serum at relatively high concentrations where it can be found attached to lipoproteins or albumin [127]. S1P and Sph are readily inter-convertible by specific intracellular S1P phosphatases [128, 129]. Although many of S1P's effects are exerted by intracellular action, a family of specific G-protein coupled receptors, S1P receptors (S1PR), have been described (Reviewed in [130]).

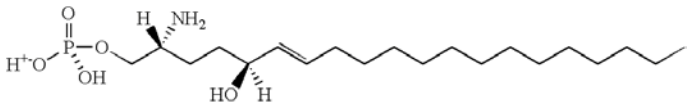

Figure 2.2.3.1. Sphingosine 1-phosphate

2.2.4. Ceramide 1-phosphate and Ceramide kinase (CERK)

Ceramide -1-phosphate (C1P) is a major metabolite of ceramide. C1P was thought to be not biologically active until 1995, when it was first described as a stimulator of DNA synthesis in rat fibroblast [131, 132]. Later, C1P has been described as a pro-survival agent capable of stimulating proliferation in different cell types, including fibroblasts macrophages and myoblasts [131, 133-136], as well as inhibiting apoptosis [137-142]. Moreover, C1P has been shown to affect cell proliferation and inflammation through activation of PLA2 and increases in production of arachidonic acid [143, 144]. In fact C1P in concordance with S1P studies, is able to stimulate the formation of PGE2 and promote the inflammatory process [123]. Our group has recently established that C1P can induce cell migration in Raw 264.7 macrophages [145] and we have also described the association between cell migration and Monocyte Chemoattractant Protein 1 (MCP-1) release in macrophages [146]. More recently, it has been demonstrated that C1P is a negative regulator of TNF-α production induced by Lipopolysaccharide (LPS) [147]. In this connection, C1P has also been described to have anti-inflammatory effects in HEK-293 cells, as it can block LPS-induced cytokine expression [148].

Ceramide-1-phosphate is synthesized in mammalian cells by the direct phosphorylation of ceramide by ceramide kinase (CERK). At present, CERK is the only enzyme known to produce C1P in mammalian cells [149]. This enzyme was first observed in brain synaptic vesicles [150] as a calcium stimulated lipid kinase. After this initial finding, CERK was later found in human leukemia HL-60 cells [151].

The CERK protein sequence has 537 amino acids with two protein sequence motifs: an N-terminus that encompasses a sequence motif known as a pleckstrin homology (PH) domain (amino acids 32–121); and a C-terminal region containing a Ca^{2+}/calmodulin binding domain (amino acids 124–433). Using site-directed mutagenesis, it was found that leucine 10 in the PH domain is essential for its catalytic activity [152], and it was also reported that the interaction between this PH domain of CERK and 4,5-bisphosphate regulates plasma membrane targeting and C1P levels [153].

It has been postulated that a transport protein (ceramide transport protein or CERT) is required for CERK to phosphorylate ceramide. This protein utilizes ceramide transported to the trans-Golgi apparatus. This fact was discovered by silencing of CERT

with specific siRNA resulting in strong inhibition of newly synthesized C1P [144]. However, this hypothesis is controversial because it was also reported that transport of ceramides to the vicinity of CERK was not dependent on CERT [154]. Hence, there are still some questions concerning this concept that require further investigation.

However, it has been reported that bone marrow-derived macrophages from CERK null mice (CERK-/- mice) still have significant levels of C1P, which suggests that there could be other metabolic pathways for generating C1P [154]. We have previously speculated that two alternative pathways for the generation of C1P in cells might be the transfer of a long acyl-CoA chain to S1P by a putative acyl transferase, or cleavage of SM by a PLD-like activity, similar to the existing arthropod or bacterial SMase D. However, at the present time, CERK is considered to be the only C1P source in mammalian cells. Concerning enzyme regulation it has been clearly established that CERK is absolutely dependent on Ca^{2+} ions for activity, and more recently it has been proposed to be regulated by phosphorylation/dephosphorylation processes [155].

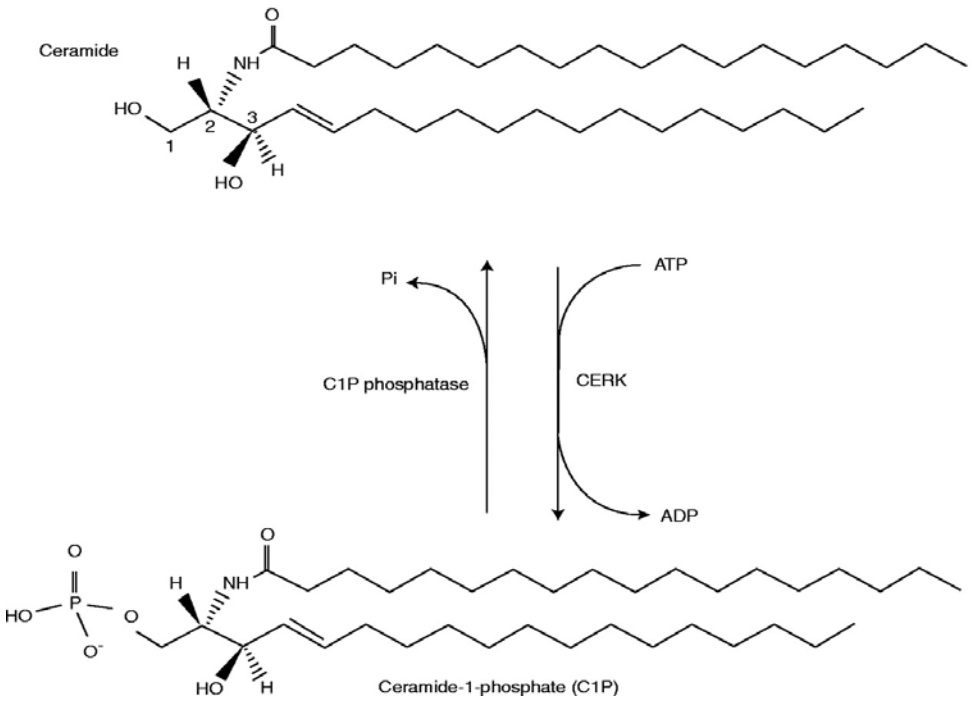

Figure 2.2.4. Conversion of ceramide in C1P by Ceramide Kinase enzymatic action (taken from [156]).

2.2.5. Putative receptor of C1P

It has recently been shown that not all of C1P's effects can be reproduced by increasing intracellular C1P levels. For instance, C1P can induce cell migration in Raw 264.7 cells but it is not possible to stimulate chemotaxis by increasing intracellular C1P levels (i.e, with IL-1β or with the calcium ionophore A23187) [145]. This result suggests that there may be some kind of interaction between C1P and the plasma membrane that cannot be achieved intracellularly. In order to elucidate the existence of a possible C1P receptor binding experiments between C1P and cell membranes were performed. The receptor turned out to be a Gi protein-coupled receptor (GPCR) with low affinity for its substrate (Kd=7.8 μM) [145]. Activation of the this receptor may be physiologically possible since the concentration of C1P in serum is about 20 μM [157].

3. SPHINGOLIPIDS AND OBESITY

3.1. Bioactive sphingolipids in obesity

The contribution of aberrant production of bioactive lipids to pathophysiological changes associated with obesity has risen to the forefront of lipid research. Increased diacylglycerol has been appreciated as a cause of insulin resistance, but emerging data support a role for sphingolipids, such as ceramides, sphingosine and ceramide 1-phosphate in other metabolic diseases.

3.1.1. Ceramides in obesity

Ceramide, a lipid signaling molecule, is not only involved in cellular processes such as differentiation, cell proliferation and cell death [158-160], but also in the pathogenesis of a variety of diseases including obesity, diabetes, atherosclerosis and cardiovascular disease [161-168]. It has been demonstrated that ceramide and sphingosine inhibit insulin action and signaling in cultured cells [167], and it is also shown that inhibition of ceramide synthesis by using the specific serine palmitoyltransferase (SPT) inhibitor myriocin ameliorated obesity-induced insulin resistance [168]. Furthermore, ceramide and sphingosine content in adipocytes during adipogenesis are decreased compared to those of preadipocytes, while the number of lipid droplets and the triglyceride content,

which are differentiation biomarkers, gradually increase [169]. These data are consistent with the observation of a significant decrease in both, the sphingomielyn and ceramide levels in adipose tissue of obese mice compared with a lean mice [170]. Given the diverse signaling properties of sphingolipids, it can be hypothesized that these lipids might mediate the pathology associated with metabolic disease.

3.1.2. Possible role of C1P in obesity

It is known that C1P has emerged as a crucial bioactive sphingolipid. Specifically, C1P was shown to potently stimulate cell migration [145, 146], and promote inflammation [123, 156, 171, 172]. Since chronic inflammation and cell migration are key events in obesity, C1P may contribute to obesity development.

3.1.2.1. C1P and the control of inflammation

Inflammation is one of the major components of the pathogenesis of Type 2 diabetes mellitus (T2DM), which is closely related to obesity. Sphingolipids acts as a potential players in the process of inflammation and clinical data suggest a correlation between ceramide, inflammation, and insulin resistance [173, 174]. However, our group have demonstrated that many of the pro-inflammatory effects of ceramide can be attributed to its phosphorylated form ceramide 1-phosphate [175]. C1P can bind directly to phospholipase A2 (PLA2) [176] and allosterically activate the enzyme leading to release of arachidonic acid (AA) and subsequent prostaglandin formation [177]. AA is a polyunsaturated fatty acid that is present in phospholipids and can act as a second messenger in inflammatory pathways. AA can be also secreted to the extracellular medium and activate other cells in paracrine manner. AA can be generated by the action of phospholipase A2 (PLA2) activity, which cleaves the fatty acid in the second position within the phospholipid molecule. AA can also be generated from diacylglycerol (DAG) through cleavage by diacylglycerol lipase. Besides, AA is a precursor of other pro-inflammatory molecules, such as, prostaglandins, leukotrienes or epoxyeicosatrienoic acid. It has been reported that C1P can activate group IV cPLA2 [178] by increasing the enzyme affinity for its substrate, mainly phosphatidylcholine [179].

In addition to that, Ceramide kinase (CERK), a key enzyme involved in the generation of C1P, is upregulated in type 2 diabetes mellitus (T2DM). Since obesity-associated T2DM is an inflammatory disease, increased CERK activity would serve to execute a pro-inflammatory scenario contributing towards pathology.

3.1.2.2. C1P and cell migration.

Macrophage populations in tissues are determined by the rates of recruitment of monocytes from the bloodstream into the tissue, the rates of macrophage proliferation and apoptosis, and the rate of macrophage migration or efflux. Recently, our group demonstrated that C1P potently stimulates macrophage migration, which has also been associated to inflammatory responses [145, 146]. In addition, our recent work indicates that phosphatidic acid (PA), which is a lipid precursor for phospholipid and triacylglycerol biosynthesis, and is also a signaling metabolite, can also bind to the C1P receptor to counteract C1P-stimulated cell migration [180]. This action could only be observed when C1P was added exogenously, which suggested that C1P could interact with a putative membrane receptor in order to induce macrophage chemotaxis [145]. This receptor, located in the plasma membrane, is specific for C1P and is coupled to Gi proteins. Ligation of this receptor with C1P causes phosphorylation of ERK1-2, and PKB, and inhibition of these pathways completely abolished C1P-stimulated macrophage migration. Moreover, blockade of the transcription factor NF-κB resulted in a full inhibition of macrophage migration. These observations suggest that MEK/ERK1-2, PI3-K/PKB (or Akt) and NF-κB are crucial signalling pathways for regulation of cell migration by C1P.

An understanding of the molecular regulation of obesity-associated processes is of key interest for developing therapeutic strategies to control obesity and related pathologies, as well as cardiovascular diseases and cancer.This particular research area could help to clarify whether C1P or the activity of the enzymes that control their metabolism, could serve as targets for developing new pharmacological strategies for treatment of illnesses such as obesity, in which cell migration and chronic inflammation play a key role.

4. REFERENCES

1. Swinburn, B.A., G. Sacks, K.D. Hall, K. McPherson, D.T. Finegood, M.L. Moodie and S.L. Gortmaker, *The global obesity pandemic: shaped by global drivers and local environments.* Lancet, 2011. **378**(9793): p. 804-14.
2. *Obesity: preventing and managing the global epidemic. Report of a WHO consultation.* World Health Organ Tech Rep Ser, 2000. **894**: p. i-xii, 1-253.
3. Hossain, P., B. Kawar and M. El Nahas, *Obesity and diabetes in the developing world--a growing challenge.* N Engl J Med, 2007. **356**(3): p. 213-5.
4. Mokdad, A.H., E.S. Ford, B.A. Bowman, W.H. Dietz, F. Vinicor, V.S. Bales and J.S. Marks, *Prevalence of obesity, diabetes, and obesity-related health risk factors, 2001.* Jama, 2003. **289**(1): p. 76-9.
5. Dorresteijn, J.A., F.L. Visseren and W. Spiering, *Mechanisms linking obesity to hypertension.* Obes Rev, 2012. **13**(1): p. 17-26.
6. Franssen, R., H. Monajemi, E.S. Stroes and J.J. Kastelein, *Obesity and dyslipidemia.* Med Clin North Am, 2011. **95**(5): p. 893-902.
7. Kahn, S.E., R.L. Hull and K.M. Utzschneider, *Mechanisms linking obesity to insulin resistance and type 2 diabetes.* Nature, 2006. **444**(7121): p. 840-6.
8. McCarthy, M.I., *Genomics, type 2 diabetes, and obesity.* N Engl J Med, 2010. **363**(24): p. 2339-50.
9. Drong, A.W., C.M. Lindgren and M.I. McCarthy, *The genetic and epigenetic basis of type 2 diabetes and obesity.* Clin Pharmacol Ther, 2012. **92**(6): p. 707-15.
10. Masuoka, H.C. and N. Chalasani, *Nonalcoholic fatty liver disease: an emerging threat to obese and diabetic individuals.* Ann N Y Acad Sci, 2013. **1281**: p. 106-22.
11. Speliotes, E.K., *Genetics of common obesity and nonalcoholic fatty liver disease.* Gastroenterology, 2009. **136**(5): p. 1492-5.
12. Rocha, V.Z. and P. Libby, *Obesity, inflammation, and atherosclerosis.* Nat Rev Cardiol, 2009. **6**(6): p. 399-409.
13. Hansson, G.K. and P. Libby, *The immune response in atherosclerosis: a double-edged sword.* Nat Rev Immunol, 2006. **6**(7): p. 508-19.
14. Tzotzas, T., P. Evangelou and D.N. Kiortsis, *Obesity, weight loss and conditional cardiovascular risk factors.* Obes Rev, 2011. **12**(5): p. e282-9.
15. Apovian, C.M. and N. Gokce, *Obesity and cardiovascular disease.* Circulation, 2012. **125**(9): p. 1178-82.
16. Khandekar, M.J., P. Cohen and B.M. Spiegelman, *Molecular mechanisms of cancer development in obesity.* Nat Rev Cancer, 2011. **11**(12): p. 886-95.
17. Hursting, S.D. and S.M. Dunlap, *Obesity, metabolic dysregulation, and cancer: a growing concern and an inflammatory (and microenvironmental) issue.* Ann N Y Acad Sci, 2012. **1271**: p. 82-7.
18. Dixit, V.D., *Adipose-immune interactions during obesity and caloric restriction: reciprocal mechanisms regulating immunity and health span.* J Leukoc Biol, 2008. **84**(4): p. 882-92.
19. Weisberg, S.P., D. McCann, M. Desai, M. Rosenbaum, R.L. Leibel and A.W. Ferrante, Jr., *Obesity is associated with macrophage accumulation in adipose tissue.* J Clin Invest, 2003. **112**(12): p. 1796-808.
20. Xu, H., G.T. Barnes, Q. Yang, G. Tan, D. Yang, C.J. Chou, J. Sole, A. Nichols, J.S. Ross, L.A. Tartaglia and H. Chen, *Chronic inflammation in fat plays a crucial role in the development of obesity-related insulin resistance.* J Clin Invest, 2003. **112**(12): p. 1821-30.
21. Hotamisligil, G.S., N.S. Shargill and B.M. Spiegelman, *Adipose expression of tumor necrosis factor-alpha: direct role in obesity-linked insulin resistance.* Science, 1993. **259**(5091): p. 87-91.

22. Lumeng, C.N., S.M. Deyoung, J.L. Bodzin and A.R. Saltiel, *Increased inflammatory properties of adipose tissue macrophages recruited during diet-induced obesity*. Diabetes, 2007. **56**(1): p. 16-23.
23. Oliver, E., F. McGillicuddy, C. Phillips, S. Toomey and H.M. Roche, *The role of inflammation and macrophage accumulation in the development of obesity-induced type 2 diabetes mellitus and the possible therapeutic effects of long-chain n-3 PUFA.* Proc Nutr Soc, 2010. **69**(2): p. 232-43.
24. Heilbronn, L.K. and L.V. Campbell, *Adipose tissue macrophages, low grade inflammation and insulin resistance in human obesity.* Curr Pharm Des, 2008. **14**(12): p. 1225-30.
25. Wozniak, S.E., L.L. Gee, M.S. Wachtel and E.E. Frezza, *Adipose tissue: the new endocrine organ? A review article.* Dig Dis Sci, 2009. **54**(9): p. 1847-56.
26. Lefterova, M.I. and M.A. Lazar, *New developments in adipogenesis.* Trends Endocrinol Metab, 2009. **20**(3): p. 107-14.
27. Kissebah, A.H. and G.R. Krakower, *Regional adiposity and morbidity.* Physiol Rev, 1994. **74**(4): p. 761-811.
28. Curat, C.A., A. Miranville, C. Sengenes, M. Diehl, C. Tonus, R. Busse and A. Bouloumie, *From blood monocytes to adipose tissue-resident macrophages: induction of diapedesis by human mature adipocytes.* Diabetes, 2004. **53**(5): p. 1285-92.
29. Schaffler, A., J. Scholmerich and C. Buchler, *Mechanisms of disease: adipocytokines and visceral adipose tissue--emerging role in intestinal and mesenteric diseases.* Nat Clin Pract Gastroenterol Hepatol, 2005. **2**(2): p. 103-11.
30. Schipper, H.S., B. Prakken, E. Kalkhoven and M. Boes, *Adipose tissue-resident immune cells: key players in immunometabolism.* Trends Endocrinol Metab, 2012. **23**(8): p. 407-15.
31. Cildir, G., S.C. Akincilar and V. Tergaonkar, *Chronic adipose tissue inflammation: all immune cells on the stage.* Trends Mol Med, 2013. **19**(8): p. 487-500.
32. Catalan, V., J. Gomez-Ambrosi, A. Rodriguez and G. Fruhbeck, *Adipose tissue immunity and cancer.* Front Physiol, 2013. **4**: p. 275.
33. Jager, A. and V.K. Kuchroo, *Effector and regulatory T-cell subsets in autoimmunity and tissue inflammation.* Scand J Immunol, 2010. **72**(3): p. 173-84.
34. Nishimura, S., I. Manabe, M. Nagasaki, K. Eto, H. Yamashita, M. Ohsugi, M. Otsu, K. Hara, K. Ueki, S. Sugiura, K. Yoshimura, T. Kadowaki and R. Nagai, *CD8+ effector T cells contribute to macrophage recruitment and adipose tissue inflammation in obesity.* Nat Med, 2009. **15**(8): p. 914-20.
35. Feuerer, M., L. Herrero, D. Cipolletta, A. Naaz, J. Wong, A. Nayer, J. Lee, A.B. Goldfine, C. Benoist, S. Shoelson and D. Mathis, *Lean, but not obese, fat is enriched for a unique population of regulatory T cells that affect metabolic parameters.* Nat Med, 2009. **15**(8): p. 930-9.
36. Winer, S., Y. Chan, G. Paltser, D. Truong, H. Tsui, J. Bahrami, R. Dorfman, Y. Wang, J. Zielenski, F. Mastronardi, Y. Maezawa, D.J. Drucker, E. Engleman, D. Winer and H.M. Dosch, *Normalization of obesity-associated insulin resistance through immunotherapy.* Nat Med, 2009. **15**(8): p. 921-9.
37. Winer, D.A., S. Winer, L. Shen, P.P. Wadia, J. Yantha, G. Paltser, H. Tsui, P. Wu, M.G. Davidson, M.N. Alonso, H.X. Leong, A. Glassford, M. Caimol, J.A. Kenkel, T.F. Tedder, T. McLaughlin, D.B. Miklos, H.M. Dosch and E.G. Engleman, *B cells promote insulin resistance through modulation of T cells and production of pathogenic IgG antibodies.* Nat Med, 2011. **17**(5): p. 610-7.
38. Olefsky, J.M. and C.K. Glass, *Macrophages, inflammation, and insulin resistance.* Annu Rev Physiol, 2010. **72**: p. 219-46.
39. Le, K.A., S. Mahurkar, T.L. Alderete, R.E. Hasson, T.C. Adam, J.S. Kim, E. Beale, C. Xie, A.S. Greenberg, H. Allayee and M.I. Goran, *Subcutaneous adipose tissue macrophage infiltration is associated with hepatic and visceral fat deposition,*

hyperinsulinemia, and stimulation of NF-kappaB stress pathway. Diabetes, 2011. **60**(11): p. 2802-9.

40. Cinti, S., G. Mitchell, G. Barbatelli, I. Murano, E. Ceresi, E. Faloia, S. Wang, M. Fortier, A.S. Greenberg and M.S. Obin, *Adipocyte death defines macrophage localization and function in adipose tissue of obese mice and humans.* J Lipid Res, 2005. **46**(11): p. 2347-55.
41. Murano, I., G. Barbatelli, V. Parisani, C. Latini, G. Muzzonigro, M. Castellucci and S. Cinti, *Dead adipocytes, detected as crown-like structures, are prevalent in visceral fat depots of genetically obese mice.* J Lipid Res, 2008. **49**(7): p. 1562-8.
42. Liu, J., A. Divoux, J. Sun, J. Zhang, K. Clement, J.N. Glickman, G.K. Sukhova, P.J. Wolters, J. Du, C.Z. Gorgun, A. Doria, P. Libby, R.S. Blumberg, B.B. Kahn, G.S. Hotamisligil and G.P. Shi, *Genetic deficiency and pharmacological stabilization of mast cells reduce diet-induced obesity and diabetes in mice.* Nat Med, 2009. **15**(8): p. 940-5.
43. Wu, D., A.B. Molofsky, H.E. Liang, R.R. Ricardo-Gonzalez, H.A. Jouihan, J.K. Bando, A. Chawla and R.M. Locksley, *Eosinophils sustain adipose alternatively activated macrophages associated with glucose homeostasis.* Science, 2011. **332**(6026): p. 243-7.
44. Balistreri, C.R., C. Caruso and G. Candore, *The role of adipose tissue and adipokines in obesity-related inflammatory diseases.* Mediators Inflamm, 2010. **2010**: p. 802078.
45. Diez, J.J. and P. Iglesias, *The role of the novel adipocyte-derived hormone adiponectin in human disease.* Eur J Endocrinol, 2003. **148**(3): p. 293-300.
46. Fruebis, J., T.S. Tsao, S. Javorschi, D. Ebbets-Reed, M.R. Erickson, F.T. Yen, B.E. Bihain and H.F. Lodish, *Proteolytic cleavage product of 30-kDa adipocyte complement-related protein increases fatty acid oxidation in muscle and causes weight loss in mice.* Proc Natl Acad Sci U S A, 2001. **98**(4): p. 2005-10.
47. Ahima, R.S., *Metabolic actions of adipocyte hormones: focus on adiponectin.* Obesity (Silver Spring), 2006. **14 Suppl 1**: p. 9S-15S.
48. Schwartz, M.W., S.C. Woods, D. Porte, Jr., R.J. Seeley and D.G. Baskin, *Central nervous system control of food intake.* Nature, 2000. **404**(6778): p. 661-71.
49. Elmquist, J.K., R. Coppari, N. Balthasar, M. Ichinose and B.B. Lowell, *Identifying hypothalamic pathways controlling food intake, body weight, and glucose homeostasis.* J Comp Neurol, 2005. **493**(1): p. 63-71.
50. Schwartz, M.W., D.G. Baskin, T.R. Bukowski, J.L. Kuijper, D. Foster, G. Lasser, D.E. Prunkard, D. Porte, Jr., S.C. Woods, R.J. Seeley and D.S. Weigle, *Specificity of leptin action on elevated blood glucose levels and hypothalamic neuropeptide Y gene expression in ob/ob mice.* Diabetes, 1996. **45**(4): p. 531-5.
51. Vong, L., C. Ye, Z. Yang, B. Choi, S. Chua, Jr. and B.B. Lowell, *Leptin action on GABAergic neurons prevents obesity and reduces inhibitory tone to POMC neurons.* Neuron, 2011. **71**(1): p. 142-54.
52. Schwartz, M.W., R.J. Seeley, S.C. Woods, D.S. Weigle, L.A. Campfield, P. Burn and D.G. Baskin, *Leptin increases hypothalamic pro-opiomelanocortin mRNA expression in the rostral arcuate nucleus.* Diabetes, 1997. **46**(12): p. 2119-23.
53. Cheung, C.C., D.K. Clifton and R.A. Steiner, *Proopiomelanocortin neurons are direct targets for leptin in the hypothalamus.* Endocrinology, 1997. **138**(10): p. 4489-92.
54. Fernandez-Riejos, P., S. Najib, J. Santos-Alvarez, C. Martin-Romero, A. Perez-Perez, C. Gonzalez-Yanes and V. Sanchez-Margalet, *Role of leptin in the activation of immune cells.* Mediators Inflamm, 2010. **2010**: p. 568343.
55. Arner, E., P.O. Westermark, K.L. Spalding, T. Britton, M. Ryden, J. Frisen, S. Bernard and P. Arner, *Adipocyte turnover: relevance to human adipose tissue morphology.* Diabetes, 2010. **59**(1): p. 105-9.
56. Spalding, K.L., E. Arner, P.O. Westermark, S. Bernard, B.A. Buchholz, O. Bergmann, L. Blomqvist, J. Hoffstedt, E. Naslund, T. Britton, H. Concha, M. Hassan, M. Ryden, J. Frisen and P. Arner, *Dynamics of fat cell turnover in humans.* Nature, 2008. **453**(7196): p. 783-7.

57. Rosen, E.D. and B.M. Spiegelman, *Molecular regulation of adipogenesis.* Annu Rev Cell Dev Biol, 2000. **16**: p. 145-71.
58. Feve, B., *Adipogenesis: cellular and molecular aspects.* Best Pract Res Clin Endocrinol Metab, 2005. **19**(4): p. 483-99.
59. Lilla, J., D. Stickens and Z. Werb, *Metalloproteases and adipogenesis: a weighty subject.* Am J Pathol, 2002. **160**(5): p. 1551-4.
60. Christiaens, V. and H.R. Lijnen, *Role of the fibrinolytic and matrix metalloproteinase systems in development of adipose tissue.* Arch Physiol Biochem, 2006. **112**(4-5): p. 254-9.
61. Khan, T., E.S. Muise, P. Iyengar, Z.V. Wang, M. Chandalia, N. Abate, B.B. Zhang, P. Bonaldo, S. Chua and P.E. Scherer, *Metabolic dysregulation and adipose tissue fibrosis: role of collagen VI.* Mol Cell Biol, 2009. **29**(6): p. 1575-91.
62. Selvarajan, S., L.R. Lund, T. Takeuchi, C.S. Craik and Z. Werb, *A plasma kallikrein-dependent plasminogen cascade required for adipocyte differentiation.* Nat Cell Biol, 2001. **3**(3): p. 267-75.
63. Farmer, S.R., *Transcriptional control of adipocyte formation.* Cell Metab, 2006. **4**(4): p. 263-73.
64. Rosen, E.D. and O.A. MacDougald, *Adipocyte differentiation from the inside out.* Nat Rev Mol Cell Biol, 2006. **7**(12): p. 885-96.
65. Lehmann, J.M., L.B. Moore, T.A. Smith-Oliver, W.O. Wilkison, T.M. Willson and S.A. Kliewer, *An antidiabetic thiazolidinedione is a high affinity ligand for peroxisome proliferator-activated receptor gamma (PPAR gamma).* J Biol Chem, 1995. **270**(22): p. 12953-6.
66. Tontonoz, P., E. Hu, J. Devine, E.G. Beale and B.M. Spiegelman, *PPAR gamma 2 regulates adipose expression of the phosphoenolpyruvate carboxykinase gene.* Mol Cell Biol, 1995. **15**(1): p. 351-7.
67. Ramji, D.P. and P. Foka, *CCAAT/enhancer-binding proteins: structure, function and regulation.* Biochem J, 2002. **365**(Pt 3): p. 561-75.
68. Wu, Z., Y. Xie, N.L. Bucher and S.R. Farmer, *Conditional ectopic expression of C/EBP beta in NIH-3T3 cells induces PPAR gamma and stimulates adipogenesis.* Genes Dev, 1995. **9**(19): p. 2350-63.
69. Wagner, E.R., B.C. He, L. Chen, G.W. Zuo, W. Zhang, Q. Shi, Q. Luo, X. Luo, B. Liu, J. Luo, F. Rastegar, C.J. He, Y. Hu, B. Boody, H.H. Luu, T.C. He, Z.L. Deng and R.C. Haydon, *Therapeutic Implications of PPARgamma in Human Osteosarcoma.* PPAR Res, 2010. **2010**: p. 956427.
70. DeLong, C.J., Y.J. Shen, M.J. Thomas and Z. Cui, *Molecular distinction of phosphatidylcholine synthesis between the CDP-choline pathway and phosphatidylethanolamine methylation pathway.* J Biol Chem, 1999. **274**(42): p. 29683-8.
71. Cole, L.K. and D.E. Vance, *A role for Sp1 in transcriptional regulation of phosphatidylethanolamine N-methyltransferase in liver and 3T3-L1 adipocytes.* J Biol Chem, 2010. **285**(16): p. 11880-91.
72. Jacobs, R.L., Y. Zhao, D.P. Koonen, T. Sletten, B. Su, S. Lingrell, G. Cao, D.A. Peake, M.S. Kuo, S.D. Proctor, B.P. Kennedy, J.R. Dyck and D.E. Vance, *Impaired de novo choline synthesis explains why phosphatidylethanolamine N-methyltransferase-deficient mice are protected from diet-induced obesity.* J Biol Chem, 2010. **285**(29): p. 22403-13.
73. Medzhitov, R., *Origin and physiological roles of inflammation.* Nature, 2008. **454**(7203): p. 428-35.
74. Gordon, S., *The macrophage.* Bioessays, 1995. **17**(11): p. 977-86.
75. Nishimura, S., I. Manabe, M. Nagasaki, Y. Hosoya, H. Yamashita, H. Fujita, M. Ohsugi, K. Tobe, T. Kadowaki, R. Nagai and S. Sugiura, *Adipogenesis in obesity requires close interplay between differentiating adipocytes, stromal cells, and blood vessels.* Diabetes, 2007. **56**(6): p. 1517-26.

76. Nishimura, S., I. Manabe, M. Nagasaki, K. Seo, H. Yamashita, Y. Hosoya, M. Ohsugi, K. Tobe, T. Kadowaki, R. Nagai and S. Sugiura, *In vivo imaging in mice reveals local cell dynamics and inflammation in obese adipose tissue.* J Clin Invest, 2008. **118**(2): p. 710-21.
77. Strissel, K.J., Z. Stancheva, H. Miyoshi, J.W. Perfield, 2nd, J. DeFuria, Z. Jick, A.S. Greenberg and M.S. Obin, *Adipocyte death, adipose tissue remodeling, and obesity complications.* Diabetes, 2007. **56**(12): p. 2910-8.
78. Weisberg, S.P., D. Hunter, R. Huber, J. Lemieux, S. Slaymaker, K. Vaddi, I. Charo, R.L. Leibel and A.W. Ferrante, Jr., *CCR2 modulates inflammatory and metabolic effects of high-fat feeding.* J Clin Invest, 2006. **116**(1): p. 115-24.
79. Nara, N., Y. Nakayama, S. Okamoto, H. Tamura, M. Kiyono, M. Muraoka, K. Tanaka, C. Taya, H. Shitara, R. Ishii, H. Yonekawa, Y. Minokoshi and T. Hara, *Disruption of CXC motif chemokine ligand-14 in mice ameliorates obesity-induced insulin resistance.* J Biol Chem, 2007. **282**(42): p. 30794-803.
80. Kabon, B., A. Nagele, D. Reddy, C. Eagon, J.W. Fleshman, D.I. Sessler and A. Kurz, *Obesity decreases perioperative tissue oxygenation.* Anesthesiology, 2004. **100**(2): p. 274-80.
81. Shi, H., M.V. Kokoeva, K. Inouye, I. Tzameli, H. Yin and J.S. Flier, *TLR4 links innate immunity and fatty acid-induced insulin resistance.* J Clin Invest, 2006. **116**(11): p. 3015-25.
82. Suganami, T., J. Nishida and Y. Ogawa, *A paracrine loop between adipocytes and macrophages aggravates inflammatory changes: role of free fatty acids and tumor necrosis factor alpha.* Arterioscler Thromb Vasc Biol, 2005. **25**(10): p. 2062-8.
83. Nguyen, M.T., H. Satoh, S. Favelyukis, J.L. Babendure, T. Imamura, J.I. Sbodio, J. Zalevsky, B.I. Dahiyat, N.W. Chi and J.M. Olefsky, *JNK and tumor necrosis factor-alpha mediate free fatty acid-induced insulin resistance in 3T3-L1 adipocytes.* J Biol Chem, 2005. **280**(42): p. 35361-71.
84. Wang, P., E. Mariman, J. Renes and J. Keijer, *The secretory function of adipocytes in the physiology of white adipose tissue.* J Cell Physiol, 2008. **216**(1): p. 3-13.
85. Scherer, P.E., *Adipose tissue: from lipid storage compartment to endocrine organ.* Diabetes, 2006. **55**(6): p. 1537-45.
86. Halberg, N., I. Wernstedt-Asterholm and P.E. Scherer, *The adipocyte as an endocrine cell.* Endocrinol Metab Clin North Am, 2008. **37**(3): p. 753-68, x-xi.
87. Chawla, A., K.D. Nguyen and Y.P. Goh, *Macrophage-mediated inflammation in metabolic disease.* Nat Rev Immunol, 2011. **11**(11): p. 738-49.
88. Mantovani, A., A. Sica, S. Sozzani, P. Allavena, A. Vecchi and M. Locati, *The chemokine system in diverse forms of macrophage activation and polarization.* Trends Immunol, 2004. **25**(12): p. 677-86.
89. Lumeng, C.N., J.L. Bodzin and A.R. Saltiel, *Obesity induces a phenotypic switch in adipose tissue macrophage polarization.* J Clin Invest, 2007. **117**(1): p. 175-84.
90. Odegaard, J.I. and A. Chawla, *Alternative macrophage activation and metabolism.* Annu Rev Pathol, 2011. **6**: p. 275-97.
91. Oh, D.Y., H. Morinaga, S. Talukdar, E.J. Bae and J.M. Olefsky, *Increased macrophage migration into adipose tissue in obese mice.* Diabetes, 2012. **61**(2): p. 346-54.
92. Harford, K.A., C.M. Reynolds, F.C. McGillicuddy and H.M. Roche, *Fats, inflammation and insulin resistance: insights to the role of macrophage and T-cell accumulation in adipose tissue.* Proc Nutr Soc, 2011. **70**(4): p. 408-17.
93. Calle, E.E. and R. Kaaks, *Overweight, obesity and cancer: epidemiological evidence and proposed mechanisms.* Nat Rev Cancer, 2004. **4**(8): p. 579-91.
94. Beretta, M., M. Bauer and E. Hirsch, *PI3K signaling in the pathogenesis of obesity: The cause and the cure.* Adv Biol Regul, 2015. **58**: p. 1-15.
95. Bost, F., M. Aouadi, L. Caron and B. Binetruy, *The role of MAPKs in adipocyte differentiation and obesity.* Biochimie, 2005. **87**(1): p. 51-6.

96. Ma, Z., G. Wang, X. Chen, Z. Ou and F. Zou, *Association of STAT3 common variations with obesity and hypertriglyceridemia: protective and contributive effects.* Int J Mol Sci, 2014. **15**(7): p. 12258-69.
97. Wunderlich, C.M., N. Hovelmeyer and F.T. Wunderlich, *Mechanisms of chronic JAK-STAT3-SOCS3 signaling in obesity.* Jakstat, 2013. **2**(2): p. e23878.
98. Chen, J., *Multiple signal pathways in obesity-associated cancer.* Obes Rev, 2011. **12**(12): p. 1063-70.
99. Plotnikov, A., E. Zehorai, S. Procaccia and R. Seger, *The MAPK cascades: signaling components, nuclear roles and mechanisms of nuclear translocation.* Biochim Biophys Acta, 2011. **1813**(9): p. 1619-33.
100. Fuentes, P., M.J. Acuna, M. Cifuentes and C.V. Rojas, *The anti-adipogenic effect of angiotensin II on human preadipose cells involves ERK1,2 activation and PPARG phosphorylation.* J Endocrinol, 2010. **206**(1): p. 75-83.
101. Wang, T., Y. Wang, Y. Kontani, Y. Kobayashi, Y. Sato, N. Mori and H. Yamashita, *Evodiamine improves diet-induced obesity in a uncoupling protein-1-independent manner: involvement of antiadipogenic mechanism and extracellularly regulated kinase/mitogen-activated protein kinase signaling.* Endocrinology, 2009. **149**(1): p. 358-66.
102. Sebolt-Leopold, J.S. and R. Herrera, *Targeting the mitogen-activated protein kinase cascade to treat cancer.* Nat Rev Cancer, 2004. **4**(12): p. 937-47.
103. Huang, P., J. Han and L. Hui, *MAPK signaling in inflammation-associated cancer development.* Protein Cell, 2011. **1**(3): p. 218-26.
104. Huang, X.F. and J.Z. Chen, *Obesity, the PI3K/Akt signal pathway and colon cancer.* Obes Rev, 2009. **10**(6): p. 610-6.
105. Kim, J.H., R.A. Bachmann and J. Chen, *Interleukin-6 and insulin resistance.* Vitam Horm, 2009. **80**: p. 613-33.
106. Sun, B. and M. Karin, *Obesity, inflammation, and liver cancer.* J Hepatol, 2012. **56**(3): p. 704-13.
107. Spiegel, S., *Sphingosine 1-phosphate: a prototype of a new class of second messengers.* J Leukoc Biol, 1999. **65**(3): p. 341-4.
108. Hannun, Y.A. and L.M. Obeid, *The Ceramide-centric universe of lipid-mediated cell regulation: stress encounters of the lipid kind.* J Biol Chem, 2002. **277**(29): p. 25847-50.
109. Zheng, W., J. Kollmeyer, H. Symolon, A. Momin, E. Munter, E. Wang, S. Kelly, J.C. Allegood, Y. Liu, Q. Peng, H. Ramaraju, M.C. Sullards, M. Cabot and A.H. Merrill, Jr., *Ceramides and other bioactive sphingolipid backbones in health and disease: lipidomic analysis, metabolism and roles in membrane structure, dynamics, signaling and autophagy.* Biochim Biophys Acta, 2006. **1758**(12): p. 1864-84.
110. Kolesnick, R. and D.W. Golde, *The sphingomyelin pathway in tumor necrosis factor and interleukin-1 signaling.* Cell, 1994. **77**(3): p. 325-8.
111. Hannun, Y.A., *The sphingomyelin cycle and the second messenger function of ceramide.* J Biol Chem, 1994. **269**(5): p. 3125-8.
112. Hannun, Y.A. and L.M. Obeid, *Ceramide: an intracellular signal for apoptosis.* Trends Biochem Sci, 1995. **20**(2): p. 73-7.
113. Dressler, K.A., S. Mathias and R.N. Kolesnick, *Tumor necrosis factor-alpha activates the sphingomyelin signal transduction pathway in a cell-free system.* Science, 1992. **255**(5052): p. 1715-8.
114. Gomez-Munoz, A., *Modulation of cell signalling by ceramides.* Biochim Biophys Acta, 1998. **1391**(1): p. 92-109.
115. Mathias, S., K.A. Dressler and R.N. Kolesnick, *Characterization of a ceramide-activated protein kinase: stimulation by tumor necrosis factor alpha.* Proc Natl Acad Sci U S A, 1991. **88**(22): p. 10009-13.
116. Mathias, S. and R. Kolesnick, *Ceramide: a novel second messenger.* Adv Lipid Res, 1993. **25**: p. 65-90.

117. Okazaki, T., A. Bielawska, R.M. Bell and Y.A. Hannun, *Role of ceramide as a lipid mediator of 1 alpha,25-dihydroxyvitamin D3-induced HL-60 cell differentiation.* J Biol Chem, 1990. **265**(26): p. 15823-31.
118. Menaldino, D.S., A. Bushnev, A. Sun, D.C. Liotta, H. Symolon, K. Desai, D.L. Dillehay, Q. Peng, E. Wang, J. Allegood, S. Trotman-Pruett, M.C. Sullards and A.H. Merrill, Jr., *Sphingoid bases and de novo ceramide synthesis: enzymes involved, pharmacology and mechanisms of action.* Pharmacol Res, 2003. **47**(5): p. 373-81.
119. Cowart, L.A. and Y.A. Hannun, *Selective substrate supply in the regulation of yeast de novo sphingolipid synthesis.* J Biol Chem, 2007. **282**(16): p. 12330-40.
120. Maceyka, M., S.G. Payne, S. Milstien and S. Spiegel, *Sphingosine kinase, sphingosine-1-phosphate, and apoptosis.* Biochim Biophys Acta, 2002. **1585**(2-3): p. 193-201.
121. Smith, E.R., A.H. Merrill, L.M. Obeid and Y.A. Hannun, *Effects of sphingosine and other sphingolipids on protein kinase C.* Methods Enzymol, 2000. **312**: p. 361-73.
122. Taha, T.A., Y.A. Hannun and L.M. Obeid, *Sphingosine kinase: biochemical and cellular regulation and role in disease.* J Biochem Mol Biol, 2006. **39**(2): p. 113-31.
123. Chalfant, C.E. and S. Spiegel, *Sphingosine 1-phosphate and ceramide 1-phosphate: expanding roles in cell signaling.* J Cell Sci, 2005. **118**(Pt 20): p. 4605-12.
124. Spiegel, S., D. English and S. Milstien, *Sphingosine 1-phosphate signaling: providing cells with a sense of direction.* Trends Cell Biol, 2002. **12**(5): p. 236-42.
125. Spiegel, S. and S. Milstien, *Sphingosine-1-phosphate: an enigmatic signalling lipid.* Nat Rev Mol Cell Biol, 2003. **4**(5): p. 397-407.
126. Spiegel, S. and S. Milstien, *Sphingosine 1-phosphate, a key cell signaling molecule.* J Biol Chem, 2002. **277**(29): p. 25851-4.
127. Watterson, K., H. Sankala, S. Milstien and S. Spiegel, *Pleiotropic actions of sphingosine-1-phosphate.* Prog Lipid Res, 2003. **42**(4): p. 344-57.
128. Waggoner, D.W., A. Gomez-Munoz, J. Dewald and D.N. Brindley, *Phosphatidate phosphohydrolase catalyzes the hydrolysis of ceramide 1-phosphate, lysophosphatidate, and sphingosine 1-phosphate.* J Biol Chem, 1996. **271**(28): p. 16506-9.
129. Brindley, D.N., D. English, C. Pilquil, K. Buri and Z.C. Ling, *Lipid phosphate phosphatases regulate signal transduction through glycerolipids and sphingolipids.* Biochim Biophys Acta, 2002. **1582**(1-3): p. 33-44.
130. Pyne, S., S.C. Lee, J. Long and N.J. Pyne, *Role of sphingosine kinases and lipid phosphate phosphatases in regulating spatial sphingosine 1-phosphate signalling in health and disease.* Cell Signal, 2009. **21**(1): p. 14-21.
131. Gomez-Munoz, A., P.A. Duffy, A. Martin, L. O'Brien, H.S. Byun, R. Bittman and D.N. Brindley, *Short-chain ceramide-1-phosphates are novel stimulators of DNA synthesis and cell division: antagonism by cell-permeable ceramides.* Mol Pharmacol, 1995. **47**(5): p. 833-9.
132. Gomez-Munoz, A., L.M. Frago, L. Alvarez and I. Varela-Nieto, *Stimulation of DNA synthesis by natural ceramide 1-phosphate.* Biochem J, 1997. **325 (Pt 2)**: p. 435-40.
133. Arana, L., P. Gangoiti, A. Ouro, I.G. Rivera, M. Ordonez, M. Trueba, R.S. Lankalapalli, R. Bittman and A. Gomez-Munoz, *Generation of reactive oxygen species (ROS) is a key factor for stimulation of macrophage proliferation by ceramide 1-phosphate.* Exp Cell Res, 2012. **318**(4): p. 350-60.
134. Gangoiti, P., C. Bernacchioni, C. Donati, F. Cencetti, A. Ouro, A. Gomez-Munoz and P. Bruni, *Ceramide 1-phosphate stimulates proliferation of C2C12 myoblasts.* Biochimie, 2012. **94**(3): p. 597-607.
135. Gangoiti, P., M.H. Granado, S.W. Wang, J.Y. Kong, U.P. Steinbrecher and A. Gomez-Munoz, *Ceramide 1-phosphate stimulates macrophage proliferation through activation of the PI3-kinase/PKB, JNK and ERK1/2 pathways.* Cell Signal, 2008. **20**(4): p. 726-36.
136. Kim, T.J., Y.J. Kang, Y. Lim, H.W. Lee, K. Bae, Y.S. Lee, J.M. Yoo, H.S. Yoo and Y.P. Yun, *Ceramide 1-phosphate induces neointimal formation via cell proliferation and cell cycle progression upstream of ERK1/2 in vascular smooth muscle cells.* Exp Cell Res, 2011. **317**(14): p. 2041-51.

137. Gangoiti, P., M.H. Granado, L. Arana, A. Ouro and A. Gomez-Munoz, *Involvement of nitric oxide in the promotion of cell survival by ceramide 1-phosphate.* FEBS Lett, 2008. **582**(15): p. 2263-9.
138. Gomez-Munoz, A., J.Y. Kong, K. Parhar, S.W. Wang, P. Gangoiti, M. Gonzalez, S. Eivemark, B. Salh, V. Duronio and U.P. Steinbrecher, *Ceramide-1-phosphate promotes cell survival through activation of the phosphatidylinositol 3-kinase/protein kinase B pathway.* FEBS Lett, 2005. **579**(17): p. 3744-50.
139. Gomez-Munoz, A., J.Y. Kong, B. Salh and U.P. Steinbrecher, *Ceramide-1-phosphate blocks apoptosis through inhibition of acid sphingomyelinase in macrophages.* J Lipid Res, 2004. **45**(1): p. 99-105.
140. Granado, M.H., P. Gangoiti, A. Ouro, L. Arana and A. Gomez-Munoz, *Ceramide 1-phosphate inhibits serine palmitoyltransferase and blocks apoptosis in alveolar macrophages.* Biochim Biophys Acta, 2009. **1791**(4): p. 263-72.
141. Miranda, G.E., C.E. Abrahan, D.L. Agnolazza, L.E. Politi and N.P. Rotstein, *Ceramide-1-phosphate, a new mediator of development and survival in retina photoreceptors.* Invest Ophthalmol Vis Sci, 2011. **52**(9): p. 6580-8.
142. Levi, M., M.M. Meijler, A. Gomez-Munoz and T. Zor, *Distinct receptor-mediated activities in macrophages for natural ceramide-1-phosphate (C1P) and for phosphoceramide analogue-1 (PCERA-1).* Mol Cell Endocrinol, 2010. **314**(2): p. 248-55.
143. Pettus, B.J., K. Kitatani, C.E. Chalfant, T.A. Taha, T. Kawamori, J. Bielawski, L.M. Obeid and Y.A. Hannun, *The coordination of prostaglandin E2 production by sphingosine-1-phosphate and ceramide-1-phosphate.* Mol Pharmacol, 2005. **68**(2): p. 330-5.
144. Lamour, N.F., R.V. Stahelin, D.S. Wijesinghe, M. Maceyka, E. Wang, J.C. Allegood, A.H. Merrill, Jr., W. Cho and C.E. Chalfant, *Ceramide kinase uses ceramide provided by ceramide transport protein: localization to organelles of eicosanoid synthesis.* J Lipid Res, 2007. **48**(6): p. 1293-304.
145. Granado, M.H., P. Gangoiti, A. Ouro, L. Arana, M. Gonzalez, M. Trueba and A. Gomez-Munoz, *Ceramide 1-phosphate (C1P) promotes cell migration Involvement of a specific C1P receptor.* Cell Signal, 2009. **21**(3): p. 405-12.
146. Arana, L., M. Ordonez, A. Ouro, I.G. Rivera, P. Gangoiti, M. Trueba and A. Gomez-Munoz, *Ceramide 1-phosphate induces macrophage chemoattractant protein-1 release: involvement in ceramide 1-phosphate-stimulated cell migration.* Am J Physiol Endocrinol Metab, 2013. **304**(11): p. E1213-26.
147. Jozefowski, S., M. Czerkies, A. Lukasik, A. Bielawska, J. Bielawski, K. Kwiatkowska and A. Sobota, *Ceramide and ceramide 1-phosphate are negative regulators of TNF-alpha production induced by lipopolysaccharide.* J Immunol, 2010. **185**(11): p. 6960-73.
148. Hankins, J.L., T.E. Fox, B.M. Barth, K.A. Unrath and M. Kester, *Exogenous ceramide-1-phosphate reduces lipopolysaccharide (LPS)-mediated cytokine expression.* J Biol Chem, 2011. **286**(52): p. 44357-66.
149. Sugiura, M., K. Kono, H. Liu, T. Shimizugawa, H. Minekura, S. Spiegel and T. Kohama, *Ceramide kinase, a novel lipid kinase. Molecular cloning and functional characterization.* J Biol Chem, 2002. **277**(26): p. 23294-300.
150. Bajjalieh, S.M., T.F. Martin and E. Floor, *Synaptic vesicle ceramide kinase. A calcium-stimulated lipid kinase that co-purifies with brain synaptic vesicles.* J Biol Chem, 1989. **264**(24): p. 14354-60.
151. Dressler, K.A. and R.N. Kolesnick, *Ceramide 1-phosphate, a novel phospholipid in human leukemia (HL-60) cells. Synthesis via ceramide from sphingomyelin.* J Biol Chem, 1990. **265**(25): p. 14917-21.
152. Kim, T.J., S. Mitsutake, M. Kato and Y. Igarashi, *The leucine 10 residue in the pleckstrin homology domain of ceramide kinase is crucial for its catalytic activity.* FEBS Lett, 2005. **579**(20): p. 4383-8.

153. Kim, T.J., S. Mitsutake and Y. Igarashi, *The interaction between the pleckstrin homology domain of ceramide kinase and phosphatidylinositol 4,5-bisphosphate regulates the plasma membrane targeting and ceramide 1-phosphate levels.* Biochem Biophys Res Commun, 2006. **342**(2): p. 611-7.
154. Boath, A., C. Graf, E. Lidome, T. Ullrich, P. Nussbaumer and F. Bornancin, *Regulation and traffic of ceramide 1-phosphate produced by ceramide kinase: comparative analysis to glucosylceramide and sphingomyelin.* J Biol Chem, 2008. **283**(13): p. 8517-26.
155. Baumruker, T., F. Bornancin and A. Billich, *The role of sphingosine and ceramide kinases in inflammatory responses.* Immunol Lett, 2005. **96**(2): p. 175-85.
156. Lamour, N.F. and C.E. Chalfant, *Ceramide-1-phosphate: the "missing" link in eicosanoid biosynthesis and inflammation.* Mol Interv, 2005. **5**(6): p. 358-67.
157. Mietla, J.A., D.S. Wijesinghe, L.A. Hoeferlin, M.D. Shultz, R. Natarajan, A.A. Fowler, 3rd and C.E. Chalfant, *Characterization of eicosanoid synthesis in a genetic ablation model of ceramide kinase.* J Lipid Res, 2013. **54**(7): p. 1834-47.
158. Geilen, C.C., T. Wieder and C.E. Orfanos, *Ceramide signalling: regulatory role in cell proliferation, differentiation and apoptosis in human epidermis.* Arch Dermatol Res, 1997. **289**(10): p. 559-66.
159. Olivera, A., A. Romanowski, C.S. Rani and S. Spiegel, *Differential effects of sphingomyelinase and cell-permeable ceramide analogs on proliferation of Swiss 3T3 fibroblasts.* Biochim Biophys Acta, 1997. **1348**(3): p. 311-23.
160. Obeid, L.M., C.M. Linardic, L.A. Karolak and Y.A. Hannun, *Programmed cell death induced by ceramide.* Science, 1993. **259**(5102): p. 1769-71.
161. Chatterjee, S., *Sphingolipids in atherosclerosis and vascular biology.* Arterioscler Thromb Vasc Biol, 1998. **18**(10): p. 1523-33.
162. Shimabukuro, M., Y.T. Zhou, M. Levi and R.H. Unger, *Fatty acid-induced beta cell apoptosis: a link between obesity and diabetes.* Proc Natl Acad Sci U S A, 1998. **95**(5): p. 2498-502.
163. Auge, N., A. Negre-Salvayre, R. Salvayre and T. Levade, *Sphingomyelin metabolites in vascular cell signaling and atherogenesis.* Prog Lipid Res, 2000. **39**(3): p. 207-29.
164. Unger, R.H. and L. Orci, *Diseases of liporegulation: new perspective on obesity and related disorders.* Faseb J, 2001. **15**(2): p. 312-21.
165. Hojjati, M.R., Z. Li, H. Zhou, S. Tang, C. Huan, E. Ooi, S. Lu and X.C. Jiang, *Effect of myriocin on plasma sphingolipid metabolism and atherosclerosis in apoE-deficient mice.* J Biol Chem, 2005. **280**(11): p. 10284-9.
166. Summers, S.A. and D.H. Nelson, *A role for sphingolipids in producing the common features of type 2 diabetes, metabolic syndrome X, and Cushing's syndrome.* Diabetes, 2005. **54**(3): p. 591-602.
167. Summers, S.A., *Ceramides in insulin resistance and lipotoxicity.* Prog Lipid Res, 2006. **45**(1): p. 42-72.
168. Holland, W.L., J.T. Brozinick, L.P. Wang, E.D. Hawkins, K.M. Sargent, Y. Liu, K. Narra, K.L. Hoehn, T.A. Knotts, A. Siesky, D.H. Nelson, S.K. Karathanasis, G.K. Fontenot, M.J. Birnbaum and S.A. Summers, *Inhibition of ceramide synthesis ameliorates glucocorticoid-, saturated-fat-, and obesity-induced insulin resistance.* Cell Metab, 2007. **5**(3): p. 167-79.
169. Choi, K.M., Y.S. Lee, M.H. Choi, D.M. Sin, S. Lee, S.Y. Ji, M.K. Lee, Y.M. Lee, Y.P. Yun, J.T. Hong and H.S. Yoo, *Inverse relationship between adipocyte differentiation and ceramide level in 3T3-L1 cells.* Biol Pharm Bull, 2011. **34**(6): p. 912-6.
170. Samad, F., K.D. Hester, G. Yang, Y.A. Hannun and J. Bielawski, *Altered adipose and plasma sphingolipid metabolism in obesity: a potential mechanism for cardiovascular and metabolic risk.* Diabetes, 2006. **55**(9): p. 2579-87.
171. Wijesinghe, D.S., P. Subramanian, N.F. Lamour, L.B. Gentile, M.H. Granado, Z. Szulc, A. Bielawska, A. Gomez-Munoz and C.E. Chalfant, *The chain length specificity for the activation of group IV cytosolic phospholipase A2 by ceramide-1-phosphate. Use of the*

dodecane delivery system for determining lipid-specific effects. J Lipid Res, 2009. **50**(10): p. 1986-95.
172. Wijesinghe, D.S., N.F. Lamour, A. Gomez-Munoz and C.E. Chalfant, *Ceramide kinase and ceramide-1-phosphate.* Methods Enzymol, 2007. **434**: p. 265-92.
173. de Mello, V.D., M. Lankinen, U. Schwab, M. Kolehmainen, S. Lehto, T. Seppanen-Laakso, M. Oresic, L. Pulkkinen, M. Uusitupa and A.T. Erkkila, *Link between plasma ceramides, inflammation and insulin resistance: association with serum IL-6 concentration in patients with coronary heart disease.* Diabetologia, 2009. **52**(12): p. 2612-5.
174. Gill, J.M. and N. Sattar, *Ceramides: a new player in the inflammation-insulin resistance paradigm?* Diabetologia, 2009. **52**(12): p. 2475-7.
175. Gomez-Munoz, A., P. Gangoiti, M.H. Granado, L. Arana and A. Ouro, *Ceramide-1-phosphate in cell survival and inflammatory signaling,* in *Adv Exp Med Biol*. 2010. p. 118-30.
176. Subramanian, P., M. Vora, L.B. Gentile, R.V. Stahelin and C.E. Chalfant, *Anionic lipids activate group IVA cytosolic phospholipase A2 via distinct and separate mechanisms.* J Lipid Res, 2007. **48**(12): p. 2701-8.
177. Pettus, B.J., A. Bielawska, S. Spiegel, P. Roddy, Y.A. Hannun and C.E. Chalfant, *Ceramide kinase mediates cytokine- and calcium ionophore-induced arachidonic acid release.* J Biol Chem, 2003. **278**(40): p. 38206-13.
178. Pettus, B.J., A. Bielawska, P. Subramanian, D.S. Wijesinghe, M. Maceyka, C.C. Leslie, J.H. Evans, J. Freiberg, P. Roddy, Y.A. Hannun and C.E. Chalfant, *Ceramide 1-phosphate is a direct activator of cytosolic phospholipase A2.* J Biol Chem, 2004. **279**(12): p. 11320-6.
179. Subramanian, P., R.V. Stahelin, Z. Szulc, A. Bielawska, W. Cho and C.E. Chalfant, *Ceramide 1-phosphate acts as a positive allosteric activator of group IVA cytosolic phospholipase A2 alpha and enhances the interaction of the enzyme with phosphatidylcholine.* J Biol Chem, 2005. **280**(18): p. 17601-7.
180. Ouro, A., L. Arana, I.G. Rivera, M. Ordonez, A. Gomez-Larrauri, N. Presa, J. Simon, M. Trueba, P. Gangoiti, R. Bittman and A. Gomez-Munoz, *Phosphatidic acid inhibits ceramide 1-phosphate-stimulated macrophage migration.* Biochem Pharmacol, 2014. **92**(4): p. 642-50.

Objectives

3. OBJECTIVES

It is well established that ceramide 1-phosphate (C1P) regulates important biological functions, including cell growth, and survival, and it is also implicated in inflammatory responses. Since sphingolipid metabolism is altered in obesity, we hypothesized that C1P and CERK could be implicated in obesity-associated processes such as inflammation, macrophage migration and adipogenesis. In this connection, the activity of phosphatidylethanolamine methyl transferase (PEMT) has recently been implicated in adipogenesis and obesity. Therefore, the present thesis was undertaken to examine the possible participation of C1P and CERK in these processes. Accordingly, the objectives proposed in this thesis are as follows:

1. To study the possible implication of MMPs and actin polymerization in C1P-induced macrophage migration and to elucidate the pathways implicated in this process.

2. To study the role of Cerk and C1P in adipocyte differentiation.

3. To determine whether PEMT deficiency affects pro-inflammatory and/or anti-inflammatory cytokine production in WAT from pemt $^{-/-}$ and pemt $^{+/+}$ mice.

4. To evaluate the possible implication of PEMT in macrophage polarization in WAT from pemt $^{-/-}$ and pemt$^{+/+}$ mice.

5. To determine whether PEMT could regulate macrophage migration and to elucidate the pathways implicated in this process.

Materials and Methods

3. MATERIALS AND METHODS

1. MATERIALS

1.1. Reagents

Supplier	Reactives
Abnova	Adipogenesis assay kit
Applied Biosystems (Ambion)	MAPK2 siRNA PI3K siRNA FRAP1 (mTOR) siRNA MMP-2 siRNA MMP-9 siRNA Paxillin siRNA Negative siRNA
Avanti Polar Lipids	C16 Ceramide 1-phosphate
BIO RAD	BCA protein assay kit Nitrocellulose membranes Protein markers
BIO-SERV	High fat diet (HFD) #F3282
Calbiochem-Novabiochem Corporation	(3-(4,5-dimethylthiazole-2-yl)-5-(3-carboxymethoxyphenyl)-2-(4-sulfophenyl)-2H-tetrazolium (MTS) Phenazine methosulfate (PMS) (2R)-2-[(4-Biphenylylsulfonyl)amino]-3-phenylpropionic Acid (MMP-2/9 inhibitor I)
Cayman Chemical	NBD-C6 Ceramide
Cell Signaling Technology	Ab Akt1 Ab p-Akt (Ser 473) Ab p42/p44 (ERK1/2) Ab p-p42/44 (Thr 202/Tyr 204) (p-ERK1/2) Ab p-C/EBPβ Ab mTOR1

	Ab MMP-2 **Ab MMP-9** **Ab p-mTOR1 (Ser2448)** **Ab p-paxillin** **Ab paxillin** **Ab p85 subunit of PI3K** **Ab PPARγ** **Rabbit secondary Ab**
eBioscience	**Mouse CCL2 (MCP-1) ELISA Ready-SET-Go!** **Mouse TNFalpha ELISA Ready-SET-Go!** **Mouse IL-10 ELISA Ready-SET-Go!** **Mouse IL-6 Elisa Ready-SET-Go!** **Anti-mouse CD11c-A488 Ab** **Anti-mouse CD68-PE Ab**
Gibco (Invitrogen)	**Fetal Bovine Serum (FBS)** **Newborn calf serum (NCS)** **Opti-MEM**
Life Technologies	**Phalloidin – Alexa Fluor 488** **SYBR Green RT-PCR Master Mix**
Lonza	**DMEM**
LSBio	**Ab PEMT**
Matreya, LLC	**N-Hexadecanoyl-D-erythro-sphingosine-1-phosphate** **(N-Palmitoyl-Ceramide 1-phosphate) (C1P)**
Molecular Probes (Invitrogen)	**Oligofectamine™**
Peprotech	**Mouse IL-4 ELISA Development Kit** **Mouse IL-1α ELISA Development Kit** **Mouse IL-1β ELISA Development Kit** **Mouse Leptin ELISA Development Kit** **Mouse VEGF ELISA Development Kit** **Mouse RANTES ELISA Development Kit**
Promega	**CellTiter96® AQueous One Solution (MTS)**

RaybioTech	**Mouse inflammation antibody array (AAM-INF-1)**
Santa Cruz Biotechnology, Inc.	**Ab CERK** **Ab GAPDH** **Ab IL-1β** **siRNA Akt1** **siRNA CERK** **siRNA IL-1β**
Sigma-Aldrich	**Acrylamide/bisacrylamide** **Ammonium persulfate** **Bovine Serum Albumin (BSA)** **Coomassie Blue** **Dexamethasone** **Eosin** **Fibronectin** **Gentamicin** **Hematoxylin** **Insulin** **3-Isobutyl-1-methylxanthine (IBMX)** **L-glutamine** **LY294002** **Oil Red O** **PD98059** **Pertussis toxin** **Protease Inhibitor Cocktail (PIC)** **Rosiglitazone** **SB239063** **Scott's Tap Water substitute Concentrate (Blueing Agent)** **SP600126** **Tween-20**
TOCRIS	**10-DEBC** **Cytochalasin D** **Rapamycin**

	Stattic	
Universal ProbeLibrary- Assay desing center - Roche	**qmht CD11c-F**	**qmht CD11c -R**
	qmht CD64-F	**qmht CD64-R**
	qmht CD206-F	**qmht-CD206-R**
	qmht CD163-F	**qmht CD163-R**
	qmht MCP-1-F	**qmht MCP-1-R**
	qmht IL-10-F	**qmht IL-10-R**
	qmht CD68-F	**qmht CD68-R**
	qmht F4/80-F	**qmht F4/80-R**

pC1 empty vector and pC1-PEMT plasmid were kindly provided by Prof. Dennis Vance (Heritage Medical Research Centre, University of Alberta (Edmonton), Canada).

1.2. Cell lines

1.2.1. *J774A.1 cell line*

The J774A.1 cell line is a monocyte/macrophage cell line obtained from BALB/c mice with reticulum cell sarcoma. This cell line was purchased from American Type Culture Collection (ATCC) (Manassas, VA, USA) and cultured following the manufacturer´s indications. Cells were grown in 175 cm^2 flask in DMEM supplemented with 10% heat-inactivated FBS, 50 mg/l gentamicin, 200 µM L-glutamine and 1 g/l glucose. Cells were incubated in a humidified 5% CO_2 incubator at 37 °C and subcultured every 2-3 days, maintaining the cell concentration between 0.5-2 x 10^6 cells/ml.

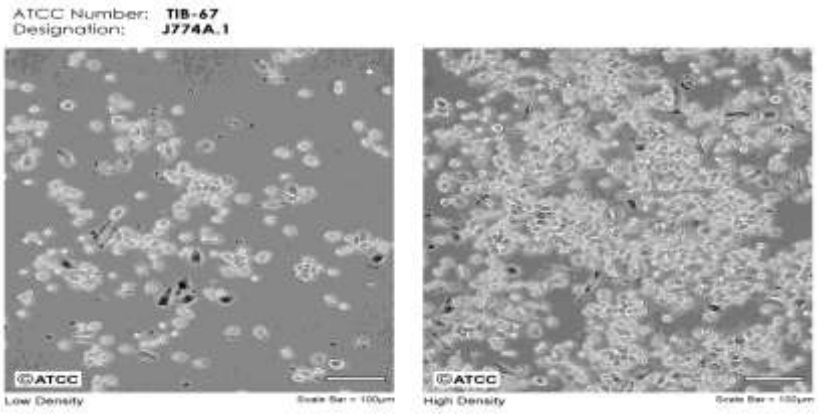

Figure 1.2.1.1. Micrograph of J774A.1 cells taken from the ATCC website

1.2.2. *3T3-L1 cell line*

The 3T3-L1 cell line is a fibroblast cell line purchased from American Type Culture Collection (ATCC) (Manassas, VA, USA) and cultured following the manufacturer's indications. Cells were grown in 175 cm^2 flask in DMEM supplemented with 10% heat-inactivated bovine calf serum (NCS), 50 mg/l gentamicin, 200 µM L-glutamine and 4.5 g/l glucose. Cells were incubated in a humidified 5% CO_2 incubator at 37 °C and subcultured every 3-4 days, before the culture reached 70% to 80% confluence.

These cells undergo a pre-adipose to adipose- like phenotype conversion, characterized by rapid proliferation which can be inhibited by contact. High levels of serum in the medium enhanced fat accumulation.

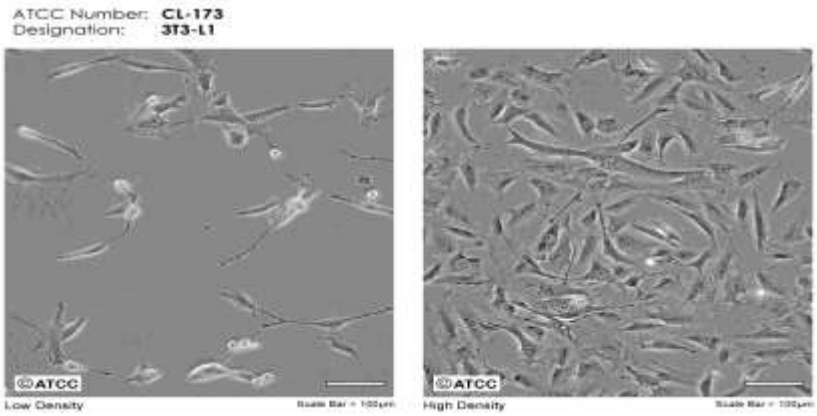

Figure 1.2.2.1 Micrograph of 3T3-L1 cells taken from the ATCC website

2. ANIMAL HANDLING AND DIETS

All procedures were approved by the University of Alberta's Institutional Animal Care Committee in accordance with guidelines of the Canadian Council on Animal Care. 8-9 weeks old *Pemt*$^{+/+}$ and *Pemt*$^{-/-}$ mice (backcrossed >7 generations) were housed with free access to water and high fat diet (HFD) for 10 weeks. Tissues were collected in the morning and stored at -80 °C until analysis.

3. METHODS

3.1. Delivery of C1P to cells in culture

An aqueous dispersion (in the form of liposomes) of C1P was added to cultured cells as previously described [1-3]. Specifically, stock solutions were prepared by sonicating C1P (5 mg) in sterile nanopure water (3 ml) on ice using a probe sonicator until a clear dispersion was obtained. The final concentration of C1P in the stock solution was ~2.62 mM. This procedure is considered preferable to dispersions prepared by adding C1P in organic solvents, because droplet formation is minimized and there are no organic solvent effects on the cells.

C1P was then added to the culture medium in the micromolar range (10-20 μM). These concentrations of C1P are within the physiological range, as previously reported by Mietla and co-workers for mouse serum [4].

3.2. Determination of cell migration. Boyden chamber assay

Macrophage migration was measured using a Boyden chamber-based cell migration assay, also called transwell migration assay. Twenty four-well chemotaxis chambers (Transwell, Corning Costar) were used for the experiments. Before starting the migration experiments, transwell chambers were precoated with 30 μl of fibronectin (0.2 μg/μl) to allow cell attachment. Cell suspensions (100 μl, 5 x 10^4 cells) were then added to the upper wells of the 24-well chemotaxis chambers. Agonists diluted in 300 μL medium supplemented with 0.2% fatty-acid free Bovine Serum Albumin (BSA) were then added to the lower wells. The cells were incubated in the upper chamber for 1 hour inside the incubator in order to ensure cell adhesion. When used, inhibitors were added to the upper wells and pre-incubated 1 hour prior to agonist addition. Then inhibitors and agonists were added to the lower wells and next, chambers holding the cells were moved into agonist containing lower compartments (Figure 3.2.1).

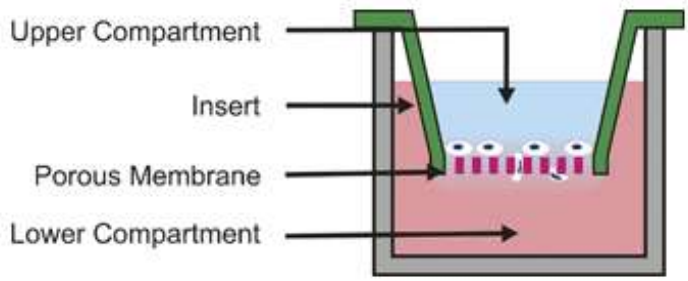

Figure 3.2.1. Schematic representation of a Boyden-chamber based cell migration assay.

After the indicated incubation time, non-migrated cells were removed with a cotton swab, and the filters were fixed with Formaldehyde (5% in PBS) for 30 minutes. Then, formaldehyde was removed and the filters were stained with hematoxylin for 2 hours. After removing hematoxylin with water, the filters were immersed in an acid alcohol solution (70% ethanol:HCL acid 50:1, v/v) for a few seconds, and they were then submerged in blueing agent for 2 minutes. Next, filters were rehydrated with ethanol and further stained with eosin for another 2 minutes. After hematoxilyn-eosin staining, the filters were placed on microscopy slides using mineral oil, avoiding bubbles between slides and coverslips. Cell migration was measured by counting the number of migrated cells in a Nikon Elipse 90i microscope equipped with the NIS-Elements 3.0 software. J774A.1 cells were counted in 8 randomly selected microscopy fields per well, at 20× magnification. The number of migrated cells was normalized by the number of migrated cells in the control chambers.

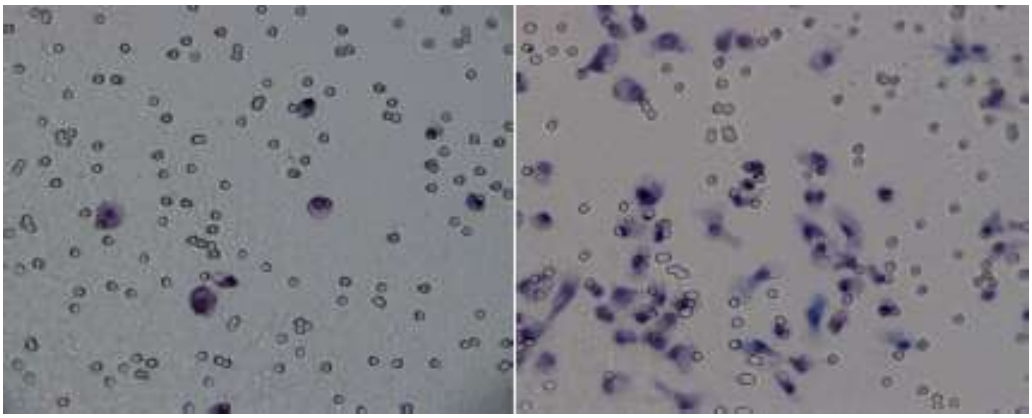

Figure 3.2.2. Micrographs of the migrated cells in the 8 μm pore filters. Cells were incubated with vehicle (left panel) or 20 μM C1P (right panel).

3.3. Cell viability assay (MTS-Formazan method)

Cell viability and proliferation can be determined using the MTS-formazan colorimetric assay. This assay is based on the rate of reduction of the tetrazolium dye, the (3-(4,5 dimethylthiazol-2-yl)-5-(3-carboxymethoxyphenyl)-2-(4-sulfophenyl)-2H-tetrazolium or MTS. MTS in the presence of phenazine methosulfate (PMS) (5% v/v diluted in Phosphate-buffered Saline (PBS) containing Mg^{2+} and Ca^{2+}), reacts with mitochondrial dehydrogenases producing a formazan product that has a maximum absorbance at 490-500 nm in PBS. Generated formazan is proportional to the number of viable cells in culture for up to 15000 cells. (Figure 3.3.1, taken from Gangoiti P. et al, unpublished work).

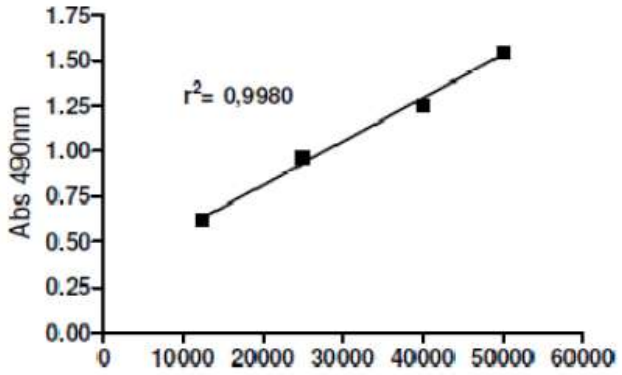

Figure 3.3.1. Generated formazan is proportional to the number of viable cells in culture. The indicated cell number was seeded in 96-wells plates in RPMI 1640 supplemented with 10% FBS and 20% L-cell conditioned medium. 20 μl MTS/PMS was added into each well and after 2 hours absorbance was measured at 490nm. Absorbance of the medium (without cells) was subtracted from each absorbance value and results are the mean ± SEM of three independent experiments. R^2= 0.998 indicates the linearity between cell number and absorbance values.

- **J774A.1 cells** were seeded at 5 x 10^3 cells/well in 96-well plates and incubated overnight in DMEM supplemented with 10% FBS. The next day, the medium was replaced with fresh FBS-starving media in the presence or in the absence of agonists and/or inhibitors and cells were incubated for 24 hours.

- **3T3-L1 cells** were seeded at 9 x 10^3 cells/well in 96-well plates and incubated in DMEM 10% NCS until confluence. Post-confluent cells were

then cultured in the adipogenic induction medium (AIM) in the presence or in the absence of agonist and/or inhibitors and cells were incubated for the indicated periods of time.

After the indicated incubation time, 20 µl of a mixture of MTS and PMS was added to the wells and incubated under the same conditions for 2 hours. Absorbance of the plates was read at 490 nm and absorbance of the medium (without cells) was subtracted from all absorbance values.

3.4. Western blotting

Each cell type was seeded under different conditions in order to obtain the desired confluency and protein concentration:

- **J774A.1** cells were incubated in 60 mm diameter dishes at 2.5 x 10^5 cells/dish and were grown in DMEM containing 10% FBS overnight.

- **3T3-L1** cells were incubated in 6-well plates at 1.2 x 10^5 cells/well and were grown in DMEM containing 10% NCS until they were about 90-100% confluent. Cells were then cultured in adipogenenic induction media (AIM).

Then, all cell types were incubated with or without agonists for the indicated incubation times. Cells were then washed with PBS and harvested with ice-cold homogenization buffer (50 mM HEPES, 137 mM NaCl, 1 mM $MgCl_2$, 1mM $CaCl_2$, 1% (v/v) NP-40, 10% (v/v) glycerol, 2.5 mM EDTA, 10 mM $Na_4P_2O_7$, 1 µg/ml protease inhibitor cocktail), as described [5]. Samples were lysed by sonication and protein concentration was determined by a protein concentration commercial kit (*BioRad*).
Samples (20-40 µg protein/sample) were mixed with 4x loading buffer (125 mM Tris pH 6.8, 50% (v/v) glycerol, 4% SDS, 0.08% (p/v) bromophenol and 50 µl/ml β-mercaptoethanol). Samples were then heated at 90ºC for 10 minutes and loaded into polyacrilamide gels (15%, 12% or 7.5% acrylamide) to perform protein separation by SDS-PAGE. Electrophoresis was run (120 V for 2 hours aprox.) in electrophoresis buffer (1.92 M Glycin, 0.25 M Tris-HCl and 1% SDS).

Proteins were then transferred into nitrocellulose membranes. Transference was run at 400 mA for 1 hour and 15 minutes in ice-cold transfer buffer (14.4 g/l glycin, 3 g/l Tris

and 20% Methanol). In order to avoid unspecific antibody binding, nitrocellulose membrane was blocked for 1 hour with 5% skim milk in Tris-buffered saline (TBS) containing 0.01% NaN_3 and 0.1% Tween 20, pH 7.6. The skim milk was then removed and nitrocellulose membranes were incubated overnight with primary antibody diluted in TBS/0.1%Tween (1:1000) at 4 ºC. After three washes with TBS/0.1% Tween 20, membranes were incubated with Horseradish Peroxidase (HRP) -conjugated secondary antibody at 1:4000 dilution in TBS/0.1% Tween 20 for 1 hour. Bands were visualized by enhanced chemiluminescence and exposed films were analyzed with ImageJ software in order to measure arbitrary intensity.

3.5. Gelatin zymography

MMP-2 and MMP-9 enzymatic activities were determined by SDS-PAGE gelatin zymography. Cells (5 x 10^5 cells/plate) were seeded in 60-mm diameter plates in DMEM containing 10% FBS and incubated for 3-4 hours in order to allow cell attachment. Then, cells were washed and medium was replaced by serum-free DMEM. After 2 hours, agonists were added, and cells were further incubated for the indicated time. After incubation, supernatants were collected and centrifuged 5 minutes at 10000 × g to remove any particulate material. Then, supernatants were centrifuged again at 3200 x g for 10 minutes in 30K centrifugal filters devices in order to concentrate the sample. Samples were mixed (3:1) with sample buffer. Then, 50 µl (40-50 µg) supernatant was loaded and separated in 12% SDS-PAGE containing 0.1% (w/v) gelatin. Gels were incubated in the presence of 2.5% Triton X-100 at room temperature for 2 hours with shaking. Cells were then incubated overnight at 37°C in a buffer containing 5 mM $CaCl_2$, 150 mM NaCl, and 50 mM Tris (pH 7.5). Thereafter, gels were stained with 0.5% Coomassie Blue for 1 hour, with shaking. Then, gels were submerged in a buffer containing 45% methanol, 10% acetic acid and 45% H_2O. Proteolysis was detected as a white band against a blue background. The activity of MMP-2 and MMP-9 was determined by scanning of the bands and densitometry was quantified with ImageJ software. The gelatinolytic activity of MMP-2 and MMP-9 is given in arbitrary units.

3.6. Measurement of actin polymerization by flow cytometry

J774A.1 cells were seeded in 60 mm plates (2.5 x 10^5 cells/well) and incubated in DMEM containing 10% FBS overnight. Then, medium was replaced with free-serum DMEM and further incubated for 2 hours. Agonists and/or inhibitors were then added and after the indicated incubation time, cells were washed and scrapped in 0.5 ml PBS containing 1% BSA. Cells were then collected and centrifuged at 2200 rpm for 5 minutes at 4ºC. Then, supernatant was discarded and cells were fixed in 200 µl paraformaldehide 4% (in PBS) solution for 15 minutes at room temperature. After fixation, cells were washed with PBS containing 1% BSA and resuspended in 200 µl of 0.005% digitonin solution in PBS for 20 minutes in order to permeabilize cell membranes. Cells were then blocked with 1% BSA in PBS for 30 minutes in order to avoid unspecific antibody binding. Finally, cells were washed with PBS and incubated with fluorescent phalloidin (stock solution 6.6 µM) diluted (1:40) in PBS-1% BSA for 30 minutes at room temperature and in dark conditions. Cells were then washed with PBS and resuspended in 0.5 ml PBS with 1% BSA. Cell suspensions were transferred into cytometry tubes. Alexa Fluor 488-fluorescence was measured by flow cytometry using an air-cooled 488 nm argon-ion laser (FACSCalibur, BD Biosciences) and data were analyzed using the CellQuest software (Becton Dickinson), according to the manufacturer´s instructions.

3.7. Quantitative Enzyme-Linked Immunosorbent Assays (ELISA)

3.7.1. Determination of IL-1β concentration in J774A.1 cell culture medium

J774A.1 cells (1.5 x 10^5 cells/well) were seeded in 6-well plates and incubated overnight in DMEM containing 10% FBS. The next day, cells were washed twice with PBS and the medium was replaced by serum-free DMEM. Cells were further incubated in serum deprivation conditions for 2 hours. After 2 hours of incubation, agonists and/or inhibitors were added and cells were incubated for the indicated periods of time. Cell medium was then collected into microcentrifuge tubes and cells were counted for later normalization of the results. The medium was centrifuged at 10000 × g for 5 minutes at 4ºC and the supernatant was used for performing the ELISA assay.

The IL-1β concentration in the medium was determined using a "Mouse Standard ELISA Development Kit" (*PeproTech*) and the manufacturer's protocol was followed. Briefly, a 96-well high reactivity plate was precoated with a specific cytokine antibody to IL-1β and incubated overnight at room temperature. Once the capture antibody was adhered to the plate, the wells were washed and blocked with 1% Bovine Serum Albumin (BSA) in PBS for 1 hour. After blocking, 100 µl of each sample was added in duplicate to the wells. Along with the samples, serial dilutions of a standard solution of IL-1β were also added to the plate. Samples were incubated for 2.5 hours at room temperature and after incubation, wells were washed again and the biotinylated-detection antibody was added. This antibody binds to the IL-1β capture antibody complexes. After 2 hours of incubation at room temperature and the subsequent washes, an Avidin-HRP solution was added to the wells and reactions with biotinylated-detection antibody were allowed to proceed for 30 minutes. Finally after the last wash step, a 2,2′-Azino-bis(3-ethylbenzothiazoline-6-sulfonic acid) diammonium salt (ABTS) solution was added as the substrate. The reaction catalyzed by the enzyme in the presence of the ABTS substrate generates a chromophoric product that enables a colorimetric change (Figure 3.7.1.1.). The absorbance was then read at 405 and 650 nm using a PowerWave™ XS (BioTek) microplate reader provided with Gen5 software. To process the data correctly, absorbance values obtained at 650 nm were subtracted from the values obtained at 405 nm in order to avoid any possible interference, and the standard solutions were used to perform a calibration curve. Sample concentration values (pg/ml) obtained by the calibration curve were normalized considering the total volume of the supernatants collected and the number of cells counted in each well (pg/10^6 cells).

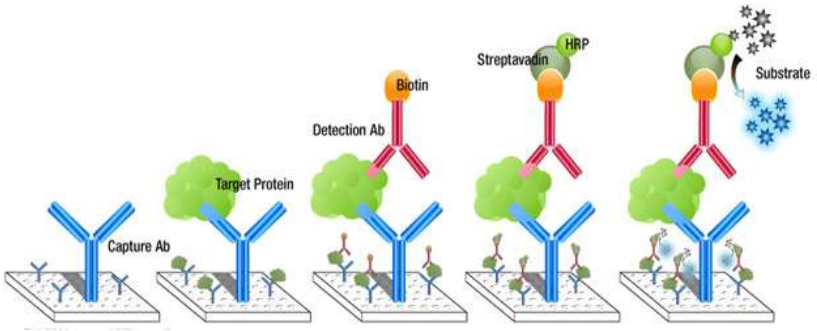

Figure 3.7.1.1. Schematic representation of sandwich ELISA format experiment.

3.7.2. Determination of MCP-1, TNFα, IL-4, IL-10, RANTES, Leptin and IL-1α concentration in White adipose tissue

White adipose tissue was thawed and homogenized with 1ml ice-cold homogenization buffer (50 mM HEPES, 137 mM NaCl, 1 mM $MgCl_2$, 1mM $CaCl_2$, 1% (v/v) NP-40, 10% (v/v) glycerol, 2.5 mM EDTA, 10 mM $Na_4P_2O_7$, 1 µg/ml protease inhibitor cocktail). Then, homogenates were sonicated and centrifuged at 10000 × g for 10 minutes at 4 ºC and the supernatant was then used for the ELISA assay. In order to determine the protein concentration of each sample, the BCA protein assay kit (Bio-Rad) was used.

3.7.2.1. Determination of MCP-1, TNFα and IL-10 concentration in white adipose tissue.

MCP-1, TNF-α and IL-10 concentration was determined using a ¨*Mouse ELISA Ready-Set-Go! Kit* "(*eBioscience*) for each cytokine according to the protocol provided by the manufacturer. Briefly, a 96-well high reactivity plate was precoated with a specific cytokine antibody for MCP-1, TNF-α or IL-10 and incubated overnight at 4 ºC. The next day, wells were washed and blocked with 1% BSA in PBS for 1 hour. Samples were diluted at a 1:3 dilution rate and 100 µl of each diluted sample was then added in duplicate to the wells. Along with the samples, serial dilutions of a standard solution for each cytokine were also added to the plate. Samples were incubated for 2.5 hours. After incubation, wells were washed again and the biotinylated-detection antibody was added. This antibody binds to the MCP-1, TNF-α or IL-10 capture antibody complexes. After 1 hour of incubation at room temperature and subsequent washes, an Avidin-HRP solution was added to the wells and reactions with biotinylated-detection antibody were allowed to proceed for 30 minutes. Finally after the last wash steps, a 3',3',5,5'-tetramethylbenzidine (TMB) solution was added as a substrate and the reaction produced a chromophoric product that prompted a colorimetric change (Figure 3.7.1.1.). The reaction was then stopped with 2N H_2SO_4 and the absorbance was read at 450 and 570 nm using a PowerWave™ XS (BioTek) microplate reader provided with Gen5 software. To process the data correctly, the absorbance values obtained at 570 nm were subtracted from the values obtained at 450 nm so as to avoid possible interferences, and the standard solutions were used to perform a calibration curve. Sample concentration values (pg/ml) obtained by the calibration curve were normalized considering the total

volume of the supernatants collected and the protein quantity in each sample (pg/mg protein).

3.7.2.2. Determination of RANTES, IL1-α, IL-4 and Leptin concentration in white adipose tissue.

RANTES, IL1-α, IL-4 and Leptin concentration was determined using a "Mouse Standard ELISA Development Kit" (PeproTech) for each cytokine according to the manufacturer's protocol.

Briefly, a 96-well high reactivity plates were precoated with a specific cytokine antibody for RANTES, IL1-α, IL-4 and Leptin, and incubated overnight. The next day, wells were washed and blocked with 1% Bovine Serum Albumin (BSA) in PBS for 1 hour. Samples were diluted at a 1:3 dilution rate and 100 µl of each diluted sample was then added in duplicate to the wells. Along with the samples, serial dilutions of a standard solution for each cytokine were also added to the plate. Samples were incubated for 2.5 hours and after incubation, wells were washed again and the biotinylated-detection antibody was added. This antibody binds to the RANTES, IL1-α, IL-4 and Leptin capture antibody complexes. After 2 hour incubation at room temperature and subsequent washes, an Avidin-HRP solution was added to the wells and reactions with biotinylated-detection antibody were allowed to proceed for 30 minutes. Finally, after the last wash steps, a 2,2′-Azino-bis(3-ethylbenzothiazoline-6-sulfonic acid) diammonium salt (ABTS) solution was added as a substrate. The reaction catalyzed by the enzyme in the presence of the ABTS substrate produces a chromophoric product that enables a colorimetric change (Figure 3.7.1.1.). The absorbance was then read at 405 and 650 nm using a PowerWave™ XS (BioTek) microplate reader provided with Gen5 software. To process the data correctly, the absorbance values obtained at 650 nm were subtracted from the values obtained at 405 nm so as to avoid possible interference, and the standard solutions were used to perform a calibration curve. Sample concentration values (pg/ml) obtained by the calibration curve were normalized considering the total volume of the supernatants collected and the protein quantity in each sample (pg/mg protein).

3.7.3. Determination of cytokine release in 3T3-L1 differentiated cells.

3T3-L1 preadipocytes were seeded in 6-well plates (1.2 x 10^5 cells/well) and grown to confluence in DMEM supplemented with 10% newborn calf serum. Confluent cells (day 0) were treated with adipogenic induction medium (DMEM 10% FBS + 0.5 mM IBMX + 1μg/ml insulin + 0.25μM Dexametasone + 2μM Rosiglitazone) in the presence or in the absence of 20 μM of C1P. After 2 days, the medium was removed and cells were further incubated in maintenance medium (DMEM 10% FBS + 1μg/ml insulin) with or without 20 μM of C1P for another 2 days. Cells were then fed every two days with DMEM supplemented with 10% FBS and 1μg/ml insulin, in the presence or in the absence of 20 μM of C1P until the 10^{th} day of the differentiation process. Cell medium was then collected, centrifuged at 10000 × g for 5 minutes at 4 ºC and the supernatant was used for the ELISA assay.

3.7.3.1. Determination of Leptin, IL-4 and VEGF concentration in 3T3-L1 differentiated cells.

Leptin, IL-4 and VEGF concentration was determined using a "Mouse Standard ELISA Development Kit" (*PeproTech*) for each cytokine and the manufacturer's protocol was followed as described in 3.7.2.2 section. Sample concentration values (pg/ml) obtained by the calibration curve were normalized considering the total volume of the collected supernatants and the protein quantity in each sample (pg/mg protein).

3.7.3.2. Determination of MCP-1, IL-10, IL-6 and TNF-α concentration in 3T3-L1 differentiated cells.

MCP-1, TNF-α, IL-6 and IL-10 concentration was determined using a ¨*Mouse ELISA Ready-Set-Go! Kit* "(*eBioscience*) for each cytokine according to the manufacturer's protocol as described in 3.7.2.1 section. Sample concentration values (pg/ml) obtained by the calibration curve were normalized considering the total volume of the supernatants collected and the protein quantity in each sample (pg/mg protein).

3.8. 3T3-L1 preadipocytes differentiation protocol

3T3-L1 cells (20000-30000 cells/ cm^2 of the plate) were cultured and grown in DMEM supplemented with 10% newborn calf serum (NCS) until they were about 90-100% confluent. Confluent cells were further incubated for 2 days. Then, confluent cells (day

0) were treated with adipogenic induction medium (DMEM %10FBS + 0.5mM IBMX + 1μg/ml insulin + 0.25μM Dexametasone + 2μM Rosiglitazone) with or without agonists or inhibitors. After 2 days, medium was removed and cells were further incubated in maintenance medium (DMEM %10 FBS + 1μg/ml insulin) with or without agonists or inhibitors for another 2 days. Cells were then fed every two days with DMEM supplemented with 10% FBS and 1μg/ml insulin, with or without agonists or inhibitors. Agonists and/or inhibitors were added every time the medium was changed.

3.9. Oil Red staining protocol

3T3-L1 preadipocytes were seeded (6 x 10^4 cells/well) in 24-well plates and grown in DMEM supplemented with 10% newborn calf serum (NCS) until they were about 90-100% confluent. Confluent cells were further incubated for 2 days. Then, confluent cells (day 0) were treated with adipogenic induction medium (AIM) in the presence or in the absence of agonists or inhibitors and differentiated following the above described 3T3-L1 preadipocyte differentiation protocol (section 3.8). Thereafter, in order to quantify accumulation of intracellular lipid droplets at any time during adipogenesis process, oil red stock solution (150 mg oil red was dissolved in 50 ml isopropanol, 3 mg/ml) was prepared. After that, cells were washed with PBS and 0.5 ml of previously diluted Oil Red solution (3 parts of 3mg/ml Oil Red solution were mixed with 2 parts of H_2O) was added to each well, including control without cells. Cells were then incubated with oil red solution for 15-20 minutes at room temperature. Cells were then washed with water and after removal of the last wash, stained plates were photographed in a Nikon Eclipse TS100 microscope. Finally, 200 μl isopropanol (dye extraction solution) was added per well and incubated for 30 minutes in a plate shaker. Then, 50 μl of extracted dye was transferred into a 96-well plate and quantified by reading absorbance in a plate reader at 510 nm. The dye extracted from the controls (wells without cells) represents non-specific binding of the dye to the plate. Thus, this value must be subtracted from the absorbance of experimental wells to obtain more accurate assessment of specific staining.

3.10. Triacylglycerol assay kit

3T3-L1 preadipocytes were cultured in 96-well plates (9 x 10^3 cells/well) and grown in DMEM supplemented with 10% newborn calf serum (NCS) until they were about 90-

100% confluent. Confluent cells were further incubated for 2 days. Then, confluent cells (day 0) were treated with adipogenic induction medium (AIM) in the presence or in the absence of agonists and/or inhibitors and differentiated following the above described 3T3-L1 preadipocyte differentiation protocol (section 3.8). For triglyceride (TG) testing, the manufacturer´s instructions were followed. Briefly, after treating cells with the desired agonists and/or inhibitors, cells were washed with PBS and 100 µl lipid extraction solution per well was added. Then, the plates were cover with an adhesive film to prevent evaporation and incubated in a heating block at 90-100ºC for 30 minutes. In order to ensure that triglycerides were completely dissolved in the lipid extraction buffer, plates were cooled while shaking. After this, 50 µl/well of standard dilutions and 5-50 µl of the lipid extracts were transferred to the 96-well plate and assay buffer was added in order to bring the volume to 50 µl. Then, 2 µl of lipase was added to each well containing either sample or standard, mixed and incubated 10 minutes at room temperature so that TG will be converted to glycerol and fatty acids. Then, 50 µl of the reaction mix (46 µl adipogenesis assay buffer + 2 µl Probe + 2 µl Enzyme mix) was added to each well and incubated at 37 ºC for 30 minutes in the dark. Finally, the absorbance values were read at 570 nm in a plate reader. Protein concentration of the lipid extract was determined by a protein concentration commercial kit (BCA, *BioRad*) and it was used as an internal control to normalize the lipid concentration in the sample.

3.11. Semi-quantitative detection of inflammation-related cytokines.

White adipose tissue was thawed and homogenized in 1ml raybio cell lysis buffer (diluted 1:2 in water) with 1 µl protease inhibitor cocktail (PIC). Then, homogenates were sonicated and centrifuged at 10000 × g for 10 minutes at 4 ºC. After that, protein concentration was determined using a protein concentration commercial kit (Bio-Rad) and supernatant was used for performing the cytokine array following manufacturer's indications.

The semi-quantitative detection of the cytokines was performed using RayBio Mouse cytokine antibody array (RayBiotech). First, membranes were blocked for 30 minutes with blocking buffer at room temperature. After subsequent washes, 1ml of 10 fold diluted samples (250 µg-500 µg protein) was added to the membrane and incubated

overnight at 4 ºC. In order to ensure maximum reactivity, different wash steps were performed at room temperature. Then, biotinylated antibody cocktail was added and membranes were incubated for 2 hours at room temperature. After the detection antibody, HRP-Streptavidin was added and membranes were further incubated for 2 hours. Finally, detection solutions were added and cytokine dots were visualized by enhanced chemiluminescence. Exposed films were analyzed by ImageJ software in order to measure arbitrary intensity (Figure 3.11.1.).

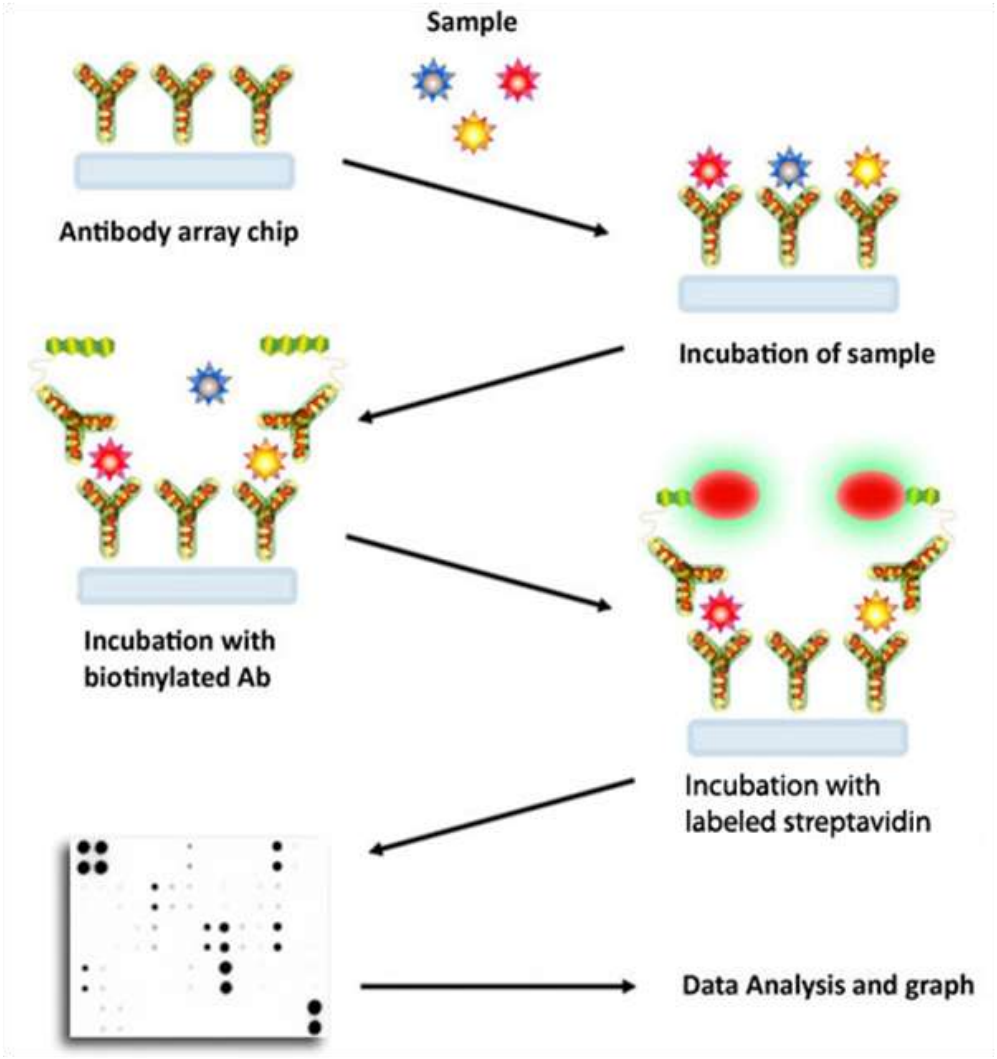

Figure 3.11.1. Schematic representation of the semi-quantitative multichemokine detection

Table 3.11.2 shows the membrane conformation of the chemokines detected with RayBio mouse inflammation antibody array

	A	B	C	D	E	F	G	H	I	J	K	L
1	POS	POS	NEG	NEG	BLANK	BLC	CD30 Ligand	Eotaxin 1	Eotaxin 2	Fas Ligand	Fractalkine	G-CSF
2	POS	POS	NEG	NEG	BLANK	BLC	CD30 Ligand	Eotaxin 1	Eotaxin 2	Fas Ligand	Fractalkine	G-CSF
3	GM-CSF	IFN gamma	IL-1 alpha	IL-1 beta	IL-2	IL-3	IL-4	IL-6	IL-9	IL-10	IL-12 p40/70	IL-12 p70
4	GM-CSF	IFN gamma	IL-1 alpha	IL-1 beta	IL-2	IL-3	IL-4	IL-6	IL-9	IL-10	IL-12 p40/70	IL-12 p70
5	IL-13	IL-17	I-TAC	KC	Lepin	LIX	XCL1	MCP 1	M-CSF	MIG	MIP-1 alpha	MIP-1 gamma
6	IL-13	IL-17	I-TAC	KC	Lepin	LIX	XCL1	MCP 1	M-CSF	MIG	MIP-1 alpha	MIP-1 gamma
7	RANTES	SDF-1	TCA 3	TECK	TIMP 1	TIMP 2	TNF alpha	sTNFR I	sTNFR II	BLANK	BLANK	POS
8	RANTES	SDF-1	TCA 3	TECK	TIMP 1	TIMP 2	TNF alpha	sTNFR I	sTNFR II	BLANK	BLANK	POS

Table 3.11.2. Membrane conformation of the chemokines detected with RayBio mouse inflammation antibody array.

3.12. Small interfering RNA (siRNA) transfection protocol

Small interfering RNAs (siRNAs) assemble into endoribonuclease-containing complexes known as RNA-induced silencing complexes (RISCs). RISC is a multiprotein complex that incorporates one strand of a siRNA to be used it as a template for recognizing complementary mRNA. When the RISC complex finds a complementary strand, it activates a ribonuclease and cleaves the RNA. Cleavage of cognate RNA takes place near the middle of the bounded region by the siRNA strand. After the cleavage of the target mRNA, translation of the protein is inhibited so that the expression of the targeted protein is silenced. siRNA protocols were performed following the manufacturer's instructions.

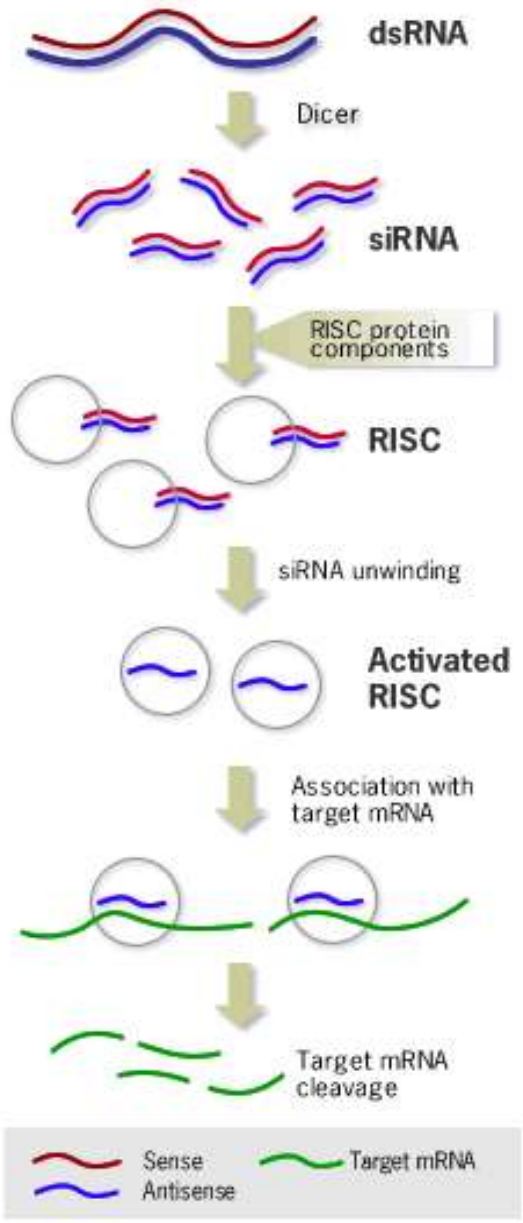

Figure 3.12.1 The mechanism of RNA interference (iRNA)

3.12.1. siRNA transfection protocol for IL-1β release experiments in J774A.1 macrophages

J774A.1 cells were seeded in 60 mm diameter dishes (2 x 10^5 cells/plate) in DMEM containing 10% FBS. Four hours later, medium was removed and cells were washed twice with sterile PBS. Cells were incubated during 24 hours in 1600 μl opti-MEM and siRNA was added following the procedure below:

Solution A: 8 µl of Oligofectamine + 30 µl of opti-MEM (mixed and incubated for 5-10 minutes)

Solution B: 20 µl of siRNA (from 20 µM siRNA stock) + 350 µl of opti-MEM

Solution A was added to Solution B and mixed gently by pipetting. The mixture was incubated at room temperature for 15 minutes and 400 µl of the siRNA mixture was then added into each plate. Cells were then incubated for 5 hours and after that 2 ml of opti-MEM supplemented with 20% FBS was added into the plates, without removing the transfection mixture. This culture was further incubated for 24 hours and the medium was replaced by fresh DMEM containing 10% FBS.

After 24 hours incubation in 10% supplemented DMEM, the cells were scrapped and counted in order to be seeded (1.5 x 10^5 cells) in 6-well plates and further incubated for 24 hours. After 24 hours, the medium was replaced by serum-free DMEM and incubated for 2 hours. After 2 hour of incubation, 20 µM of C1P was added and cells were incubated for the indicated periods of time. Cell medium was then collected into microcentrifuge tubes and cells were counted for later normalization of the results. The medium was centrifuged at 10000 × g for 5 minutes at 4 ºC and the supernatant was used for performing the ELISA assay following "Quantitative Enzyme-Linked Immunosorbent Assays (ELISA)" protocol (section 3.7.1). Remaining cells were lysed and analyzed through Western blotting experiments in order to determine the silencing efficiency of the siRNA treatment.

3.12.2. siRNA transfection protocol for migration experiments in J774A.1 macrophages

Macrophages were seeded in 60 mm diameter dishes (2.0 x 10^5 cells/well) in DMEM containing 10% FBS. The medium was replaced by 1.6 ml opti-MEM and cells were then incubated for 24 hours. The siRNA was added following the procedure below:

Solution A: 8 µl of Oligofectamine + 30 µl of opti-MEM (mixed and incubated for 5-10 minutes)

Solution B: 20 µl of siRNA (from 20 µM siRNA stock) + 350 µl of opti-MEM

Solution A was added into solution B and mixed gently by pipetting. The mixture was incubated at room temperature for 15 minutes and 400 µl of the siRNA mixture was added into each plate. Cells were then incubated for 5 hours and, after that period of time, 2 ml of opti-MEM containing 10% FBS was added into the plates, without removing transfection mixture. This culture was further incubated for 24 hours and the medium was replaced by fresh DMEM containing 10% FBS.

24 hours after medium replacement, cells were scrapped and counted in order to be seeded (5 x 10^4 cells/well) in upper wells of 24-well chambers coated with fibronectin. Migration assays were performed following "Determination of cell migration. Boyden chamber assay" protocol (section 3.2). Remaining cells were lysed and analyzed by Western blotting in order to determine the efficiency of the siRNA treatment.

3.12.3. siRNA transfection protocol for gelatin zymography experiments in J774A.1macrophages

J774A.1 cells were seeded in 60 mm diameter dishes (2 x 10^5 cells/plate) in DMEM containing 10% FBS. Four hours later, medium was removed and cells were washed twice with sterile PBS. Cells were incubated during 24 hours in 1600 µl opti-MEM (without antibiotics) and siRNA was added following the procedure below:

Solution A: 8 µl of Oligofectamine + 30 µl of opti-MEM (mixed and incubated for 5-10 minutes)

Solution B: 20 µl of siRNA (from 20 µM siRNA stock) + 350 µl of opti-MEM

Solution A was added to Solution B and mixed gently by pipetting. The mixture was incubated at room temperature for 15 minutes and 400 µl of the siRNA mixture was then added into each plate. Cells were then incubated for 5 hours and, after that, 2 ml of opti-MEM supplemented with 20% FBS was added into the plates, without removing the transfection mixture. This culture was further incubated for 24 hours and the medium was replaced by fresh DMEM containing 10% FBS.

After 24 hours incubation in 10% FBS supplemented DMEM, the cells were scrapped, counted and seeded (5 x 10^5 cells/plate) in 60 mm diameter dishes and further incubated for 3-4 hours in order to allow cell attachment. Then, the medium was replaced by

serum-free DMEM and incubated for 2 hours. After 2 hours of incubation, 20 μM C1P was added and cells were incubated for the indicated periods of time. Cell supernatant was then collected into microcentrifuge tubes and cells were counted for later normalization of the results. The medium was centrifuged at 10000 × g for 5 minutes at 4 ºC and the supernatant was used for performing gelatin zymography following "Gelatin zymography" protocol (section 3.5). Cells were lysed and analyzed through Western blotting experiments in order to determine the silencing efficiency of the siRNA treatment.

3.12.4. siRNA transfection protocol for Western blot experiments in J774A.1 macrophages.

J774A.1 cells were seeded in 60 mm diameter dishes (2.5 x 10^5 cells/plate) in DMEM containing 10% FBS. Four hours later, medium was removed and cells were washed twice with sterile PBS. Cells were incubated during 24 hours in 1600 μl opti-MEM and siRNA was added following the procedure below:

Solution A: 8 μl of Oligofectamine + 30 μl of opti-MEM (mixed and incubated for 5-10 minutes)

Solution B: 20 μl of siRNA (from 20 μM siRNA stock) + 350 μl of opti-MEM

Solution A was added to Solution B and mixed gently by pipetting. The mixture was incubated at room temperature for 15 minutes and 400 μl of the plasmid mixture was then added into each plate. Cells were then incubated for 5 hours and after that, 2 ml of opti-MEM supplemented with 20% FBS was added into the plates, without removing the transfection mixture. This culture was further incubated for 16-24 hours. After 16-24 hours of incubation in 10% FBS supplemented DMEM, cells were scrapped and counted in order to be seeded (2.5 x 10^5 cells/well) in 60 mm dishes and further used for Western blotting assays. Remaining cells were lysed and analyzed by Western blotting in order to determine the efficiency of the siRNA treatment.

3.12.5. siRNA transfection protocol for flow cytometry analysis in J774A.1 macrophages.

J774A.1 cells were seeded in 60 mm diameter dishes (2 x 10^5 cells/plate) in DMEM containing 10% FBS. Four hours later, medium was removed and cells were washed

twice with sterile PBS. Cells were incubated during 24 hours in 1600 µl opti-MEM (without antibiotics) and siRNA was added following the procedure below:

Solution A: 8 µl of Oligofectamine + 30 µl of opti-MEM (mixed and incubated for 5-10 minutes)

Solution B: 20 µl of siRNA (from 20 µM siRNA stock) + 350 µl of opti-MEM

Solution A was added to Solution B and mixed gently by pipetting. The mixture was incubated at room temperature for 15 minutes and 400 µl of the siRNA mixture was then added into each plate. Cells were then incubated for 5 hours and after that 2 ml of opti-MEM supplemented with 20% FBS was added into the plates, without removing the transfection mixture. This culture was further incubated for 24 hours and the medium was replaced by fresh DMEM containing 10% FBS.

After 24 hours of incubation in 10% FBS supplemented DMEM, the cells were scrapped and counted in order to be seeded (2.5 x 10^5 cells/plate) in 60 mm diameter dishes and further incubated for 24 hours. Then, the medium was replaced by serum-free DMEM and incubated for 2 hours. After 2 hours, 20 µM of C1P was added and cells were incubated for the indicated periods of time. Cells were collected into microcentrifuge tubes and flow cytometry assays were performed following "Measurement of actin polymerization by flow cytometry" protocol (section 3.6). Remaining cells were lysed and analyzed through Western blotting in order to determine the silencing efficiency of the siRNA treatment.

3.12.6. siRNA transfection (by electroporation) protocol for adipogenesis assays in 3T3-L1 cells

3T3-L1 cells were seeded in 100 mm diameter dishes (5 x 10^5 cells/plate) and incubated in DMEM containing 10% NCS until confluence. 48 hours after confluence, medium was removed and cells were washed with sterile PBS and 500 µl trypsin-EDTA was added in order to detach cells. Cells were then centrifuged at 130 × g for 7 minutes and resuspended in 500 µl free-serum DMEM. Cell suspension was transferred into an electroporation cuvette and 20 µl of siRNA (from 20µM siRNA stock) was added. Then, after gently shaking the cuvette for few seconds, cells were electroporated using

the Electro Square Porator (ECM 830) following the conditions shown in Figure 3.12.6.1.

Voltage	Pulse length	# pulses	Interval	Polarity
1000V	30μS	1	100ms	Unipolar

Figure 3.12.6.1 Optimal conditions for 3T3-L1 electroporation

After electroporation, the cell suspension was transferred into 15 ml tubes containing 3T3-L1 adipogenic induction medium and cells were counted. Finally, cells were seeded to confluence (2 x 10^4 cells/well in 96-well plate; 1,2 x 10^5 cells/well in 24-well plate; 5 x 10^5 cells/well in 6-well plate) and differentiated until day 4 of the differentiation process. Then, cells were used for Oil red experiments and Triglyceride assay kit, in order to measure lipid and triglyceride content, respectively. Cell lysates were also analyzed through Western blot analysis in order to determine the silencing efficiency of the siRNA treatment.

3.13. PEMT plasmid overexpression for migration assays in J774A.1 macrophages

J774A.1 cells were seeded in 60 mm diameter dishes (2 x 10^5 cells/plate) in DMEM containing 10% FBS. Four hours later, the medium was removed and cells were washed twice with sterile PBS. Cells were incubated for 24 hours in 1600 μl opti-MEM (without antibiotics) and the pC1 (empty vector) or pC1-PEMT plasmid were added following the procedure below:

Solution A: 8 μl of Oligofectamine + 30 μl of opti-MEM (mixed and incubated for 5-10 minutes)

Solution B: 2.9 μl plasmid (from 1.35μg/μl stock) + 370 μl of opti-MEM

Solution A was added to Solution B and mixed gently by pipetting. The mixture was incubated at room temperature for 15 minutes and 400 μl of the plasmid mixture was then added into each plate. Cells were then incubated for 5 hours and after that 2 ml of opti-MEM supplemented with 20% FBS was added into the plates, without removing the transfection mixture. This culture was further incubated for 16-24 hours. After 16-24 hours, cells were scrapped and counted in order to be seeded (5 x 10^4 cells/well) in

upper wells of 24-well chambers coated with fibronectin. The cell migration protocol was performed as mentioned before (section 3.2). Remaining cells were lysed and analyzed by Western blotting in order to determine the PEMT transfection efficiency.

3.14. PEMT plasmid overexpression for Western blot analysis in J774A.1 macrophages

J774A.1 cells were seeded in 60 mm diameter dishes (2 x 10^5 cells/plate) in DMEM containing 10% FBS. Four hours later, the medium was removed and cells were washed twice with sterile PBS. Cells were incubated for 24 hours in 1600 μl opti-MEM (without antibiotics) and pC1 (empty vector) or pC1-PEMT plasmid were added following the procedure below:

Solution A: 8 μl of Oligofectamine + 30 μl of opti-MEM (mixed and incubated for 5-10 minutes)

Solution B: 2.9 μl plasmid (from 1.35μg/μl stock) + 370 μl of opti-MEM

Solution A was added to Solution B and mixed gently by pipetting. The mixture was incubated at room temperature for 15 minutes and 400 μl of the plasmid mixture was then added into each plate. Cells were then incubated for 5 hours and after that 2 ml of opti-MEM supplemented with 20% FBS was added into the plates, without removing the transfection mixture.

After 16-24 hours incubation in 10% FBS supplemented DMEM, cells were scrapped and counted in order to be seeded (2.5 x 10^5 cells/well) in 60 mm dishes and further used for western blot assays. Remaining cells were lysed and analyzed by Western blotting in order to determine the PEMT transfection efficiency.

3.15. Determination of CERK activity using NBD-Ceramide as the enzyme substrate in cell homogenates

3T3-L1 preadipocytes were seeded in 6-well plates (1.2 x 10^5 cells/well) and grown to confluence with DMEM supplemeted with 10% NCS. 48 hours after confluence, cells were treated with adipogenic induction medium (AIM: DMEM 10% FBS + 0.5 mM IBMX + 1μg/ml insulin + 0.25μM Dexametasone + 2μM Rosiglitazone) or growth medium (GM). After 2 days, adipogenicinduction medium was removed and cells were

further incubated in maintenance medium (DMEM 10% FBS + 1μg/ml insulin). Cells were then fed every two days with DMEM supplemented with 10% FBS and 1μg/ml insulin until day 10 after induction of differentiation. Cells were then washed, scrapped in 100 μl of PBS:PIC (1000:1) solution, and sonicated. Again, a fluorescent CERK assay, adapted for a microplate reader, was performed using the method described by Don and Rosen [6]. Briefly, cell lysates (50-100 μg total protein) were mixed with reaction buffer (100 μl, 20 mM Hepes (pH 7.4), 10 mM KCl, 15 mM MgCl2, 15 mM $CaCl_2$, 10% glycerol, 1 mM DTT, 1 mM ATP) containing 10 μM NBD-ceramide. Reactions were allowed to proceed for 30 minutes in the dark before the lipid extraction was performed. Then, 250 μl chloroform:methanol (2:1) was added and samples were vortexed and centrifuged at 10000 × g for 1.5 minutes. 100 μl of the upper aqueous phase was transferred to a 96-well plate and measured with a Synergy HT (Biotek) plate reader equipped with Gen5 software. NBD fluorescence was quantified with a 495 nm excitation filter and a 520 nm emission filter.

3.16. RT-PCR for M1 and M2 macrophage markers in white adipose tissue

This technique was performed in Dr. Dennis Vance´s laboratory at the Heritage Medical Research Centre, University of Alberta (Edmonton, Canada).

3.16.1. RNA isolation from tissue by Trizol

RNA was isolated from mouse white adipose tissue using tryzol. Briefly, after mice were euthanized, tissue was harvested and treated with trizol. Then, the tissue lysates were splited into 1 ml aliquots in RNAse-free microfuge tubes, placed at room temperature for 5 minutes to ensure disruption of nucleoprotein complexes and spin at 13000 × g for 10 minutes at 4 ºC, to remove fibrous material. Supernatant was then transferred to a clean nuclease-free microfuge tube and 200 μl of chloroform was added for each ml of lysate. Lysates were then vortexed and incubated at room temperature for 5 minutes. After that, samples were centrifuged again at 13000 × g for 15 minutes at 4 ºC. The upper (aqueous) phase was transferred to an RNAse-free tube and an equal volume of isopropanol was added to the collected aqueous phase. Then, tubes were vortexed and kept on ice for at least 15 minutes to allow RNA precipitation. The samples were then centrifuged at 13000 × g for 15 minutes at 4 ºC. Supernatant was

then carefully removed by pipetting, 1ml of 75% ethanol prepared in nuclease-free water was added and samples were then gently mixed by pipetting. Samples were then centrifuged again at 13000 × g for 10 minutes at 4ºC. Supernatant was then removed and tubes were left to air dry for 5 minutes. Finally, 50 µl of nuclease-free water was added, vortexed and kept on ice for 10 minutes. Isolated RNA was quantified using the ND-1000 spectrophotometer (*NanoDrop*) and samples were then stored at -80 ºC until used.

3.16.2. DNAse 1 treatment of RNA for RT-PCR and qPCR protocols

2 µg of isolated RNA were taken from each sample and DEPC water was added to RNA to obtain a final volume of 8 µl. In a separate tube, enough DNAse 1 (amplification grade, *invitrogen*) and DNAse buffer (10x, supplied) were mixed in 1:1 proportion. Then, DNAse and buffer (total of 2 µl) was added to each RNA sample and samples were gently mixed by pipetting at room temperature for 15 minutes. Then, samples were put on ice and 1 µl of 25 mM EDTA solution was added, vortexed and centrifuged. Finally, samples were heated at 65 ºC for 10 minutes in order to kill the enzyme activity. After that, RNA samples were ready to perform Reverse Transcription-Polymerase Chain Reaction (RT-PCR) in order to obtain cDNA.

Briefly, 1 µl oligo (Dt) was added to each sample, mixed and kept at 65-70 ºC for 10 minutes and placed on ice for 5 minutes. Each RNA sample was then mixed in PCR tubes with a Reverse Transcription Master Mix solution, containing 4 µL 5X First Strand Buffer, RT Buffer, 0.4 µl dNTPs Mix (25 mM), 2 µl DTT, 0.6 µl DEPC-treated dH_2O and 1 µl SuperScript II Reverse Transcriptase. As a control, a master mix solution was prepared without reverse transcriptase. Instead of reverse transcriptase 1.6 µl of nuclease-free water was added. The plate was then carried to a Mastercycler Gradient thermal cycler with the following thermal profile: an initial step at 42 ºC for 50 minutes, a second step of 94 ºC for 15 minutes and a final step at 4 ºC for 60 minutes. Reactions were then allowed to happen and cDNA obtained was then stored at -80 ºC until used.

3.16.3. q-PCR

For q-PCR, cDNA template was diluted (1/100) in sterile dH_2O so that it can be added in a volume of 4 µl to each tube to reach a final reaction volume of 20 µl per tube. Then, 16 µl master mix reaction was added to each tube. This master mix reaction contained

for 1 reaction: 0.8 µl forward and 0.8 µl reverse primers (from 10 µM stock), 10 µl qPCR Supermix containing SYBR Green, and 4.4 µl of sterile dH_2O. The master mix was vortexed and 16 µl of this was dispensed into the wells of the PCR plate, which was placed in the aluminium PCR set up block, chilled on ice. Next, 4 µl of diluted cDNA template was added into each well and a clear adhesive cover was positioned over the PCR plate so that it covered all wells. The plate was then mixed using Eppendorf MixMate plate mixer set for 1000 rpm for 1 minute. After mixing, the plates were centrifuged at 1000 rpm for 30 seconds in the Eppendorf desktop centrifuge using the plate spinner buckets. Finally, quantitative real-time PCR (qPCR) was performed using Step One Plus qPCR system following a 3 step cycling protocol, which consists on an initial step at 94 ºC for 4 minutes, a cycling step of 94 ºC for 30 seconds (desnaturalization), 60 ºC for 30 seconds (annealing) and 72 ºC for 30 seconds (extension) and a final step at 72 ºC. The last cycle was followed by a melting curve analysis to ensure that a reaction free of products has been performed. Diluted standard curves were used as external standards. The level of fluorescence emitted from SYBR green dye when incorporated to double-stranded DNA was detected.

The mRNA expression of the samples was normalized to CD68 mRNA, which is a generic macrophage marker, and qPCR data were directly exported from Step One Plus qPCR machine.

The following genes were measured:

Target template	**SEQUENCE**	**Melting temperature Tm (ºC)**	**Amplicon (bp)**	**Reference sequence**
CD11c	F: 5´- tctgctgctgctggctatc - 3´ R: 5´- gtcccgtctgagacaaactgt -3´	60 59	111 111	**NM_0213342**
MCP-1	F: 5´- cagcaagatgatcccaatga - 3´ R: 5´- cctctctcttgagcttggtga -3´	59 59	104 104	**NM_011333**
CD206	F: 5´- catgttccgaaatgttgaagg- 3´ R: 5´- gcccgaagatgaagctagaa -3´	60 59	127 127	**NM_008625.2**
CD163	F: 5´- tggggaaagcattactgtca- 3´ R: 5´- aatctccacctccacaatgc -3´	59 59	123 123	**NM_053094.2**
IL-10	F: 5´- cgactccttaatgcaggacttt- 3´ R: 5´- ttgatttctgggccatgc -3´	59 60	117 117	**NM_010548.2**

F4/80	F: 5´- ccctcgggctgtgagattgtg- 3´ R: 5´- tggccaaggcaagacataccag -3´	60.1 60.1	172 172	**NM_090708**
CD68	F: 5´- gcggctccctgtgtgtctgat- 3´ R: 5´- gggcctgtggctggtcgtag -3´	61.5 61.5	157 157	**NM_009853**

Table 3.15.3.1. Primers used in qPCR

3.17. M1 macrophage phenotype detection by immunofluorescence staining of white adipose tissue (WAT)

Mouse white adipose tissue was collected and fixed in 10% buffered formalin and processed overnight. Tissue samples were then embedded in paraffin wax and sectioned at 5 μm. Slides were then dried out overnight and were stored until analysis. For tissue staining, tissue sections were deparafinnized in xylene for three 5-minute incubation periods. Then, sections were rehydrated by washing them twice with 100% ethanol for 10 minutes each, then with 95% ethanol for another 10 minutes each and finally, the tissue sections were washed in deionized water for 1 minute with stirring. After removing the liquid excess from the slides, they were blocked with 20% normal goat serum for 60 minutes to suppress non-specific binding. Tissue sections were then incubated with CD11c- Alexa Flour 488-conjugated antibody or CD68- PE-conjugated antibody (1/80 dilution) for 60 minutes at room temperature. Slides were then rinsed with PBS (x3), sealed and imaged on a Leika DM IRE2 microscope. This protocol was carried out at the HistoCore service of the Heritage Medical Research Centre (University of Alberta).

3.18. *Statistical analyses*

Statystical analyses were performed using two-tailed Student's t-test, with the level of significance set at $p<0.05$.

Significancy and used symbols:

Symbol	Significance
n.s.	**p>0.05, not significant**
*	**p<0.05, significant**
**	**p<0.01, significant**
***	**p<0.001, significant**

symbol has been used instead of * symbol to compare inhibitor-treated cells versus C1P-treated cells

4. REFERENCES

1. Gomez-Munoz, A., J.Y. Kong, B. Salh and U.P. Steinbrecher, *Ceramide-1-phosphate blocks apoptosis through inhibition of acid sphingomyelinase in macrophages.* J Lipid Res, 2004. **45**(1): p. 99-105.
2. Gangoiti, P., M.H. Granado, S.W. Wang, J.Y. Kong, U.P. Steinbrecher and A. Gomez-Munoz, *Ceramide 1-phosphate stimulates macrophage proliferation through activation of the PI3-kinase/PKB, JNK and ERK1/2 pathways.* Cell Signal, 2008. **20**(4): p. 726-36.
3. Gomez-Munoz, A., J.Y. Kong, K. Parhar, S.W. Wang, P. Gangoiti, M. Gonzalez, S. Eivemark, B. Salh, V. Duronio and U.P. Steinbrecher, *Ceramide-1-phosphate promotes cell survival through activation of the phosphatidylinositol 3-kinase/protein kinase B pathway.* FEBS Lett, 2005. **579**(17): p. 3744-50.
4. Mietla, J.A., D.S. Wijesinghe, L.A. Hoeferlin, M.D. Shultz, R. Natarajan, A.A. Fowler, 3rd and C.E. Chalfant, *Characterization of eicosanoid synthesis in a genetic ablation model of ceramide kinase.* J Lipid Res, 2013. **54**(7): p. 1834-47.
5. Hundal, R.S., A. Gomez-Munoz, J.Y. Kong, B.S. Salh, A. Marotta, V. Duronio and U.P. Steinbrecher, *Oxidized low density lipoprotein inhibits macrophage apoptosis by blocking ceramide generation, thereby maintaining protein kinase B activation and Bcl-XL levels.* J Biol Chem, 2003. **278**(27): p. 24399-408.
6. Don, A.S. and H. Rosen, *A fluorescent plate reader assay for ceramide kinase.* Anal Biochem, 2008. **375**(2): p. 265-71.

Chapter 1

4. CHAPTER 1: Matrix metalloproteinase -2 and -9 (MMP-2 and MMP-9) are implicated in C1P-induced macrophage migration.

1. INTRODUCTION

The concept of adipose tissue remodeling refers to a combination of matrix synthesis and degradation, with the deposition of specific proteins in response to physiological requirements for growth, expansion or tissue repair, and pathological processes such as inflammation, aging or disease [1]. In particular, the development of obesity is associated with a variety of modifications of the adipose tissue, including adipogenesis, angiogenesis and proteolysis of the extracellular matrix (ECM) [2]. In an obese state, adipose tissue responds dynamically to alterations in nutrient excess through adipocyte hypertrophy and hyperplasia, giving rise to an accelerated adipose tissue remodeling, where expression of ECM components and fragments derived from tissue-remodeling processes can influence ECM overproduction and immune cell recruitment and activation. These changes actively contribute to obesity-associated chronic inflammation.

1.1. Extracellular matrix (ECM)

The extracellular matrix (ECM) is a three-dimensional, non cellular structure that is present in all tissues and is essential for the maintenance of tissue integrity. It is composed of around 300 proteins, known as core matrisome, which includes proteins such as collagen, proteoglicans (PGs) and glycoproteins. The ECM forms a milieu surrounding cells that reciprocally influences cellular functions and thereby modulate cell biology [3]. The ECM is extremely versatile and performs many functions in addition to its structural role. As a major component of the microenvironment of the cell, the ECM takes part in most basic cell behaviors, from cell proliferation, adhesion and migration, to cell differentiation and cell death [3]. ECM dynamics can result from changes in the ECM composition or in the ECM arrangement. In addition, ECM is also subject to sustained remodeling, which is mediated by reciprocal interactions between the ECM and its resident cellular components [4]. Consistent with the numerous cell biological functions in which ECM participates, ECM remodeling needs to be tightly

regulated and the most significant enzymes in ECM remodeling are metalloproteinases (MMPs) [5], which are able to degrade or modify all the protein components outside or inside the cell. Despite multiple regulatory mechanisms, ECM dynamics can go awry when activities of ECM remodeling proteins are deregulated, resulting in devastating consequences manifested in various human diseases [6].

1.2. Matrix metalloproteinases (MMPs)

MMPs comprise a large family of structurally related Zn^{2+}-dependent proteolytic enzymes. Each MMP has a specific target substrate that defines its denomination, such as collagenases (MMP-1, MMP-13, MMP-8, MMP-18) that are active against fibrillar collagen; gelatinases (MMP-2 and MMP-9), which are responsible for IV type collagen degradation, vasculature remodeling, angiogenesis, inflammation and atherosclerotic plaque rupture [7]; stromelysins (MMP-3, MMP-10, MMP-11) that degrade noncollagen components of the ECM; matrilysins (MMP-7 and MMP-26); membrane-type MMPs (MT-MMPs) that are transmembrane molecules, and other less characterized members.

MMPs are expressed in several cell types. In particular, gelatinases A and B (MMP-2 and -9) are secreted by several vascular cell types, including endothelial cells, pericytes and podocytes, fibroblasts and myofibroblasts, monocyte derived macrophages and local tissue macrophages [8]. MMP-2 is constitutively expressed on cell surface, while MMP-9 is stored in secretory granules in different cell types and it is inducible by exogenous stimuli, such as cytokines, growth factors or altered cell-matrix contacts [8, 9].

The main activity of these enzymes is to degrade ECM proteins (collagen, gelatins, fibronectin and laminin) by cleavage of internal peptide bonds. Generally, MMPs are expressed at low levels but are rapidly induced at times of active tissue remodeling. Most MMPs are secreted as inactive proenzymes and require proteolytic processing to become active. Their activity is modulated through interactions with tissue inhibitors of MMPs (TIMPs). Consequently, the net MMP activity in tissues is locally determined by the balance between the levels of activated MMPs and TIMPs [10].

1.2.1. Biological roles of MMPs

Extracellular proteases are required for numerous developmental and disease-related processes including migration, invasion, proliferation, apoptosis, differentiation, inflammation, angiogenesis, and host defense. The ability to degrade extracellular proteins is essential for any individual cell to interact properly with its immediate surrounding and for multicellular organisms to develop and function normally.

MMPs can act at different levels during development and normal physiology (Figure 1.2.1.1). Concerning cell migration, ECM needs to be degraded [11] and MMPs are the main enzymes involved in this action. In addition to ECM remodeling, MMPs also promote the activation of the cytoskeleton to provide cell movement, and they also modulate cell-surface adhesive molecules to provide traction. All these processes, which are regulated by MMPs, are required for cells to change from an adhesive phenotype to a migratory phenotype in order to move. Moreover, these enzymes can change ECM microenvironment, which results in an alteration in cellular behavior. Besides, they also modulate the activity of biologically active molecules such as growth factors or growth factor receptors, by cleaving or by releasing them from the ECM. MMPs are also responsible for the activation or inactivation of chemokines and cytokines [12] and they may alter the balance of protease activity by cleaving the enzymes or their inhibitors.

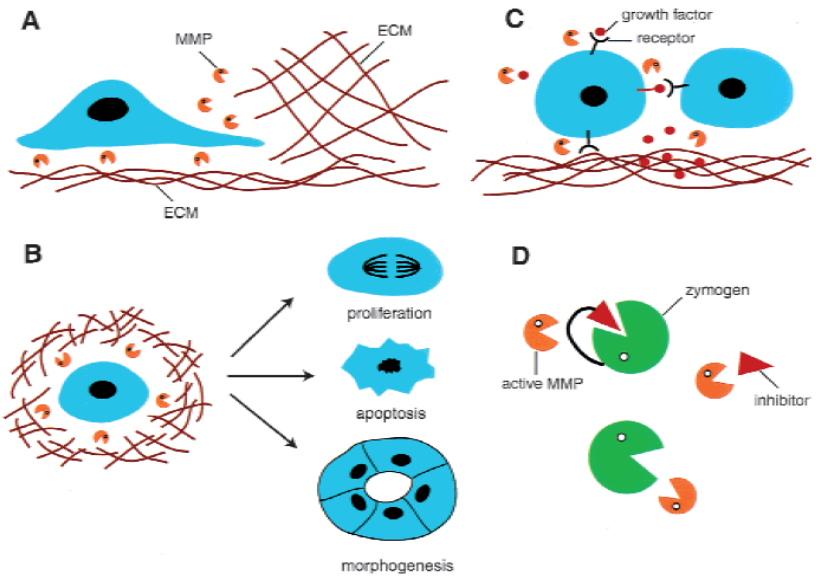

Figure 1.2.1.1. Diverse functions of matrix metalloproteinases. (A) MMPs may affect cell migration by turning cells from an adhesive to non-adhesive phenotype and by degrading the ECM. (B) MMPs may alter ECM microenvironment leading to cell proliferation, apoptosis, or morphogenesis. (C) MMPs may modulate the activity of biologically active molecules such as

growth factors or growth factor receptors by cleaving or by releasing them from the ECM. (D) MMPs may alter the balance of protease activity by cleaving the enzymes or their inhibitors. This figure was taken from [13].

1.2.2. MMPs in obesity

Several studies have suggested that MMPs play important roles in obesity-mediated adipose tissue remodeling [14-18]. MMP-9 expression is increased in adipose tissue with obesity and insulin resistance [15]. Moreover, MMP-9 expression is increased in adipocytes in response to co-culture with macrophages. In addition, upregulation of the expression of MMP-2, MMP-3, MMP-12, MMP-19 and MMP-14 in adipose tissue from genetically obese mice and diet-induced obesity mice has been found [16]. Reportedly, circulating levels of MMP-2 and MMP-9 are increased in obese patients, suggesting an abnormal extracellular matrix metabolism present in these subjects [19]. Therefore, it can be concluded that these enzymes play a key role in ECM degradation, which is an essential step in both physiological and pathological processes like obesity.

1.3. Macrophage migration

Macrophages are present in almost all tissues of the organism where they play a central role in clearance of microorganisms, initiation and mediation of immune and inflammatory responses, and tissue repair. Nevertheless, tissue infiltration of macrophages also exacerbates pathological processes, such as chronic inflammation, neurodegenerative disorders, cancer development, and obesity [20-23]. For a successful migration, cells have to trespass many barriers, in particular the dense meshwork of interconnected fibers that conforms the extracellular matrix (ECM). Although ECM is a physical barrier that impedes cell migration, macrophages are able to go through most, if not all, tissues of the body. To reach their final destination, transmigration through the endothelial wall must be followed by migration through basal membranes and within interstitial tissues [24]. Although macrophage migration in two dimensions has been thoroughly studied [25, 26], recent evidence indicates that macrophages can also migrate in a three-dimensional (3D) environment.

2D migration is characterized by a series of events, which begin with cell polarization in response to extracellular signals. Cell polarization is accompanied by cytoskeleton modifications such as actin polymerization, which triggers the formation of a lamellipodium at the leading edge of the cell rear (Figure 1.3.1). Since actin

polymerization is largely responsible for the dynamic nature of the cytoskeleton, many cellular movements are driven by the cytoskeletal actin reorganization. The efficacy of 2D cell motility relies on highly coordinated dynamic assembly and disassembly cycles of adhesion sites from the front to the rear part of the cell [27, 28]. Most of the cell surface receptors for cell adhesion to ECM structures belong to the integrin family. Furthermore, the majority of proteases that are known to be involved in 2D macrophage migration act directly or indirectly on integrin deactivation. This can occur either by direct cleavage of the integrin extracellular domains or by proteolysis of the integrin ligands.

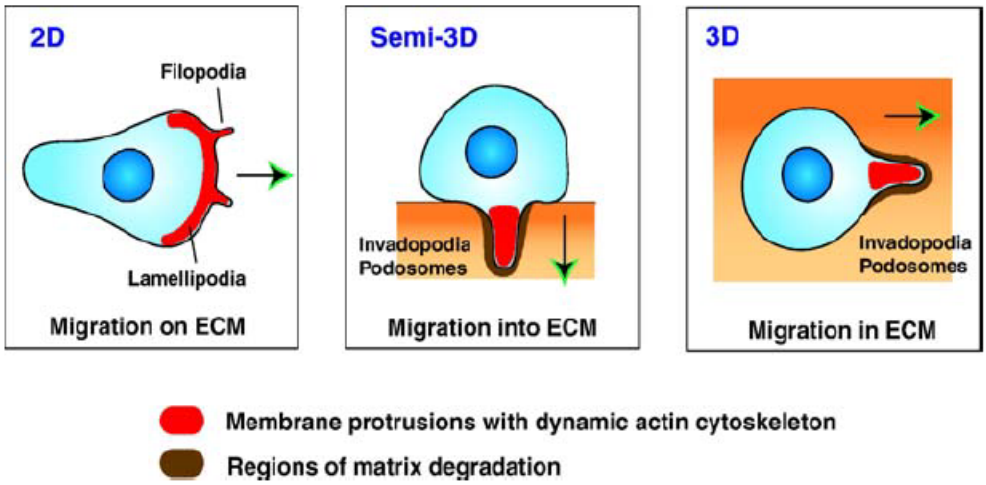

Figure 1.3.1: Cell migration and membrane protrusions in different environments. Cell migrating on 2D substrates form membrane protrusions called fillopodia and lamellipodia at the leading edge. Cells entering into the migrating in a dense rigid ECM in 3D need to form membrane protrusions at the invading front, such as invadopodia and podosomes that have an ECM remodeling activity. Formation of these structures is driven by localized actin polymerization. Taken from [29].

3D cell migration involves two main classes of movement: amoeboid (protease-independent) and mesenchymal migration (protease-dependent) [11]. Cells that perform the amoeboid migration are characterized by a rounded cell shape and a lack of both strong adhesive interactions and proteolytic matrix degradation. Mesenchymal migration is much slower and its cells are characterized by an elongated cell shape with long membrane protrusions, the presence of strong adhesion sites and proteolytic degradation of the ECM [22]. Recent 3D migration studies indicate that macrophages use the amoeboid mode to migrate into fibrillar collagen I and the protease-dependent mesenchymal mode to migrate inside dense ECMs [30, 31]. Contrary to other cell types,

macrophages are able to form podosomes at the tip of cell protrusions, which are cell-matrix contacts with an inherent ability to lyse extracellular matrix (figure 1.3.1) [32-34]. This is achieved by localized release of matrix-lytic factors, especially proteases of the matrix metalloproteinase family [35]. Podosomes show a typical architecture: a core structure consisting of F-actin and actin-associated proteins, and a ring structure of plaque proteins such as paxillin.

The fact that proteases could be dispensable for macrophages to migrate is not completely clear. A recent report shows that macrophages from matrix metalloproteinase (MMP) Mmp-$9^{-/-}$ mice exhibit transmatrix migrating activity similar to that of wild-type cells [36] and, *in vivo*, macrophage tissue infiltration is not affected in experimental atherosclerosis performed in Mmp13-/- or Mmp-14-/- (MT1-MMP) mice [37, 38]. However, other recent work indicates that *in vivo* macrophage migration during embryonic development is MMP dependent in frog and zebrafish and also that macrophages from MT1-MMP-deficient mice have defective tissue infiltration capacity [39]. Therefore, it is rather difficult to conclude the specific role of proteases in macrophage migration.

Cell migration is also regulated by chemokines, a family of small cytokines or signaling proteins secreted by cells in response to signals such as proinflammatory cytokines, which play an important role in selectively recruiting monocytes, neutrophils, and lymphocytes toward the chemokine source. These chemokines act as intercellular messengers to control cell migration and activation of specific subsets of leukocytes. In addition, chemokines contribute to the regulation of gene expression in target cells and they also regulate cell proliferation and apoptosis. It has been described that the levels of these proteins are elevated in several inflammatory diseases. Although it is not clear whether excessive chemokine production might be the cause or the consequence of these diseases, it has been reported that neutralizing endogenous chemokines reduces symptoms in autoimmune diseases, chronic inflammation and cancer treatment (reviewed in [40]).

1.3.1. C1P and cell migration

Within the sphingolipid family, there are some sphingolipids that have been shown to behave as bioactive lipids. Some of the most important ones are considered to be phosphorylated species such as sphingosine 1-phosphate (S1P) and ceramide 1-

phosphate (C1P), which play an important role in intracellular signaling and in cell-to-cell communication [41, 42]. While most of the research work over the past decades has been focused on the role of S1P in trafficking and migration over several cell types, the role of C1P has been more recently discovered. Our group demonstrated the potent chemotactic effect of C1P in macrophages, an action that requires interaction of C1P with a Pertussis toxin (Ptx)-sensitive receptor [43]. Also, we established for the first time that C1P induces release of Monocyte Chemoattractant Protein-1 (MCP-1) in J774A.1 macrophages, human THP-1 monocytes and 3T3-L1 preadipocytes [44].

In this thesis, we wanted to examine whether C1P was able to conduct macrophage migration through MMP activation, actin polymerization and cytokine release, which are key events in cell migration.

2. RESULTS

2.1. C1P induces MMP-2 and MMP-9 protein expression and activity in J774A.1 macrophages.

In a previous work we had established that C1P can induce cell migration in macrophages through activation of a putative plasma membrane receptor [43]. It is also known that MMPs are the main enzymes involved in extracellular matrix remodeling, which plays an essential role in cell migration. Since C1P induces J774A.1 macrophage migration and the role of MMPs in this process is crucial, it was important to find whether C1P was able to induce MMP-2 and MMP-9 protein expression and activation in the macrophages.

To test the effect of C1P on MMP-2 and MMP-9, we incubated J774A.1 macrophages with C1P at 20 μM, which according to our previous work is the optimal concentration of C1P to induce cell migration in these cells [44]. We observed that C1P was able to induce MMP-2 and MMP-9 expression in a time-dependent manner, with a maximum effect at 24 hours and 8 hours, respectively (Figure 2.1.1).

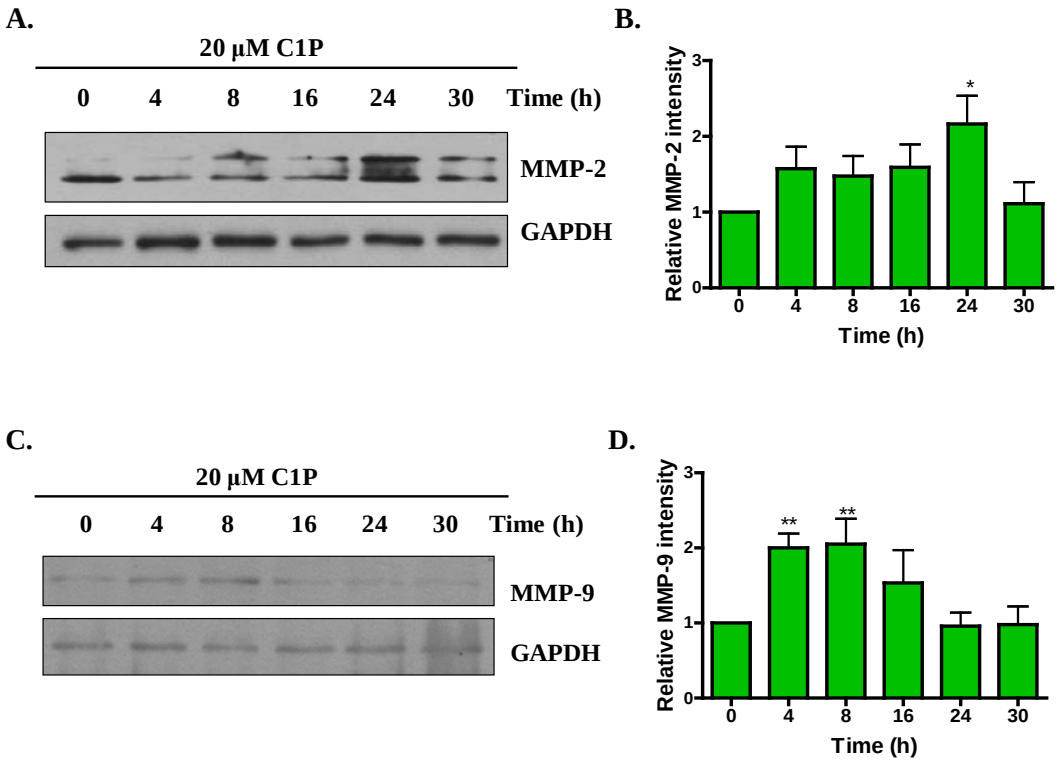

Figure 2.1.1 C1P induces MMP-2 and MMP-9 expression in J774A.1 macrophages. Cells were seeded in 60 mm dishes (2.5 x 10^5 cells/dish) and incubated overnight in DMEM supplemented with 10% FBS. The next day, the cells were washed with PBS and the medium was replaced with medium without serum. After 2 hours in medium without serum, 20 µM of C1P was added. Cells were then harvested at the indicated time points. **A.** MMP-2 was detected by Western blotting using specific antibody to MMP-2. Equal loading of protein was monitored using a specific antibody to GAPDH. Similar results were obtained in each of 4 replicate experiments. **B.** Results of scanning densitometry of the exposed film. Data are expressed as arbitrary units of intensity relative to control values and are the mean ± SEM of 4 independent experiments (*$p<0.05$). **C.** MMP-9 was detected by Western blotting using specific antibody to MMP-9 and equal loading of protein was monitored using a specific antibody to GAPDH. Similar results were obtained in each of 5 replicate experiments. **D.** Results of scanning densitometry of the exposed film. Data are expressed as arbitrary units of intensity relative to control values and are the mean ± SEM of 5 independent experiments (**$p<0.01$).

In addition to studying the possible role of C1P in MMP-2 and MMP-9 expression, we also wanted to test whether C1P induces MMP-2 and MMP-9 activation. For this, gelatin zymographic analyses were performed. These experiments revealed that C1P also induces MMP-2 and MMP-9 activation in a time-dependent manner with a maximum effect at 24 hours (Figure 2.1.2A and B). In order to ensure that these MMP activations were not just increments in their basal activity but rather activations caused by C1P, similar experiments with control samples and C1P-treated samples were carried

out. It was observed that C1P induced MMP-2 and MMP-9 activation (Figure 2.1.2 C and D).

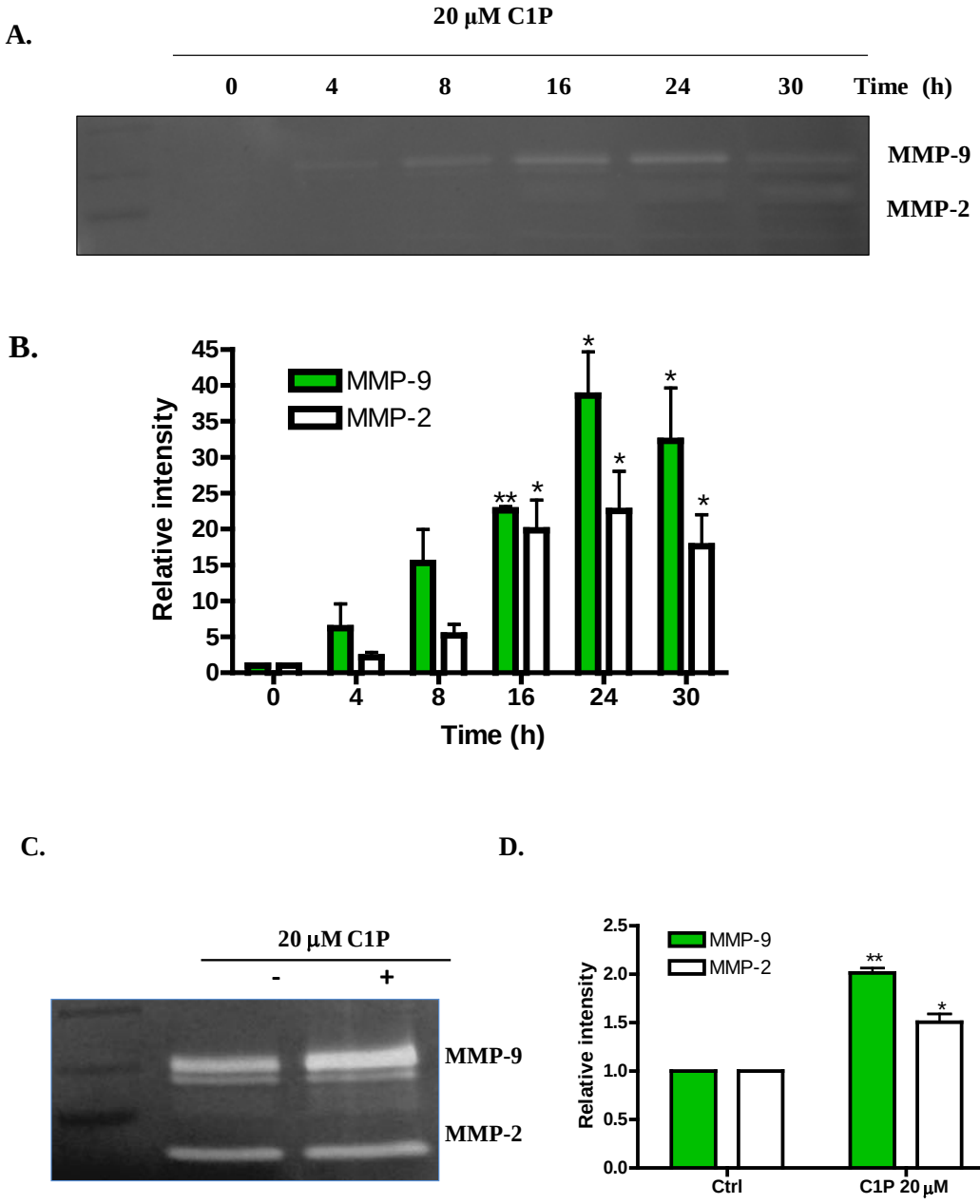

Figure 2.1.2. C1P induces MMP-2 and MMP-9 activity. A. Cells were seeded in 60 mm dishes (5 x 10^5 cells/dish) and incubated in DMEM supplemented with 10% FBS for 3-4 hours in order to allow cell attachment. Cells were then washed and serum-free DMEM was added. After 2 hours, 20 μM of C1P was added and the supernatant was collected and concentrated after the indicated time points. **A.** MMP-2 and MMP-9 activity was determined by gelatin zymography, as described in *Materials and Methods*. **B.** Results of scanning densitometry of the gel. Data are expressed as arbitrary units of intensity and are the mean ± SEM of 4 independent experiments (*p< 0.05,**p<0.01). **C.** Cells were incubated and treated as in A, except that cells were treated with vehicle or 20 μM of C1P for 24 hours. Then, MMP-2 and MMP-9 activities were determined by gelatin zymography. **D.** Results of scanning densitometry of the gel. Data

are expressed as arbitrary units of intensity and are the mean ± SEM of 3 independent experiments (*p< 0.05, ** p<0.01).

2.2. PI3K and ERK kinases are implicated in C1P-induced MMP-2 and MMP-9 activation.

Some of the best characterized pathways linked to cell motility functions are the Phosphoinositide 3-kinase (PI3K)/Protein kinase B (PKB) and the Mitogen activated protein kinase (MAPK)/Extracellular signal-regulated kinase (ERK) pathways [41-44]. To test if these pathways were involved in C1P-induced MMP-2 and MMP-9 activities we performed gelatin zymography assays using siRNA technology in order to silence the corresponding genes encoding these kinases.

We observed that silencing of PI3K and ERK in J774A.1 macrophages completely blocked C1P-induced gelatinase activity (Figure 2.2.1). These results suggest that both PI3K and ERK kinases are important downstream effectors of C1P, which promotes MMP-9 and MMP-2 activation.

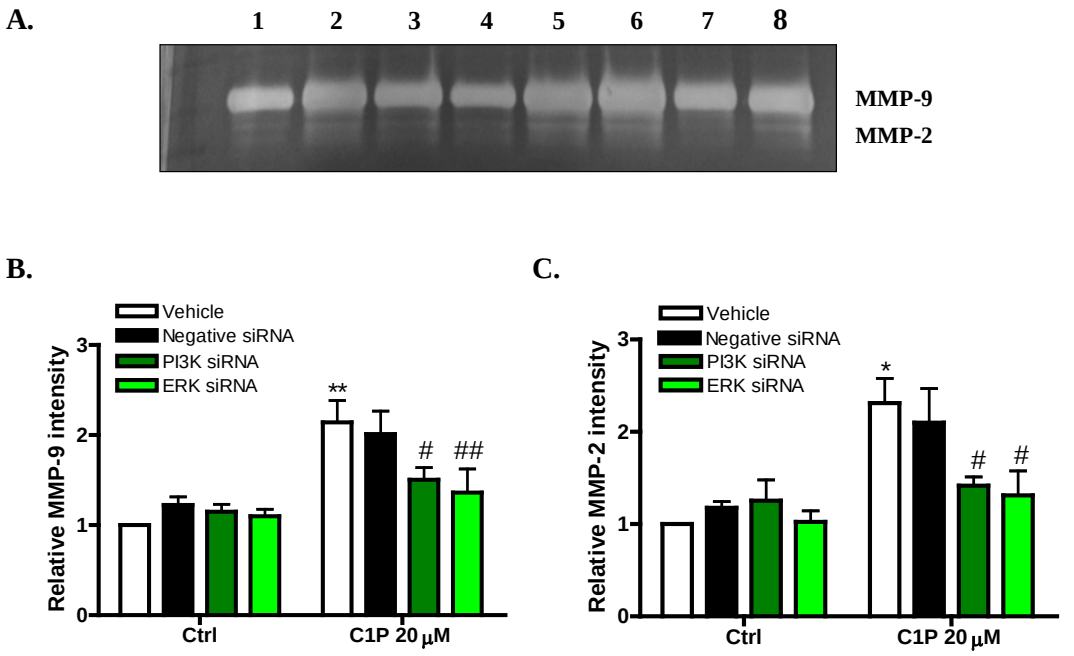

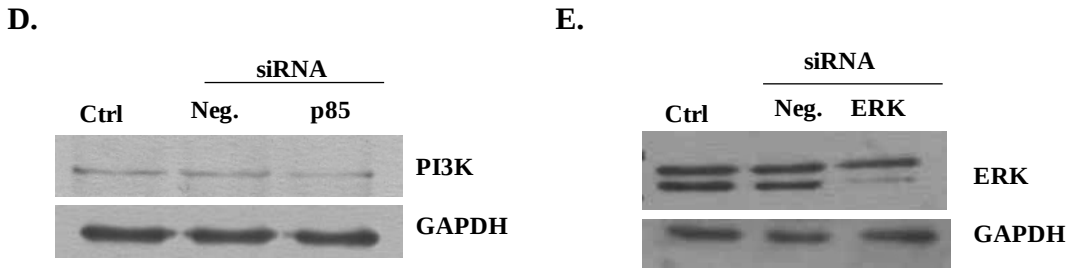

Figure 2.2.1. PI3K and ERK pathways are involved in C1P-induced MMP-2 and MMP-9 activation. Cells were seeded in 60 mm dishes (2 x 10^5 cells/dish) and treated with vehicle (open bars, line 1 and 5), negative siRNA (black bars, line 2 and 6), PI3K siRNA (dark green bars, line 3 and 7), or ERK siRNA (light green bars, line 4 and 8), as described in *Materials and Methods*. Cells were then scrapped and counted in order to be seeded in 60 mm dishes (5 x 10^5 cells/dish). Cells were further incubated for 3-4 hours in DMEM supplemented with 10% FBS in order to allow cell attachment. Cells were then washed and the medium was changed to serum-free DMEM. After 2 hours of incubation, the cells were further incubated with vehicle (1.- Ctrl, 2.- Negative siRNA, 3.- PI3K siRNA and 4.- ERK siRNA) or 20 μM of C1P (5.- C1P 20μM, 6.- C1P + negative siRNA, 7.- C1P + PI3K siRNA and 8.- C1P + ERK siRNA) for 24 hours. The culture medium was collected and concentrated. **A.** MMP-2 and MMP-9 activity was determined by gelatin zymography. **B**. Results of scanning densitometry of MMP-9 in the gel. Data are expressed as arbitrary units of intensity and are the mean ± SEM of 5 independent experiments (** $p< 0.01$, ## $p<0.01$, #$p<0.05$). **C.** Results of scanning densitometry of MMP-2 in the gel. Data are expressed as arbitrary units of intensity and are the mean ± SEM of 5 independent experiments (* $p< 0.05$, # $p< 0.05$). **D.** After treatment with PI3K siRNA, cells were collected and the PI3K siRNA inhibitory efficiency was confirmed by Western blotting using specific antibody to PI3K. Equal loading of protein was monitored using specific antibody to GAPDH. Similar results were obtained in each of 2 independent experiments. **E.** After treatment with ERK siRNA, cells were collected and the ERK siRNA inhibitory efficiency was confirmed by Western blotting using specific antibody to ERK. Equal loading of protein was monitored using a specific antibody to GAPDH. Similar results were obtained in each of 2 independent experiments.

As mentioned before, our group previously demonstrated that C1P stimulates cell migration through interaction with a putative specific C1P receptor which was found to be a Gi protein-coupled receptor (GPCR) [43]. To test if C1P-induced Akt and ERK phosphorylation is dependent on the activation of a GPCR, we used Pertussis toxin (Ptx), a widely used toxin secreted by *Bordetella pertussis*, which upon addition to eukaryotic cells causes inhibition of GPCRs on the cell surface. Therefore, all of the signaling pathways that are dependent on this kind of interaction will be consequently blocked. It was observed that C1P-stimulated Akt and ERK phosphorylation were highly sensitive to Ptx treatment (Figure 2.2.2).

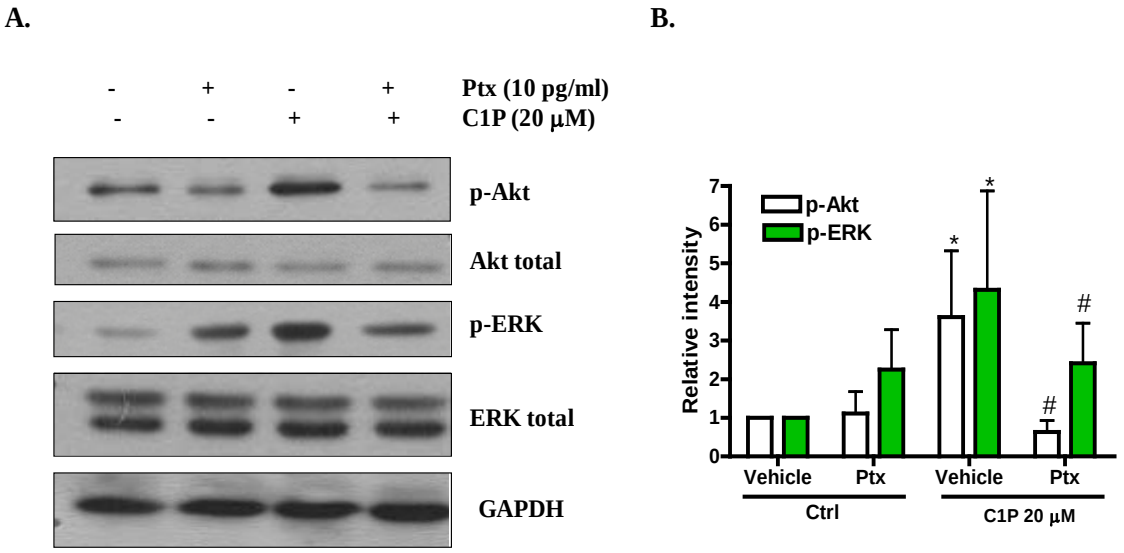

Figure 2.2.2. Pertussis toxin (Ptx) inhibits C1P-induced Akt and ERK phosphorylation in J774A.1 macrophages. Cells were seeded in 60 mm plates (2.5 x 10^5 cells/dish) and incubated overnight in DMEM supplemented with 10% FBS. Cells were then washed and the medium was replaced by serum-free DMEM. After 2 hours, cells were incubated with 10 pg/ml Ptx for 16 hours and then 20 μM of C1P or vehicle was added for 10 minutes. Cells were then harvested in lysis buffer and samples were analyzed by Western blotting. **A.** The presence of phosphorylated protein was detected using a specific antibody to each phosphorylated kinase, p-Akt and p-ERK, respectively. Equal loading of protein was monitored using specific antibody to total protein of each kinase and to GAPDH. **B**. Results of scanning densitometry of the exposed film. Data are expressed as arbitrary units of intensity and are the mean ± SEM of 3 independent experiments (*$p< 0.05$, # $p< 0.05$).

2.3. MMP-2 and MMP-9 gelatinases are implicated in C1P-induced macrophage migration.

Although in a previous work we had established that C1P induced cell migration in macrophages, the mechanisms involved in this process were poorly described. Considering that C1P stimulates MMP-2 and MMP-9 activities, we wanted to assess whether MMP-2 and MMP-9 would be implicated in C1P-induced cell migration. We performed cell migration assays using a selective MMP-2/9 inhibitor and, as shown in Figure 2.3.1, this inhibitor was able to reduce C1P-promoted cell migration potently.

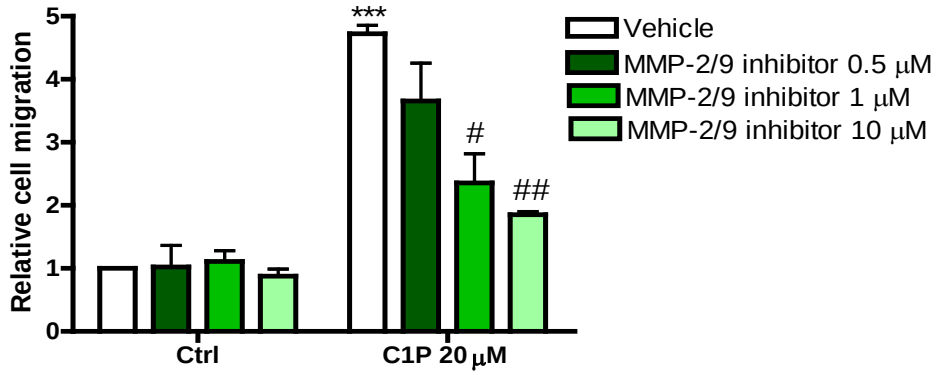

Figure 2.3.1. Inhibition of MMP-2 and MMP-9 almost completely blocks C1P-induced cell migration. Macrophage migration was measured using a Boyden chamber-based cell migration assay. Cells (5 x10^4 cells/well) were seeded in the upper wells of 24-well chambers coated with fibronectin, and pre-incubated for 1 hour with vehicle (open bars) or with either 0.5, 1 or 10 μM of MMP-2/9 inhibitor (filled bars). After 1 hour of incubation, either vehicle or 20 μM of C1P were added. Cells were further incubated for 24 hours and cell migration was determined as indicated in *Materials and Methods*. Data are expressed as the number of migrated cells relative to the number of cells migrated in the control chamber and are the mean ± SEM of 4 independent experiments performed in duplicate (***p>0.001, # p<0.05, ## p<0.01).

The implication of MMP-2 and MMP-9 on C1P-induced cell migration was also studied using siRNA in order to silence the corresponding genes encoding these enzymes. It was observed that silencing of MMP-2 and MMP-9 completely blocked C1P-induced macrophage migration (Figure 2.3.2).

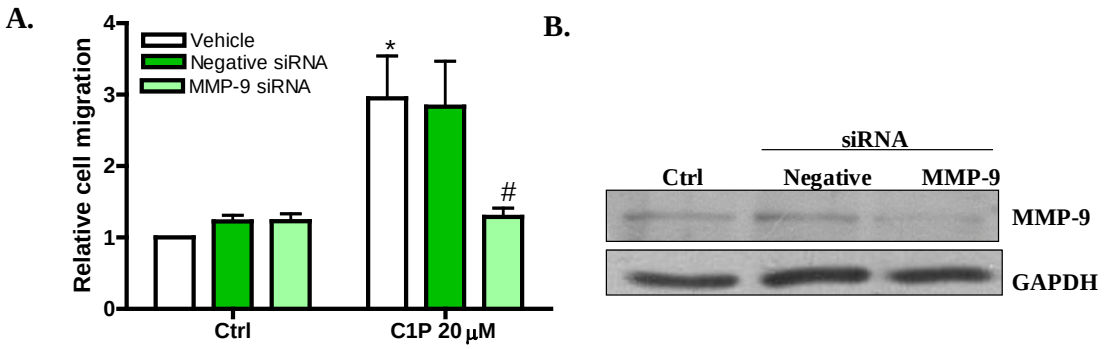

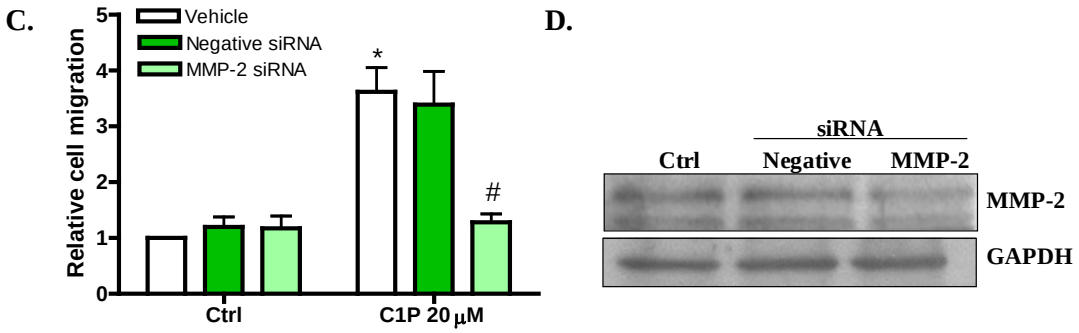

Figure 2.3.2. MMP-2 and MMP-9 siRNA inhibit C1P-stimulated cell migration in J774A.1 macrophages. Cells were seeded in 60 mm dishes (2 x 10^5 cells/dish) and siRNA treatment was performed as indicated in *Materials and Methods*. Cells were treated with MMP-9 siRNA (panel A and B) or MMP-2 siRNA (panel C and D) as well as with the negative siRNA or vehicle, as indicated. After treatment with siRNA, cells were incubated with fresh DMEM supplemented with 10% FBS for 24 hours. Cells were then scrapped and counted. **A.** Cells (5 x 10^4 cells/well) were seeded in the upper wells of 24-well chambers coated with fibronectin. After 1 hour of preincubation, either vehicle (control) or 20 μM of C1P were added in the lower chambers. Cells were then incubated for 24 hours and cell migration was determined as indicated in *Materials and Methods*. Data are expressed as the number of migrated cells relative to the number of cells migrated in the control chamber and are the mean ± SEM of 4 independent experiments performed in duplicate (* $p<0.05$, # $p<0.05$). **B.** MMP-9 siRNA inhibitory efficiency was confirmed by Western blotting using specific antibody to MMP-9. Equal loading of protein was monitored using a specific antibody to GAPDH. Similar results were obtained in each of 2 independent experiments. **C.** Cells (5 x 10^4 cells/well) were seeded in the upper wells of 24-well chambers coated with fibronectin. After 1 hour of preincubation, either vehicle (control) or 20 μM of C1P were added in the lower chambers. Cells were then incubated for 24 hours and cell migration was determined as indicated in *Materials and Methods*. Data are expressed as the number of migrated cells relative to the number of cells migrated in the control chamber and are the mean ± SEM of 3 independent experiments performed in duplicate (* $p<0.05$, # $p<0.05$). **D.** MMP-2 siRNA inhibitory efficiency was confirmed by Western blotting using specific antibody to MMP-2. Equal loading of protein was monitored using a specific antibody to GAPDH. Similar results were obtained in each of 2 independent experiments.

All these data suggest a different pathway for C1P to induce cell migration, in which the gelatinases MMP-2 and MMP-9 are the main enzymes involved and their activation is regulated by PI3K and ERK kinases.

2.4. Actin polymerization is implicated in C1P-induced macrophage migration

Due to their ability to degrade ECM, MMPs are important enzymes involved in cell migration. However, the ECM degradation mechanism by itself does not grant cell migration. Furthermore, cell migration is a complex process in which cell shape

undergoes morphological changes, mainly due to actin polymerization. Actin is a globular multi-functional protein that forms microfilaments. It is found in almost all eukaryotic cells and it can be present as either a free monomer called G-actin (globular) or as part of a linear polymer microfilament called F-actin (filamentous), both of which are essential for vital cellular functions, such as cell mobility or cell contraction processes during cell division.

Since actin polymerization is largely responsible for the dynamic nature of the cytoskeleton, we wanted to study whether the polymerization of cytoskeletal actin filaments was implicated in C1P-induced macrophage migration. Noteworthy, we observed that disturbances of actin cytoskeleton organization promoted by Cytochalasin D blocked C1P-induced macrophage migration (Figure 2.4.1).

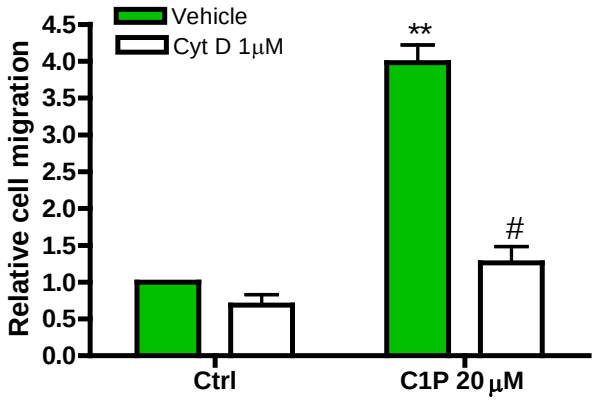

Figure 2.4.1. Cytochalasin D blocks C1P-induced macrophage migration. Macrophage migration was measured using a Boyden chamber-based cell migration assay. Cells (5 x 10^4 cells/well) were seeded in the upper wells of 24-well chambers coated with fibronectin, and pre-incubated for 1 hour with vehicle (filled bars) or with 1 μM of Cytochalasin D, an actin polymerization inhibitor (open bars). After 1 hour of incubation, either vehicle or 20 μM of C1P was added. Cells were further incubated for 24 hours and cell migration was measured as described in *Materials and Methods*. Results are expressed as the number of migrated cells relative to the number of cells migrated in the control chamber and are the mean ± SEM of 3 independent experiments performed in duplicate (** $p<0.01$, # $p<0.05$).

Due to the importance of actin polymerization in the process of cell migration, and taking into consideration that C1P-induced macrophage migration was blocked with a specific actin polymerization inhibitor, we next decided to study whether C1P was able to induce actin polymerization in J774A.1 macrophages. In order to visualize F-actin by flow cytometry we used Phalloidin, a class of toxins that belongs to the Phallotoxins

family. Due to their selective binding to F-actin, phalloidin-derived molecules containing fluorescent tags were used in our experiments to visualize actin filaments. As shown in Figure 2.4.2, we observed that C1P stimulates polymerization of cytoskeletal actin filaments. However, we found that C1P-induced actin polymerization was not MMP-2/9 dependent.

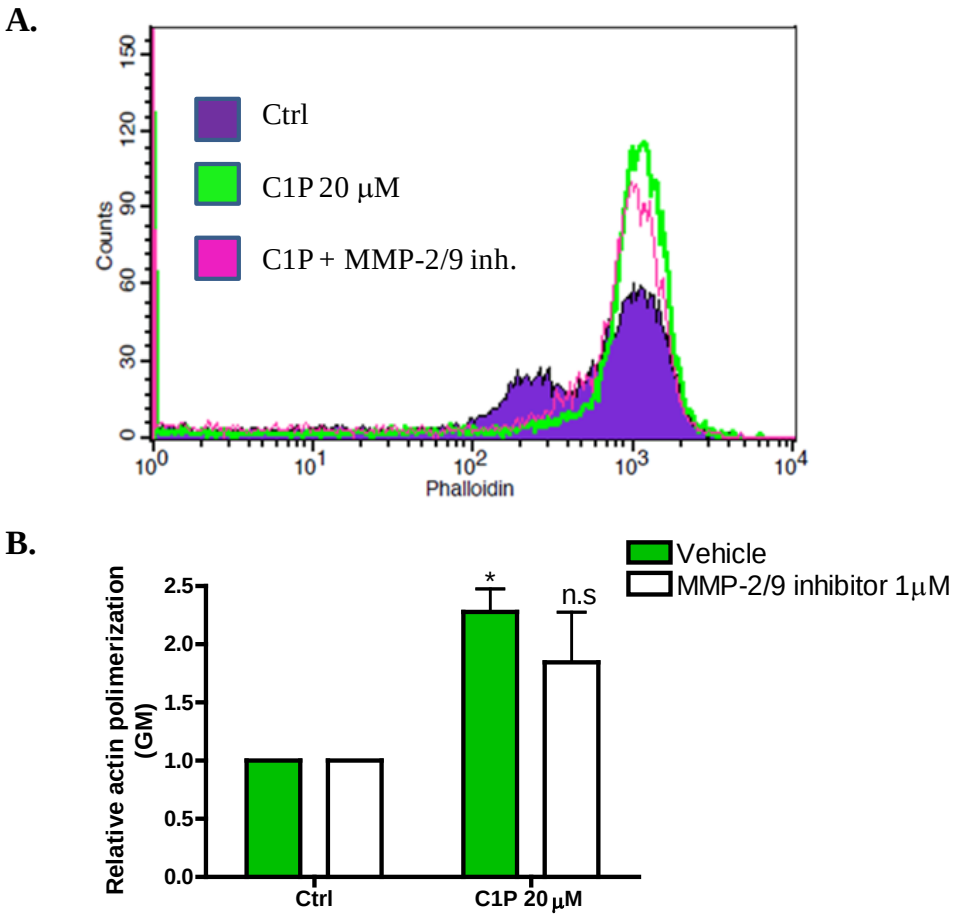

Figure 2.4.2. C1P induces actin polymerization in J774A.1 cells, an action that is not MMP-2/9 dependent. J774A.1 cells were seeded in 60 mm plates (2.5 x 10^5 cells/well) and incubated in DMEM containing 10% FBS, overnight. The medium was then changed to serum-free DMEM and further incubated for 2 hours. After 2 hours, cells were pretreated with vehicle or 1 μM of MMP-2/9 inhibitor for 30 minutes. After 30 minutes of preincubation, either vehicle or 20 μM of C1P were added to the cells. Cells were incubated for 24 hours and actin polymerization was determined as indicated in *Materials and Methods*. Samples were then analyzed by flow cytometry. **A.** A representative histogram obtained after the treatment with vehicle (solid purple area), 20 μM C1P (green line), or C1P 20 μM with 1 μM of MMP-2/ 9 inhibitor (pink line). Similar results were obtained in 3 independent experiments **B.** Results are expressed as the phalloidin- Alexa Flour 488 GeoMean of fluorescence intensity (GM) ± SEM of 3 independent experiments (*p< 0.05).

Since C1P-induced actin polymerization is not MMPs-dependent, we hypothetized that MMP-2 and MMP-9 might be downstream effectors of actin polymerization. To understand the role of actin polymerization on MMP-2 and MMP-9 expression in J774A.1 macrophages, we treated macrophages with Cytochalasin D, and we found that actin polymerization is required for C1P-stimulated MMP-2 and MMP-9 expression (Figure 2.4.3), suggesting that C1P induces actin polymerization before inducing MMP-2 and MMP-9 expression.

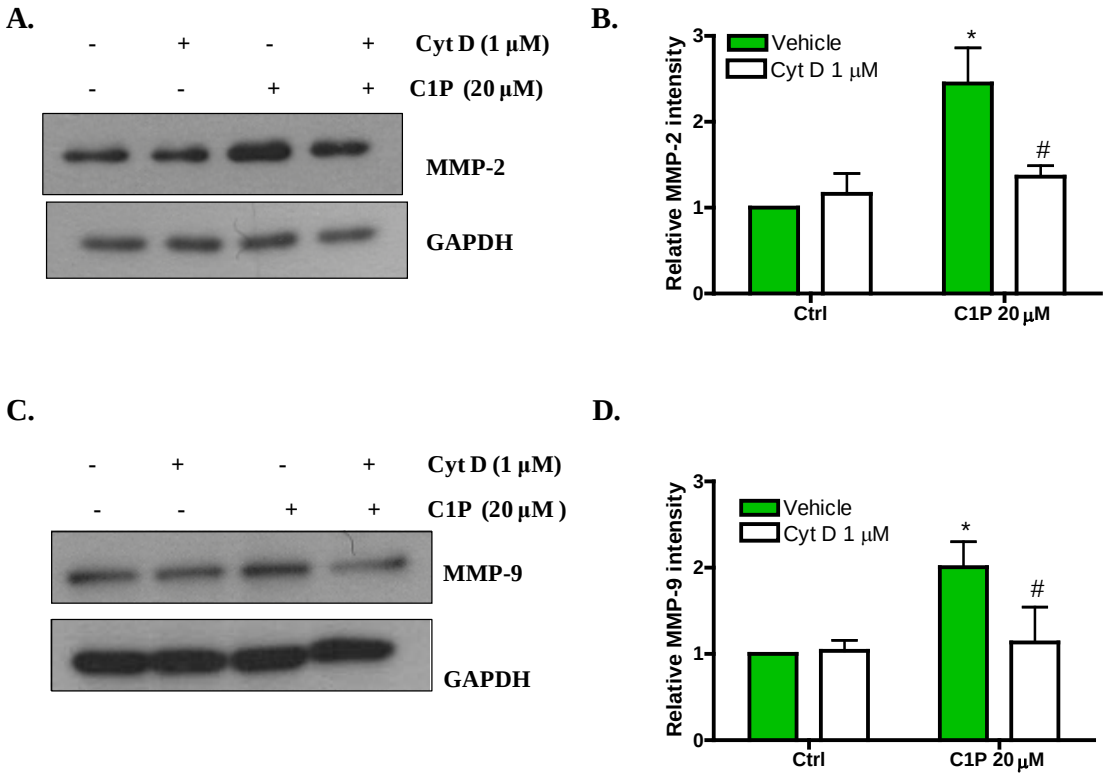

Figure 2.4.3. Cytochalasin D blocks C1P-induced MMP-2 and MMP-9 expression. Cells were seeded in 60 mm dishes (2.5 x 10^5 cells/dish) and incubated overnight in DMEM supplemented with 10% FBS. The next day, the cells were washed and the medium was replaced with medium without serum. After 2 hours, cells were incubated with either vehicle or 1 μM cytochalasin D for 30 minutes prior to 20 μM of C1P addition. **A.** After 24 hours of incubation with 20 μM of C1P, cells were harvested and the presence of MMP-2 protein was detected by Western blotting using specific antibody to MMP-2. Equal loading of protein was monitored using a specific antibody to GAPDH. **B.** Results of scanning densitometry of exposed film. Data are expressed as arbitrary units of intensity of the MMP-2 protein and are the mean ± SEM of 5 independent experiments (*p< 0.05, #p< 0.05). **C.** After 8 hours of incubation with 20 μM of C1P, cells were harvested and the presence of MMP-9 was detected by Western blotting using specific antibody to MMP-9 protein. Equal loading of protein was monitored using a specific antibody to GAPDH. **D.** Results of scanning densitometry of exposed film. Data are expressed as arbitrary units of intensity of the MMP-9 protein and are the mean ± SEM of 5 independent experiments (*< 0.05, #p< 0.05).

2.5. Paxillin is involved in C1P-induced actin polymerization in J774A.1 cells

Focal adhesions form a structural link between the ECM and the actin cytoskeleton, thus, they involve important signaling pathways in cell growth and migration. Their components, which are focal adhesion proteins, propagate cell signals that start with the activation of integrins. This is followed by the junction to ECM proteins, such as fibronectin, collagen and laminin. Importantly, focal adhesion proteins, including paxillin, bind to many proteins that are involved in promoting changes in the actin cytoskeleton organization, which are necessary for cell motility events.

Since, C1P induces actin polymerization, we hypothesized that paxillin could be involved in this action. Therefore, to investigate the signaling processes involved in C1P-induced actin polymerization, we initially examined the ability of C1P to induce paxillin phosphorylation. We found that C1P was able to induce paxillin phosphorylation in a time-dependent manner, with a maximum effect at 1 hour of incubation (Figure 2.5.1).

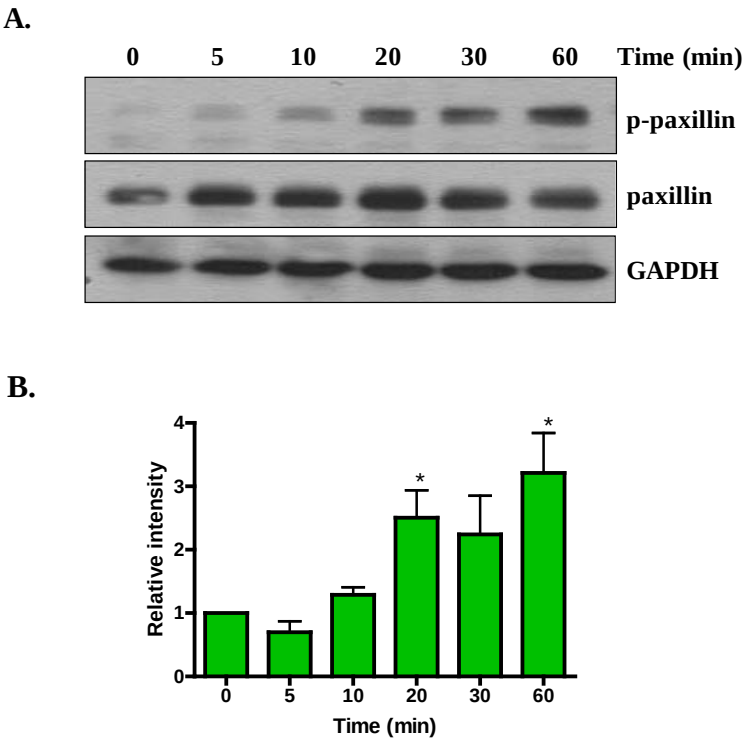

Figure 2.5.1. C1P induces paxillin phosphorylation. Cells were seeded in 60 mm dishes (2.5 x 10^5 cells/dish) and incubated overnight in DMEM supplemented with 10% FBS. The next day, cells were washed and serum-free DMEM was added. After 2 hours, 20 μM of C1P was added and cells were harvested at the indicated time points. **A**. The presence of p-paxillin protein was detected by Western blotting using specific antibody to phosphorylated paxillin. Equal loading of protein was monitored using specific antibody to GAPDH and total paxillin. **B.** Results of

scanning densitometry of exposed film. Data are expressed as arbitrary units of intensity of phosphorylated paxillin and are the mean ± SEM of 4 independent experiments (*p< 0.05).

To further demonstrate the implication of paxillin in C1P-induced actin polymerization, we performed siRNA experiments to block the expression of paxillin. After siRNA treatment, F-actin content was measured by flow cytometry. We found that paxillin silencing was able to inhibit C1P-induced actin polymerization in J774A.1 cells (Figure 2.5.2.), suggesting a possible role of paxillin in C1P-induced actin polymerization.

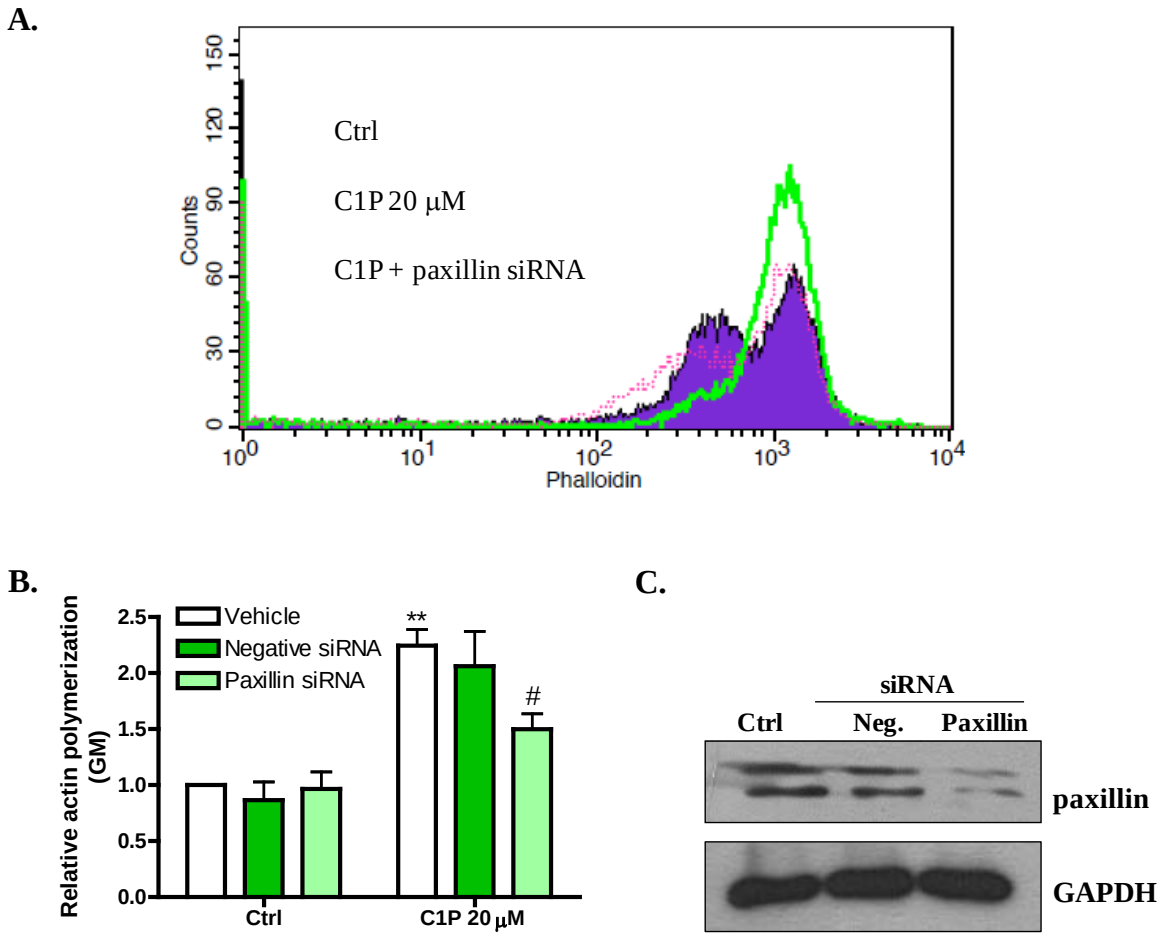

Figure 2.5.2. Paxillin is involved in C1P-induced actin polymerization. Cells were seeded in 60 mm dishes (2 x 10^5 cells/dish) and treated with vehicle, negative siRNA or paxillin siRNA, as described in *Materials and Methods*. Cells were then scrapped, counted and seeded in 60 mm dishes (2.5 x 10^5 cells/dish). The next day, cells were washed and the medium was changed to serum-free DMEM. After 2 hours of incubation, the cells were further incubated with vehicle or 20 µM of C1P for 24 hours. After 24 hours, cells were harvested and actin polymerization was measured, as described in *Materials and Methods* **A.** Representative histogram obtained after the treatment with vehicle (solid purple area), 20 µM of C1P (green line), or with 20 µM of C1P with paxillin siRNA (pink line) for 24 hours. Similar results were obtained in 5 independent experiments. **B.** Results of relative actin polymerization. Data are expressed as the phalloidin-

Alexa Flour 488 GeoMean of fluorescence intensity (GM) ± SEM of 5 independent experiments (#p< 0.05, **p<0.01). **C.** After siRNA treatment, cells were collected and the paxillin siRNA inhibitory efficiency was confirmed by Western blotting using specific antibody against paxillin. Equal loading of protein was monitored using a specific antibody to GAPDH. Similar results were obtained in each of 2 independent experiments.

To evaluate whether C1P induces paxillin phosphorylation through prior intreraction with its putative receptor, the macrophages were pre-treated with Ptx. We found that Ptx at a concentration as low as 10 pg/ml completely blocked C1P-induced paxillin phosphorylation (Figure 2.5.3). Therefore, it is quite possible that C1P action on paxillin phosphorylation requires the interaction of C1P with its Ptx-sensitive GPCR.

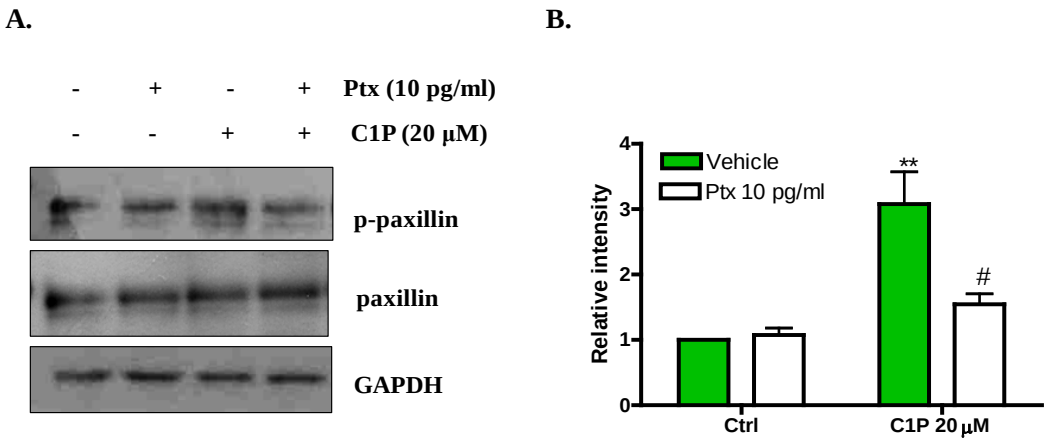

Figure 2.5.3. Pertussis toxin inhibits C1P-induced paxillin phosphorylation. Cells were seeded in 60 mm dishes (2.5 x 10^5 cells/dish) and incubated overnight in DMEM supplemented with 10% FBS. Cells were then treated with 10 pg/ml Ptx for 16 hours. After 16 hours, cells were treated with either vehicle or 20 μM of C1P for 1 hour. After 1 hour, cells were harvested. **A**. The presence of phosphorylated paxillin protein (p-paxillin) was detected by Western blotting using specific antibody to p-paxillin. Equal loading of protein was monitored using specific antibody to GAPDH and total paxillin. **B.** Results of scanning densitometry of exposed film. Data are expressed as arbitrary units of intensity of p-paxillin and are the mean ± SEM of 6 independent experiments (#p< 0.05, **p<0.01).

The next step was to investigate the signaling pathways involved in paxillin phosphorylation. Our group previously demonstrated the implication of MAPK in C1P-induced antiapoptotic, cell proliferation and cell migration effects in different cell types [44-46]. MEK1 and MEK2, also known as MAPKK or MAPK2, are important kinases that participate in this pathway. Once activated, they are able to stimulate ERK1/2

through direct phosphorylation of loop residues Thr202/Tyr204 and Thr185/Tyr187, respectively.

Since, paxillin is involved in C1P-induced actin polymerization, which is a key mechanism for the cell migration process, and C1P-induced cell migration is dependent on MAPK pathway, we hypothesized that paxillin may be a target protein of ERK. Therefore, to determine if this pathway is implicated in C1P-induced paxillin phosphorylation, siRNA technology was used to silence ERK1/2 protein expression. We found that ERK1/2 silencing caused a marked reduction in C1P-induced paxillin phosphorylation (Figure 2.5.4), suggesting that ERK1/2 are involved in this process.

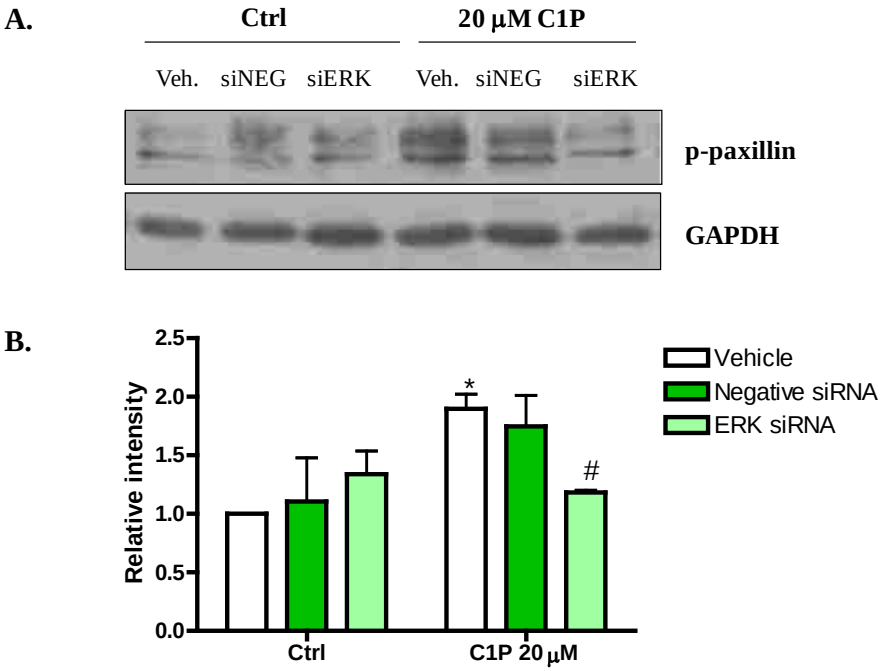

Figure 2.5.4. ERK is implicated in C1P-induced paxillin phosphorylation. Cells were seeded in 60 mm dishes (2 x 10^5 cells/dish) and the siRNA treatment was performed as indicated in *Materials and Methods*. Cells were treated with vehicle (open bars), negative siRNA (dark green bars) or ERK siRNA (light green bars). After treatment with siRNA, cells were incubated with fresh DMEM supplemented with 10% FBS for 24 hours. After 24 hours, cells were scrapped and counted. Cells were then seeded in 60 mm dishes (2.5 x 10^5cells/well) and incubated overnight in DMEM supplemented with 10% FBS. The next day, the medium was replaced with serum-free DMEM for 2 hours. After 2 hours, cells were treated with either vehicle or 20 μM of C1P for 1 hour. Cells were then harvested. **A.** The presence of p-paxillin protein was detected by Western blotting using specific antibody to phosphorylated paxillin. Equal loading of protein was monitored using specific antibody to GAPDH. **B.** Results of scanning densitometry of exposed film. Data are expressed as arbitrary units of intensity of phosphorylated paxillin and are the mean ± SEM of 3 independent experiments (*$p < 0.05$, #$p < 0.05$)**.**

Altogether, these data suggest that actin polymerization is a new important event implicated in C1P-induced MMP-2 and MMP-9 expression and, consequently in C1P-induced macrophage migration. In addition, paxillin, a focal adhesion protein which is a target protein for ERK kinase, plays a key role in this migration-associated signaling pathway.

2.6. C1P induces IL-1β release in J774A.1 macrophages.

We have previously reported that C1P is a potent chemoattractant agent for macrophages and that C1P exerts this action through interaction with a putative receptor for C1P [43]. Also, we established for the first time that C1P induces release of Monocyte Chemoattractant Protein-1 (MCP-1) in J774A.1 macrophages, human THP-1 monocytes and 3T3-L1 preadipocytes [44]. In addition to C1P, the production of MCP-1 can be induced in response to inflammatory cytokines, such as interleukin-1 (IL-1), IL-4, tumor necrosis factor (TNF-α), or interferon-γ.

Since cell migration and inflammation are closely related events in both pathological and physiological processes, and because of the importance of interleukin-1β (IL-1β) in inflammatory responses and immunity, it was important to know whether C1P was able to induce IL-1β release in macrophages. Therefore, we cultured J774A.1 macrophages in the presence or absence of C1P and measured IL-1β concentration in the culture medium after incubation with different C1P concentrations (Figure 2.6.1a) and after different incubation times (Figure 2.6.1b). We observed that C1P significantly stimulated IL-1β release in a concentration- and time-dependent manner.

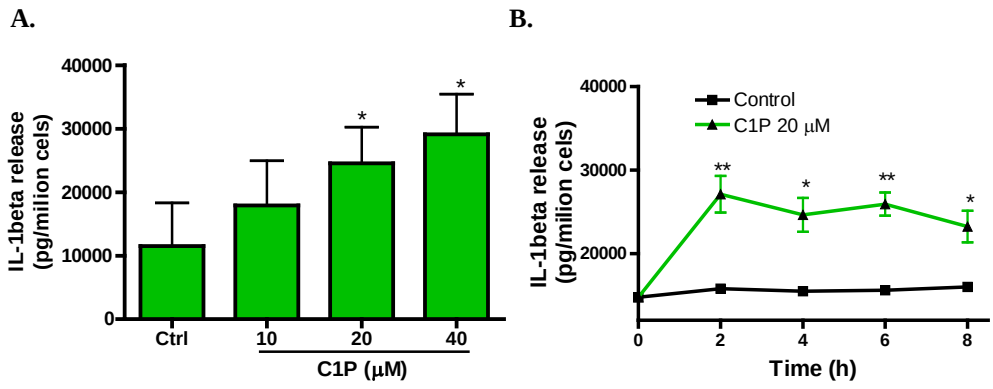

Figure 2.6.1. C1P induces IL-1β release in J774A.1 macrophages. Cells were seeded in 6-well plates (1.5 x 10^5 cells/dish) and incubated overnight in DMEM supplemented with 10% FBS. The next day, the cells were washed and the medium was replaced by serum-free DMEM for 2 hours. **A.** After 2 hours of incubation, cells were further incubated with the indicated

concentrations of C1P for 2 hours. Then, the medium was collected and centrifuged. IL-1β concentrations were measured using ELISA kits, as indicated in *Materials and Methods*. Results are normalized to total cell number and are the mean ± SEM of 3 independent experiments performed in duplicate (*p<0.05). **B**. After 2 hours, cells were incubated with 20 μM of C1P for the indicated time periods and the IL-1β concentration in the medium was determined. IL-1β values were normalized to the total cell number and the results are expressed as the mean ± SEM of 3 independent experiments (*p< 0.05, **p<0.01)**.**

2.7. ERK and PI3K are implicated in C1P-induced IL-1β release.

Some of the best characterized kinases linked to cell motility functions are PI3K and ERK. Both kinases can be activated by many different stimuli, including growth factors, cytokines, virus infection, ligands for heterotrimeric G protein-coupled receptors, transforming agents and carcinogens. The PI3K/PKB and MEK/ERK pathways have been described to lead to activation of transcription factors, such as nuclear factor kappa-light-chain-enhancer of activated B cells (NF-κB). NF-κB signaling plays an important role in inflammation. This transcription factor is present in cells in an inactive state and does not require new protein transcription to exert its action. Therefore, it participates in a variety of cell responses such as cell proliferation, protection of apoptosis, immune system regulation, inflammation and cell migration.

Although PI3K and ERK are some of the most important kinases related to inflammation, we wanted to study the possible implication of other signaling kinases and transcription factors in C1P-induced IL-1β release. To determine which signaling pathways are involved in this C1P-induced IL-1β release, we performed ELISA experiments using selective inhibitors for these kinases and transcription factors: PD98059 for the MEK1 protein, Ly294002 for PI3K, SP600125 for JNK, SB202190 for p38, and Stattic for STAT3. We observed that ERK and PI3K kinases were the only kinases implicated in C1P-induced IL-1β release (Figure 2.7.1).

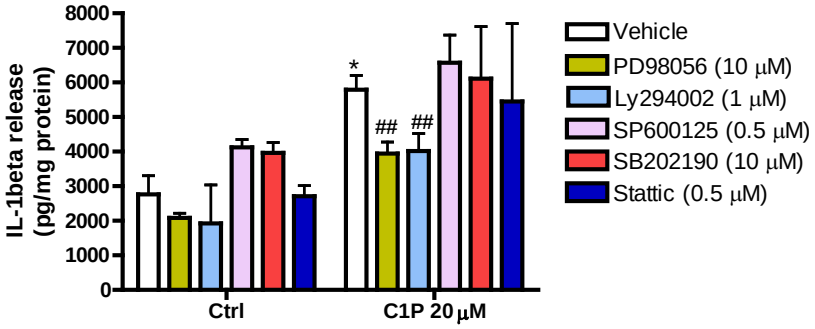

Figure 2.7.1. ERK and PI3K are implicated in C1P-induced IL-1β release. Cells were seeded in 6-well plates (1.5 x 10^5 cells/dish) and incubated overnight in DMEM supplemented with 10% FBS. The next day, the cells were washed and the medium was replaced by serum-free DMEM for 2 hours. After 2 hours of incubation, cells were pre-incubated with the indicated concentrations of inhibitor for 30 minutes before 20 μM C1P addition, and cells were further incubated for 2 hours. Then, the medium was collected and centrifuged. IL-1β concentrations were measured using an ELISA kit, as indicated in *Materials and Methods*. IL-1β values were normalized to the total protein amount and the results are expressed as the mean ± SEM of 4 independent experiments performed in duplicate (*p< 0.05, ##p<0.01)**.**

In order to confirm the results obtained with the pharmacological inhibitors PD98059 and Ly294002, siRNA technology experiments were performed to silence the corresponding genes encoding these kinases. We observed that silencing of ERK and PI3K significantly blocked C1P-induced IL-1β release (Figure 2.7.2).

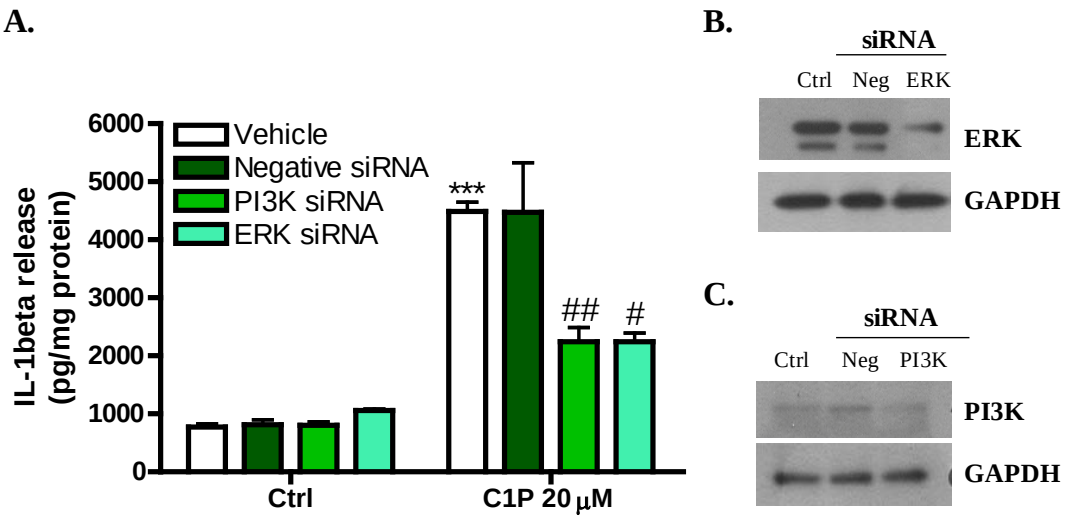

Figure 2.7.2. PI3K and ERK are implicated in C1P-induced IL-1β release in J774A.1 macrophages. Cells were seeded in 60 mm dishes (2 x 10^5 cells/dish) and the siRNA treatment was performed as indicated in *Materials and Methods*. Cells were then scrapped and counted in order to be seeded (1.5 x 10^5 cells/dish) in 6-well plates. The next day, cells were washed and the medium was replaced by serum-free DMEM. After 2 hours of incubation, cells were further incubated with or without 20 μM of C1P for 2 hours. **A.** The culture medium was collected and the IL-1β content was determined by ELISA, as described in *Materials and Methods*. IL-1β concentration was normalized to the total protein content and data are expressed as the mean ± SEM of 4 independent experiments performed in duplicate (***p<0.001, ##p<0.01, #p< 0.05)**.** **B**. After siRNA treatment, cells were collected and the ERK siRNA inhibitory efficiency was confirmed by Western blotting using specific antibody against ERK. Equal loading of protein was monitored using a specific antibody to GAPDH. Similar results were obtained in each of 2 independent experiments. **C**. After siRNA treatment, cells were collected and the PI3K siRNA inhibitory efficiency was confirmed by Western blotting using specific antibody against p85.

Equal loading of protein was monitored using a specific antibody to GAPDH. Similar results were obtained in each of 2 independent experiments.

In order to test the implication of IL1-β in C1P-induced cell migration, we performed migration experiments using siRNA technology to silence the corresponding gene encoding this cytokine. We found that silencing of IL-1β in J774A.1 macrophages does not block C1P-induced macrophage migration. These data suggest that IL-1β release is not required for C1P-induced cell migration (Figure 2.7.3).

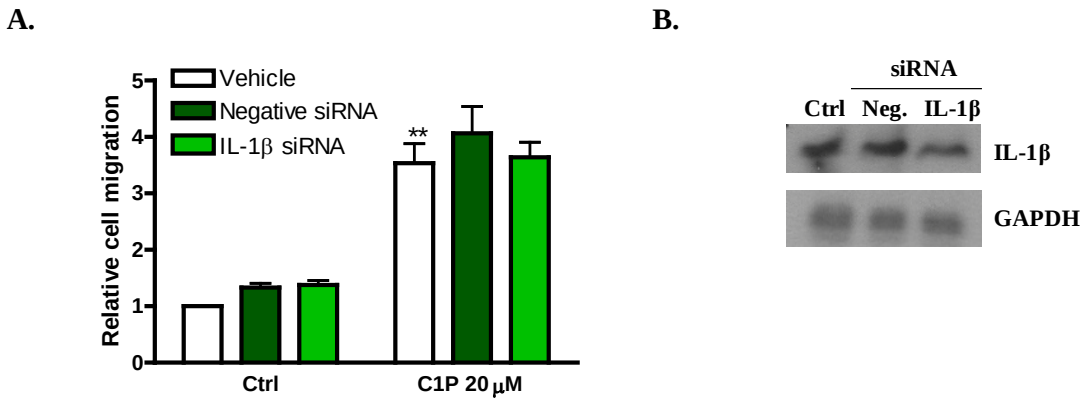

Figure 2.7.3. IL-1β siRNA does not block C1P-stimulated cell migration in J774A.1 cells. Cells were seeded in 60 mm dishes (2 x 10^5 cells/dish) and the siRNA treatment was performed as indicated in *Materials and Methods*. Cells were treated with IL-1β siRNA as well as with the negative siRNA and the vehicle. After treatment with siRNA, cells were incubated with fresh DMEM supplemented with 10% FBS for 24 h. Cells were then scrapped and counted. **A.** Cells (5 x 10^4 cells/well) were seeded in the upper wells of 24-well chambers coated with fibronectin. After 1 hour of preincubation, either vehicle or 20 μM of C1P were added in the lower chambers. Cells were then incubated for 24 h and cell migration was determined as described in *Materials and Methods*. Data are expressed as the number of migrated cells relative to the number of cells migrated in the control chamber and are the mean ± SEM of 4 independent experiments (**p<0.01). **B.** IL-1β siRNA inhibitory efficiency was confirmed by Western blotting using a specific antibody to IL-1β. Equal loading of protein was monitored using a specific antibody to GAPDH. Similar results were obtained in each of 2 independent experiments.

2.8. Lack of toxicity of the inhibitors used in this work

All commonly used chemical inhibitors in cell signaling studies have been described to be toxic for cells at certain concentrations or incubation times. To test if any of the above used inhibitors were toxic for the J774A.1 macrophages at the indicated times and concentrations we performed cell viability assays. We observed that none of these

pharmacological inhibitors caused a significant decrease in cell viability of macrophages (Figure 2.8.1). PD98059, Ly294002, SP600125, SB202190, and Stattic were previously tested and none of these inhibitors were toxic for J774A.1 cells. Fig. 2.8.1 shows that cytochalasin and the MMP-2/9 inhibitor were also not toxic at the concentrations and time points used in these studies.

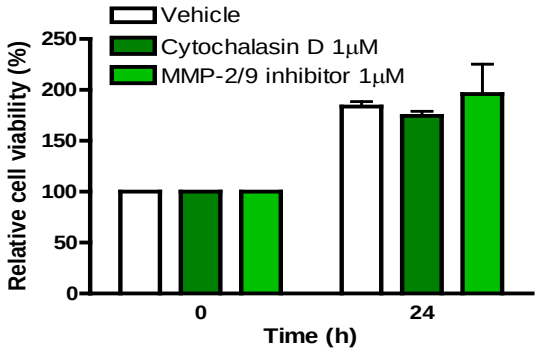

Figure 2.8.1. Cell viability after treatment with various chemical inhibitors. Cells were seeded in 96-well plates (5 x 10^3 cells/well) and incubated overnight in DMEM supplemented with 10% FBS. The next day, the cells were washed and the medium was replaced with medium without serum. After 2 hours of incubation, cells were treated with the chemical inhibitors at the indicated concentrations and cell viability was measured after 24 hours of incubation. Cell viability was determined using the MTS-formazan assay as indicated in *Materials and Methods.* Results are the mean ± SEM of 3 independent experiments performed in triplicate.

Altogether, these data demonstrate that C1P promotes MMP-2 and MMP-9 expression and activation as well as actin polymerization, which act as mediators of C1P-stimulated cell migration. Based on our data, paxillin is implicated in C1P-induced actin polymerization. Besides, actin polymerization is necessary for C1P to induce MMP-2 and MMP-9 expression, suggesting an interconection between actin polimerization and MMPs. In this connection, PI3K/Akt and MEK/ERK are important upstream effectors of these action, since after the blockade of both ERK and PI3K kinases, C1P-induced MMPs activity was attenuated and ERK inhibition also diminished paxillin phosphorylation. On the other hand, despite the fact that C1P induces IL-1β release, this cytokine is not implicated in C1P-induced J774A.1 macrophage migration.

3. DISCUSSION

Inflammation is a set of cellular and humoral reactions, which defends the organism from infection and tissue damage, leading ultimately to the restoration of functional and morphological integrity of affected tissues [47, 48]. Inflammation can be classified as either acute or chronic. Acute inflammation, can be defined as a physiological process generated by the body in response to injury, infection, or irritation, and is vital for the healing process. However, when this process becomes chronic it may contribute to a variety of diseases, including obesity or even cancer.

Cell migration is a key event in the inflammatory response and it requires strict coordination. Macrophages are one of the most important immune cells involved in this protective response due to their migratory ability. Moreover, these highly motile cells are able to migrate and enter various tissues under inflammatory and non-inflammatory conditions and assume different functions and phenotypes according to the cues they receive from the environment. In inflammatory diseases, such as obesity or cancer, immune cells need to remodel and degrade ECM in order to migrate from the blood vessels into the damaged tissue, where they activate and differentiate into mature macrophages. Once activated, macrophages actively secrete and cause an imbalance of cytokines, chemokines, and mediators of inflammation. Hence, macrophages play a critical role in the initiation, maintenance, and resolution of inflammation and mediate many inflammatory diseases, such as atherosclerosis [49], obesity [50] and cancer [51].

There are some bioactive lipids that can exert biological functions as signaling molecules. One of these bioactive sphingolipid is ceramide 1-phosphate (C1P), whose implication in the regulation of cell biology has extensively been studied by our group. C1P was described as a mitogenic and pro-survival agent capable of stimulating proliferation in different cell types, including fibroblasts, macrophages and myoblasts [45, 46, 52-55]. Also, our group has recently demonstrated that C1P can act as a chemoattractant molecule for J774A.1 macrophages. This effect required the interaction of C1P with a *Pertussis Toxin* (Ptx)- sensitive receptor [43].

Due to the importance of the cell migration process in physiological and pathological settings, its regulation needs to be further studied. Much evidence accumulated recently has established that cell-matrix and cell-cell interactions are also important in regulating this process. Interestingly, in the remodeling of the cell-matrix and cell-cell interactions,

matrix metalloproteinases (MMPs) play key regulatory roles. Previous reviews have focused on the physiological and pathological roles of MMPs in blood vessels [56, 57].

In this thesis we have shown that C1P is able to induce MMP-2 and MMP-9 expression in a time-dependent manner. In addition, gelatin zymography showed that MMP-9 and MMP-2 activity was induced by C1P. Moreover, experiments using MMP-2/MMP-9 selective inhibitor and siRNA to silence MMP-2 and MMP-9 demonstrated that these proteins take part in the signaling cascade that leads to C1P-induced macrophage migration. These results suggest that MMP-2 and MMP-9 play a key role in the activation of cell migration by C1P.

Migration of cells is shown to be influenced by ERK since inhibition of ERK by MEK inhibitor U0126 or PD98059 reduces cell migration in various cell types [58]. Also, PI3K/Akt/mTOR signaling axis has emerged as a pivotal node of many cell growth and proliferation processes [59-61]. Concerning signaling pathways, gelatin zymographic analysis of medium from the C1P-treated J774A.1 macrophages revealed that C1P-induced MMP-2 and MMP-9 activity requires the activation of ERK and PI3K, which are key kinases located in the Mitogen activated protein kinase (MAPK) pathway and the PI3K/Akt (PKB) pathway, respectively. Here, we found that gelatinases are downstream targets of ERK1/2 and PI3K, which are involved in C1P-induced macrophage migration.

The linkage of the actin cytoskeleton to extracellular matrix (ECM) through focal adhesion sites provides a physical path for cells to exert traction forces on substrates during cellular processes such as migration. Cell migration involves two processes: first, the contact with external (chemoattractants) cues, and second a controlled generation of mechanical forces that will lead to conspicuous deformation of the cell body. This second process relies on the protrusion of the leading edge of the cell, its adhesion to the underlying substratum, retraction of the rear and de-adhesion [28]. The advancing of the leading edge is driven by actin polymerization under the plasma membrane which supports extension of the plasma membrane in the form of lamellipodia and filopodia [62]. In this work, we found for the first time that C1P significantly increases actin polymerization in J774A.1 macrophages. Also, we demonstrated that disturbances of actin cytoskeleton organization induced by Cytochalasin D abolished C1P-induced macrophage migration. Moreover, alterations in the cytoskeletal architecture that are

reflected in some cell shape changes are well known to accompany modifications in the gene expression of different cell types: mammary epithelium cells, chondrocytes, adipocyte precursors, and cells from synovial tissues. Unemori and Werb reported that disruption of the actin cytoskeleton stimulated procollagenase and stromelysin secretion in rabbit synovial fibroblasts. These results led to the speculation that perturbation of the actin microfilaments might be linked to the expression of genes involved in the initiation of extracellular matrix degradation [63]. In the current study, we performed experiments to discover whether changes in cytoskeleton polymerization modulate the expression of MMPs in J774A.1 macrophages. We observed that treatment of the cells with Cytochalasin D, which causes disruption of actin stress fibers, resulted in loss of C1P-induced MMP-2 and MMP-9 expression. All these data suggest that alterations in the cytoskeleton and subsequent cell shape changes, such as actin polymerization, exert specific effects on the expression of MMP-2 (also known as gelatinase-A) and MMP-9 (also known as gelatinase –B), whose activation is crucial for C1P-induced macrophage migration. These results can be correlated with different works that have established a connection between actin polymerization and MMPs expression. These studies showed that MMP-9 was suppressed by an alteration in cell shape in melanoma cells [64] and that MMP-2 activation was regulated by the reorganization of the polymerized actin in human palmar fascial fibroblasts [65], which demonstrate that an alteration in cell shape influences MMP-9 as well as MMP-2 in different cell types.

We next evaluated the proteins involved in C1P-induced actin polymerization. Polymerization of actin filaments and their interaction with the plasma membrane is mediated, among others, by paxillin. Paxillin is an adaptor protein involved in multiple protein-protein interactions. These protein-protein interactions are important for protrusion of the leading edge and the formation/disassembly of focal adhesions in moving cells [66, 67]. Moreover, paxillin phosphorylation was found to be required for migration of rat bladder carcinoma NBT-II cells [66]. Therefore, we wanted to demonstrate whether this adhesion-protein was implicated in C1P-stimulated actin polymerization. We observed that C1P rapidly increases paxillin phosphorylation in a time-dependent manner. In addition, C1P-induced actin polymerization was decreased after silencing paxillin with specific siRNA, suggesting that paxillin plays a key role in C1P- induced actin polymerization, which is a key event on the cell migration process.

Concerning signaling pathways, our group previously demonstrated the ability of C1P to activate both Akt and ERK kinases in J774A.1 macrophages, minutes after the stimulation takes place [44]. Our studies revealed that this activation was blocked after Ptx-treatment, suggesting that C1P action on Akt and ERK phosphorylation requires the interaction of C1P with the Ptx-sensitive GPCR. In connection with these observations, we found that Ptx was able to decrease C1P-induced paxillin phosphorylation and furthermore, ERK inhibition also attenuated C1P-induced paxillin phosphorylation, suggesting that C1P-induced paxillin phosphorylation was regulated by ERK.

On the other hand, we also demonstrated the role of C1P in cytokine release since inflammation and cell migration are closely related processes. It is known that C1P induces MCP-1 release in J774A.1 cell line [44], which is a potent chemoattractant for macrophages. In this thesis we found that C1P is able to induce IL-1β release in J774A.1 macrophages in a time- and concentration-dependent manner. In addition, using selective inhibitors and siRNA technology to silence gene encoding different kinases, we established that PI3K and ERK are key regulators of C1P-induced IL-1β release. However, although IL-1β induces neutrophil migration [68], IL-1β was not required for C1P-induced J774A.1 macrophage migration, since the blockade of IL-1β with siRNA did not abolish C1P-induced macrophage migration. Therefore, it can be concluded that MCP-1, but not IL-1β, acts as chemoattractant for macrophages [44].

Overall, in this thesis we found for the first time that C1P was able to induce MMP-2 and MMP9 activation and actin polymerization in J774A.1 macrophages, two distinct processes which are interconnected and very closely implicated in cell migration process. In addition, C1P-induced actin polymerization was accompanied by paxillin phosphorylation, an important focal adhesion protein which facilitates actin cytoskeletal reorganization and therefore, takes part in cell migration process. On the other hand, C1P also stimulates IL-1β release, although this cytokine is not required for C1P-induced cell migration. Unlike MCP-1, IL-1β may not act as a chemoattractant for macrophages. Concerning signaling pathways, C1P-induced paxillin phosphorylation was ERK-dependent while C1P-induced MMPs activity was ERK- and PI3K-dependent, both of which are key kinases in cell motility. The scheme shown below emphasizes the new signaling pathways involved in C1P- stimulated migration.

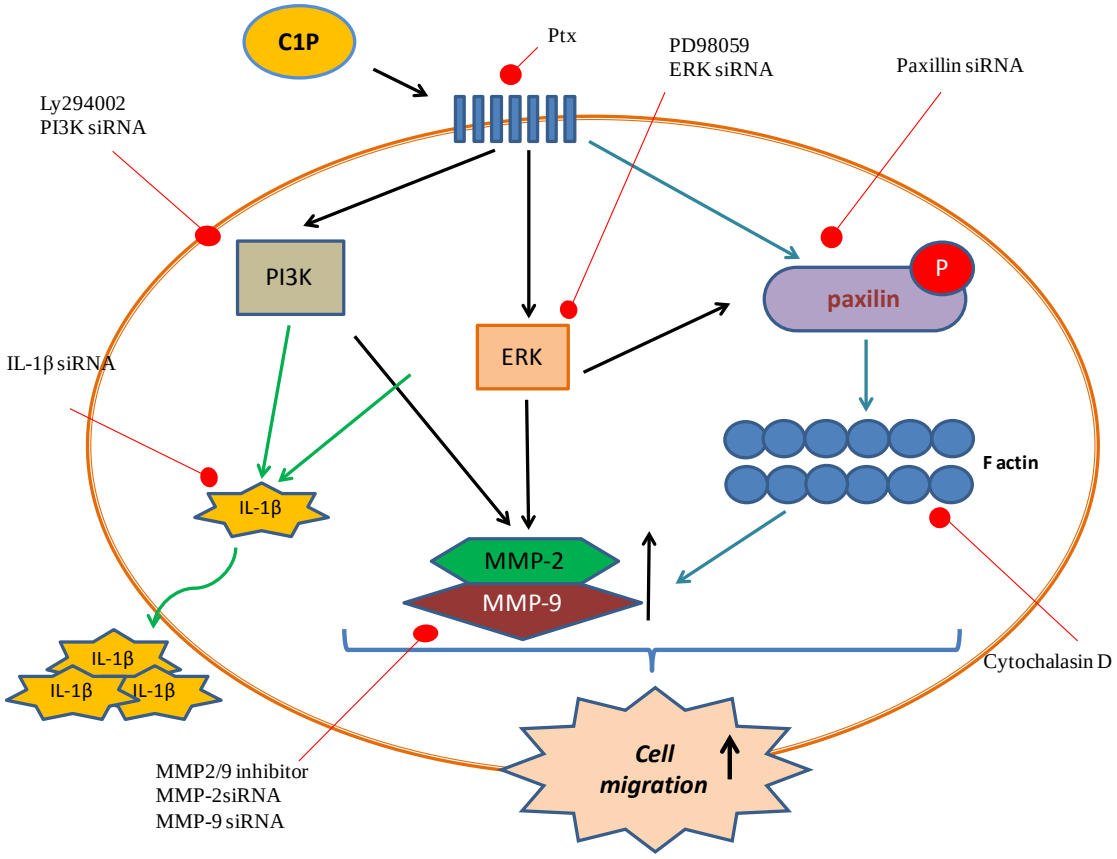

Figure 3.1. Working model for the implication of C1P in cell migration in J774A.1 macrophages.

4. REFERENCES

1. Lee, M.J., Y. Wu and S.K. Fried, *Adipose tissue remodeling in pathophysiology of obesity.* Curr Opin Clin Nutr Metab Care, 2010. **13**(4): p. 371-6.
2. Crandall, D.L., G.J. Hausman and J.G. Kral, *A review of the microcirculation of adipose tissue: anatomic, metabolic, and angiogenic perspectives.* Microcirculation, 1997. **4**(2): p. 211-32.
3. Hynes, R.O., *The extracellular matrix: not just pretty fibrils.* Science, 2009. **326**(5957): p. 1216-9.
4. Daley, W.P., S.B. Peters and M. Larsen, *Extracellular matrix dynamics in development and regenerative medicine.* J Cell Sci, 2008. **121**(Pt 3): p. 255-64.
5. Cawston, T.E. and D.A. Young, *Proteinases involved in matrix turnover during cartilage and bone breakdown.* Cell Tissue Res, 2010. **339**(1): p. 221-35.
6. Muschler, J. and C.H. Streuli, *Cell-matrix interactions in mammary gland development and breast cancer.* Cold Spring Harb Perspect Biol, 2010. **2**(10): p. a003202.
7. Jaiswal, A., A. Chhabra, U. Malhotra, S. Kohli and V. Rani, *Comparative analysis of human matrix metalloproteinases: Emerging therapeutic targets in diseases.* Bioinformation, 2011. **6**(1): p. 23-30.
8. Bourboulia, D. and W.G. Stetler-Stevenson, *Matrix metalloproteinases (MMPs) and tissue inhibitors of metalloproteinases (TIMPs): Positive and negative regulators in tumor cell adhesion.* Semin Cancer Biol, 2010. **20**(3): p. 161-8.
9. Amalinei, C., I.D. Caruntu and R.A. Balan, *Biology of metalloproteinases.* Rom J Morphol Embryol, 2007. **48**(4): p. 323-34.
10. Gomez, D.E., D.F. Alonso, H. Yoshiji and U.P. Thorgeirsson, *Tissue inhibitors of metalloproteinases: structure, regulation and biological functions.* Eur J Cell Biol, 1997. **74**(2): p. 111-22.
11. Even-Ram, S. and K.M. Yamada, *Cell migration in 3D matrix.* Curr Opin Cell Biol, 2005. **17**(5): p. 524-32.
12. Van Lint, P. and C. Libert, *Chemokine and cytokine processing by matrix metalloproteinases and its effect on leukocyte migration and inflammation.* J Leukoc Biol, 2007. **82**(6): p. 1375-81.
13. Vu, T.H. and Z. Werb, *Matrix metalloproteinases: effectors of development and normal physiology.* Genes Dev, 2000. **14**(17): p. 2123-33.
14. Catalan, V., J. Gomez-Ambrosi, A. Rodriguez, B. Ramirez, C. Silva, F. Rotellar, M.J. Gil, J.A. Cienfuegos, J. Salvador and G. Fruhbeck, *Increased adipose tissue expression of lipocalin-2 in obesity is related to inflammation and matrix metalloproteinase-2 and metalloproteinase-9 activities in humans.* J Mol Med (Berl), 2009. **87**(8): p. 803-13.
15. Unal, R., A. Yao-Borengasser, V. Varma, N. Rasouli, C. Labbate, P.A. Kern and G. Ranganathan, *Matrix metalloproteinase-9 is increased in obese subjects and decreases in response to pioglitazone.* J Clin Endocrinol Metab, 2010. **95**(6): p. 2993-3001.
16. de Meijer, V.E., D.Y. Sverdlov, H.D. Le, Y. Popov and M. Puder, *Tissue-specific differences in inflammatory infiltrate and matrix metalloproteinase expression in adipose tissue and liver of mice with diet-induced obesity.* Hepatol Res, 2012. **42**(6): p. 601-10.
17. Chavey, C., B. Mari, M.N. Monthouel, S. Bonnafous, P. Anglard, E. Van Obberghen and S. Tartare-Deckert, *Matrix metalloproteinases are differentially expressed in adipose tissue during obesity and modulate adipocyte differentiation.* J Biol Chem, 2003. **278**(14): p. 11888-96.
18. Scroyen, I., L. Cosemans and H.R. Lijnen, *Effect of tissue inhibitor of matrix metalloproteinases-1 on in vitro and in vivo adipocyte differentiation.* Thromb Res, 2009. **124**(5): p. 578-83.
19. Derosa, G., I. Ferrari, A. D'Angelo, C. Tinelli, S.A. Salvadeo, L. Ciccarelli, M.N. Piccinni, A. Gravina, F. Ramondetti, P. Maffioli and A.F. Cicero, *Matrix*

metalloproteinase-2 and -9 levels in obese patients. Endothelium, 2008. **15**(4): p. 219-24.
20. Yiangou, Y., P. Facer, P. Durrenberger, I.P. Chessell, A. Naylor, C. Bountra, R.R. Banati and P. Anand, *COX-2, CB2 and P2X7-immunoreactivities are increased in activated microglial cells/macrophages of multiple sclerosis and amyotrophic lateral sclerosis spinal cord.* BMC Neurol, 2006. **6**: p. 12.
21. Condeelis, J. and J.W. Pollard, *Macrophages: obligate partners for tumor cell migration, invasion, and metastasis.* Cell, 2006. **124**(2): p. 263-6.
22. Friedl, P. and B. Weigelin, *Interstitial leukocyte migration and immune function.* Nat Immunol, 2008. **9**(9): p. 960-9.
23. Wynn, T.A., A. Chawla and J.W. Pollard, *Macrophage biology in development, homeostasis and disease.* Nature, 2013. **496**(7446): p. 445-55.
24. Ley, K., C. Laudanna, M.I. Cybulsky and S. Nourshargh, *Getting to the site of inflammation: the leukocyte adhesion cascade updated.* Nat Rev Immunol, 2007. **7**(9): p. 678-89.
25. Butcher, E.C., *Leukocyte-endothelial cell recognition: three (or more) steps to specificity and diversity.* Cell, 1991. **67**(6): p. 1033-6.
26. Springer, T.A., *Traffic signals for lymphocyte recirculation and leukocyte emigration: the multistep paradigm.* Cell, 1994. **76**(2): p. 301-14.
27. Ulrich, F. and C.P. Heisenberg, *Trafficking and cell migration.* Traffic, 2009. **10**(7): p. 811-8.
28. Pollard, T.D. and G.G. Borisy, *Cellular motility driven by assembly and disassembly of actin filaments.* Cell, 2003. **112**(4): p. 453-65.
29. Yamaguchi, H. and J. Condeelis, *Regulation of the actin cytoskeleton in cancer cell migration and invasion.* Biochim Biophys Acta, 2007. **1773**(5): p. 642-52.
30. Cougoule, C., V. Le Cabec, R. Poincloux, T. Al Saati, J.L. Mege, G. Tabouret, C.A. Lowell, N. Laviolette-Malirat and I. Maridonneau-Parini, *Three-dimensional migration of macrophages requires Hck for podosome organization and extracellular matrix proteolysis.* Blood, 2010. **115**(7): p. 1444-52.
31. Van Goethem, E., R. Poincloux, F. Gauffre, I. Maridonneau-Parini and V. Le Cabec, *Matrix architecture dictates three-dimensional migration modes of human macrophages: differential involvement of proteases and podosome-like structures.* J Immunol, 2010. **184**(2): p. 1049-61.
32. Gimona, M., R. Buccione, S.A. Courtneidge and S. Linder, *Assembly and biological role of podosomes and invadopodia.* Curr Opin Cell Biol, 2008. **20**(2): p. 235-41.
33. Linder, S., C. Wiesner and M. Himmel, *Degrading devices: invadosomes in proteolytic cell invasion.* Annu Rev Cell Dev Biol, 2011. **27**: p. 185-211.
34. Van Goethem, E., R. Guiet, S. Balor, G.M. Charriere, R. Poincloux, A. Labrousse, I. Maridonneau-Parini and V. Le Cabec, *Macrophage podosomes go 3D.* Eur J Cell Biol, 2010. **90**(2-3): p. 224-36.
35. Linder, S., *The matrix corroded: podosomes and invadopodia in extracellular matrix degradation.* Trends Cell Biol, 2007. **17**(3): p. 107-17.
36. Gong, Y., E. Hart, A. Shchurin and J. Hoover-Plow, *Inflammatory macrophage migration requires MMP-9 activation by plasminogen in mice.* J Clin Invest, 2008. **118**(9): p. 3012-24.
37. Deguchi, J.O., E. Aikawa, P. Libby, J.R. Vachon, M. Inada, S.M. Krane, P. Whittaker and M. Aikawa, *Matrix metalloproteinase-13/collagenase-3 deletion promotes collagen accumulation and organization in mouse atherosclerotic plaques.* Circulation, 2005. **112**(17): p. 2708-15.
38. Schneider, F., G.K. Sukhova, M. Aikawa, J. Canner, N. Gerdes, S.M. Tang, G.P. Shi, S.S. Apte and P. Libby, *Matrix-metalloproteinase-14 deficiency in bone-marrow-derived cells promotes collagen accumulation in mouse atherosclerotic plaques.* Circulation, 2008. **117**(7): p. 931-9.
39. Sakamoto, T. and M. Seiki, *Cytoplasmic tail of MT1-MMP regulates macrophage motility independently from its protease activity.* Genes Cells, 2009. **14**(5): p. 617-26.

40. Galzi, J.L., M. Hachet-Haas, D. Bonnet, F. Daubeuf, S. Lecat, M. Hibert, J. Haiech and N. Frossard, *Neutralizing endogenous chemokines with small molecules. Principles and potential therapeutic applications.* Pharmacol Ther, 2010. **126**(1): p. 39-55.
41. Chalfant, C.E. and S. Spiegel, *Sphingosine 1-phosphate and ceramide 1-phosphate: expanding roles in cell signaling.* J Cell Sci, 2005. **118**(Pt 20): p. 4605-12.
42. Gomez-Munoz, A., P. Gangoiti, L. Arana, A. Ouro, I.G. Rivera, M. Ordonez and M. Trueba, *New insights on the role of ceramide 1-phosphate in inflammation.* Biochim Biophys Acta, 2013. **1831**(6): p. 1060-6.
43. Granado, M.H., P. Gangoiti, A. Ouro, L. Arana, M. Gonzalez, M. Trueba and A. Gomez-Munoz, *Ceramide 1-phosphate (C1P) promotes cell migration Involvement of a specific C1P receptor.* Cell Signal, 2009. **21**(3): p. 405-12.
44. Arana, L., M. Ordonez, A. Ouro, I.G. Rivera, P. Gangoiti, M. Trueba and A. Gomez-Munoz, *Ceramide 1-phosphate induces macrophage chemoattractant protein-1 release: involvement in ceramide 1-phosphate-stimulated cell migration.* Am J Physiol Endocrinol Metab, 2013. **304**(11): p. E1213-26.
45. Gangoiti, P., M.H. Granado, S.W. Wang, J.Y. Kong, U.P. Steinbrecher and A. Gomez-Munoz, *Ceramide 1-phosphate stimulates macrophage proliferation through activation of the PI3-kinase/PKB, JNK and ERK1/2 pathways.* Cell Signal, 2008. **20**(4): p. 726-36.
46. Arana, L., P. Gangoiti, A. Ouro, I.G. Rivera, M. Ordonez, M. Trueba, R.S. Lankalapalli, R. Bittman and A. Gomez-Munoz, *Generation of reactive oxygen species (ROS) is a key factor for stimulation of macrophage proliferation by ceramide 1-phosphate.* Exp Cell Res, 2012. **318**(4): p. 350-60.
47. Cildir, G., S.C. Akincilar and V. Tergaonkar, *Chronic adipose tissue inflammation: all immune cells on the stage.* Trends Mol Med, 2013. **19**(8): p. 487-500.
48. Lee, B.C. and J. Lee, *Cellular and molecular players in adipose tissue inflammation in the development of obesity-induced insulin resistance.* Biochim Biophys Acta, 2014. **1842**(3): p. 446-62.
49. Woollard, K.J. and F. Geissmann, *Monocytes in atherosclerosis: subsets and functions.* Nat Rev Cardiol, 2010. **7**(2): p. 77-86.
50. Subramanian, V. and A.W. Ferrante, Jr., *Obesity, inflammation, and macrophages.* Nestle Nutr Workshop Ser Pediatr Program, 2009. **63**: p. 151-9; discussion 159-62, 259-68.
51. Peranzoni, E., S. Zilio, I. Marigo, L. Dolcetti, P. Zanovello, S. Mandruzzato and V. Bronte, *Myeloid-derived suppressor cell heterogeneity and subset definition.* Curr Opin Immunol, 2010. **22**(2): p. 238-44.
52. Kim, T.J., Y.J. Kang, Y. Lim, H.W. Lee, K. Bae, Y.S. Lee, J.M. Yoo, H.S. Yoo and Y.P. Yun, *Ceramide 1-phosphate induces neointimal formation via cell proliferation and cell cycle progression upstream of ERK1/2 in vascular smooth muscle cells.* Exp Cell Res, 2011. **317**(14): p. 2041-51.
53. Gangoiti, P., C. Bernacchioni, C. Donati, F. Cencetti, A. Ouro, A. Gomez-Munoz and P. Bruni, *Ceramide 1-phosphate stimulates proliferation of C2C12 myoblasts.* Biochimie, 2012. **94**(3): p. 597-607.
54. Gomez-Munoz, A., P.A. Duffy, A. Martin, L. O'Brien, H.S. Byun, R. Bittman and D.N. Brindley, *Short-chain ceramide-1-phosphates are novel stimulators of DNA synthesis and cell division: antagonism by cell-permeable ceramides.* Mol Pharmacol, 1995. **47**(5): p. 833-9.
55. Gomez-Munoz, A., L.M. Frago, L. Alvarez and I. Varela-Nieto, *Stimulation of DNA synthesis by natural ceramide 1-phosphate.* Biochem J, 1997. **325 (Pt 2)**: p. 435-40.
56. Galis, Z.S. and J.J. Khatri, *Matrix metalloproteinases in vascular remodeling and atherogenesis: the good, the bad, and the ugly.* Circ Res, 2002. **90**(3): p. 251-62.
57. Newby, A.C., *Dual role of matrix metalloproteinases (matrixins) in intimal thickening and atherosclerotic plaque rupture.* Physiol Rev, 2005. **85**(1): p. 1-31.
58. Huang, C., K. Jacobson and M.D. Schaller, *MAP kinases and cell migration.* J Cell Sci, 2004. **117**(Pt 20): p. 4619-28.

59. Engelman, J.A., J. Luo and L.C. Cantley, *The evolution of phosphatidylinositol 3-kinases as regulators of growth and metabolism.* Nat Rev Genet, 2006. **7**(8): p. 606-19.
60. Dummler, B. and B.A. Hemmings, *Physiological roles of PKB/Akt isoforms in development and disease.* Biochem Soc Trans, 2007. **35**(Pt 2): p. 231-5.
61. Fayard, E., G. Xue, A. Parcellier, L. Bozulic and B.A. Hemmings, *Protein kinase B (PKB/Akt), a key mediator of the PI3K signaling pathway.* Curr Top Microbiol Immunol, 2010. **346**: p. 31-56.
62. Linder, S., K. Hufner, U. Wintergerst and M. Aepfelbacher, *Microtubule-dependent formation of podosomal adhesion structures in primary human macrophages.* J Cell Sci, 2000. **113 Pt 23**: p. 4165-76.
63. Unemori, E.N. and Z. Werb, *Reorganization of polymerized actin: a possible trigger for induction of procollagenase in fibroblasts cultured in and on collagen gels.* J Cell Biol, 1986. **103**(3): p. 1021-31.
64. MacDougall, J.R. and R.S. Kerbel, *Constitutive production of 92-kDa gelatinase B can be suppressed by alterations in cell shape.* Exp Cell Res, 1995. **218**(2): p. 508-15.
65. Tomasek, J.J., N.L. Halliday, D.L. Updike, J.S. Ahern-Moore, T.K. Vu, R.W. Liu and E.W. Howard, *Gelatinase A activation is regulated by the organization of the polymerized actin cytoskeleton.* J Biol Chem, 1997. **272**(11): p. 7482-7.
66. Petit, V., B. Boyer, D. Lentz, C.E. Turner, J.P. Thiery and A.M. Valles, *Phosphorylation of tyrosine residues 31 and 118 on paxillin regulates cell migration through an association with CRK in NBT-II cells.* J Cell Biol, 2000. **148**(5): p. 957-70.
67. Laukaitis, C.M., D.J. Webb, K. Donais and A.F. Horwitz, *Differential dynamics of alpha 5 integrin, paxillin, and alpha-actinin during formation and disassembly of adhesions in migrating cells.* J Cell Biol, 2001. **153**(7): p. 1427-40.
68. Faccioli, L.H., G.E. Souza, F.Q. Cunha, S. Poole and S.H. Ferreira, *Recombinant interleukin-1 and tumor necrosis factor induce neutrophil migration "in vivo" by indirect mechanisms.* Agents Actions, 1990. **30**(3-4): p. 344-9.

Chapter 2

5. CHAPTER 2: Implication of C1P and CERK in adipogenesis.

1. INTRODUCTION

1.1. Adipogenesis in obesity

The development of obesity is associated with extensive modifications in adipose tissue including adipogenesis, angiogenesis, and proteolysis of the extracellular matrix (ECM) [1]. In particular, adipogenesis is a highly controlled biological process that is divided in two different phases: the first stage is named “determination phase”, while the second stage is referred to as “terminal differentiation”. The determination phase leads undifferentiated cells to enter the adipogenic differentiation program becoming pre-adipocytes. Subsequently, after a phase of mitotic clonal expansion, which is a necessary step for the terminal adipocyte differentiation, preadipocytes differentiate and exhibit the phenotypical and molecular characteristics of mature adipocytes. They also acquire the machinery that is necessary for lipid transport and synthesis, insulin action and the secretion of adipocyte-specific proteins [2]. The aberrant increase in fat mass that is observed in obesity is due to a dysregulation of both phases of the differentiation process resulting in an increase in the number of adipocytes (hyperplasia) and/or adipocyte size (hypertrophy).

1.1.1. 3T3-L1 cell differentiation process

Two different kinds of *in vitro* experimental models, essential for the determination of the mechanisms involved in adipocyte proliferation, differentiation and adipokine secretion, are currently available: preadipocyte cell lines, which are already committed to the adipocyte lineage, and multipotent stem cell lines, that are able to transform into different cell lineages including adipose, bone and muscle lineages. Many of the findings on adipocytes and adipogenesis come from *in vitro* studies based on murine immortalized preadipocyte cell lines such as 3T3-L1 and 3T3-F442A, which are derived from disaggregated 17-19-day-old Swiss 3T3 mouse embryos.

Most available models of murine preadipocytes, once they reach confluence and thereby growth arrest, can be induced into a differentiation process using an adipogenic cocktail of inducers, which consists of insulin, dexamethasone, rosiglitazone and 3-isobutyl-1-methylxanthine (IBMX). Dexamethasone is a synthetic glucocorticoid (GC) agonist that is traditionally used to stimulate the GC receptor, whereas rosiglitazone is an insulin sensitizer that makes the cells more responsive to insulin. IBMX is a potent inhibitor of cyclic nucleotide phosphodiesterases that increases intracellular cAMP levels considerably [3]. These proadipogenic compounds initiate a series of events that regulate staging of the differentiation program. Immediately after induction of differentiation, cyclic AMP response element-binding protein (CREB) becomes phosphorylated and activates the expression of CCAAT/Enhancer Binding Protein beta (C/EBPβ). After that, C/EBPβ acquires DNA- binding activity as the preadipocytes reenter the cell cycle. Following a delay of 16–20 h after induction, preadipocytes synchronously reenter the cell cycle [3, 4] and undergo several rounds of postconfluent mitosis, referred to as mitotic clonal expansion (MCE). The cells then exit the cell cycle, lose their fibroblastic morphology, accumulate cytoplasmic triglyceride, and acquire the appearance and metabolic features of adipocytes [3]. Triglyceride accumulation is closely correlated with an increased rate of *de novo* lipogenesis and a coordinate rise in the expression of the enzymes of fatty acid and triacylglycerol biosynthesis [5, 6].

1.1.2. Transcriptional control of adipocyte outcome

The differentiation of preadipocytes into adipocytes is regulated by an elaborate network of transcription factors, which are responsible for the coordinated induction and silencing of more than 2000 genes related to the regulation of adipocyte in both morphology and physiology (Figure 1.1.2.1) [7]. The adipogenic cascade can be divided into at least two waves of transcription factors that drive the adipogenic program. The first stage of adipogenesis consists of the transient induction of C/EBP-β and C/EBP-δ, which can be stimulated *in vitro* by a hormonal differentiation cocktail [8]. C/EBP-β and C/EBP-δ begin to accumulate within 24 h of adipogenesis induction and the cells re-take the cell cycle and execute MCE synchronously [9] (Figure 1.1.2.1A). In the conversion from G1 to S stage, C/EBP-β is hyperphosphorylated and sequentially activated by glycogen synthase kinase-3β and mitogen-activated protein kinase

(MAPK). Then, both C/EBP-β and C/EBP-δ induce expression of PPARγ and C/EBPα, the key transcriptional regulators of adipocyte differentiation. PPARγ and C/EBPα initiate positive feedback to induce their own expression and also activate a large number of downstream target genes whose expression determines the adipocyte. By day 2 of the differentiation course, C/EBP-α protein is phosphorylated by the cyclin D3, inducing a proliferation inhibition effect on the cells, which allows to begin the final differentiation phase of adipogenesis [10] (Figure 1.1.2.1B). By day 8 after differentiation induction, more than 90% of the adipocytes are already mature.

In addition to PPARγ and C/EBPs, several other transcription factors are likely to play an important role in the molecular control of adipogenesis. These proteins include Kruppel-like factors (KLFs), cAMP response element binding protein (CREB), early growth response 2 (Krox20), and sterol regulatory element-binding protein 1c (SREBP-1c).

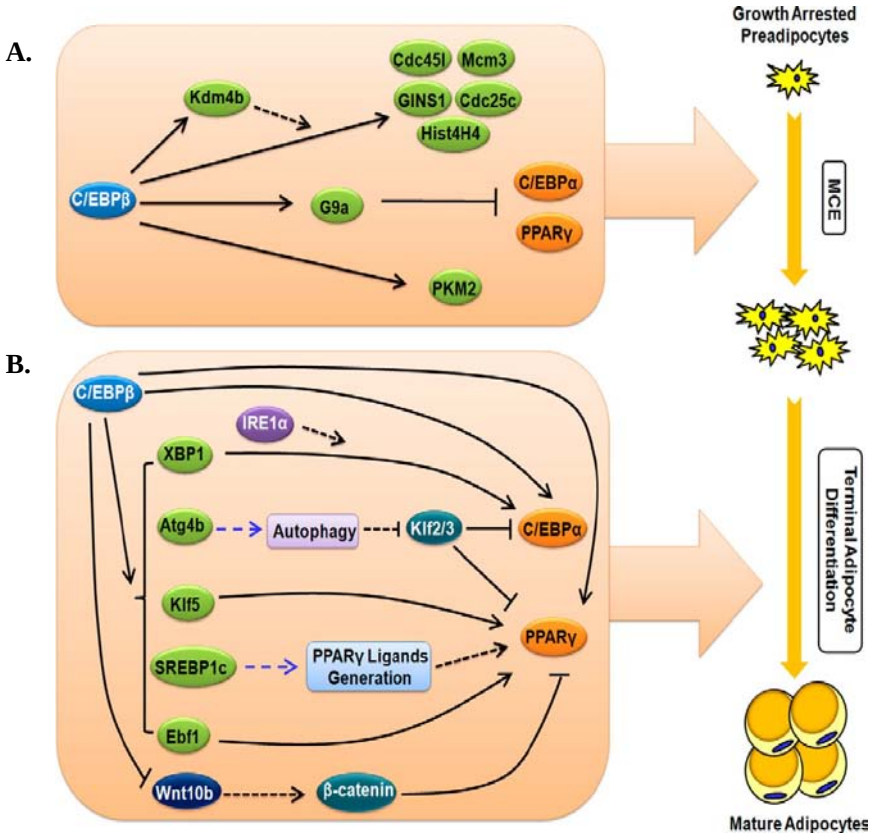

Figure 1.1.2.1. Transcriptional regulation of adipocyte differentiation. A. At the early stage of 3T3-L1 adipocyte differentiation, C/EBPβ transactivates the expression of multiple cell cycle-related genes to facilitate MCE, a required step for terminal differentiation. Moreover, C/EBPβ activates the expression of G9a, which delays the expression of C/EBPα and PPARγ, two anti-proliferation factors, so as to ensure MCE. In addition, C/EBPβ activates de expression

of some other transcriptional factors and inhibits the expression of Wnt10b, an anti-adipogenic factor. **B.** Together, these effects ultimately lead to the activation or up-regulation of C/EBP-α and PPARγ, thereby promoting terminal differentiation. Taken from [11].

1.1.3. MAPK signaling pathway in adipogenesis

The commitment of an undifferentiated cell to the adipogenic lineage requires the fine regulation of a complex network of transcription factors, cofactors, and signaling intermediates from numerous pathways [12, 13]. The mitogen-activated protein kinases (MAPKs) are a superfamily of serine/threonine kinases that regulate both cytoplasmic events and gene expression [14, 15] and they are involved in many cellular processes such as proliferation, differentiation, and stress response [16]. A primary role of the MAPKs in adipogenesis has been proposed [17, 18], although the significance of the involvement of these kinases is not clear. In fact, some authors suggest that MAPKs, in particular the extracellular signal-regulated kinases 1 and 2 (ERK1/2) are required in the proliferative phase of differentiation, and blockade of ERK activity in 3T3-L1 cells or in mice inhibited adipogenesis [17, 19, 20]. In addition, other works found that either in 3T3-L1 cells [21] or in other cellular models [22], ERK activity is necessary for the expression of the crucial adipogenic regulators C/EBPα, β and δ, and PPARγ. Conversely, other groups have proposed an inhibitory role for ERK1/2 in adipogenesis [23, 24]. It has been reported that ERK1 activity leads to activation of PPARγ in the terminal differentiation phase, which inhibits differentiation [18]. Therefore, the ERK pathway can display both positive and negative effects throughout adipogenesis.

1.2. Sphingolipids in obesity

The contribution of aberrant production of bioactive lipids to pathophysiological changes associated with obesity has risen to the forefront of lipid research. In particular, ceramide, a lipid signaling molecule, is not only involved in diverse cellular processes such as differentiation, cell proliferation and cell death [25-27], but also in the pathogenesis of a variety of diseases such as obesity, diabetes, and cardiovascular diseases including atherosclerosis [28-35]. It was demonstrated that ceramide and sphingosine inhibited insulin action and signaling in cultured cells [34] and that inhibition of ceramide synthesis using the specific serine palmitoyltransferase (SPT) inhibitor myriocin ameliorated obesity-induced insulin resistance [35]. Furthermore, ceramide and sphingosine levels of adipocytes during adipogenesis were decreased

compared to those of preadipocytes, while the number of lipid droplets and the triglyceride content, which are differentiation biomarkers, gradually increased [36]. These data are consistent with the observation of a significant decrease in both the sphingomielyn and ceramide levels in adipose tissue of obese mice compared with a lean mice [37]. Therefore, sphingolipid content in tissue undergoes dramatic alterations in metabolic diseases. Given the diverse signaling properties of sphingolipids, it can be considered that these lipids might mediate the pathology associated with metabolic disease.

Understanding the molecular mechanisms that regulate adipogenesis can be a crucial step for developing novel therapeutic strategies to control obesity and obesity-related pathologies. For this reason, the purpose of this study was to assess whether ceramide kinase (CERK) and ceramide 1-phosphate (C1P) might be able to regulate adipocyte cell differentiation.

2. RESULTS

2.1. Adipogenic induction medium (AIM) induces 3T3-L1 cell differentiation.

Due to their potential ability to differentiate from fibroblast to adipocytes, 3T3-L1 cells are widely used for studying adipogenesis and the biochemistry of adipocytes. Although it has been described that rosiglitazone, insulin, 3-isobutylmethylxanthine (IBMX), dexamethasone and FBS are potent prodifferentiative agents [38], we wanted to examine whether adipogenic induction medium (AIM), which is a medium consisting of DMEM 10% FBS and an adipogenic cocktail (0.5 mM IBMX, 1μg/ml insulin, 0.25 μM dexamethasone and 2μM Rosiglitazone) induces 3T3-L1 cell differentiation.

Induction of 3T3-L1 cell differentiation triggers deep phenotypical changes of preadipocytes that become spherical and filled with lipid droplets, displaying many morphological and biochemical characteristics of adipocytes differentiated *in vivo*. To confirm that adipogenesis was accompanied by a phenotypical change, we treated 3T3-L1 cells with AIM and then took some time-lapse micrographs of 3T3-L1 cells after AIM treatment. Oil Red O staining was used to visualize fat droplets within the

differentiated adipocytes, according to the methods described in a previous report [39]. As shown in Figure 2.1.1, AIM induces 3T3-L1 cell differentiation.

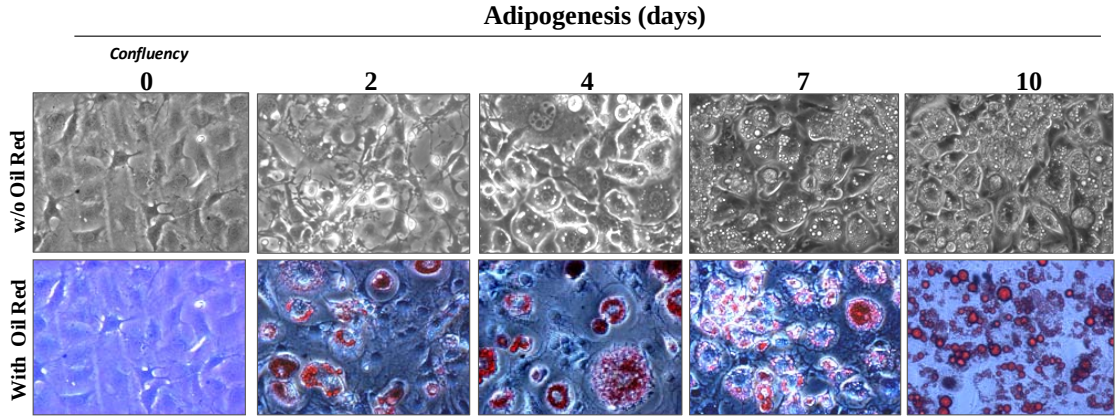

Figure 2.1.1. Adipogenic induction medium (AIM) promotes 3T3-L1 cell differentiation. 3T3-L1 cells were seeded in 6-well plates (1.2 x 10^5 cells/well) and they were grown in DMEM containing 10% NCS until they were about 90-100% confluent. Cells were further incubated for 2 days before inducing cell differentiation. After two days, cells were subjected to adipogenic induction media (AIM) in order to induce cell differentiation, as described in *Materials and Methods*. At the indicated time points, cells were treated with or without Oil Red and fat droplets were visualized with a Nikon Eclipse TS100 microscope at 20x magnification.

In addition to fat droplets, other adipogenic biomarkers were tested to confirm whether AIM induces differentiation in 3T3-L1 cells. It has already been described that during adipogenesis cells start gaining some adipogenic markers, including CCAAT-enhancer-binding protein beta (C/EBPβ) and peroxisome proliferator-activated receptor gamma (PPARγ). Therefore, we examined those adipogenic markers. We observed that AIM caused upregulation of both p-C/EBPβ and PPARγ expression in a time dependent manner. The maximum grade of expression was attained at 4th day for C/EBPβ and 7th day for PPARγ (Figure 2.1.2).

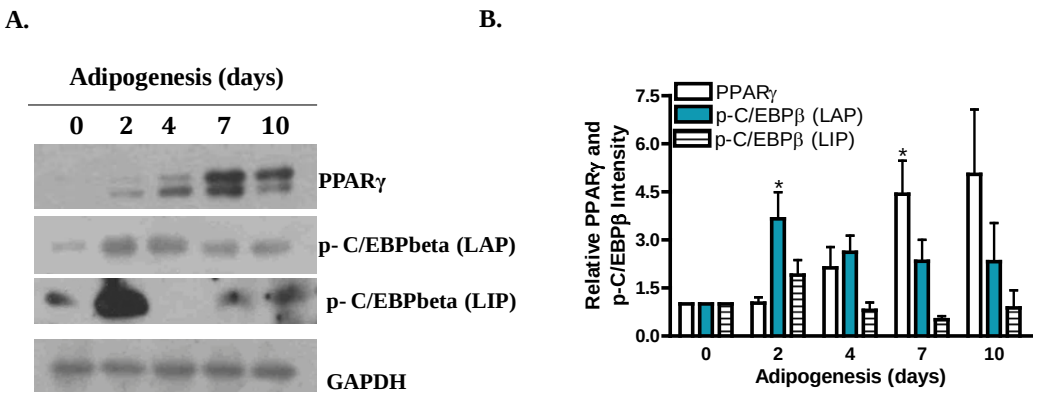

Figure 2.1.2 PPARγ expression and C/EBPβ phosphorylation increase during differentiation of 3T3-L1 cells. 3T3-L1 cells were seeded in 6-well plates (1.2 x 10^5 cells/well) and they were grown in DMEM containing 10% NCS until they were about 90-100% confluent. Confluent cells were further incubated for 2 days before induction of cell differentiation. After two days, cells were treated with adipogenic induction media (AIM) in order to induce cell differentiation, as described in *Materials and Methods.* Cells were then harvested after indicated periods of time. **A.** PPARγ and p-C/EBPβ were detected by Western blotting using specific antibodies and equal loading of protein was assessed with an antibody against GAPDH. Similar results were obtained in each of 3 replicate experiments. **B.** Results of scanning densitometry of the exposed film. Data are expressed as arbitrary units of intensity relative to control value and are the mean ± SEM of 3 independent experiments (*p<0.05).

2.2. CERK activity is required during 3T3-L1 cell differentiation process.

Sphingolipid metabolism has been previously described to be implicated in the pathogenesis of a variety of diseases including obesity, diabetes, and cardiovascular diseases [28-35]. Due to the importance of this group of lipids in obesity-associated diseases and taking into consideration that the ceramide content is decreased in differentiated 3T3-L1 adipocytes [36], we hypothesized that Ceramide Kinase (CERK), the enzyme that converts ceramide to ceramide 1-phosphate, might be implicated in this process. To address this question, we induced 3T3-L1 cell differentiation with AIM and CERK expression and activity were measured. As shown in Figure 2.2.1, CERK expression gradually increased during adipogenesis.

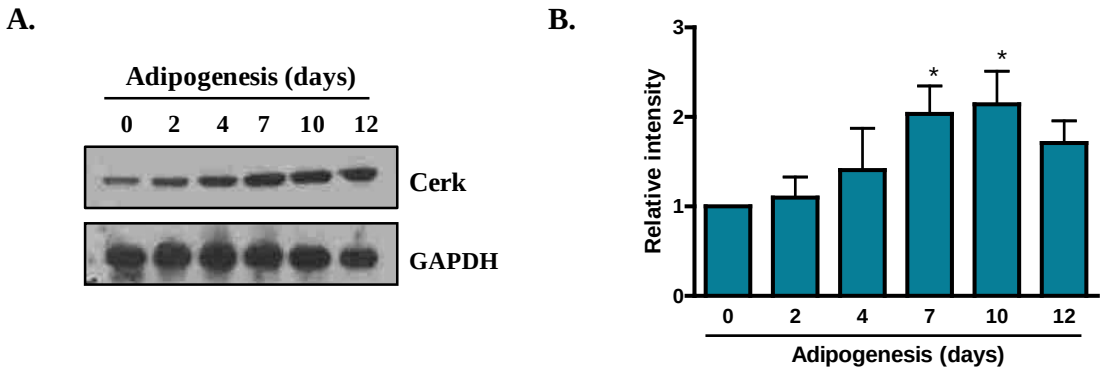

Figure 2.2.1. CERK expression increases during adipogenesis. 3T3-L1 cells were seeded in 6-well plates (1.2 x 10^5 cells/well) and they were grown in DMEM containing 10% NCS until they were about 90-100% confluent. Cells were then further incubated for 2 days before inducing cell differentiation. After two days, cells were cultured in AIM in order to induce cell differentiation, as described in *Materials and Methods.* **A.** Cells were then harvested at the indicated times after differentiation and prepared for Western blot analysis. CERK expression was detected by Western blotting using a specific antibody to CERK and equal loading of

protein was assessed with an antibody against GAPDH. Similar results were obtained in each of 4 replicate experiments. **B.** Results of the scanning densitometry of exposed film. Data are expressed as arbitrary units of intensity and are the mean ± SEM of 4 independent experiments (*p<0.05).

The implication of CERK in adipogenesis was also tested with a direct enzyme assay. We observed that CERK activity was higher in differentiated adipocytes, whereas preadipocytes showed less enzyme activity (Figure 2.2.2).

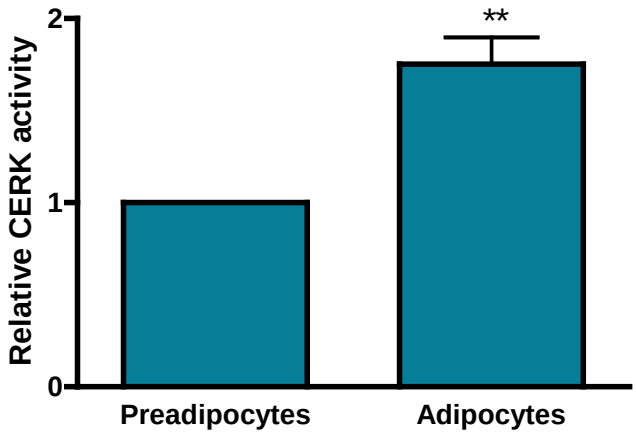

Figure 2.2.2. CERK activity is increased in differentiated 3T3-L1 adipocytes. 3T3-L1 cells were seeded in 6-well plates (1.2 x 10^5 cells/well) and they were grown in DMEM containing 10% NCS until they were about 90-100% confluent. Confluent cells were further incubated for 2 days before inducing cell differentiation. After two days, cells were cultured in either GM or AIM. GM-treated cells were maintained in DMEM 10% NCS whereas AIM-treated cells were induced to differentiation until day 10, as described in *Materials and Methods*. On day 10 after induction of differentiation, cells were harvested and CERK activity assay was performed as described in *Materials and Methods*. Data are expressed as the mean ± SEM of 5 independent experiments (**p<0.01).

To further confirm the implication of CERK in adipogenesis, siRNA technology was used in order to silence the gene encoding CERK. Undifferentiated 3T3-L1 cells were transfected with CERK siRNA by electroporation and after that, the differentiation process was induced. On day 4 of induction of differentiation, adipocyte differentiation was assessed by staining lipid droplets with Oil Red O, and the absorbance of extracted Oil Red O was quantified. As shown in Figure 2.2.3a, the more intense staining value was found in non-transfected cells (control), while the less intense staining value was found in CERK siRNA-treated cells. In addition, a TG assay kit was used to quantify triglyceride content and we found that CERK silencing caused a marked reduction in

TG concentration in differentiated cells (Figure 2.2.3b). These data suggest that CERK is involved in 3T3-L1 cell differentiation.

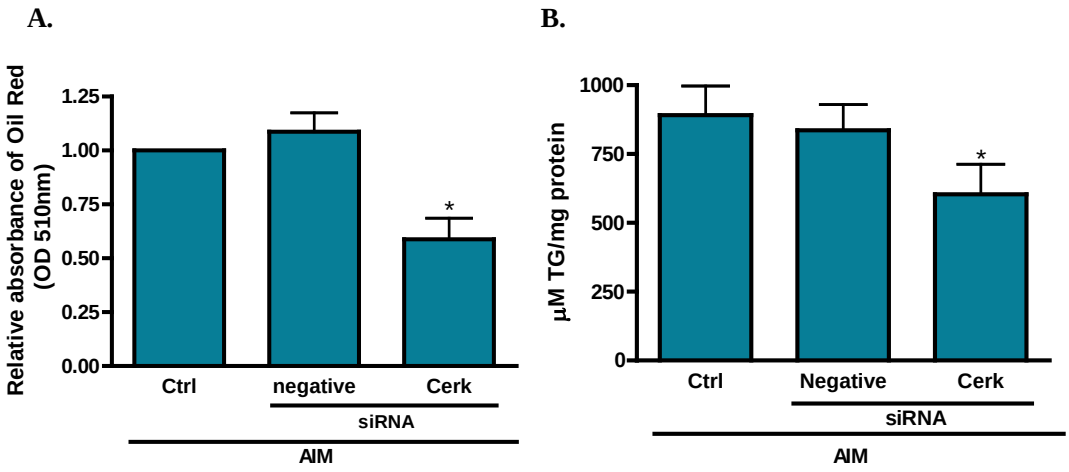

Figure 2.2.3. CERK siRNA inhibits 3T3-L1 cell differentiation. 3T3-L1 cells were seeded in 100 mm diameter dishes (5 x 10^5 cells/plate) in DMEM containing 10% NCS until they were confluent. 48h after confluence, medium was removed and cells were washed with sterile PBS and 500µl trypsin-EDTA was added in order to detach cells. Cells were then electroporated as described in *Materials and Methods*. **A.** Electroporated cells were seeded in confluence (1,2 x 10^5 cells/well) in 24-well plate and differentiated until day 4. On day 4 after induction of differentiation, cells were stained with Oil Red O, as indicated in *Materials and Methods*. Lipid droplets were quantified by measuring absorbance of each well. Absorbance of empty wells (without cells) was subtracted to the rest of values. Data are expressed as the mean ± SEM of 5 independent experiments (*$p<0.05$). **B.** Electroporated cells were seeded in confluence (2 x 10^4 cells/well) in 96-well plate and differentiated until day 4. On day 4, TG amount was measured using TG assay as described in *Materials and Methods.* Results are normalized to the protein concentration and are the mean ± SEM of 4 independent experiments performed in triplicate (*$p<0.05$).

To demonstrate the knock-down ability of specific CERK siRNA, we tested CERK expression and found that it was efficiently silenced by CERK siRNA (Figure 2.2.4).

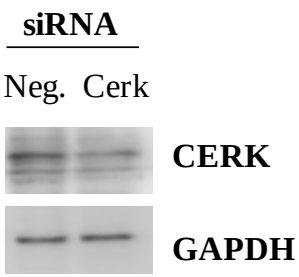

Figure 2.2.4. CERK siRNA efficiently silences CERK protein expression in 3T3-L1 cells. Cells were seeded in 60 mm dishes and electroporated with CERK siRNA, as described in *Materials and Methods*. Electroporated cells were seeded in confluence (5 x 10^5 cells/well) in 6-well plate and differentiated until day 4. On day 4 after induction of differentiation, cells were harvested and CERK expression was detected by Western blotting using specific antibody to CERK. Equal loading of protein was assessed with an antibody against GAPDH. Similar results were obtained in other 2 experiments.

It has been demonstrated that ceramide concentration in differentiated adipocytes is decreased during adipogenesis, whereas the ceramide content is increased in non-differentiated preadipocytes [36]. Consistent with this observation, we found that CERK activation is a key event in adipocyte differentiation, which leads to an increase of intracellular C1P levels, and subsequently decrease of ceramide amount. To further study the implication of the CERK/C1P axis in adipogenesis, we wanted to examine whether extracellular C1P was involved in this process.

2.3. Exogenous ceramide 1-phosphate (C1P) decreases adipogenesis.

To examine the effects of exogenous C1P on adipocyte differentiation, confluent 3T3-L1 cells were grown in growth medium (GM) or in AIM for 10 days, both in the absence or in the presence of different concentrations of C1P.

As mentioned above, one of the main features of adipogenesis is the lipid accumulation inside the cell. Since morphological changes notably illustrate the consequences of all these internal modifications induced by AIM, some micrographs of cells were taken in the presence or absence of C1P in the 10^{th} day after inducing the differentiation process, with or without Oil Red staining, which was used to detect intracellular lipid droplets. We observed that cells grown in GM did not accumulate lipid droplets. By contrast, cells exposed to AIM accumulated lipid droplets. Surprisingly, C1P significantly decreased the formation of lipid droplets, in a dose-dependent manner (Figure 2.3.1a). In addition to micrographs, the Oil Red O dye that cells incorporated was also quantified every 2-3 days. As shown in Figure 2.3.1b, after treatment with 20 μM of C1P, the absorbance of Oil Red decreased, meaning that less lipid droplets were detected inside those cells. However, cells that were differentiated in the absence of C1P showed much more lipid accumulation. Therefore, it seems that exogenous C1P

decreases cell differentiation, at 20 μM of C1P (Figure 2.3.1), a concentration that is within physiological levels, at least in mice [40].

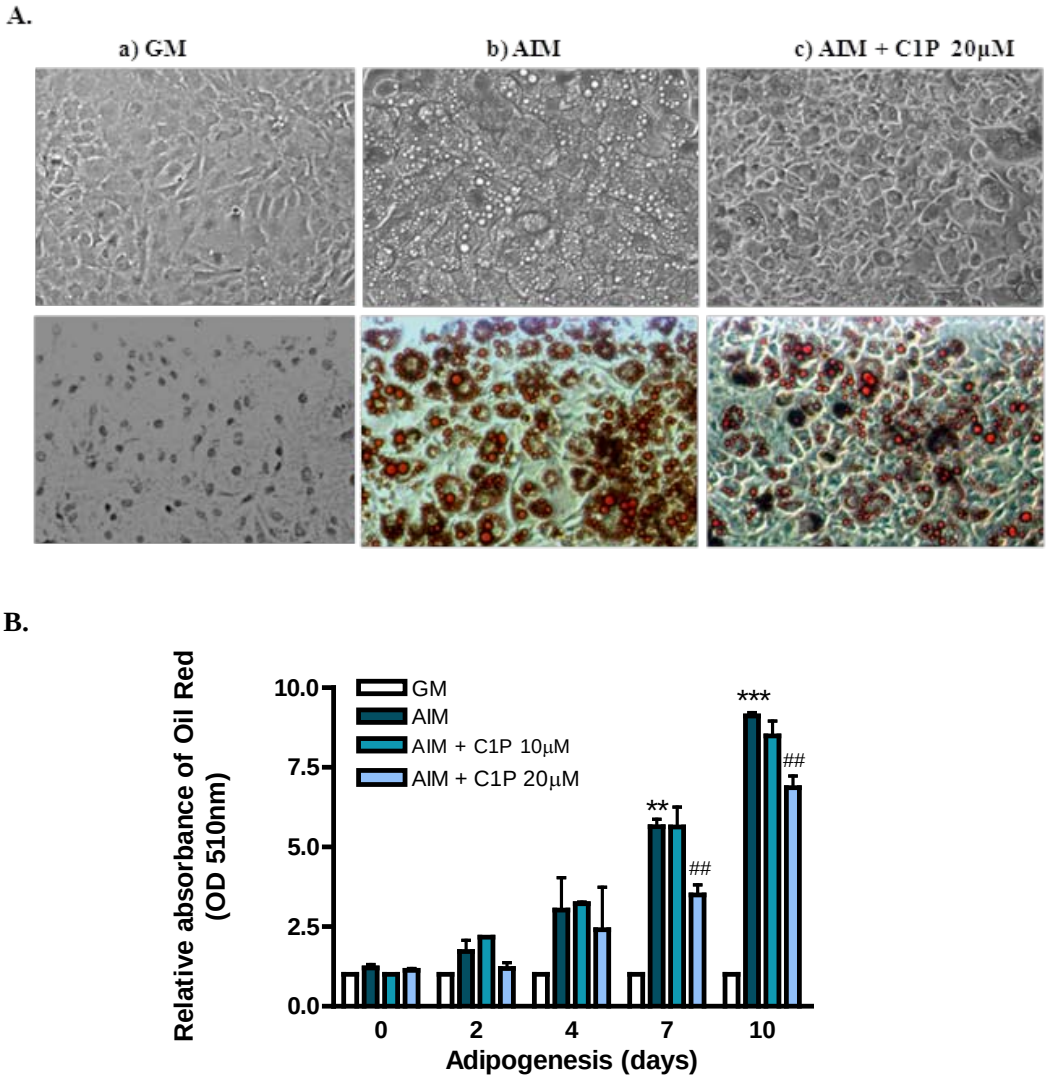

Figure 2.3.1 Ceramide 1-phosphate decreases adipogenesis in 3T3-L1 cells. 3T3-L1 cells were seeded in 24-well plates (6 x 10^4 cells/well) and they were grown in DMEM containing 10% NCS until they were about 90-100% confluent. Confluent cells were further incubated for 2 days before inducing cell differentiation. After two days, cells were subjected to growth medium (GM) or Adipogenic Induction Medium (AIM) with or without C1P. The medium was changed every 2 days and C1P was added each time. Cells were stained with Oil Red O at the indicated time points after differentiation, as described in *Material and Methods.* **A.** On day 10 after differentiation, micrographs of the stained and non-stained cells were taken. All micrographs shown were obtained with a Nikon Eclipse TS100 microscope. **B.** For quantitative analysis of Oil Red staining, the Oil Red O was dissolved in isopropanol and absorbance of the dye was measured in order to quantify lipid droplets. The absorbance of empty wells (without cells) was subtracted from the absorbance of experimental wells. Results are the mean ± SEM of 5 independent experiments performed in triplicate (*$p<0.05$).

Accumulation of fat droplets is not the only feature of differentiated cells. Adipogenesis is accompanied by increased expression of adipogenic transcription factors and adipocyte-specific genes. As mentioned above, there is a wide range of adipogenic markers that can be used to define the change of state between fibroblast and adipocyte phenotype. Some of the adipogenic markers that have been used are C/EBPβ, PPARγ, triglyceride (TG) content and leptin release.

To further characterize the effect of C1P on adipocyte differentiation, we analyzed the TG content in the cells. Confluent 3T3-L1 cells were differentiated with AIM in the presence or absence of C1P until the 10th day after induction of differentiation. At this time, triglyceride assay was performed. This TG assay indicated that the TG content was increased in differentiated cells compared to preadipocytes, and treatment with C1P reduced TG content in 3T3-L1 differentiated cells (Figure 2.3.2). These data are consistent with the results shown above.

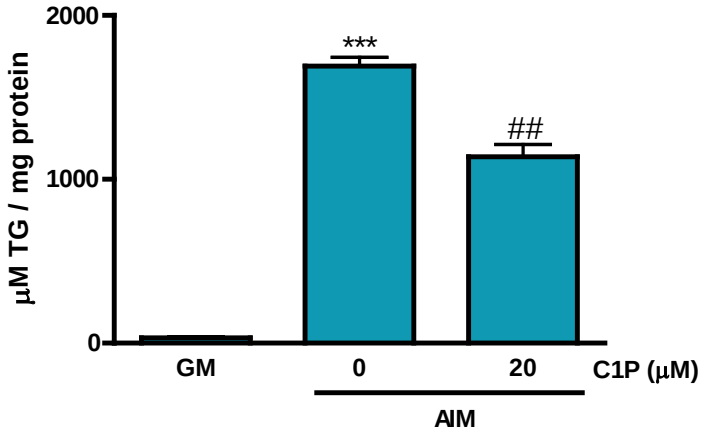

Figure 2.3.2. Exogenous ceramide 1-phosphate decreases TG concentration in 3T3-L1 cells. 3T3-L1 cells were seeded in 96-well plates (9 x 10^3 cells/well) and they were grown in DMEM containing 10% NCS until they were about 90-100% confluent. Cells were then further incubated for 2 days before inducing cell differentiation. After two days, cells were cultured in growth medium (GM) or Adipogenic Induction Medium (AIM) with or without 20 μM of C1P. The medium was changed every 2 days and C1P was added each time. On the 10th day after inducing cell differentiation, TG concentration was measured using the TG assay as described in *Materials and Methods.* Results are normalized to protein concentration of each sample and are the mean ± SEM of 4 independent experiments performed in triplicate (***p<0.001, ##p<0.01).

As mentioned above cell differentiation is related to important changes in the cell pattern of protein expression. In particular, during this process C/EBPβ is phosphorylated and this leads to an increase in PPARγ expression. Therefore, in order

to ensure that C1P attenuates the differentiation process, 3T3-L1 cells were differentiated in the presence or absence of C1P and the phosphorylation of C/EBPβ and PPARγ expression were measured, at 4th and 7th day after induction of differentiation, respectively. Under these conditions, we found that C/EBPβ phosphorylation as well as PPARγ expression were decreased in differentiated cells treated with C1P (Figure 2.3.3), which suggests that C1P promotes antiadipogenic activity in 3T3-L1 cells by downregulating the adipogenic markers C/EBPβ and PPARγ .

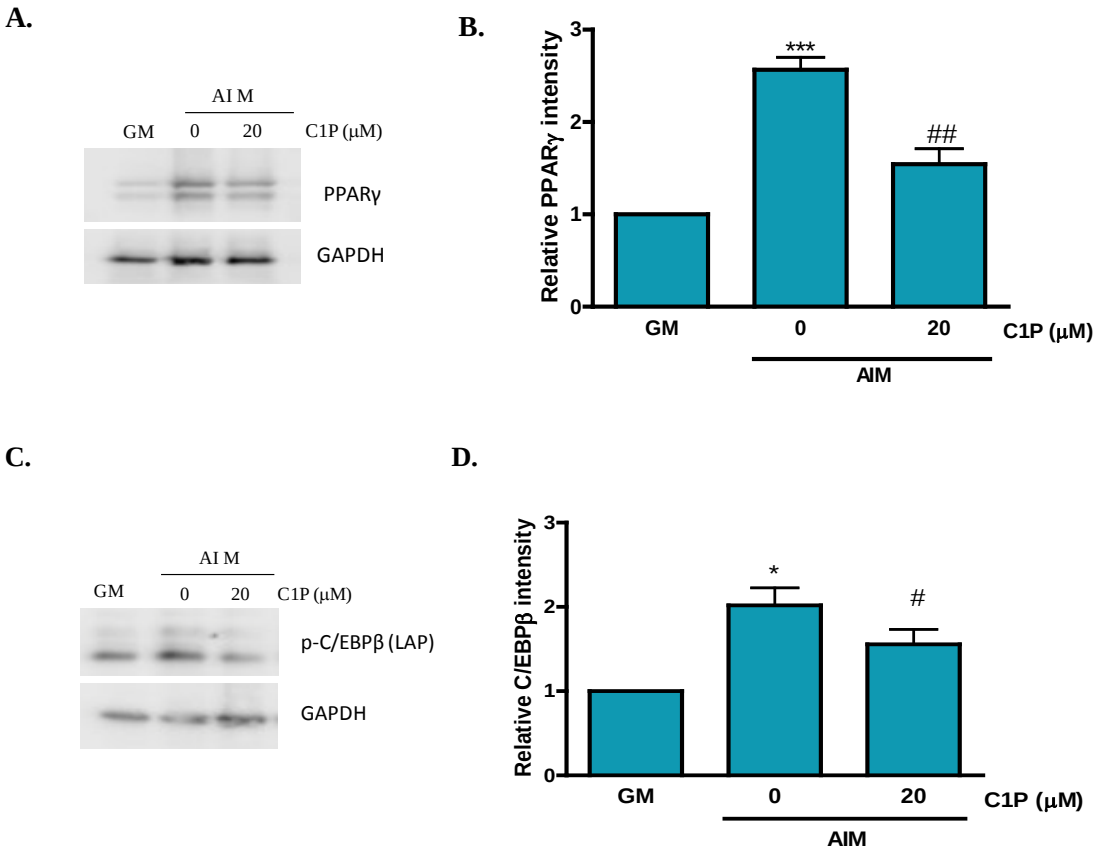

Figure 2.3.3. Ceramide 1-phosphate decreases PPARγ expression and C/EBPβ phosphorylation in 3T3-L1 differentiated cells. 3T3-L1 cells were seeded in 6-well plates (1.2 x 10^5 cells/well) and grown in DMEM containing 10% NCS until they were about 90-100% confluent. Confluent cells were further incubated for 2 days before inducing cell differentiation. After two days, cells were cultured in growth medium (GM) or Adipogenic Induction Medium (AIM), with or without 20 μM of C1P. The medium was changed every 2 days and agonist was added each time. **A.** On day 7, cell lysates were prepared and PPARγ expression was detected by Western blotting using specific antibody to PPARγ and equal loading of protein was assessed with an antibody against GAPDH. Similar results were obtained in each of 6 replicate experiments. **B.** Results of the scanning densitometry of exposed film. Data are expressed as arbitrary units of intensity and are the mean ± SEM of 6 independent experiments (***p<0.001, ##p<0.01). **C.** On day 4, cell lysates were prepared and C/EBPβ phosphorylation was detected by Western blotting using specific antibody to p-C/EBPβ and equal loading of protein was

assessed with an antibody against GAPDH. Similar results were obtained in other 2 experiments. **D.** Results of the scanning densitometry of exposed film. Data are expressed as arbitrary units of intensity and are the mean ± SEM of 3 independent experiments (*p<0.05, #p<0.05).

In order to ensure that C1P acted as an antiadipogenic agent in 3T3-L1 cells, we also examined whether C1P was able to reduce leptin secretion in 3T3-L1. Leptin is a hormone secreted by adipocytes in the obese state and its role is to regulate fat storage. Firstly, leptin levels were measured after induction of differentiation with AIM. We observed that 10 days after induction of differentiation, when most of cells are already differentiated, leptin secretion was significantly increased (Figure 2.3.4a). However, 10 days after induction of differentiation, C1P-treated cells showed a reduction in leptin release (Figure 2.3.4b), which is also consistent with our previous data shown above.

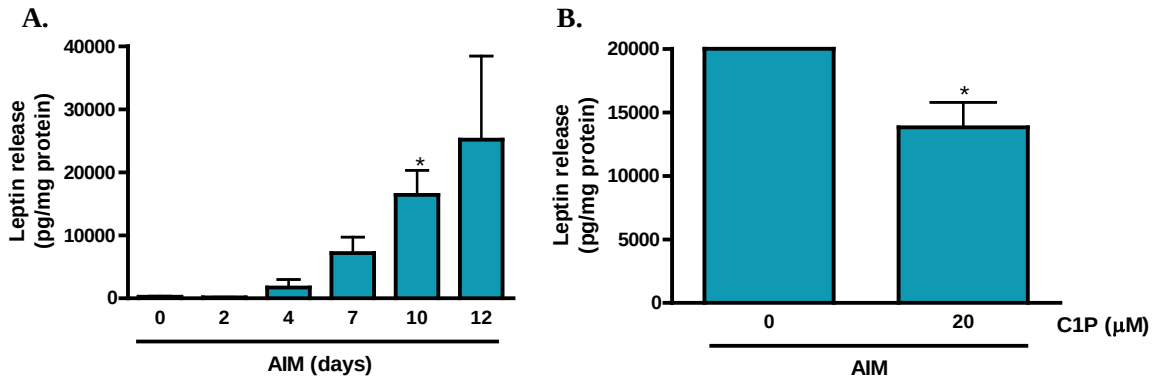

Figure 2.3.4. C1P decreases adipogenic induction medium (AIM)–induced leptin release. 3T3-L1 cells were seeded in 6-well plates (1.2 x 10^5 cells/well) and they were grown in DMEM containing 10% NCS until they were about 90-100% confluent. Confluent cells were further incubated for 2 days before inducing cell differentiation. **A.** After two days, cells were subjected to adipogenic induction media (AIM) in order to induce cell differentiation, as described in *Materials and Methods.* Then, culture medium was collected at indicated time points, centrifuged and the cells were harvested in lysis buffer in order to measure protein concentration. The leptin concentration in supernatant was measured using an ELISA kit, as indicated in *Materials and Methods*. Results are normalized to the protein concentration and are the mean ± SEM of 4 independent experiments perfomed in duplicate (*p<0.05). **B.** After two days, cells were subjected to adipogenic induction media (AIM) in presence or absence of 20 μM of C1P. The medium was changed every 2 days and C1P was added each time. On day 10, the culture medium was collected, centrifuged and the cells were harvested in lysis buffer in order to measure protein concentration. Leptin concentration in supernatant was measured using an ELISA kit. Results are normalized to the protein concentration and are the mean ± SEM of 5 independent experiments performed in duplicate (*p<0.05).

Since obesity is associated with low grade chronic inflammation, we tested to see whether cells induced to differentiate in presence of C1P would affect the levels of pro or anti-inflammatory cytokines. However, C1P had no significant effect either on pro-inflammatory or anti-inflammatory cytokine release in differentiated adipocytes (Figure 2.3.5).

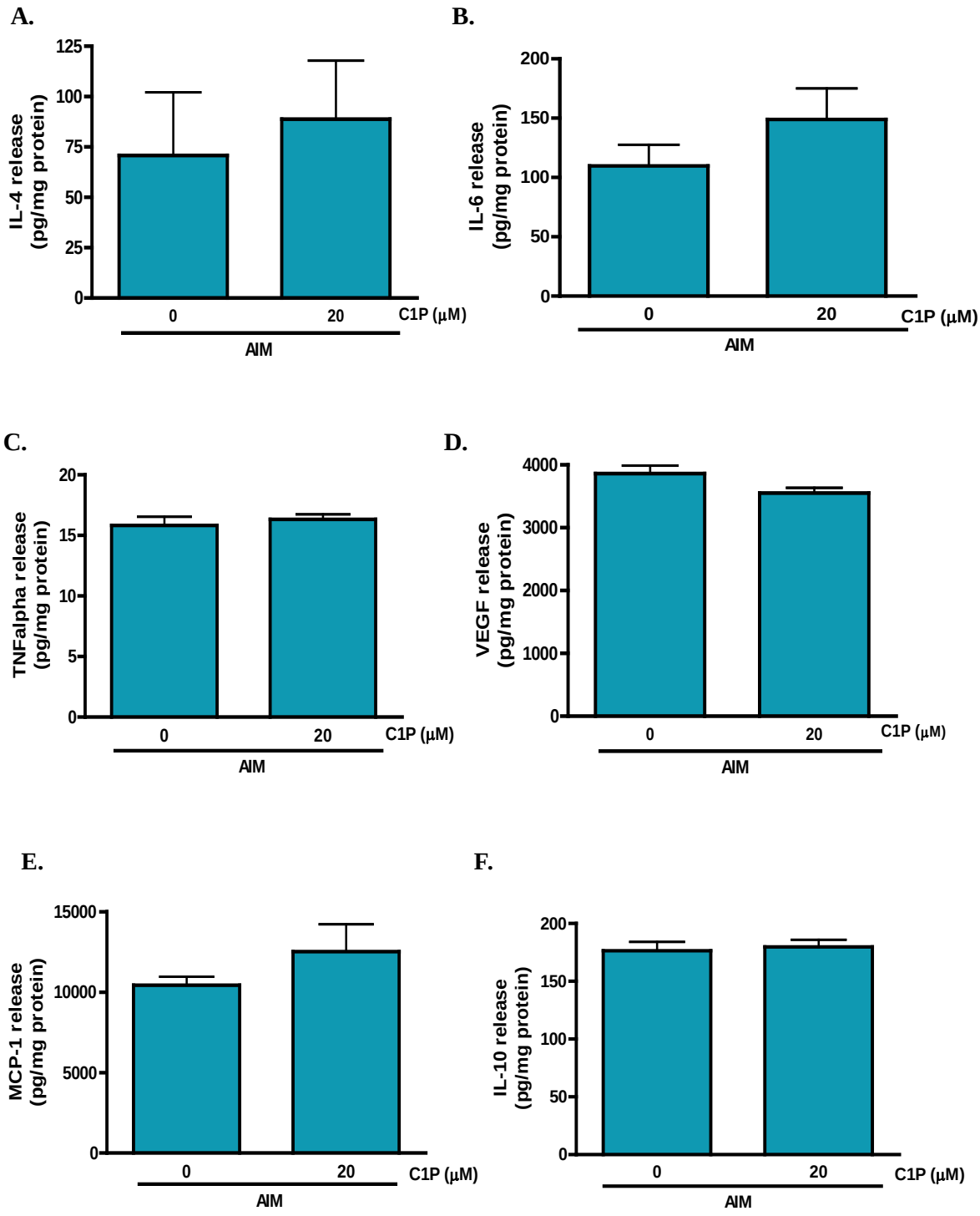

Figure 2.3.5. C1P affected neither pro-inflammatory nor anti-inflammatory cytokine release in differentiated adipocytes. A-F. 3T3-L1 cells were seeded in 6-well plates (1.2 x 10^5 cells/well) and they were grown in DMEM containing 10% NCS until they were about 90-100% confluent. Confluent cells were further incubated for 2 days before inducing cell differentiation. After two days, cells were cultured in adipogenic induction media (AIM), with or without 20 μM of C1P. The medium was changed every 2 days and C1P was added each time, as described in *Material and Methods*. On day 10, the medium was collected and centrifuged and the cells were harvested in lysis buffer in order to measure protein concentration. Cytokine levels were measured using ELISA kits, as indicated in the *Materials and Methods*. Results were normalized to the protein concentration and are the mean ± SEM of 4 independent experiments performed in duplicate.

The above results demonstrate that some adipogenic markers such as lipid droplet accumulation, TG content, leptin release, C/EBPβ phosphorylation and PPARγ expression are downregulated by C1P, which suggest an antiadipogenic role of C1P in 3T3-L1 cells.

2.4. Ceramide 1-phosphate induces sustained ERK phosphorylation under AIM conditions.

Once the antiadipogenic potential of C1P was established, the next step was to examine which signaling pathways might be involved in the ability of C1P to inhibit adipogenesis. Recent studies have shown that several agonists can modulate adipogenic differentiation by regulating MAPK activity, thereby highlighting the important roles of MAPKs in adipocyte differentiation [41, 42]. In particular, ERK seems to be necessary in the early stage of adipocyte differentiation, but not in the terminal stage of cell differentiation. This kinase could be involved in the whole process of adipogenesis displaying both positive and negative effects. We first established the implication of ERK during the differentiation process of 3T3-L1. To this aim, we induced 3T3-L1 cell differentiation by treating the cells with AIM and then ERK phosphorylation was measured every 2-3 days until the 10^{th} day after induction of differentiation. We observed that ERK phosphorylation in undifferentiated cells (day 0) was higher than in differentiated cells, indicating that ERK activity decreases during adipogenesis (Figure 2.4.1).

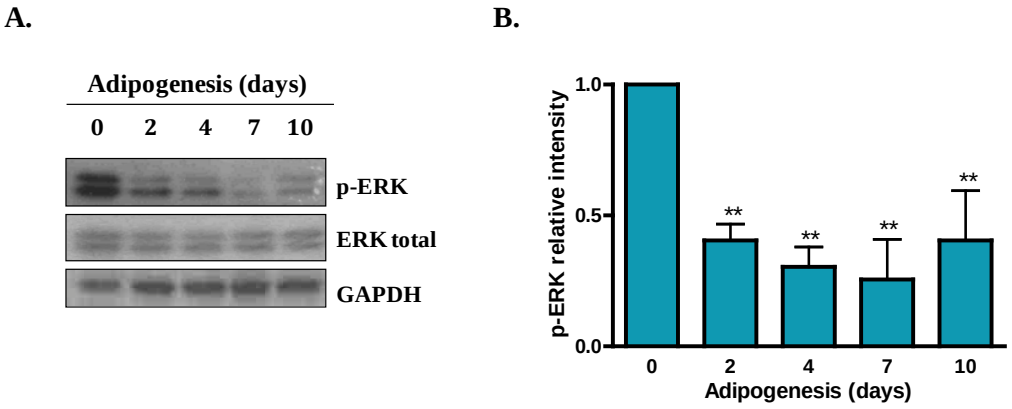

Figure 2.4.1 ERK phosphorylation decreases during adipogenesis in 3T3-L1 cells. 3T3-L1 cells were seeded in 6-well plates (1.2 x 10^5 cells/well) and they were grown in DMEM containing 10% NCS until they were about 90-100% confluent. Confluent cells were further incubated for 2 days. After two days, cells were treated with adipogenic induction media (AIM) in order to induce cell differentiation, as described in *Materials and Methods.* Cells were then harvested after the indicated periods of time. **A.** ERK phosphorylation was detected by Western blotting using a specific antibody to p-ERK and equal loading of protein was assessed with an antibody against GAPDH or total ERK expression. Similar results were obtained in each of 3 replicate experiments. **B.** Results of scanning densitometry of the exposed film. Data are expressed as arbitrary units of intensity relative to control value and are the mean ± SEM of 3 independent experiments (**p<0.01).

To evaluate whether C1P could induce ERK phosphorylation during 3T3-L1 cell differentiation process, confluent cells were treated with AIM in the presence or absence of 20 μM of C1P and ERK phosphorylation was measured by western blotting. We observed that C1P successfully promoted prolonged ERK phosphorylation, which reached maximum values at 1-4 h and was still potently elevated after 16 h of treatment with C1P. It was also observed that phosphorylation of ERK was higher at the early stages of the differentiation process (Figure 2.4.2). These results suggest that C1P could inhibit adipogenesis via sustained activation of ERK.

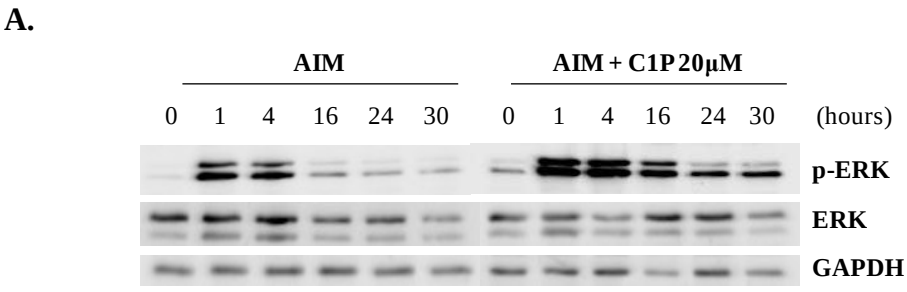

B.

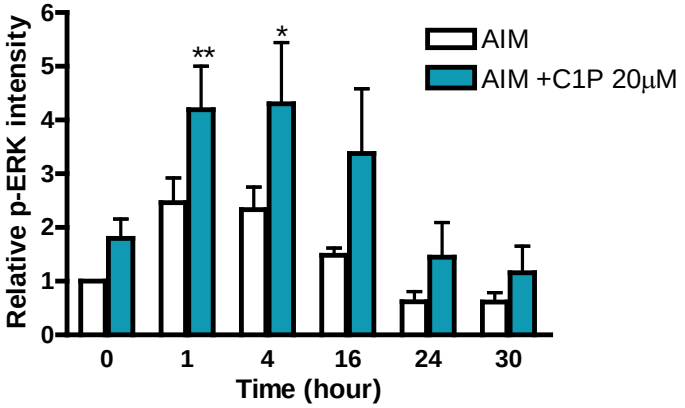

Figure 2.4.2. Ceramide 1-phosphate induces sustained ERK phosphorylation under AIM conditions. 3T3-L1 cells were seeded in 6-well plates (1.2 x 10^5 cells/well) and grown in DMEM containing 10% NCS until they were about 90-100% confluent. Cells were then further incubated for 2 days before inducing cell differentiation. After two days, cells were treated with AIM in the presence or in the absence of 20 μM of C1P. The media was changed every 2 days and C1P was added each time. Cell lysates were prepared at the indicated times after differentiation, as indicated. **A.** The phosphorylation of ERK1/2 and total ERK expression were detected by Western blotting using specific antibodies to p-ERK and ERK, respectively. Equal loading of protein was assessed with an antibody against GAPDH. Similar results were obtained in other 4 independent experiments. **B.** Results of the scanning densitometry of exposed film. Data are expressed as arbitrary units of intensity and are the mean ± SEM of 5 independent experiments (*p<0.05, **p<0.01).

Our group previously demonstrated the existence of a specific membrane binding site, possibly a receptor, for C1P. Ligation of C1P to this receptor stimulated cell migration, and this effect was completely abolished by pretreatment of the cells with pertussis toxin (the toxin secreted by *Bordetella pertussis*) [43], suggesting that the receptor belongs to the family of Gi protein-coupled receptors (GPCR). Therefore, we tested to see whether the inhibitory effect of C1P on adipogenesis was a receptor mediated effect. It was observed that C1P-induced ERK phosphorylation during 3T3-L1 cell differentiation was highly sensitive to inhibition by treatment with Ptx, suggesting that C1P- induced ERK phosphorylation is GPCR-dependent (Figure 2.4.3).

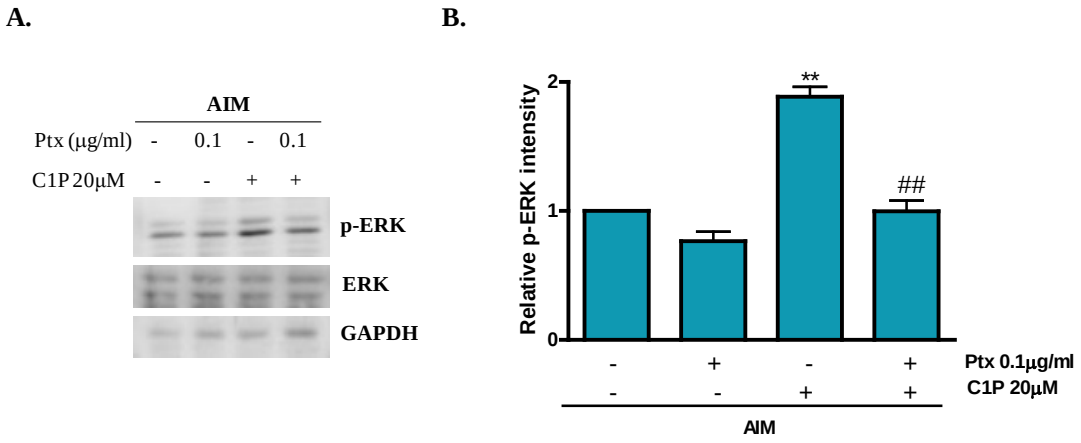

Figure 2.4.3. Pertussis toxin inhibits ceramide 1-phosphate-induced ERK phosphorylation. 3T3-L1 cells were seeded in 6-well plates (1.2 x 10^5 cells/well) and they were grown in DMEM containing 10% NCS until they were about 90-100% confluent. Confluent cells were further incubated for 2 days before inducing cell differentiation. After two days, cells were incubated overnight (for about 16h) with 0.1 μg/ml of Ptx. After treatment with Ptx, cells were cultured in AIM, with or without 20 μM of C1P for 1 h. **A.** Cells were then harvested and prepared for Western blot analysis. p-ERK1/2 and ERK were detected by Western blotting using specific antibodies to p-ERK and ERK, respectively. Equal loading of protein was assessed with an antibody against GAPDH. Similar results were obtained in each of 5 replicate experiments. **B.** Results of the scanning densitometry of exposed film. Data are expressed as arbitrary units of intensity and are the mean ± SEM of 5 independent experiments (**p<0.01, ##p<0.01).

2.5. Ceramide 1-phosphate prevents adipogenic differentiation through the ERK pathway.

Since activation of ERK was implicated in the suppression of adipogenesis, we hypothesized that C1P could inhibit adipogenesis through the ERK pathway. It is known that mitogen-activated protein kinase kinase (MEK) is an upstream kinase of ERK, and so activation of ERK is prevented by blocking MEK activity. To determine whether C1P was able to inhibit adipocyte differentiation via ERK, experiments were performed using the selective MEK inhibitor PD98059.

Confluent cells were induced to differentiate in the presence or in the absence of C1P with or without PD98059. Subsequently, fat droplets were stained with Oil Red O and quantified. As shown in Figure 2.5.1, the absorbance of extracted Oil Red O, in the presence of PD98059 (20 μM) was restored, and therefore co-treatment with PD98059 significantly reversed C1P-mediated inhibition of lipid accumulation in a dose-

dependent manner. To further confirm the essential roles of ERK in C1P-mediated suppression of adipogenic differentiation, we assessed the TG amount in the cells. Consistently, we observed that co-treatment with PD98059 also reverted C1P-attenuated TG amount (Figure 2.5.1) in 3T3-L1 cells. Taken together, these data show that ERK plays an essential role in inhibiting adipogenesis by C1P.

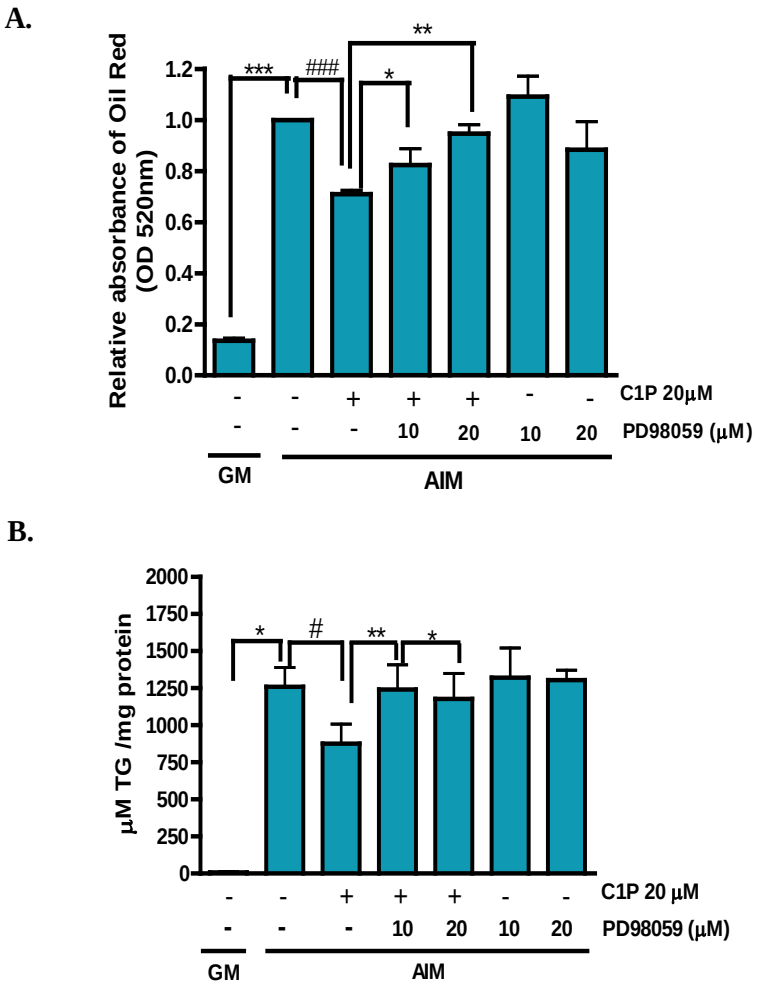

Figure 2.5.1. MEK/ERK pathway is implicated in C1P-promoted antiadipogenic activity. 3T3-L1 cells were seeded in 24-well plates (6 x 10^4 cells/well) and they were grown in DMEM containing 10% NCS until they were about 90-100% confluent. Confluent cells were further incubated for 2 days before inducing cell differentiation. After two days, cells were pre-treated with either vehicle or the indicated concentrations of PD98059 for 1h prior to adipogenic induction. After 1h, cells were cultured in GM or AIM with or without 20 μM of C1P, and in the presence or absence of PD98059 at the indicated concentrations for 10 days. The medium was changed every 2 days and agonists and inhibitors were added each time **A.** On day 10 after induction of differentiation, cells were stained with Oil Red O, as indicated in *Materials and Methods*. For quantitative analysis of the Oil Red staining, the dye was dissolved in isopropanol and the absorbance of Oil Red O was measured in order to quantify lipid droplets. Results are expressed relative to control (AIM) values and the absorbance of the dye of the empty wells

(without cells) was subtracted from the absorbance of the dye of the sample wells. Results are the mean ± SEM of 5 independent experiments performed in triplicate (*p<0.05, **p<0.01, ***p<0.001, ###p<0.001). **B.** On day 10 after induction of differentiation, TG amount was measured using TG assay as described in *Materials and Methods.* Results are normalized to the protein concentration and are the mean ± SEM of 3 independent experiments performed in triplicate (*p<0.05, #p<0.05, **p<0.01).

2.6. C1P suppresses adipocyte differentiation in a Gi protein-coupled receptor (GPCR)-dependent manner.

As mentioned above, C1P-induced ERK phosphorylation during cell differentiation is GiPCR-dependent, which suggest the possible involvement of a putative specific C1P receptor. From the above results, we hipothesized that C1P might be able to block adipogenesis by phosphorylation of ERK via GPCR. To test this, we induced cell diferentiation in the presence or absence of C1P with or without Ptx, which causes inhibition of GPCRs on the cell surface. To examine whether Ptx was able to revert C1P action, fat droplets were stained with Oil Red O and micrographs of differentiated 3T3-L1 cells were taken. This allowed quatification of internalized oil red dye by differentiated cells. We observed that co-treatment with Ptx reversed C1P-attenuated lipid droplets accumulation (Figure 2.6.1.a and Figure 2.6.1b). In addition, C1P-reduced TG amount was also increased after treatment with Ptx (Figure 2.6.1c). Therefore, Ptx, as well as PD98059, significantly restores C1P-attenuated adipogenesis, which suggest that blockade of GiPCR avoid the inhibitory action of C1P in adipogenesis (Figure 2.6.1).

A.

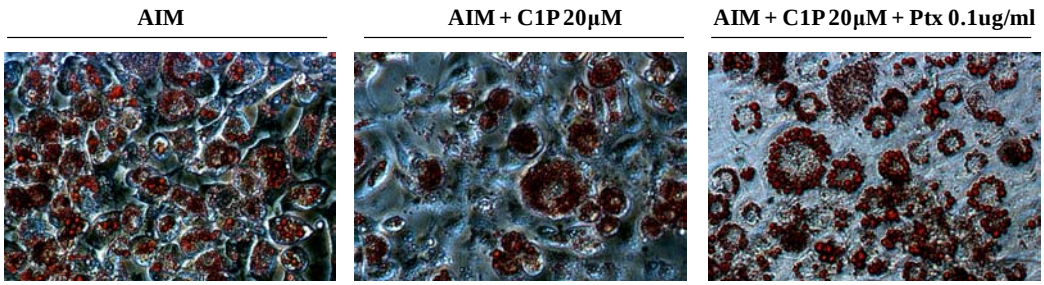

B.

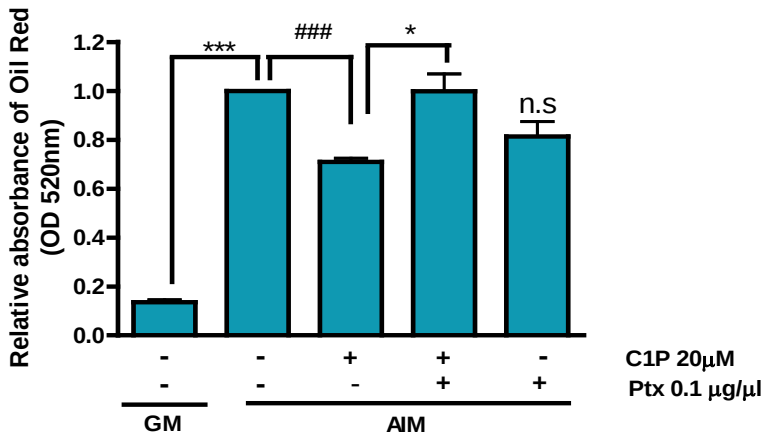

C.

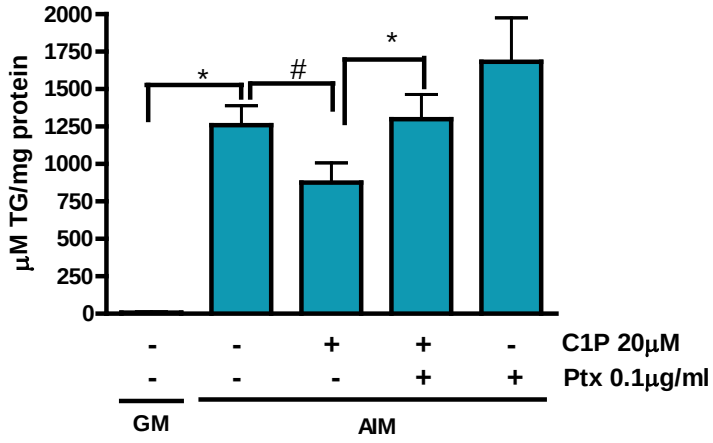

Figure 2.6.1. Ptx restores C1P-induced reduction of TG concentration in 3T3-L1 cells. 3T3-L1 cells were seeded in 24-well plates (6 x 10^4 cells/well) in order to quantify lipid accumulation and cells were seeded in 96-well plates (9 x 10^3 cells/well) for measurement of TG concentration. Cells were grown in DMEM containing 10% NCS until they were about 90-100% confluent. Confluent cells were further incubated for 2 days before inducing cell differentiation. After two days, cells were incubated overnight (for about 16h) with 0.1 µg/ml of Ptx. The cells were then cultured in AIM, with or without 20 µM of C1P in the presence or absence of Ptx for 10 days. The medium was changed every 2 days and agonists and inhibitors were added each time **A.** On day 10 after induction of differentiation, cells were stained with Oil Red O, as indicated in *Materials and Methods.* Micrographs of randomly selected fields were taken with a Nikon Eclipse TS100 microscope at 20x magnification. **B.** On day 10, cells were stained with Oil Red O, as indicated in *Materials and Methods*. For quantitative analysis of Oil Red staining, the Oil Red O was dissolved in isopropanol and absorbance of the dye was measured in order to quantify lipid droplets. Results are expressed relative to control (AIM) value and the absorbance of the dye of the empty wells (without cells) was subtracted from the absorbance of sample wells. Results are the mean ± SEM of 5 independent experiments performed in triplicate (*p<0.05, ***p<0.001, ###p<0.001). **C.** On day 10 after induction of differentiation, TG amount was measured using a TG assay kit as described in *Materials and Methods.* Results are normalized to the protein amount and are the mean ± SEM of 3 independent experiments performed in triplicate (*p<0.05, #p<0.05).

To ensure that C1P-attenuated 3T3-L1 cell differentiation was GPCR-dependent, we determined the role of Ptx on the expression of PPARγ, which is one of the most important adipogenic markers. We found that Ptx restores C1P-reduced PPARγ expression (Figure 2.6.2), which is consistent with the data shown above.

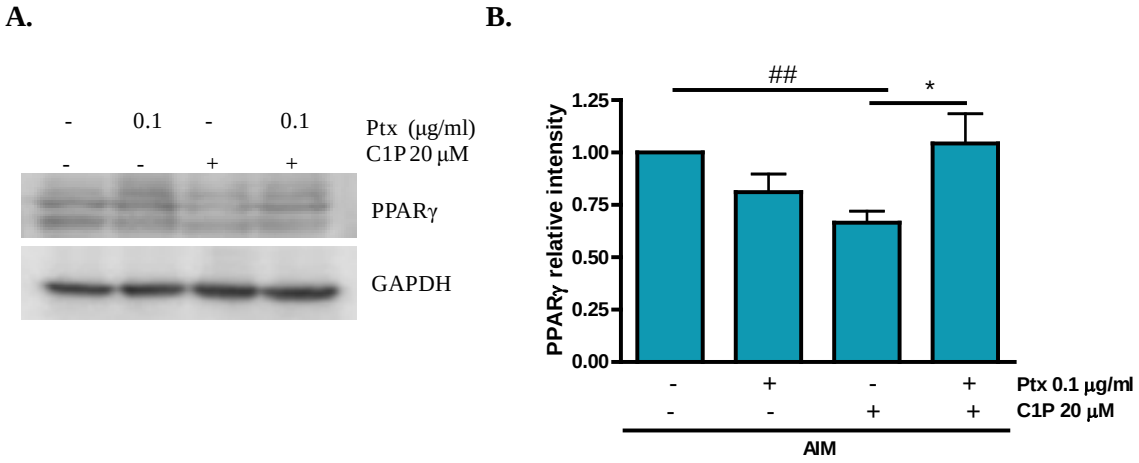

Figure 2.6.2. Ptx blocks the inhibitory effect of C1P on PPARγ expression in differentiated cells. 3T3-L1 cells were seeded in 6-well plates (1.2 x 10^5 cells/well) and they were grown in DMEM containing 10% NCS until they were about 90-100% confluent. Cells were then further incubated for 2 days before inducing cell differentiation. After two days, cells were pretreated with Ptx at 0.1μg/ml concentration for 16 h. After treatment with Ptx, cells were cultured in AIM, with or without 20 μM of C1P and in the presence or in the absence of Ptx for 7 days. The medium was changed every 2 days and agonists or inhibitors were added each time. **A.** On day 7 after induction of differentiation, cells were harvested and prepared for Western blot analysis. The PPARγ expression was detected by Western blotting using a specific antibody to PPARγ and equal loading of protein was assessed with an antibody against GAPDH. Similar results were obtained in other 4 independent experiments. **B.** Results of the scanning densitometry of exposed film. Data are expressed as arbitrary units of intensity and are the mean ± SEM of 5 independent experiments (*$p<0.05$, ##$p<0.01$).

Altogether, these thata suggest that C1P induces ERK phosphorylation through interaction with a GPCR. This action resulted in an antiadipogenic effect of C1P in 3T3-L1 cell differentiation.

2.7. Lack of toxicity of the inhibitors and agonists used in this work

All commonly used chemical inhibitors in cell signaling studies have been described to be toxic for cells at certain concentrations or times of incubation. To test if any of the inhibitors or agonists used in this Thesis were toxic for the cells at the indicated times and concentrations, we performed cell viability assays. We observed that neither PD98059 nor C1P caused a significant decrease in cell viability of 3T3-L1 cells at the indicated concentrations (Figure 2.7.1). However, Ptx decreased the proliferative capacity of cells, although this was not statistically significant. Also Ptx, can be used at concentrations higher than 0.1μg/ml (usually 0.5 μg/ml or even higher) to inhibit GPCR with no side effects been reported at those concentrations.

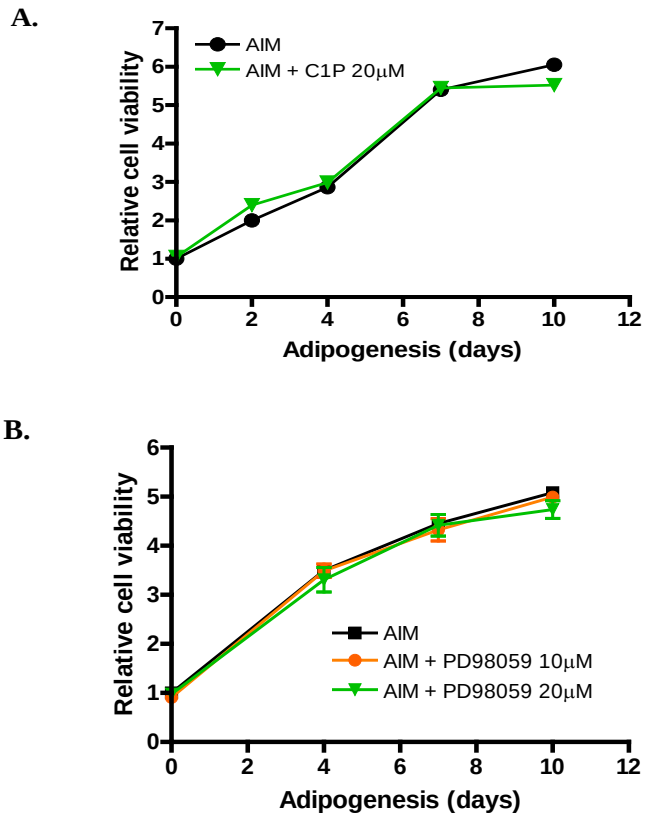

C.

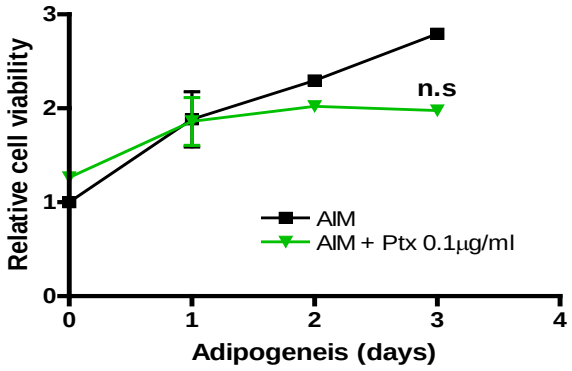

Figure 2.7.1. Cell viability after treatment with various chemical inhibitors and C1P. Cells were seeded in 96-well plate (9 x 10^3 cells/well) and incubated in DMEM supplemented with 10% NCS until they were 90-100% confluent. **A.** Two days post-confluent cells were cultured in the adipogenic induction medium (AIM), with or without 20 μM C1P and cell viability was measured at the indicated periods of time. Cell viability was determined using the MTS-formazan assay as indicated in *Materials and Methods*. Results are the mean ± SEM of 2 independent experiments performed in triplicate. **B.** Two days post-confluent cells were cultured in the adipogenic induction medium (AIM), with or without PD98059 at the indicated concentrations and cell viability was measured at the indicated periods of time. Cell viability was determined using the MTS-formazan assay as indicated in *Materials and Methods*. Results are the mean ± SEM of 2 independent experiments performed in triplicate. **C.** Two days post-confluent cells were cultured in the adipogenic induction medium (AIM), with or without 0.1 μg/ml Ptx and cell viability was measured at the indicated periods of time. Cell viability was determined using the MTS-formazan assay as indicated in *Materials and Methods*. Results are the mean ± SEM of 3 independent experiments performed in triplicate.

3. DISCUSSION

Adipocytes are the major cellular component of the adipose tissue and excessive growth, differentiation and hypertrophy of adipocytes are fundamental processes that trigger obesity. In particular, adipocyte differentiation is a multi-step process that allows a fibroblast-like preadipocyte to undergo molecular changes that facilitate its transformation into mature adipocyte [44]. In order to achieve a successful transformation into mature adipocytes, the first hallmark of the adipogenesis process is the dramatic alteration in cell shape as the cells convert from fibroblastic to spherical shape. These morphological modifications are paralleled by changes in the level and type of extracellular matrix (ECM) components and the level of cytoskeletal components [45]. Besides, the current model for adipocyte differentiation suggests that during the entire differentiation process there are several essential molecular interactions that occur among members of the CCAAT-enhancer-binding proteins (C/EBPs) and the peroxisome proliferator-activated receptor (PPAR) families. Given that adipogenesis is a key event in the development of obesity, the suppression of adipocyte differentiation is an attractive strategy for obesity therapy, and identifying molecules that regulate fat cell differentiation is crucial for the treatment of obesity and obesity-related diseases.

Sphingolipid metabolism is controlled by a complex network of highly regulated interconnected pathways leading to the production of bioactive molecules including ceramide, sphingosine, S1P and C1P. Although sphingolipids constitute a family of lipids that play important roles as structural components of biologic membranes, emerging data support a role for these bioactive sphingolipids in multiple signaling pathways regulating a variety of physiological and pathological events including cell growth and survival, differentiation, apoptosis and inflammation [25-27, 46, 47]. It is now well established that sphingolipid metabolism can be activated by a variety of conditions such as pro inflammatory cytokines (e.g., TNF-α), growth factors, oxidative stress and increased availability of FFAs. All of these conditions characterize the local milieu of the obese adipose tissue, suggesting that sphingolipid metabolism may be altered in adipose tissue in obesity.

During adipocyte differentiation, the undifferentiated fibroblast-like preadipocytes initiate expression of differentiation-related transcription factors such as PPARγ and C/EBPβ, followed by growth arrest, thereafter, they become spherical fat cells with accumulated lipid droplets [48-51]. Therefore, the population of adipocytes with lipid droplets stained with Oil Red O, a biomarker for adipocyte differentiation, is increased during adipogenesis, and this has been associated to dysregulation of sphingolipid metabolism.

Because of the significance in the regulation of sphingolipid metabolism and sphingolipid content during the cell differentiation process, general sphingolipid levels could be markedly different after the adipogenesis process is completed as a consequence of the phenotypical change from fibroblastic phenotype to spherical phenotype. During this process, the flux between the various sphingolipid metabolites is tightly controlled by several enzymes that are critical in regulating the levels and function of these bioactive molecules. In this thesis, we demonstrate that CERK, an enzyme that phosphorylates ceramide to produce ceramide 1-phosphate, plays a key role in 3T3-L1 cell differentiation. During the 3T3-L1 cell differentiation process induced by adipogenic inducers, CERK expression increased, and was higher at the late stages of adipocyte differentiation. In addition, CERK activity was also higher in differentiated adipocytes than undifferentiated 3T3-L1 preadipocytes, which did not show CERK activation. Therefore, these results suggest that during adipocyte differentiation, ceramide is phosphorylated leading to the formation of C1P. These results can be correlated with different works that have established an inverse relationship between adipocyte differentiation and ceramide levels in adipose tissue of obese mice [37] and in 3T3-L1 cells [36]. In the latter study, the authors showed that ceramide concentration in adipocytes decreased during adipogenesis compared to that in preadipocytes. Moreover, using siRNA technology, we demonstrate here that inhibition of CERK leads to significant attenuation of lipid droplets accumulation and TG content, which are adipogenic markers. The fact that CERK inhibition blocks 3T3-L1 cell differentiation may suggest a deceleration in the acquisition of the mature adipocyte phenotype. Thus, CERK activity is indeed required for adipocyte differentiation. Consistently with the results obtained in this Thesis, CERK null mice have been shown to be resistant to diet-induced obesity [52]. Interestingly, it was recently demonstrated that sphingosine kinase is also induced in 3T3-L1 cells and promotes adipogenesis by generating S1P [53].

Overall, it can be concluded that CERK may contribute to adipocyte differentiation through the production of C1P and the subsequent decrease in ceramide levels. This conclusion is supported by accumulating evidence indicating that elevation of ceramide levels is sufficient to block adipogenesis. In addition to, ceramides, other lipid metabolites including retinoic acid [54] and prostaglandin F2α [55] were also able to inhibit adipogenesis.

The scheme shown below (Figure 3.1) suggests a possible implication of CERK in adipogenesis. During this process, CERK expression and activity increase and inhibition of CERK blocks 3T3-L1 cell differentiation, probably by means of intracellular ceramide accumulation.

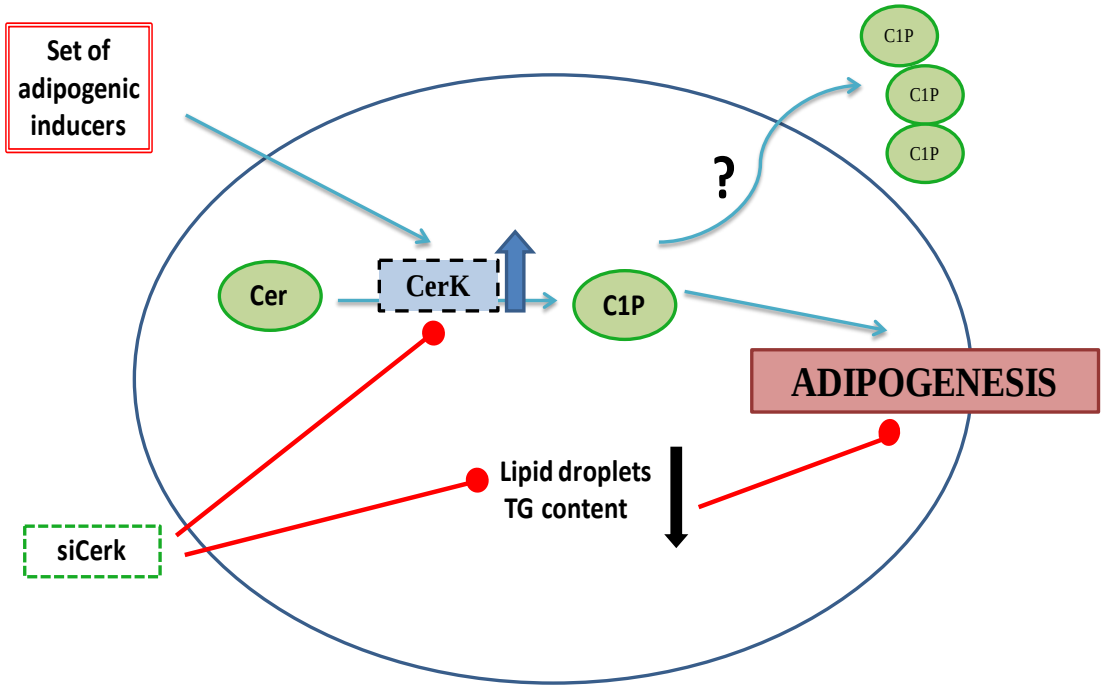

Figure 3.1. Representation of the contribution of CERK to adipocyte differentiation

Several studies have established that various secondary signaling intermediates produced by further conversion of ceramide can participate in opposite cellular processes. Certainly, ceramide and sphingosine have proapoptotic actions while the phosphorylated species, C1P and S1P, are involved in survival activities [56]. Therefore, while ceramide is regarded as antiadipogenic lipid, C1P could have the opposite effect. However, in this thesis, we demonstrate for the first time that C1P

attenuates adipogenesis in 3T3-L1 cells. Treatment with C1P during cell differentiation blocked the characteristic lipid droplets accumulation in differentiated cells. Consistent with the decrease in the amount of lipid droplets, TG content was also inhibited by C1P. Several transcription factors, including C/EBPβ and PPARγ, need to be activated during 3T3-L1 cell differentiation [9]. However, during cell differentiation C1P was able to reduce both PPARγ expression and C/EBPβ phosphorylation, which are upregulated in differentiated adipocytes.

Adipocyte differentiation is also regulated by a large number of hormones, growth factors, and cytokines. In fact, 3T3-L1 cell differentiation can be characterized by changes in the expression of numerous genes including leptin, which is produced during different stages of differentiation, leading to the characteristic changes in morphology and the accumulation of TG in the cytoplasm. Leptin is primarily secreted by adipocytes in order to regulate central and peripheral signaling pathways that ultimately lead to decreased food intake and/or increased metabolism and energy expenditure. In agreement with the data shown above, we observed that leptin secretion increased during 3T3-L1 cell differentiation, reaching maximum release value at the late stage of the differentiation process. Interestingly, treatment of 3T3-L1 cells with C1P attenuated leptin release. However, although obesity is considered a chronic inflammatory disease and thus, proinflammatory cytokine levels are increased in an obese state, C1P showed no effect on 3T3-L1 differentiated cells-induced cytokine release. These data suggest that a major antiadipogenic action of C1P is based on inhibition of leptin release.

Taken together, the data presented in this thesis establish that C1P is a potent antiadipogenic agent, being able to decrease lipid accumulation, TG concentration, adipogenic markers expression and leptin levels during the differentiation process.

The next step was to investigate into the mechanisms involved in the antiadipogenic activity of C1P. Interestingly, recent reports showed that several compounds modulate adipogenic differentiation by regulating MAPK activity [41, 42]. In particular, the ERK pathway could be involved in adipogenesis by displaying both positive and negative effects. For example, in preadipocyte cells derived from human omental adipose tissue ERK is involved in the anti-adipogenic effect of angiotensin II [57]. In addition, evodiamine, a major alkaloid compound found in Evodia fructus, was found to prevent adipocyte differentiation by sustaining the activation of ERK in 3T3-L1 [58].

Conversely, in the terminal differentiation phase ERK1 activity led to phosphorylation of PPARγ, which inhibits differentiation [18]. These contradictory data suggest that the role of ERK in adipogenesis needs to be timely regulated. Early on, ERK had to be turned on to initiate preadipocytes into the differentiation process and, thereafter, the signal transduction pathway needs to be shut-off to proceed with adipocyte maturation. In this connection, we have found that ERK phosphorylation was higher in the early stages of differentiation whereas in the late stages of the process, when adipocytes are totally differentiated, ERK phosphorylation was decreased. Based on previous work by our group, we hypothesized that C1P could regulate adipocyte differentiation via the ERK signaling pathway. We have demonstrated in this Thesis that treatment of cells with C1P at the early stages of the differentiation process increased ERK phosphorylation up to about 30 hour after induction of cell differentiation, whereas in the absence of C1P, ERK phosphorylation reached maximum value at 4 hours after induction of the differentiation process. Because of the prolonged activation of ERK by C1P, it could be speculated that activation of this kinase is essential for C1P-mediated suppression of adipogenesis. In this regard, we observed that treatment of 3T3-L1 with PD98059, an ERK inhibitor, restored C1P-mediated suppression of adipogenesis in a dose-dependent manner. This ERK inhibitor was able to also rescue the formation of lipid droplets and the content of TG in 3T3-L1 cells, even in the presence of C1P. Therefore, these results strongly suggest that the ERK pathway is responsible for the inhibition of adipogenic differentiation by extracellular C1P. However, the generation of intracellular C1P is a key event in the process of adipogenesis and unlike extracellular C1P, endogenous C1P does not inhibit adipogenesis, as intracellular C1P is unable of activating the MAPK pathway.

Our group previously demonstrated that C1P is able to stimulate cell migration through interaction with a putative specific C1P receptor which was found to be coupled to a Gi protein-coupled receptor (a GPCR, as previously mentioned) [43, 59]. Therefore, based on that work, it was hypothesized that this GPCR could be involved in C1P-induced ERK1/2 activation. To characterize this type of interaction we used Pertussis Toxin (Ptx), which upon addition to eukaryotic cells causes inhibition of GPCRs by blocking the activation of Gi proteins and therefore, all the signaling pathways that are dependent on this kind of interaction would be blocked. In this thesis, we demonstrated that C1P action on ERK phosphorylation in 3T3-L1 cells requires the interaction of C1P with a

Ptx-sensitive GPCR, as Ptx blocked C1P-estimulated ERK phosphorylation. In addition, we also observed that C1P-attenuated adipocyte differentiation was highly sensitive to treatment with Ptx. C1P-attenuated lipid droplet accumulation and TG content were increased by treatment with Ptx.

In this Thesis, we show for the first time that C1P decreases adipogenesis and we have elucidated part of the mechanism by which C1P exerts this action. The results obtained in this work indicate the CERK/C1P signaling axis appear to have an important role in the process of adipocyte differentiation. These findings may help to develop new therapeutic strategies against obesity and obesity-related diseases. The scheme shown below describes the role played by C1P in adipocyte differentiation.

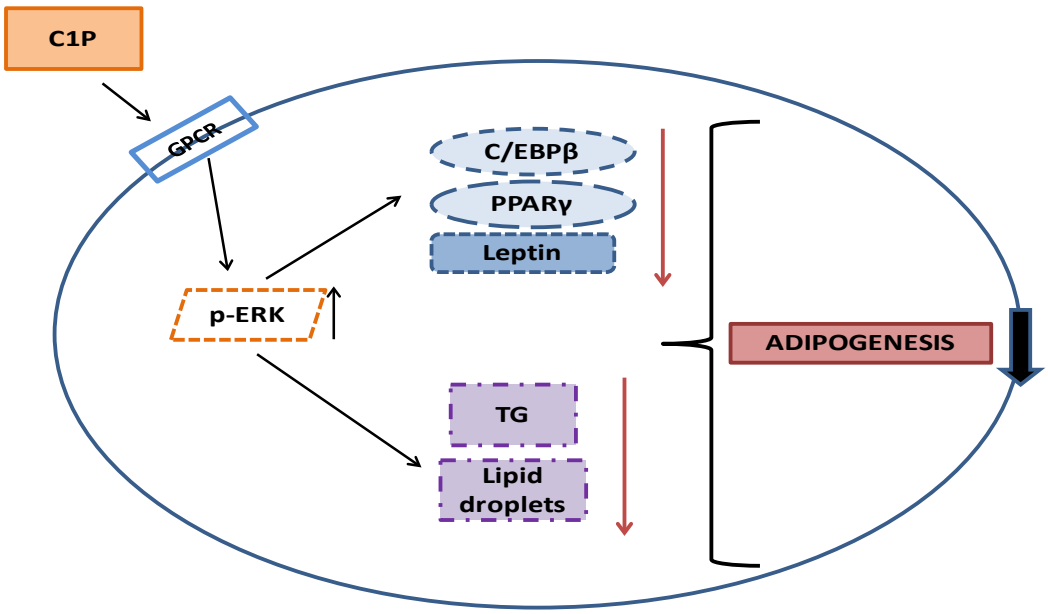

Figure 3.2. Working model for the implication of exogenous C1P in blocking adipogenesis

We propose that fluctuations in intracellular C1P levels may initially switch adipogenesis, and later provide an antiadipogenic feed-back mechanism led by exogenous C1P to reset the system to homeostasis after enhancement of CerK expression.

4. REFERENCES

1. Crandall, D.L., G.J. Hausman and J.G. Kral, *A review of the microcirculation of adipose tissue: anatomic, metabolic, and angiogenic perspectives.* Microcirculation, 1997. **4**(2): p. 211-32.
2. Feve, B., *Adipogenesis: cellular and molecular aspects.* Best Pract Res Clin Endocrinol Metab, 2005. **19**(4): p. 483-99.
3. Student, A.K., R.Y. Hsu and M.D. Lane, *Induction of fatty acid synthetase synthesis in differentiating 3T3-L1 preadipocytes.* J Biol Chem, 1980. **255**(10): p. 4745-50.
4. Davis, L.A. and N.I. Zur Nieden, *Mesodermal fate decisions of a stem cell: the Wnt switch.* Cell Mol Life Sci, 2008. **65**(17): p. 2658-74.
5. MacDougald, O.A. and M.D. Lane, *Transcriptional regulation of gene expression during adipocyte differentiation.* Annu Rev Biochem, 1995. **64**: p. 345-73.
6. Coleman, R.A., B.C. Reed, J.C. Mackall, A.K. Student, M.D. Lane and R.M. Bell, *Selective changes in microsomal enzymes of triacylglycerol phosphatidylcholine, and phosphatidylethanolamine biosynthesis during differentiation of 3T3-L1 preadipocytes.* J Biol Chem, 1978. **253**(20): p. 7256-61.
7. Farmer, S.R., *Transcriptional control of adipocyte formation.* Cell Metab, 2006. **4**(4): p. 263-73.
8. Ramji, D.P. and P. Foka, *CCAAT/enhancer-binding proteins: structure, function and regulation.* Biochem J, 2002. **365**(Pt 3): p. 561-75.
9. Tang, Q.Q., T.C. Otto and M.D. Lane, *CCAAT/enhancer-binding protein beta is required for mitotic clonal expansion during adipogenesis.* Proc Natl Acad Sci U S A, 2003. **100**(3): p. 850-5.
10. Wang, G.L., X. Shi, E. Salisbury, Y. Sun, J.H. Albrecht, R.G. Smith and N.A. Timchenko, *Cyclin D3 maintains growth-inhibitory activity of C/EBPalpha by stabilizing C/EBPalpha-cdk2 and C/EBPalpha-Brm complexes.* Mol Cell Biol, 2006. **26**(7): p. 2570-82.
11. Guo, L., X. Li and Q.Q. Tang, *Transcriptional regulation of adipocyte differentiation: a central role for CCAAT/enhancer-binding protein (C/EBP) beta.* J Biol Chem, 2015. **290**(2): p. 755-61.
12. Rosen, E.D. and O.A. MacDougald, *Adipocyte differentiation from the inside out.* Nat Rev Mol Cell Biol, 2006. **7**(12): p. 885-96.
13. Rosen, E.D., *The transcriptional basis of adipocyte development.* Prostaglandins Leukot Essent Fatty Acids, 2005. **73**(1): p. 31-4.
14. Miloso, M., A. Scuteri, D. Foudah and G. Tredici, *MAPKs as mediators of cell fate determination: an approach to neurodegenerative diseases.* Curr Med Chem, 2008. **15**(6): p. 538-48.
15. Chang, L. and M. Karin, *Mammalian MAP kinase signalling cascades.* Nature, 2001. **410**(6824): p. 37-40.
16. Zhang, Y. and C. Dong, *Regulatory mechanisms of mitogen-activated kinase signaling.* Cell Mol Life Sci, 2007. **64**(21): p. 2771-89.
17. Aubert, J., N. Belmonte and C. Dani, *Role of pathways for signal transducers and activators of transcription, and mitogen-activated protein kinase in adipocyte differentiation.* Cell Mol Life Sci, 1999. **56**(5-6): p. 538-42.
18. Bost, F., M. Aouadi, L. Caron and B. Binetruy, *The role of MAPKs in adipocyte differentiation and obesity.* Biochimie, 2005. **87**(1): p. 51-6.
19. Benito, M., A. Porras, A.R. Nebreda and E. Santos, *Differentiation of 3T3-L1 fibroblasts to adipocytes induced by transfection of ras oncogenes.* Science, 1991. **253**(5019): p. 565-8.
20. Sale, E.M., P.G. Atkinson and G.J. Sale, *Requirement of MAP kinase for differentiation of fibroblasts to adipocytes, for insulin activation of p90 S6 kinase and for insulin or serum stimulation of DNA synthesis.* Embo J, 1995. **14**(4): p. 674-84.

21. Prusty, D., B.H. Park, K.E. Davis and S.R. Farmer, *Activation of MEK/ERK signaling promotes adipogenesis by enhancing peroxisome proliferator-activated receptor gamma (PPARgamma) and C/EBPalpha gene expression during the differentiation of 3T3-L1 preadipocytes.* J Biol Chem, 2002. **277**(48): p. 46226-32.
22. Belmonte, N., B.W. Phillips, F. Massiera, P. Villageois, B. Wdziekonski, P. Saint-Marc, J. Nichols, J. Aubert, K. Saeki, A. Yuo, S. Narumiya, G. Ailhaud and C. Dani, *Activation of extracellular signal-regulated kinases and CREB/ATF-1 mediate the expression of CCAAT/enhancer binding proteins beta and -delta in preadipocytes.* Mol Endocrinol, 2001. **15**(11): p. 2037-49.
23. Kim, S.W., A.M. Muise, P.J. Lyons and H.S. Ro, *Regulation of adipogenesis by a transcriptional repressor that modulates MAPK activation.* J Biol Chem, 2001. **276**(13): p. 10199-206.
24. Janderova, L., M. McNeil, A.N. Murrell, R.L. Mynatt and S.R. Smith, *Human mesenchymal stem cells as an in vitro model for human adipogenesis.* Obes Res, 2003. **11**(1): p. 65-74.
25. Geilen, C.C., T. Wieder and C.E. Orfanos, *Ceramide signalling: regulatory role in cell proliferation, differentiation and apoptosis in human epidermis.* Arch Dermatol Res, 1997. **289**(10): p. 559-66.
26. Olivera, A., A. Romanowski, C.S. Rani and S. Spiegel, *Differential effects of sphingomyelinase and cell-permeable ceramide analogs on proliferation of Swiss 3T3 fibroblasts.* Biochim Biophys Acta, 1997. **1348**(3): p. 311-23.
27. Obeid, L.M., C.M. Linardic, L.A. Karolak and Y.A. Hannun, *Programmed cell death induced by ceramide.* Science, 1993. **259**(5102): p. 1769-71.
28. Chatterjee, S., *Sphingolipids in atherosclerosis and vascular biology.* Arterioscler Thromb Vasc Biol, 1998. **18**(10): p. 1523-33.
29. Shimabukuro, M., Y.T. Zhou, M. Levi and R.H. Unger, *Fatty acid-induced beta cell apoptosis: a link between obesity and diabetes.* Proc Natl Acad Sci U S A, 1998. **95**(5): p. 2498-502.
30. Auge, N., A. Negre-Salvayre, R. Salvayre and T. Levade, *Sphingomyelin metabolites in vascular cell signaling and atherogenesis.* Prog Lipid Res, 2000. **39**(3): p. 207-29.
31. Unger, R.H. and L. Orci, *Diseases of liporegulation: new perspective on obesity and related disorders.* Faseb J, 2001. **15**(2): p. 312-21.
32. Hojjati, M.R., Z. Li, H. Zhou, S. Tang, C. Huan, E. Ooi, S. Lu and X.C. Jiang, *Effect of myriocin on plasma sphingolipid metabolism and atherosclerosis in apoE-deficient mice.* J Biol Chem, 2005. **280**(11): p. 10284-9.
33. Summers, S.A. and D.H. Nelson, *A role for sphingolipids in producing the common features of type 2 diabetes, metabolic syndrome X, and Cushing's syndrome.* Diabetes, 2005. **54**(3): p. 591-602.
34. Summers, S.A., *Ceramides in insulin resistance and lipotoxicity.* Prog Lipid Res, 2006. **45**(1): p. 42-72.
35. Holland, W.L., J.T. Brozinick, L.P. Wang, E.D. Hawkins, K.M. Sargent, Y. Liu, K. Narra, K.L. Hoehn, T.A. Knotts, A. Siesky, D.H. Nelson, S.K. Karathanasis, G.K. Fontenot, M.J. Birnbaum and S.A. Summers, *Inhibition of ceramide synthesis ameliorates glucocorticoid-, saturated-fat-, and obesity-induced insulin resistance.* Cell Metab, 2007. **5**(3): p. 167-79.
36. Choi, K.M., Y.S. Lee, M.H. Choi, D.M. Sin, S. Lee, S.Y. Ji, M.K. Lee, Y.M. Lee, Y.P. Yun, J.T. Hong and H.S. Yoo, *Inverse relationship between adipocyte differentiation and ceramide level in 3T3-L1 cells.* Biol Pharm Bull, 2011. **34**(6): p. 912-6.
37. Samad, F., K.D. Hester, G. Yang, Y.A. Hannun and J. Bielawski, *Altered adipose and plasma sphingolipid metabolism in obesity: a potential mechanism for cardiovascular and metabolic risk.* Diabetes, 2006. **55**(9): p. 2579-87.
38. Zebisch, K., V. Voigt, M. Wabitsch and M. Brandsch, *Protocol for effective differentiation of 3T3-L1 cells to adipocytes.* Anal Biochem, 2012. **425**(1): p. 88-90.

39. Mehlem, A., C.E. Hagberg, L. Muhl, U. Eriksson and A. Falkevall, *Imaging of neutral lipids by oil red O for analyzing the metabolic status in health and disease.* Nat Protoc, 2013. **8**(6): p. 1149-54.
40. Mietla, J.A., D.S. Wijesinghe, L.A. Hoeferlin, M.D. Shultz, R. Natarajan, A.A. Fowler, 3rd and C.E. Chalfant, *Characterization of eicosanoid synthesis in a genetic ablation model of ceramide kinase.* J Lipid Res, 2013. **54**(7): p. 1834-47.
41. Chen, T.H., W.M. Chen, K.H. Hsu, C.D. Kuo and S.C. Hung, *Sodium butyrate activates ERK to regulate differentiation of mesenchymal stem cells.* Biochem Biophys Res Commun, 2007. **355**(4): p. 913-8.
42. Fu, L., T. Tang, Y. Miao, S. Zhang, Z. Qu and K. Dai, *Stimulation of osteogenic differentiation and inhibition of adipogenic differentiation in bone marrow stromal cells by alendronate via ERK and JNK activation.* Bone, 2008. **43**(1): p. 40-7.
43. Granado, M.H., P. Gangoiti, A. Ouro, L. Arana, M. Gonzalez, M. Trueba and A. Gomez-Munoz, *Ceramide 1-phosphate (C1P) promotes cell migration Involvement of a specific C1P receptor*. Cell Signal, 2009. **21**(3): p. 405-12.
44. Lefterova, M.I. and M.A. Lazar, *New developments in adipogenesis*. Trends Endocrinol Metab, 2009. **20**(3): p. 107-14.
45. Gregoire, F.M., C.M. Smas and H.S. Sul, *Understanding adipocyte differentiation.* Physiol Rev, 1998. **78**(3): p. 783-809.
46. Hannun, Y.A. and L.M. Obeid, *The Ceramide-centric universe of lipid-mediated cell regulation: stress encounters of the lipid kind.* J Biol Chem, 2002. **277**(29): p. 25847-50.
47. Futerman, A.H. and Y.A. Hannun, *The complex life of simple sphingolipids.* EMBO Rep, 2004. **5**(8): p. 777-82.
48. Ntambi, J.M. and K. Young-Cheul, *Adipocyte differentiation and gene expression.* J Nutr, 2000. **130**(12): p. 3122S-3126S.
49. Cornelius, P., O.A. MacDougald and M.D. Lane, *Regulation of adipocyte development.* Annu Rev Nutr, 1994. **14**: p. 99-129.
50. Tong, Q. and G.S. Hotamisligil, *Molecular mechanisms of adipocyte differentiation.* Rev Endocr Metab Disord, 2001. **2**(4): p. 349-55.
51. Otto, T.C. and M.D. Lane, *Adipose development: from stem cell to adipocyte.* Crit Rev Biochem Mol Biol, 2005. **40**(4): p. 229-42.
52. Mitsutake, S., T. Date, H. Yokota, M. Sugiura, T. Kohama and Y. Igarashi, *Ceramide kinase deficiency improves diet-induced obesity and insulin resistance*. FEBS Lett, 2012. **586**(9): p. 1300-5.
53. Hashimoto, T., J. Igarashi and H. Kosaka, *Sphingosine kinase is induced in mouse 3T3-L1 cells and promotes adipogenesis.* J Lipid Res, 2009. **50**(4): p. 602-10.
54. Xue, J.C., E.J. Schwarz, A. Chawla and M.A. Lazar, *Distinct stages in adipogenesis revealed by retinoid inhibition of differentiation after induction of PPARgamma.* Mol Cell Biol, 1996. **16**(4): p. 1567-75.
55. Reginato, M.J., S.L. Krakow, S.T. Bailey and M.A. Lazar, *Prostaglandins promote and block adipogenesis through opposing effects on peroxisome proliferator-activated receptor gamma*. J Biol Chem, 1998. **273**(4): p. 1855-8.
56. Zeidan, Y.H. and Y.A. Hannun, *Translational aspects of sphingolipid metabolism.* Trends Mol Med, 2007. **13**(8): p. 327-36.
57. Fuentes, P., M.J. Acuna, M. Cifuentes and C.V. Rojas, *The anti-adipogenic effect of angiotensin II on human preadipose cells involves ERK1,2 activation and PPARG phosphorylation.* J Endocrinol, 2010. **206**(1): p. 75-83.
58. Wang, T., Y. Wang, Y. Kontani, Y. Kobayashi, Y. Sato, N. Mori and H. Yamashita, *Evodiamine improves diet-induced obesity in a uncoupling protein-1-independent manner: involvement of antiadipogenic mechanism and extracellularly regulated kinase/mitogen-activated protein kinase signaling.* Endocrinology, 2009. **149**(1): p. 358-66.

59. Arana, L., M. Ordonez, A. Ouro, I.G. Rivera, P. Gangoiti, M. Trueba and A. Gomez-Munoz, *Ceramide 1-phosphate induces macrophage chemoattractant protein-1 release: involvement in ceramide 1-phosphate-stimulated cell migration.* Am J Physiol Endocrinol Metab, 2013. **304**(11): p. E1213-26.

Chapter 3

6. CHAPTER 3: Phosphatidylethanolamine N-metyltransferase (PEMT) is implicated in obesity-associated inflammation and cell migration.

1. INTRODUCTION

Several studies have demonstrated that obesity is closely related to inflammation [1-5]. In fact, obesity is now considered a chronic low-grade inflammation state, which starts in adipose tissue as it expands with excess fat and caloric intake, and involves the activation of inflammatory pathways in cells by nutrient-sensing and cytokine signaling. In particular, pro-inflammatory cytokines have been found to play a role in orchestrating the signaling mechanisms that take place in obesity-associated inflammatory responses. Consequently, obesity-associated inflammation can be regarded as a crucial factor in the development of obesity.

1.1. Obesity-associated inflammation

The inflammatory response is characterized by increased local and systemic cytokine levels along with increased number of infiltrated immune cells, with neutrophils dominating mainly in acute phases while macrophages are the main cells in chronic conditions [6]. However, obesity was shown to be associated with a slightly different type of inflammation referred to as chronic low-grade sterile inflammation or metainflammation. The chronic nature of obesity exerts a profound effect on metabolic pathways, playing one of the central roles in the development of insulin resistance (IR) [7, 8], and the interaction between immune and metabolic cells initiates and propagates the inflammatory response. In addition, inflammation results in secretion of cytokines and an enhanced production of leptin, which will activate adipose tissue T-lymphocytes and resident adipose tissue macrophages. This then leads to secretion of pro-inflammatory cytokines and chemokines from these cells, which attract immune cells including other T-lymphocytes, neutrophils, and monocytes [9-14]. Once in adipose tissue, monocytes differentiate to macrophages, and start secreting cytokines which act as an autocrine, paracrine or endocrine fashion [15-19] leading to the propagation of local inflammation in adipose tissue.

1.1.1. Macrophage infiltration into white adipose tissue (WAT)

Obesity promotes an intricate inflammatory response that involves the infiltration of immune cells to metabolic organs including adipose tissue. In an obese state, adipose-tissue-derived adipokine release and immune-cell derived cytokine release [20] increase, leading to a progressive immune cell infiltration into obese adipose tissue [9, 21], and also giving rise to an inflammatory state. Adipose tissue macrophages (ATMs), originally identified in murine fat depots by the expression of the macrophage protein F4/80, are the most abundant immune cells in adipose tissue. Although the majority of ATMs are thought to be recruited from the blood, macrophages can also proliferate within tissues in a process independent of monocytes and regulated by IL-4 [22, 23].

1.1.2. Macrophage polarization

In the present decade a new model has been developed that describes the complex mechanism of macrophage polarization [24, 25]. Due to the polarization state, macrophages configure a heterogeneous population with different functional roles [26]. In particular, adipose tissue macrophages consist of at least two different polarization states, which are classically activated “M1” pro-inflammatory macrophages and alternatively activated “M2” anti-inflammatory macrophages. Both M1 and M2 macrophages express F4/80 and CD68 surface markers, as they are generic macrophage markers. However, M1 and M2 macrophages exhibit completely different marker expression. These markers are transmembrane glycoproteins, scavenger receptors, enzymes, growth factors, hormones, cytokines and cytokine receptors with diverse functions.

1.1.2.1. Classically activated M1 pro-inflammatory macrophages.

The M1 activation is induced by intracellular pathogens, bacterial cell wall components, lipoproteins, and cytokines such as interferon gamma (IFN-γ). The M1 macrophages are characterized by a high production of nitric oxide (NO), resulting in an effective pathogen killing mechanism [24, 25, 27, 28]. In addition, M1 macrophages induce inflammatory cytokine secretion (TNF-α, IL-6, MCP-1) and therefore, they contribute to the induction of insulin resistance [29-31]. Furthermore, mice with targeted deletions in the genes for monocyte chemoattractant protein-1 (MCP-1/ccl2) and its receptor C-C motif chemokine receptor 2 (Ccr2) both have decreased ATM content, decreased inflammation in fat, and protection from high-fat diet-induced (HFD-induced) insulin resistance [32, 33].

M1 macrophages are identified based on the gene transcription or protein expression of a set of M1 markers. In fact, CD11c (integrin, alpha X) surface molecule is considered a M1 marker and its expression in ATM is considerably increased upon high-fat diet feeding [34].

1.1.2.2. Alternatively activated M2 anti-inflammatory macrophages

The alternatively activated or M2 macrophages are immune cells present in almost all organs in the body as resident cells under physiological conditions, where they act to maintain tissue homeostasis [31, 35, 36]. Based on the applied stimuli and the achieved transcriptional changes, the M2 macrophages have been classified into subdivisions [24, 27]. These are M2a, M2b, and M2c subdivisions. IL-4 and IL-13 activate M2a macrophages, immune complexes activate the M2b macrophages, and glucocorticoids and TGF-β activate the M2c.

The M2 macrophages have high phagocytosis capacity, producing extracellular matrix (ECM) components, angiogenic and chemotactic factors, and IL-10. In addition to the pathogen defense, M2 macrophages clear apoptotic cells, they can mitigate inflammatory responses, and they promote wound healing [37]. Although they are widely termed as anti-inflammatory macrophages, M2 macrophages can cause allergic inflammation, aid the growth of tumor tissues, and can act as cellular reservoirs for various pathogens [25]. Also, M2 macrophages have complex roles outside the context of inflammation, such as organ morphogenesis, tissue turnover, and endocrine signaling [24, 38-42].

M2 macrophages are reported to have a different gene expression profile, characterized by the relatively high expression of CD206 and CD163 surface markers and an increased IL-10 anti-inflammatory cytokine secretion.

CD206: C-type mannose receptor, which is a 175-kDa type I transmembrane glycoprotein, is considered a M2 macrophage marker in both mouse and human [27, 43]. Several types of tissue resident macrophages, such as cardiac resident macrophages, peritoneal macrophages, adipose tissue macrophages, placental macrophages (also known as Hofbauer cells), and macrophages of the skin express CD206 [44-49]. Lack of CD206 increases random migration of macrophages and results in the upregulation of proinflammatory cytokine production during endotoxemic lung inflammation in mouse [50]. CD206 deficiency also results in the elevated serum level of inflammatory proteins, suggesting that it has a role in the resolution of inflammation by clearing inflammatory molecules from the blood [51].

CD163: haptoglobin-hemoglobin scavenger receptor is expressed in some CD206-expressing tissue resident macrophages, such as mouse and human adipose tissue macrophages and placental macrophages [44, 45, 52, 53]. Its expression is amplified also by M-CSF, IL-6, IL-10, and glucocorticoids, while TNF-α, TGF-β, IFN-γ, and LPS reduce its expression [43, 54-56]. Macrophages coexpressing CD206 and CD163 are high IL-10, IL-1 receptor antagonist (IL-1ra), and CCL18 producers [48].

Under normal physiological conditions, 5-10% of adipose tissue cells are resident M2 macrophages. However, in obese adipose tissue, there is an imbalance in the ratio of M1/M2 macrophages, with M1 “pro-inflammatory” macrophages being enhanced and M2 “anti-inflammatory” macrophages being down-regulated, which leads to chronic inflammation and the propagation of metabolic dysfunction. Several studies reported that ATM from lean mice express many characteristic genes of M2 macrophages, which may protect adipocytes from inflammation, whereas diet-induced obesity led to a shift in the activation state to an M1 pro-inflammatory state that contributes to insulin resistance [34, 57, 58]. Therefore, sustaining the M2-like state of some tissue resident macrophages, such as Kupffer cells and adipose tissue macrophages, would diminish the production of inflammatory mediators and thus may be a therapeutic approach to treat metabolic diseases [41, 59].

1.2. Phosphatydilethanolamine N-methyltransferase (PEMT)

Phosphatidylcholine (PC) is the quantitatively major phospholipid of hepatic endoplasmic reticulum (ER) membranes in mammalian cells. The major pathway for biosynthesis of PC is the CDP-choline pathway, which is present in all eukaryotic cells. However, an alternative pathway for PC biosynthesis is the conversion of phosphatidylethanolamine (PE) to PC by PE-methyltransferase (PEMT) [60, 61]. Under normal conditions, the CDP-choline pathway accounts for 70% hepatic PC biosynthesis, and the remaining 30% is synthetized via the PEMT pathway [61].

In mice and rats the major enzymatic activity and immunoreactivity for PEMT is in the liver. In contrast, a minor activity was detected in adipose tissue, although it might also have important functions in this tissue. PEMT activity can be regulated by substrate availability, by the regulation of the enzyme expression or by transcriptional regulation.

1.2.1. Physiological functions of PEMT

PEMT is important for the biosynthesis of PC, which is a critical and essential component for membrane structure. In addition, PEMT also plays an important role in the secretion of hepatic very low density lipoproteins, since PC is quantitatively the most important phospholipid in this plasma lipoproteins [62, 63]. In order to determine whether PEMT has other function in mammalian cells, mice lacking PEMT were constructed (pemt$^{-/-}$ mice) [64]. The availability of pemt$^{-/-}$ mice permitted to determine the implication of this enzyme in atherosclerosis [65]. Moreover, it has recently been demonstrated that the lack of PEMT alters plasma VLDL levels [66] and decreases homocysteine (Hcy) levels in the plasma, suggesting that lack of PEMT protects mice from atherosclerosis [67]. Recently, it has been discovered that mice lacking PEMT are strikingly protected from high fat diet-induced obesity and insulin resistance [68]. Unlike pemt$^{+/+}$ mice, the PEMT-deficient mice held their weight constant [69], although the pemt$^{-/-}$ mice developed steatosis.

In 3T3-L1 fibroblasts PEMT expression/activity is not detected, however four days after the cells were differentiated into adipocytes, PEMT was expressed. These studies in 3T3-L1 cells demonstrated that PEMT has an important role in the stabilization of lipid droplets in 3T3-L1 adipocytes [70].

The role of PEMT in obesity and obesity-associated disorders has been firmly established based on *in vivo* and *in vitro* studies. Inflammation and cell migration are key events in obesity development, thus for a better understanding of how the lack of PEMT protects against obesity, we wanted to examine whether PEMT is implicated in obesity-associated processes such as inflammation and macrophage migration and signaling pathways involved in this action.

2. RESULTS

2.1. C1P decreases PEMT expression in 3T3-L1 differentiated cells

Recent studies have demonstrated that the lack of PEMT protects mice from the HFD-induced obesity [68]. On the other hand, we have found that C1P inhibits adipogenesis (chapter 2). As shown in Figure 2.1.1, C1P inhibits PEMT expression in 3T3-L1 differentiated adipocytes, suggesting that PEMT could be a target of C1P. Therefore, C1P could block adipogenesis not only via ERK phosphorylation, as we show in this Thesis (see chapter 2), but also by the inhibition of PEMT expression.

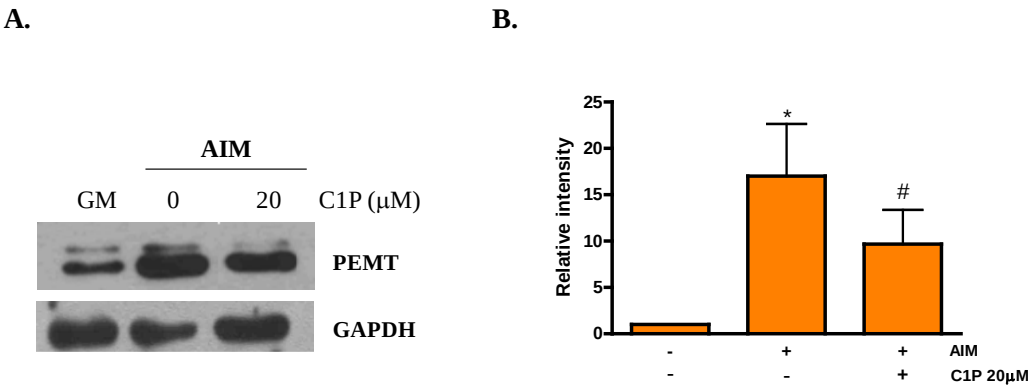

Figure 2.1.1. C1P inhibits PEMT expression in 3T3-L1 differentiated cells. 3T3-L1 cells were seeded in 6-well plates (1.2 x 10^5 cells/well) and they were grown in DMEM containing 10% NCS until they were about 90-100% confluent. Confluent cells were further incubated for 2 days before inducing cell differentiation. After two days, cells were cultured in growth medium (GM) or Adipogenic Induction Medium (AIM) with or without 20 μM of C1P. The medium was changed every 2 days and C1P was added each time. **A.** On the 7^{th} day of the differentiation process, cell lysates were prepared and PEMT expression was detected by Western blotting using a specific antibody to PEMT, and equal loading of protein was assessed with an antibody against GAPDH. Similar results were obtained in each of 5 replicate experiments. **B.** Results of the scanning densitometry of exposed film. Data are expressed as arbitrary units of intensity and are the mean ± SEM of 5 independent experiments (*$p<0.05$, #$p<0.05$).

Due to the importance of this enzyme, in this chapter we have focused on PEMT and its functions in obesity-associated processes.

2.2. Deficiency of PEMT protects mice from obesity-induced multi-cytokine release in white adipose tissue.

Obesity is considered a chronic low-grade inflammation and a wide range of different cytokines have been described to be increased in the obese state [2, 71]. In addition to demonstrating that PEMT-deficiency protects against diet-induced obesity, Vance and coworkers in collaboration with our group wanted to evaluate the effect of PEMT on cytokine release, since PEMT could also protect mice from obesity-induced inflammation. In order to test whether the lack of PEMT protects mice from obesity-induced inflammation, pemt$^{-/-}$ (PEMT-KO) and pemt$^{+/+}$ (WT) mice were fed with high fat diet for 10 weeks. After this, white adipose tissue (WAT) was used in order to perform a mouse cytokine antibody array. This array allows analysis of a variety of cytokines, chemokines and adipokines using a conventional ELISA kit. As shown in Figure 2.2.1, the expression of the adipokine leptin, some proinflammatory cytokines, including IL-1α, IL-4, and TNFα receptor I and II, and the chemokines MCP-1 and RANTES were lower in WAT from PEMT-deficient mice compared to WT mice. In addition, expression of the anti-inflammatory cytokine IL-10 was also studied and we found that its expression was slightly increased in PEMT-KO mice. These data suggest that the lack of PEMT not only protects mice from obesity, but also protects mice from obesity-associated inflammation.

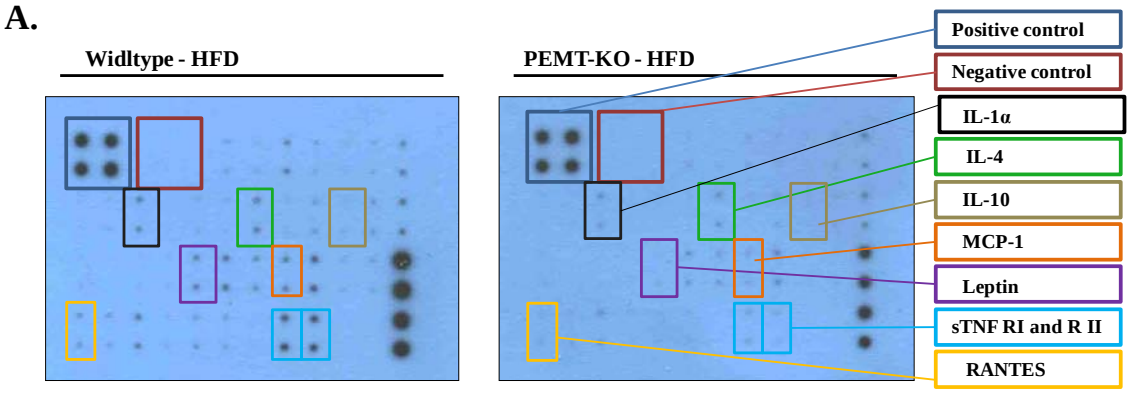

B.

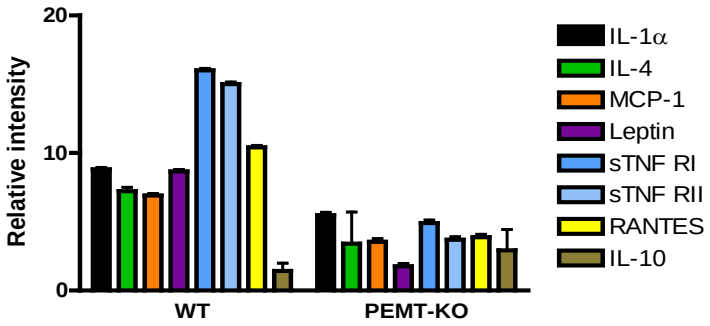

Figure 2.2.1. Lack of PEMT protects mice from HFD-induced proinflammatory cytokine release and increases anti-inflammatory cytokine release. White adipose tissue was homogenized in 1ml homogenization buffer. Adipose tissue was then centrifuged and supernatant was collected and used for the inflammation-related cytokine array. **A.** Multi-cytokine inflammatory array analysis was performed as indicated in *Materials and Methods.* **B.** Results of the scanning densitometry of the exposed film. Data are expressed as arbitrary units of intensity normalized to the protein content and are the mean ± range of 2 independent experiments.

2.3. Quantification of IL-1α, RANTES, MCP-1, IL-4, TNF-α, Leptin and IL-10 levels in WAT after HFD-feeding

Next, we tried to quantify some of the pro-inflammatory cytokines and chemokines that appeared to be more significantly decreased in PEMT-deficient mice and we also quantified the anti-inflammatory cytokine IL-10, which seems to be increased in PEMT-deficient mice. We found that after 10 weeks under a HFD, leptin levels were dramatically decreased in pemt$^{-/-}$ mice. In addition, WAT from pemt$^{-/-}$ mice had lower levels of the inflammatory cytokine TNF-α and the chemokines MCP-1 and RANTES. By contrast these mice had significantly higher levels of the anti-inflammatory cytokine IL-10 than pemt$^{+/+}$ (Figure 2.3.1) [72]. These data suggest that after 10 weeks of the HFD, *pemt*$^{-/-}$ mice showed an anti-inflammatory pattern of cytokines and chemokines in WAT, which is consistent with the results obtained in the mouse inflammation array. Altogether, the present data demonstrate that PEMT deficiency protects mice from obesity-induced inflammation.

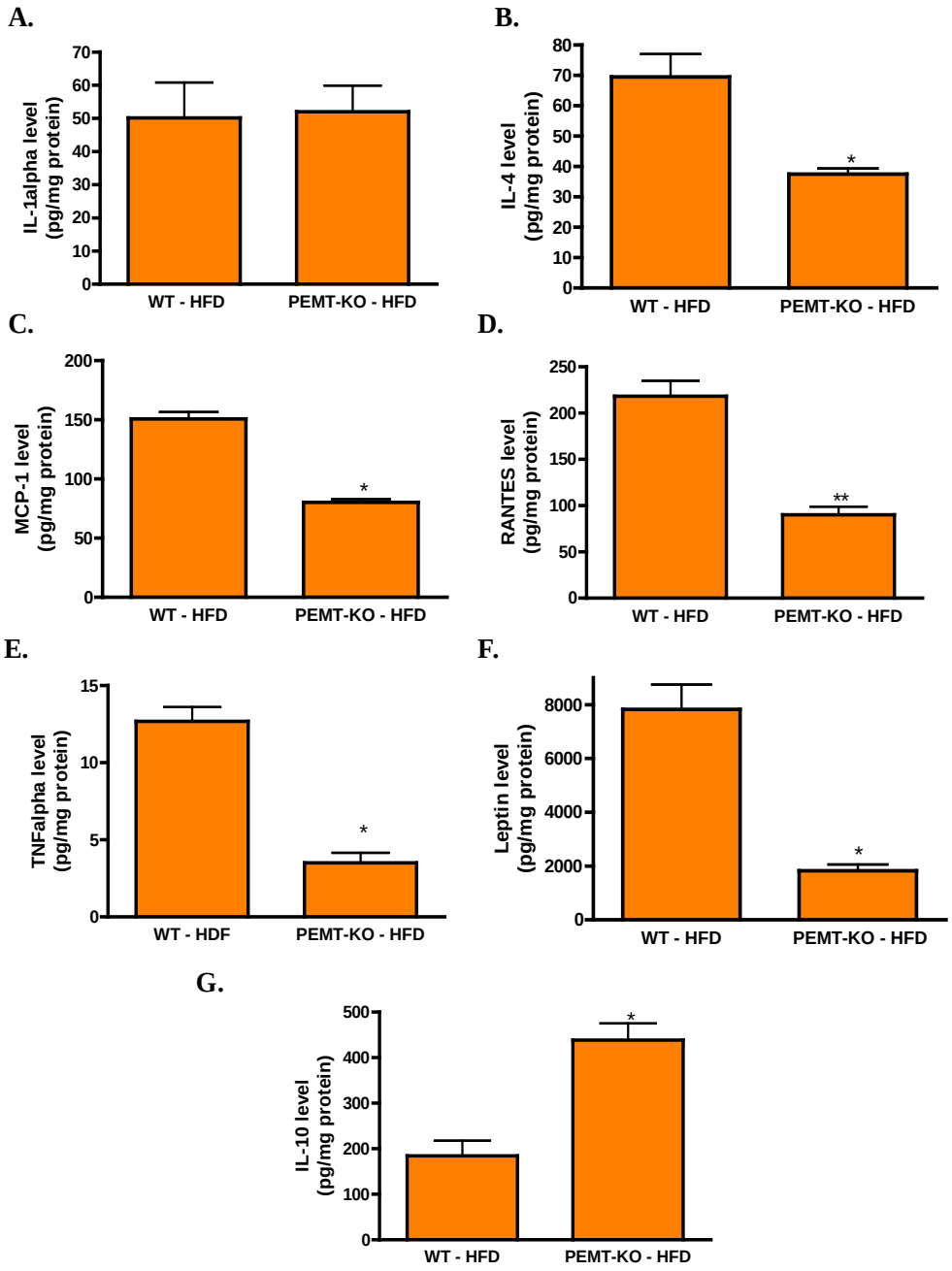

Figure 2.3.1 The lack of PEMT protects mice from HFD-induced proinflammatory cytokine release and increases the anti-inflammatory cytokine IL-10 release. White adipose tissue was homogenized in 1ml homogenization buffer. Adipose tissue was then centrifuged and supernatant was collected. Diluted (1:3) supernatants were used for ELISA experiments**. A-G** Tissue levels of proinflammatory cytokines (IL-1α, MCP-1, RANTES, TNF-α and IL-4), adipokine (Leptin) and IL-10 were quantified using ELISA kits, as indicated in *Materials and Methods*. Results are normalized to the protein concentration and are the mean ± SEM of 3 to 4 independent experiments perfomed in duplicate (*p<0.05, **p<0.01).

2.4. Deficiency of PEMT alters the phenotype of adipose tissue macrophages.

Adipose tissue inflammation, which is closely related to obesity, induces cytokine and chemokine production in order to promote recruitment of circulating monocytes, which differentiate into an M1 "pro-inflammatory" macrophage phenotype and their accumulation leads to an imbalance between M1 and M2 macrophages. Consequently, an increased cytokine production from M1 macrophages and/or reduced anti-inflammatory signals from the M2 macrophages promote adipose tissue dysfunction. Therefore, ATMs play important roles in obesity and obesity-associated disorders [9, 21, 32, 33]. Since deletion of PEMT protects mice from high fat diet-induced obesity, we hypothesized that the lack of PEMT would also reduce obesity-induced chronic inflammation. Accumulation of increased numbers of tissue macrophages is a key event in obesity-induced inflammation. Therefore, we wanted to examine whether PEMT deletion protects mice from macrophage infiltration into adipose tissue. In order to quantify macrophage numbers in adipose tissue, the mRNA expression of F4/80, which is a generic macrophage marker, was measured. It was found that WAT from PEMT-deficient mice exhibited a marked reduction in adipose tissue macrophage number, since F4/80 expression was significantly lower in WAT from pemt$^{-/-}$ mice (PEMT-KO). These data suggest that the lack of PEMT attenuates macrophage infiltration into adipose tissue (Figure 2.4.1).

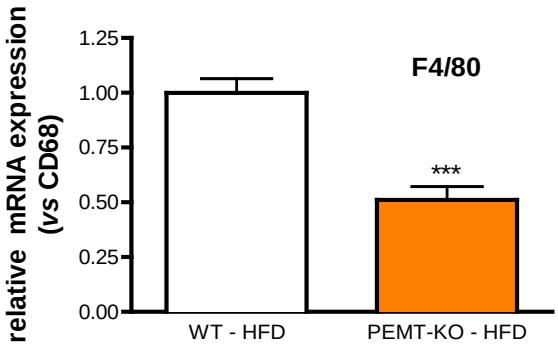

Figure 2.4.1. Relative mRNA expression for F4/80, a specific macrophage marker, is decreased in pemt-/- mice. 10 weeks after feeding mice with a high fat diet, total RNA was isolated from snap-frozen white adipose tissue using TRIzol reagent. Total RNA was treated with DNase I, then reverse-transcribed using oligo (Dt) and Superscript II reverse transcriptase. mRNA levels were determined by RT-qPCR using a Step One Plus system, as described in *Materials and Methods*. The F4/80 macrophage marker was detected using specific RNA primers. mRNA levels of specific F4/80 macrophage marker were normalized to the total CD68 mRNA. mRNA values were directly taken from Step One Plus machine. Data are the mean ±

SEM of 6 independent experiments. These results were obtained in Dr. Dennis Vance´s laboratory, at the Heritage Medical Research Centre of the University of Alberta (Edmonton, Canada).

Next, we wanted to study whether PEMT deficiency could attenuate obesity-associated inflammation by decreasing the number of classically activated M1 "proinflammatory" macrophages in adipose tissue. In order to quantify M1 and M2 macrophages, the expression of several genes characteristic of M1 and M2 were measured in WAT after 10 week of HFD.

A recent report [34] proposed that classically activated M1 macrophages or alternatively activated M2 ATMs are distinguished by the presence or the absence of CD11c. M1 ATMs produce proinflammatory cytokines, such as TNF-α, IL-6, and MCP-1, thus contributing to the induction of insulin resistance. As shown in Figure 2.4.2, CD11c and MCP-1 mRNA levels, which are M1 macrophage markers, are decreased in PEMT-KO mice, suggesting that deletion of PEMT downregulates M1 macrophage phenotype and thus, protects mice from obesity-induced inflammatory state.

A.

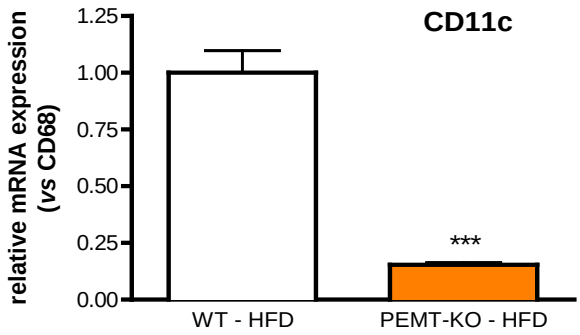

B.

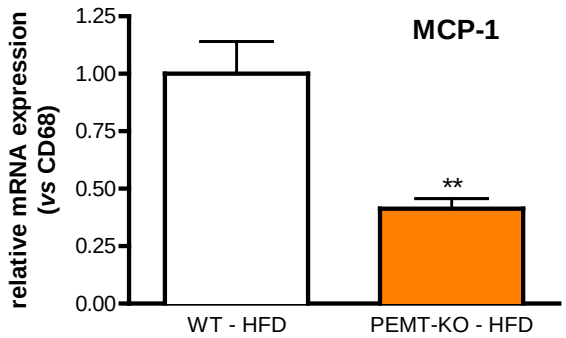

Figure 2.4.2. Assessment of M1 macrophages in WAT from HFD-fed wildtype and PEMT-KO mice. Ten weeks after feeding mice with high fat diet, total RNA was isolated from snap-frozen white adipose tissue using TRIzol reagent. Total RNA was treated with DNase I, then reverse-transcribed using oligo (Dt) and Superscript II reverse transcriptase. mRNA levels were determined by RT-qPCR using a Step One Plus system, as described in *Materials and Methods*. **A.** The CD11c M1 macrophage marker was detected using specific RNA primers. mRNA levels were normalized to the total CD68 mRNA, which is a generic macrophage marker. mRNA values were directly taken from Step One Plus machine. Data are the mean ± SEM of 6 independent experiments (***p<0.001). **B.** The MCP-1 M1 macrophage marker was detected with specific RNA primers. mRNA levels were normalized to the total CD68 mRNA, which is a generic macrophage marker. mRNA values were directly taken from Step One Plus machine. Data are the mean ± SEM of 6 independent experiments (**p<0.01). These results were obtained in Dr. Dennis Vance´s laboratory, at the Heritage Medical Research Centre of the University of Alberta (Edmonton, Canada).

On the other hand, M2 ATMs, which are the major resident macrophages in lean adipose tissue, are reported to have a different gene expression profile, characterized by the relatively high expression of CD206, CD163 and IL-10, which are involved in the repair or remodeling of tissues. In connection with the reduction of obesity-associated inflammation by PEMT, we hypothesized that M2 macrophage markers could be increased in pemt$^{-/-}$ mice. However, no difference was observed in the mRNA expression of CD206 and CD163 between pemt$^{+/+}$ mice and pemt$^{-/-}$ mice. Unlike CD206 and CD163, the mRNA expression of IL-10 cytokine of the HFD-fed PEMT-deficient mice tended to be reduced compared with those of pemt+/+ mice, although the changes are not significant (Figure 2.4.3).

A.

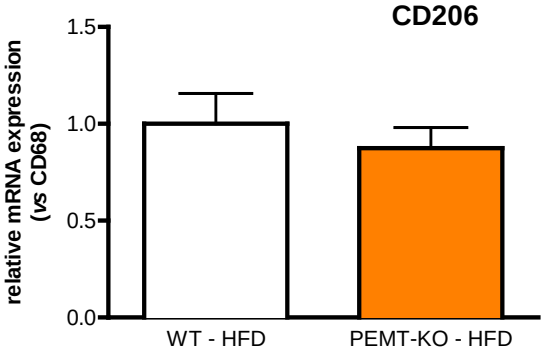

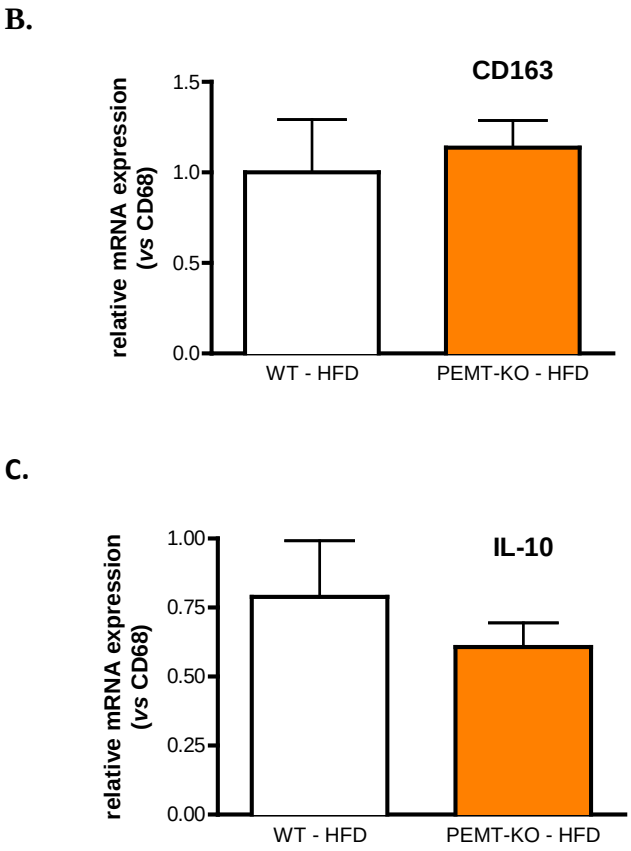

Figure 2.4.3. Assessment of M2 macrophages in WAT from HFD-fed wildtype and PEMT-KO mice. Ten weeks after feeding mice with a high fat diet, total RNA was isolated from snap-frozen white adipose tissue using TRIzol reagent. Total RNA was treated with DNase I, then reverse-transcribed using oligo (Dt) and Superscript II reverse transcriptase. mRNA levels were determined by RT-qPCR using a Step One Plus system, as described in *Materials and Methods.* **A.** The CD206 M2 macrophage marker was detected with specific RNA primers. mRNA levels were normalized to the total CD68 mRNA, which is a generic macrophage marker. mRNA values were directly taken from Step One Plus machine. Data are the mean ± SEM of 6 independent experiments. **B.** CD163 M2 macrophage marker was detected with specific RNA primers. mRNA levels were normalized to the total CD68, which is a generic macrophage marker. mRNA values were directly taken from Step One Plus machine. Data are the mean ± SEM of 6 independent experiments. **C.** The IL-10 M2 macrophage marker was detected with specific RNA primers. mRNA levels were normalized to the total CD68 mRNA. mRNA values were directly taken from Step One Plus machine. Data are the mean ± SEM of 6 independent experiments. These results were obtained in Dr. Dennis Vance´s laboratory, at the Heritage Medical Research Centre of the University of Alberta (Edmonton, Canada).

To further study whether PEMT deficiency modifies macrophage polarization, we characterized the activation state of WAT macrophages from HFD-fed $pemt^{+/+}$ and $pemt^{-/-}$ mice. In order to determine macrophage phenotype double immunofluorescence stainning was performed, first with a CD68 antibody in order to identify all macrophages, and second with a CD11c antibody to identify M1-like macrophages (Figure 2.4.4).

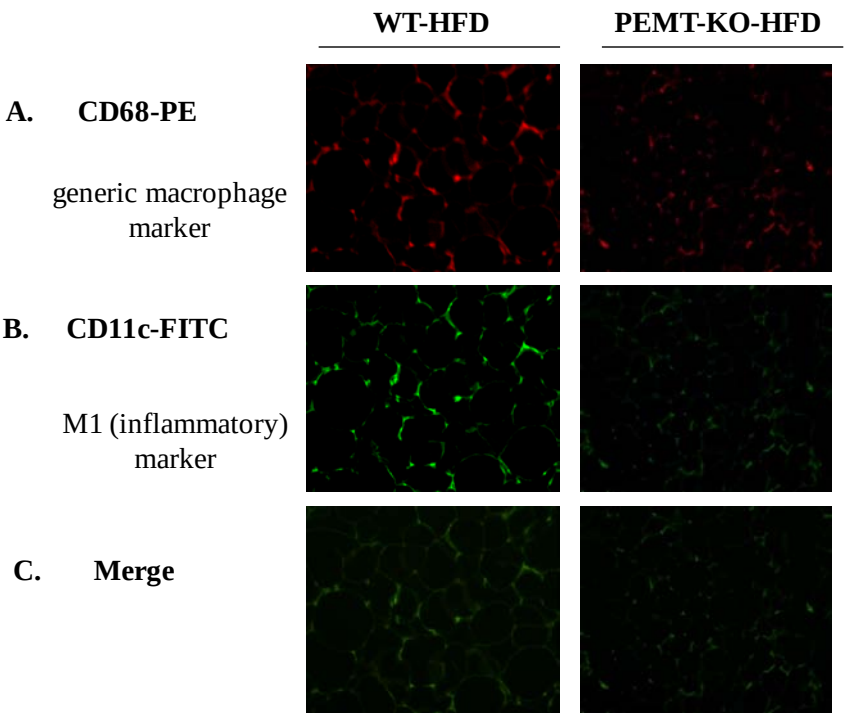

Figure 2.4.4. Immunofluorescence analysis of macrophage phenotype in WAT from HFD-fed pemt $^{+/+}$ and pemt $^{-/-}$ mice. Mouse white adipose tissue was collected and fixed in 10% formalin buffered. Fixed adipose tissue samples were immunoreacted with CD68-PE fluorescent antibody to identify all macrophages and CD11c-A488 fluorescent antibody to identify M1 (inflammatory) macrophages, following the protocol described in *Materials and Methods*. Photomicrographs of a representative field that includes white adipose tissue surrounded by macrophages. **A.** Bright-field overlay showing immunofluorescence reactivity to antibodies recognizing a general macrophage marker (CD68, red). **B.** Bright-field overlay showing a marker preferentially expressed in M1 macrophages (CD11c, green). **C.** Bright-field showing double-immunofluorescence reactivity to antibodies recognizing general macrophage marker (CD68, red), and a marker preferentially expressed in M1 macrophages (CD11c, green). This protocol was carried out at the HistoCore service of the Heritage Medical Research Centre (University of Alberta). Micrographs of white adipose tissue from wildtype and pemt-knockout mice were taken with a Leica DM IRE2 microscope.

Figure 2.4.4 shows a representative image of macrophage infiltration into WAT from pemt$^{-/-}$ and pemt$^{+/+}$ mice. There are clear differences between WAT from pemt$^{-/-}$ mice and WAT from pemt $^{+/+}$ mice after 10 week under a HFD. First, macrophage infiltration was decreased in WAT from PEMT-KO mice. Second, PEMT-deficient mice exhibited a marked reduction in accumulation of classically activated M1 “pro-inflammatory” macrophages in white adipose tissue (CD11c, a M1 “inflammatory” macrophage marker, was less expressed in WAT from PEMT-deficient mice). Third, compared to wildtype mice, PEMT-deficient mice are resistant to diet-induced hypertrophy of adipocytes in white adipose tissue, thus PEMT deficiency could hinder adipocyte

differentiation, resulting in lack of adipose hypertrophy in HFD-fed *Pemt*$^{-/-}$ mice (Figure 2.4.4). Taken together, these data suggest that PEMT deficiency attenuates the accumulation of M1 macrophages in HFD-fed WAT and it also protects from adipocyte hypertrophy, which are key events in the development of obesity and obesity-induced inflammation.

Altogether, these data demonstrate that the lack of PEMT not only protects mice from HFD-induced obesity, but also from obesity-induced inflammation, since accumulation of M1 "proinflammatory" macrophages and pro-inflammatory cytokines/chemokines levels were decreased in HFD-fed PEMT deficient mice, whereas anti-inflammatory IL-10 cytokine was increased. Therefore, the anti-inflammatory effect of PEMT deficiency would attenuate the development of obesity and obesity-associated disorders.

2.5. PEMT overexpression induces J774A.1 macrophage migration in a time-dependent manner

We have already demonstrated that the lack of PEMT modulates macrophage phenotype in adipose tissue, giving rise to a less inflammatory state. Given that the lack of PEMT decreases macrophage infiltration into adipose tissue, it was decided to examine the effect of PEMT overexpression in J774A.1 macrophages. In order to determine whether PEMT was able to promote cell migration in macrophages, we first tested the efficiency of PEMT transfection. The cells were transfected with a PEMT plasmid and then we determined PEMT expression by Western blotting. Figure 2.5.1b shows that J774A.1 macrophages were efficiently transfected. Subsequently, cell migration was assessed and we observed that transfection of PEMT in macrophages caused a significant increase in cell migration in a time dependent manner (Figure 2.5.1a). In addition, for better visualization of PEMT-induced cell migration, micrographs of the migration assay chambers were taken (Figure 2.5.1c).

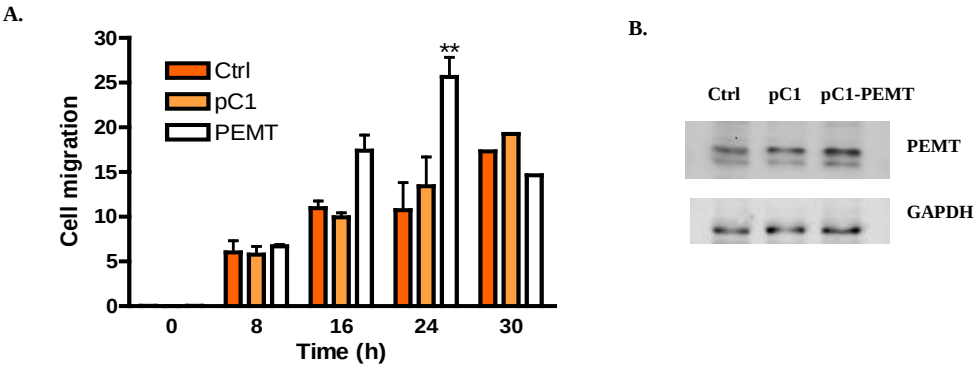

C.

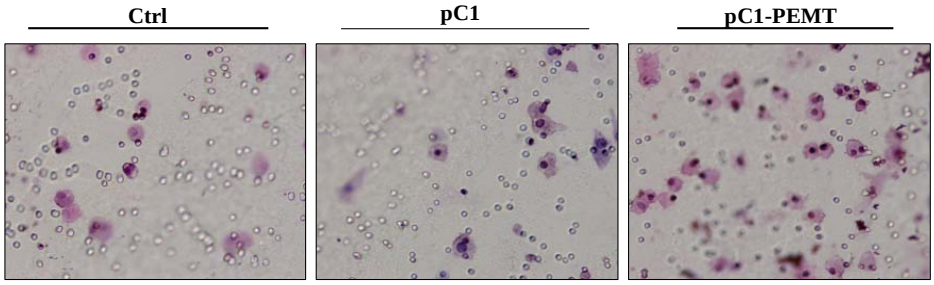

Figure 2.5.1. PEMT overexpression induces J774A.1 macrophage migration in a time-dependent manner. Cells were seeded in 60 mm dishes (2 x 10^5 cells/dish) and transfected with either pC1-PEMT plasmid, pC1 empty vector or vehicle, as described in *Materials and Methods*. Cells were then scrapped and counted. **A.** Cells (5 x 10^4 cells/well) were seeded in the upper wells of 24-well chambers coated with fibronectin and incubated for the indicated times. Cell migration was determined as indicated in *Materials and Methods*. Results are the mean ± SEM of 3 independent experiments performed in duplicate (**p<0.01). **B.** Overexpression of PEMT was confirmed by Western blotting using a specific antibody to PEMT. Equal loading of protein was monitored using a specific antibody to GAPDH. Similar results were obtained in each of 3 independent experiments. **C.** Micrographs of migrated J774A.1 cells in chambers after PEMT overexpression. Pictures were taken with a Nikon Eclipse 90i microscope.

2.6. PEMT overexpression induces ERK, Akt and mTOR phosphorylation in J774A.1 macrophages

We next studied the implication of PI3K/Akt/mTOR pathway, which is one of the best characterized pathways linked to cell motility functions, in PEMT-induced J774A.1 macrophage migration. First, we studied whether PEMT overexpression was able to induce phosphorylation of ERK, Akt and mTOR in these cells. We observed that after transfection with the PEMT plasmid, Akt1, ERK and mTOR phosphorylation was increased in J774A.1 macrophages (Figure 2.6.1), suggesting that the PI3K/Akt/mTOR pathway might be a downstream target of PEMT.

A.

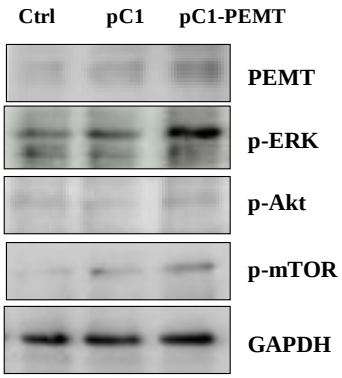

B.

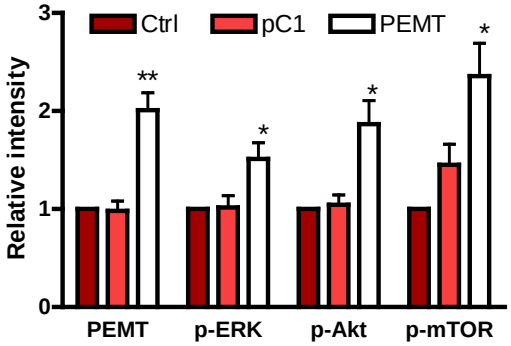

Figure 2.6.1. PEMT overexpression induces ERK, Akt and mTOR phosphorylation in J774A.1 macrophages. Cells were seeded in 60 mm dishes (2 x 10^5 cells/dish) and transfected with either pC1-PEMT plasmid, pC1 empty vector or vehicle, as described in *Materials and Methods*. **A.** Cells were then harvested and PEMT, p-ERK, p-Akt and p-mTOR were detected by Western blotting using specific antibodies. Equal loading of protein was assessed with an antibody against GAPDH. Similar results were obtained in 4 different experiments. **B.** Results of scanning densitometry of exposed film. Data are expressed as arbitrary units of intensity and are the mean ± SEM of the 4 independent experiments (*p<0.05, **p<0.01).

2.7. The PI3K/Akt1/mTOR pathway is implicated in PEMT overexpression-induced macrophage migration.

To determine the implication of the PI3K/Akt/mTOR pathway in PEMT-induced macrophage migration, cells were transfected with the PEMT plasmid and then, cell migration was performed using selective inhibitors of these three kinases: LY294002 for PI3K, 10-DEBC for Akt1 and rapamycin for mTOR. All of these reagents potently reduced PEMT-induced cell migration (Figure 2.7.1).

A.

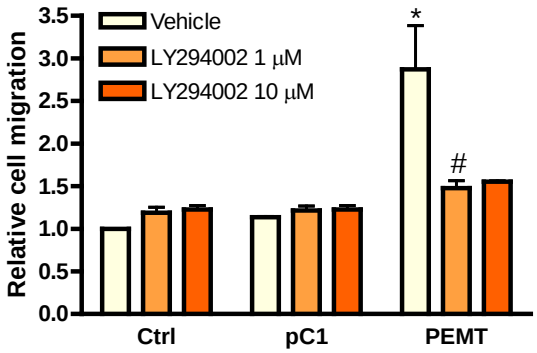

B.

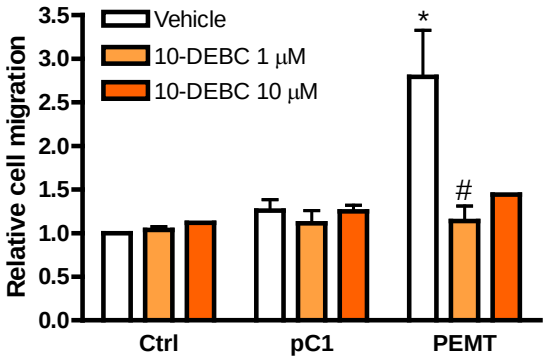

C.

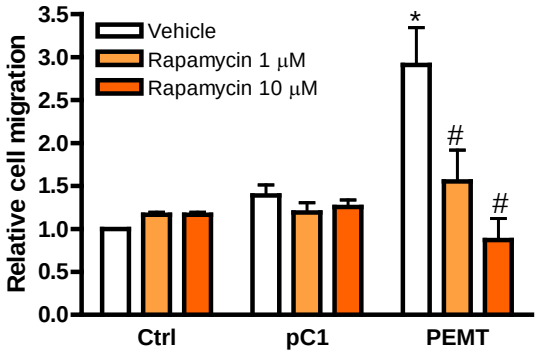

Figure 2.7.1. The PI3K/Akt1/mTOR pathway is implicated in PEMT-induced J774A.1 macrophage migration. Cells were seeded in 60 mm dishes (2 x 10^5 cells/dish) and transfected with either pC1-PEMT plasmid, pC1 empty vector or vehicle, as described in *Materials and Methods***.** Cells were then seeded in the upper wells of 24-well fibronectin precoated chambers (5 x 10^4 cells/well). After 1 hour of preincubation, cells were incubated with different inhibitors, as indicated. **A.** Cells were preincubated for 1 hour with LY294002 at the indicated concentrations. Then, either vehicle or LY294002 inhibitor was added in the lower chambers at the indicated concentrations. Cells were then incubated for 24 hours and macrophage migration was determined as indicated in *Materials and Methods.* Data are expressed as the number of migrated cells relative to the number of cells migrated in the control chamber and are the mean ± SEM of 3 independent experiments performed in duplicate (*$p<0.05$, #$p<0.05$). **B.** Cells were preincubated for 1 hour with 10-DEBC at the indicated concentrations. Then, either vehicle or LY294002 inhibitor was added in the lower chambers at the indicated concentrations. Cells were then incubated for 24 hours and cell migration was determined as indicated in *Materials and Methods.* Data are expressed as the number of migrated cells relative to the number of cells migrated in the control chamber and are the mean ± SEM of 4 independent experiments performed in duplicate (*$p<0.05$, #$p<0.05$). **C.** Cells were preincubated for 1 hour with Rapamycin at the indicated concentrations. Then, either vehicle or Rapamycin was added in the lower chambers at the indicated concentrations. Cells were then incubated for 24 hours and cell migration was determined as indicated in *Materials and Methods.* Data are expressed as the number of migrated cells relative to the number of cells migrated in the control chamber and are the mean ± SEM of 4 independent experiments performed in duplicate (*$p<0.05$, #$p<0.05$).

The implication of PI3K, Akt and mTOR in PEMT-stimulated cell migration was also studied using siRNA to silence the corresponding genes encoding these kinases. Silencing of Akt1 in J774A.1 cells completely blocked PEMT-induced cell migration (Figure 2.7.2).

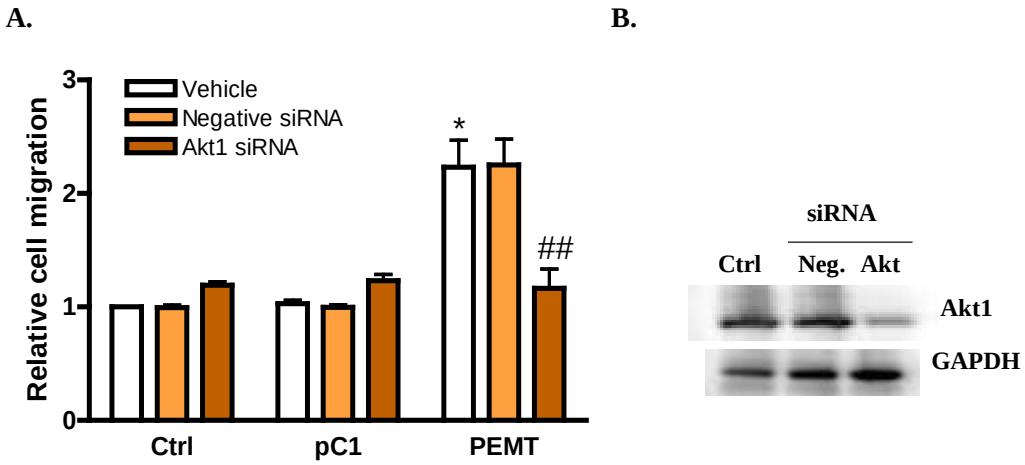

Figure 2.7.2. Akt1 siRNA blocks PEMT overexpression-induced cell migration in J774A.1 cells. Cells were seeded in 60 mm dishes (2 x 10^5 cells/dish) and siRNA transfection was performed as described in *Materials and Methods.* After siRNA treatment, cells were transfected with either pC1-PEMT plasmid, pC1 empty vector or vehicle, as indicated in *Materials and Methods.* Cells were then scrapped and counted. **A.** Cells were seeded in the upper wells of 24-well fibronectin precoated chambers (5 x 10^4 cells/well). Cells were then incubated for 24 hours and cell migration was determined as indicated in *Materials and Methods.* Data are expressed as the number of migrated cells relative to the number of cells migrated in the control chamber and are the mean ± SEM of 3 independent experiments performed in duplicate (*p<0.05, ##p<0.01). **B.** After treatment, cells were collected and the Akt1 siRNA inhibitory efficiency was confirmed by Western blotting using a specific antibody against Akt1. Equal loading of protein was monitored using a specific antibody to GAPDH. Similar results were obtained in each of 2 independent experiments.

We also found that PI3K gene silencing resulted in inhibition of PEMT overexpression-induced cell migration in J774A.1 macrophages (Figure 2.7.3)

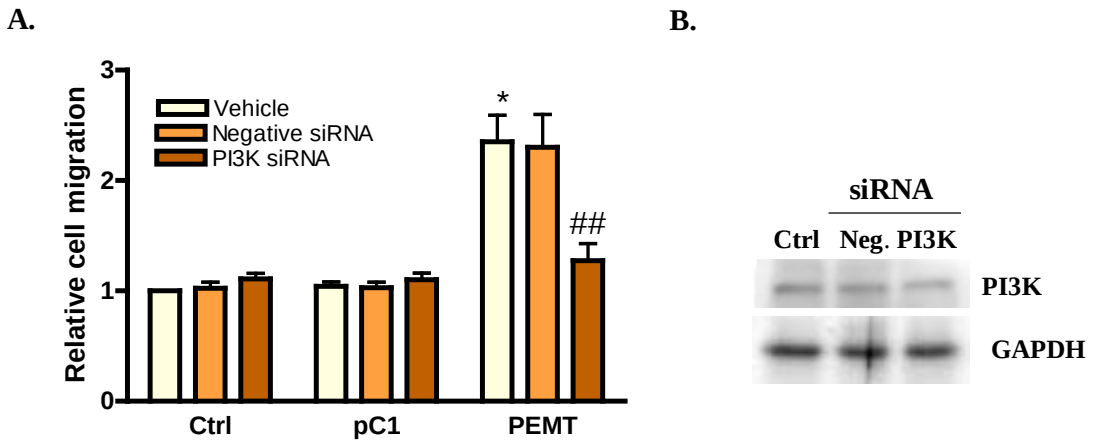

Figure 2.7.3. PI3K siRNA blocks PEMT overexpression-induced cell migration in J774A.1 cells. Cells were seeded in 60 mm dishes (2 x 10^5 cells/dish) and siRNA transfection was performed as described in *Materials and Methods.* After siRNA treatment, cells were transfected with either pC1-PEMT plasmid, pC1 empty vector or vehicle, as indicated in

Materials and Methods. Cells were then scrapped and counted. **A.** Macrophages were seeded in the upper wells of 24-well fibronectin precoated chambers (5 x 10^4 cells/well). Cells were then incubated for 24 hours and cell migration was determined as indicated in *Materials and Methods.* Data are expressed as the number of migrated cells relative to the number of cells migrated in the control chamber and are the mean ± SEM of 3 independent experiments performed in duplicate (*p<0.05, ##p<0.01). **B.** After treatment, cells were collected and the PI3K siRNA inhibitory efficiency was assessed by Western blotting using a specific antibody against PI3K. Equal loading of protein was monitored using a specific antibody to GAPDH. Similar results were obtained in each of 2 independent experiments.

Likewise, siRNA technology was used for mTOR gene silencing. We observed that mTOR1 was also required for PEMT-stimulated cell migration (Figure 2.7.4).

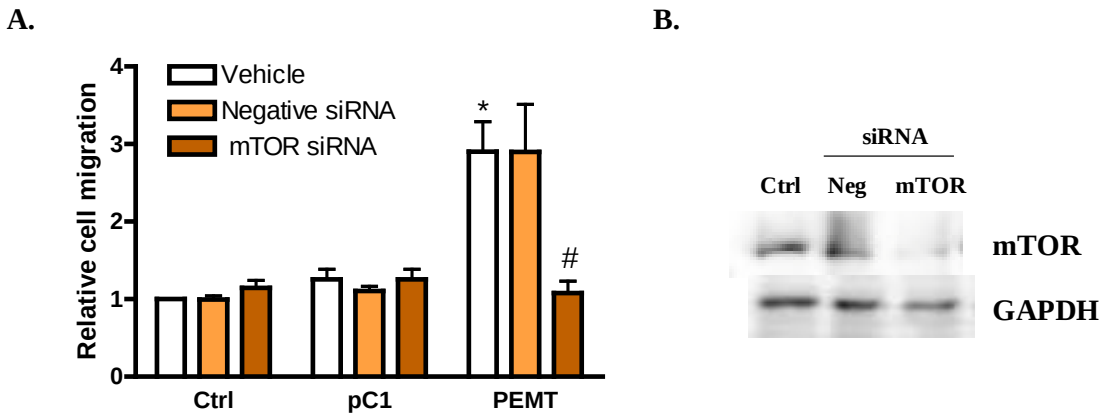

Figure 2.7.4. mTOR siRNA blocks PEMT overexpression-induced cell migration in J774A.1 cells. Cells were seeded in 60 mm dishes (2 x 10^5 cells/dish) and the siRNA treatment was performed as described in *Materials and Methods.* After siRNA treatment, cells were transfected with pC1-PEMT plasmid, pC1 empty vector or vehicle, as indicated in *Materials and Methods.* Cells were then scrapped and counted. **A.** Macrophages were seeded in the upper wells of 24-well fibronectin precoated chambers (5 x 10^4 cells/well). Cells were then incubated for 24 hours and cell migration was determined as indicated in *Materials and Methods.* Data are expressed as the number of migrated cells relative to the number of cells migrated in the control chamber and are the mean ± SEM of 3 independent experiments performed in duplicate (*p<0.05, ##p<0.01). **B.** After treatment, cells were collected and the mTOR siRNA inhibitory efficiency was confirmed by Western blotting using specific antibody against mTOR. Equal loading of protein was monitored using a specific antibody to GAPDH. Similar results were obtained in each of 2 independent experiments.

Altogether, these data demonstrate that upregulation of the PI3K/Akt1/mTOR1 pathway is one of the key signaling pathways to trigger PEMT-induced cell migration in macrophages.

Several lines of evidence indicate that cell migration is associated to receptor-mediated effects, and some of these receptors are coupled to Gi proteins. Although the mechanism by which PEMT induces macrophage migration is unknown, we tested the

possible involvement GPCRs in this process. For this, cells were transfected with the PEMT-plasmid and then cell migration experiments were performed in the presence or in the absence of Ptx, a well-known inhibitor of GPCRs, as previously mentioned. We found that Ptx was able to completely block PEMT-induced J774A.1 cell migration at a concentration as low as 10 pg/ml (Figure 2.7.5).

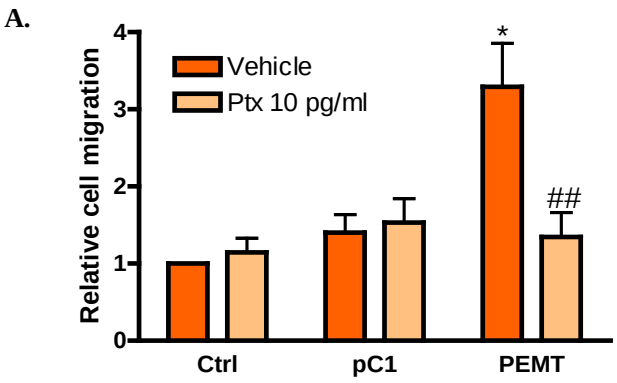

Figure 2.7.5. PEMT overexpression-induced cell migration in J774A.1 cells was GiPCR-dependent. Cells were seeded in 60 mm dishes (2 x 10^5 cells/dish) and transfected with either pC1-PEMT plasmid, pC1 empty vector or vehicle, as described in *Materials and Methods*. Cells were then counted and seeded in the upper wells of 24-well fibronectin precoated chambers (5 x 10^4 cells/well). After 1 hour of preincubation, cells were incubated with 10 pg/ml of Ptx for 4 hours in the upper chambers. Then, either vehicle or 10 pg/ml of Ptx were added in the lower chambers. Cells were then incubated for 24 hours and cell migration was determined as indicated in *Materials and Methods.* Data are expressed as the number of migrated cells relative to the number of cells migrated in the control chamber and are the mean ± SEM of 4 independent experiments performed in duplicate (*$p<0.05$, ##$p<0.01$).

2.8. Lack of toxicity of the inhibitors used in this work

All commonly used chemical inhibitors in cell signaling studies have been described to be toxic for cells at certain concentrations or incubation times. Therefore, we performed cell viability assays and showed that none of the pharmacological inhibitors used in this Thesis caused any significant decrease in cell viability (see chapter 1).

3. DISCUSSION

Chronic inflammation is an important factor linking obesity with obesity-related disorders including insulin resistance, and atherosclerosis [20, 73, 74]. Some studies suggest that a key mechanism underlying obesity-induced inflammation is the macrophage infiltration into adipose tissue, particularly in obese adipose tissue [9, 21]. These adipose tissue macrophages (ATMs) can span de spectrum from the most pro-inflammatory, M1-like, cells to anti-inflammatory, M2-like macrophages [34, 57, 75]. In obesity, the balance is tilted toward the M1-like macrophage polarization state [34], and these cells secrete a number of different proinflammatory cytokines, such as TNF-α and MCP-1. However, inflammation is not the only mechanism involved in the development of obesity-associated disorders. In fact, various abnormalities in lipid metabolism have been described, which can also impair insulin resistance [76, 77]. Therefore, chronic tissue inflammation and lipid abnormalities are not completely unrelated processes. In fact, these two systems are closely intertwined, and each of them can amplify the other in an *in vivo* pathophysiologic setting.

As mentioned above, PEMT is a major enzyme implicated in lipid metabolism. This enzyme catalyzes the methylation of phosphatidylethanolamine (PE) to phosphatidylcholine (PC). Although PC is mainly produced via the CDP-choline pathway, 30% of the PC synthesis is catalyzed by PEMT [61, 69]. *Pemt* mRNA and activity are predominantly expressed in the liver. However, PEMT activity has also been demonstrated in other tissues, including adipose tissue [69], in which *pemt* expression is induced by a HFD [70]. Furthermore, using *pemt*$^{-/-}$ mice fed a HFD, it was shown that PEMT plays a critical role in obesity and insulin resistance [68]. Consistent with these studies using animal models, it was demonstrated that human obese subjects show transcriptional upregulation of the *pemt* gene [78]. Therefore, it was hypothesized that *pemt* deficiency might protect against obesity-induced chronic inflammation.

Taking into consideration that WAT is an important endocrine organ for the secretion of cytokines and chemokines [79], we firstly examined endocrine function of white adipose tissue by comparing, both qualitatively and quantitatively, the tissue levels of cytokines and chemokines from pemt$^{-/-}$ and pemt$^{+/+}$ mice after 10 weeks of HFD feeding. We found that pemt$^{-/-}$ mice fed a HFD for 10 weeks displayed lower levels of

the inflammatory cytokine TNF-α and chemokines MCP-1 and RANTES, but significantly higher levels of the anti-inflammatory cytokine IL-10 than pemt$^{+/+}$ mice. Consequently, it could be concluded that PEMT deficiency protected against obesity-induced inflammation. However, these differences of cytokines and chemokines between pemt$^{-/-}$ and pemt$^{+/+}$ mice were not seen after 2 weeks of HFD feeding [72], and we recently suggested that the resistance to diet-induced obesity phenotype is subsequent to the fatty liver phenotype.

On another hand, adipose hypoxia and adipose hypertrophy are closely related to obesity-induced inflammation. Interestingly, adipose tissue hypertrophy leads to a release of cytokines that are responsible for macrophage recruitment into adipose tissue. Several studies suggest that adipose tissue from lean mice contains resident M2 macrophages that serve a homeostatic role and it is now widely accepted that macrophages that infiltrate into the expanded adipose tissue in obesity are derived from circulating monocytes and assume an M1 “pro-inflammatory” phenotype [53, 80]. In this thesis we show that macrophage infiltration was decreased in WAT of pemt$^{-/-}$ mice, and that the lack of PEMT reduced the mRNA expression of M1 macrophage markers, suggesting that PEMT deficiency markedly decreased the population of M1 pro-inflammatory ATMs. However, the mRNA expression of M2 “anti-inflammatory” markers, and the levels of IL-10 were not affected by PEMT deficiency. Rather than distinct macrophage populations, M1 and M2 signatures do not necessarily exclude each other and often they coexist. The resultant mixed phenotype then depends on the balance of activating and inhibitory activities as well as the tissue environment [81, 82]. Interestingly, the lack of PEMT prevented accumulation of M1 ATMs in obese adipose tissue, thereby altering the balance between inflammatory M1 and M2 ATMs.

We also found that M1 macrophage accumulation was decreased in pemt$^{-/-}$ mice, and that adipocytes were smaller in WAT from mice lacking PEMT than in wildtype mice, suggesting that PEMT deficiency protects these animals from adipocyte hypertrophy. So, it could be concluded that the lack of PEMT protects mice from macrophage infiltration and counteracts obesity-induced inflammation.

Macrophage polarization toward a classically activated (M1) or alternatively activated (M2) state depends largely on soluble factors, such as cytokines and lipid mediators [83, 84]. Interestingly, obesity promotes the mobilization of monocytes from the bone

marrow in part by activating the chemokine receptor CCR2 [32, 85, 86]. Global deficiency of *ccr2* or its ligand, *Ccl2* (MCP-1) in mice results in a failure of monocyte mobilization and is associated with protection from monocyte infiltration into adipose tissue and insulin resistance [32, 86]. The present study demonstrates that PEMT deficiency also led to a decrease in adipose tissue expression of MCP-1, suggesting that activation of the PEMT pathway may be important for subsequent production of chemokine-driven amplification loops in obesity.

Also, our data provide clear evidence that elimination of PC biosynthesis via elimination of the *pemt* gene strikingly attenuated obesity-induced inflammation. This beneficial effect is likely attributable, at least in part, to a reduction of adipocyte hypertrophy. This protection against adipocyte hypertrophy causes a reduction of macrophage infiltration into adipose tissue, where accumulation of M1 "proinflammatory" macrophages is decreased, and therefore, pro-inflammatory cytokine levels are also diminished. These findings suggest that the proinflammatory response of adipose tissue to high fat diet results in PEMT production or activation, which could serve to induce macrophage migration into adipose tissue.

The present studies also revealed that PEMT overexpression promoted macrophage migration, which we associated to significant increases in the phosphorylation of ERK1/2, Akt1 and mTOR. However, other showed that overexpression of PEMT downregulated the PI3K/Akt signaling pathway in rat hepatoma cells [87], suggesting a different role of this pathway in hepatic cancer. Of interest, we also observed that this pathway plays a key role in PEMT-induced macrophage migration. Moreover, PEMT-induced macrophage migration required participation of a Ptx-sensitive GPCR, but the mechanism by which PEMT leads to stimulation of this receptor remains unknown. Nonetheless, one might speculate that PEMT overexpression could induce release of specific cytokines that might be able to interact with GPCRs, thereby inducing cell migration. On the other hand, PEMT could also be released and somehow interact with a putative GPCR in an autocrine manner thereby leading to macrophage migration. However, this possibility is at the moment also speculative. Therefore, further studies are necessary to elucidate the mechanism by which PEMT overexpression induces cell migration.

In this Thesis, it is proposed that blockade of macrophage infiltration is one of the mechanisms by which PEMT deficiency protects against high-fat diet-induced obesity and obesity-induced inflammation, and that activation of the PI3K/Akt/mTOR pathway is, at least partially responsible for increasing macrophage migration.

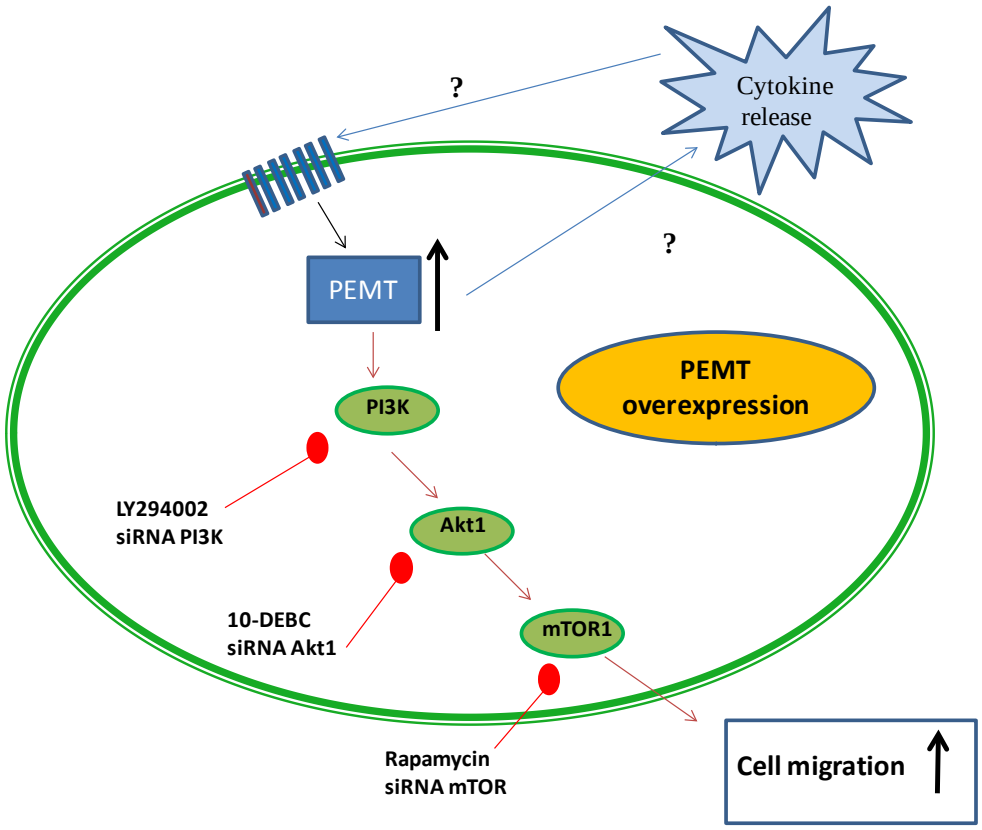

Figure 3.1. Working model for the implication of PEMT in J774A.1 macrophage migration

4. REFERENCES

1. Bullo, M., P. Casas-Agustench, P. Amigo-Correig, J. Aranceta and J. Salas-Salvado, *Inflammation, obesity and comorbidities: the role of diet.* Public Health Nutr, 2007. **10**(10A): p. 1164-72.
2. Clement, K. and S. Vignes, *[Inflammation, adipokines and obesity]*. Rev Med Interne, 2009. **30**(9): p. 824-32.
3. Ferrante, A.W., Jr., *Obesity-induced inflammation: a metabolic dialogue in the language of inflammation.* J Intern Med, 2007. **262**(4): p. 408-14.
4. Hurt, R.T., T.H. Frazier, P.J. Matheson, M.C. Cave, R.N. Garrison, C.J. McClain and S.A. McClave, *Obesity and inflammation: II.* Curr Gastroenterol Rep, 2007. **9**(4): p. 306-7.
5. Hurt, R.T., T.H. Frazier, P.J. Matheson, M.C. Cave, R.N. Garrison, C.J. McClain and S.A. McClave, *Obesity and inflammation: III.* Curr Gastroenterol Rep, 2007. **9**(4): p. 307-8.
6. Lee, B.C. and J. Lee, *Cellular and molecular players in adipose tissue inflammation in the development of obesity-induced insulin resistance.* Biochim Biophys Acta, 2014. **1842**(3): p. 446-62.
7. Heilbronn, L.K. and L.V. Campbell, *Adipose tissue macrophages, low grade inflammation and insulin resistance in human obesity.* Curr Pharm Des, 2008. **14**(12): p. 1225-30.
8. Oliver, E., F. McGillicuddy, C. Phillips, S. Toomey and H.M. Roche, *The role of inflammation and macrophage accumulation in the development of obesity-induced type 2 diabetes mellitus and the possible therapeutic effects of long-chain n-3 PUFA.* Proc Nutr Soc, 2010. **69**(2): p. 232-43.
9. Weisberg, S.P., D. McCann, M. Desai, M. Rosenbaum, R.L. Leibel and A.W. Ferrante, Jr., *Obesity is associated with macrophage accumulation in adipose tissue.* J Clin Invest, 2003. **112**(12): p. 1796-808.
10. Elgazar-Carmon, V., A. Rudich, N. Hadad and R. Levy, *Neutrophils transiently infiltrate intra-abdominal fat early in the course of high-fat feeding.* J Lipid Res, 2008. **49**(9): p. 1894-903.
11. Takeya, M., *[Monocytes and macrophages--multifaced cell population involved in inflammation, atherosclerosis, and obesity]*. Nihon Rinsho, 2005. **63 Suppl 4**: p. 117-22.
12. Sartipy, P. and D.J. Loskutoff, *Monocyte chemoattractant protein 1 in obesity and insulin resistance.* Proc Natl Acad Sci U S A, 2003. **100**(12): p. 7265-70.
13. Ilan, Y., R. Maron, A.M. Tukpah, T.U. Maioli, G. Murugaiyan, K. Yang, H.Y. Wu and H.L. Weiner, *Induction of regulatory T cells decreases adipose inflammation and alleviates insulin resistance in ob/ob mice.* Proc Natl Acad Sci U S A, 2010. **107**(21): p. 9765-70.
14. Kintscher, U., M. Hartge, K. Hess, A. Foryst-Ludwig, M. Clemenz, M. Wabitsch, P. Fischer-Posovszky, T.F. Barth, D. Dragun, T. Skurk, H. Hauner, M. Bluher, T. Unger, A.M. Wolf, U. Knippschild, V. Hombach and N. Marx, *T-lymphocyte infiltration in visceral adipose tissue: a primary event in adipose tissue inflammation and the development of obesity-mediated insulin resistance.* Arterioscler Thromb Vasc Biol, 2008. **28**(7): p. 1304-10.
15. Catalan, V., J. Gomez-Ambrosi, B. Ramirez, F. Rotellar, C. Pastor, C. Silva, A. Rodriguez, M.J. Gil, J.A. Cienfuegos and G. Fruhbeck, *Proinflammatory cytokines in obesity: impact of type 2 diabetes mellitus and gastric bypass.* Obes Surg, 2007. **17**(11): p. 1464-74.

16. Dinarello, C.A., *Role of pro- and anti-inflammatory cytokines during inflammation: experimental and clinical findings.* J Biol Regul Homeost Agents, 1997. **11**(3): p. 91-103.
17. Kabelitz, D. and R. Medzhitov, *Innate immunity--cross-talk with adaptive immunity through pattern recognition receptors and cytokines.* Curr Opin Immunol, 2007. **19**(1): p. 1-3.
18. Matsuzawa, Y., I. Shimomura, S. Kihara and T. Funahashi, *Importance of adipocytokines in obesity-related diseases.* Horm Res, 2003. **60 Suppl 3**: p. 56-9.
19. Nishimura, S., I. Manabe and R. Nagai, *Adipose tissue inflammation in obesity and metabolic syndrome.* Discov Med, 2009. **8**(41): p. 55-60.
20. Olefsky, J.M. and C.K. Glass, *Macrophages, inflammation, and insulin resistance.* Annu Rev Physiol, 2010. **72**: p. 219-46.
21. Xu, H., G.T. Barnes, Q. Yang, G. Tan, D. Yang, C.J. Chou, J. Sole, A. Nichols, J.S. Ross, L.A. Tartaglia and H. Chen, *Chronic inflammation in fat plays a crucial role in the development of obesity-related insulin resistance.* J Clin Invest, 2003. **112**(12): p. 1821-30.
22. Jenkins, S.J., D. Ruckerl, P.C. Cook, L.H. Jones, F.D. Finkelman, N. van Rooijen, A.S. MacDonald and J.E. Allen, *Local macrophage proliferation, rather than recruitment from the blood, is a signature of TH2 inflammation.* Science, 2011. **332**(6035): p. 1284-8.
23. Jenkins, S.J., D. Ruckerl, G.D. Thomas, J.P. Hewitson, S. Duncan, F. Brombacher, R.M. Maizels, D.A. Hume and J.E. Allen, *IL-4 directly signals tissue-resident macrophages to proliferate beyond homeostatic levels controlled by CSF-1.* J Exp Med, 2013. **210**(11): p. 2477-91.
24. Martinez, F.O. and S. Gordon, *The M1 and M2 paradigm of macrophage activation: time for reassessment.* F1000Prime Rep, 2014. **6**: p. 13.
25. Sica, A. and A. Mantovani, *Macrophage plasticity and polarization: in vivo veritas.* J Clin Invest, 2012. **122**(3): p. 787-95.
26. Wynn, T.A. and L. Barron, *Macrophages: master regulators of inflammation and fibrosis.* Semin Liver Dis, 2010. **30**(3): p. 245-57.
27. Murray, P.J., J.E. Allen, S.K. Biswas, E.A. Fisher, D.W. Gilroy, S. Goerdt, S. Gordon, J.A. Hamilton, L.B. Ivashkiv, T. Lawrence, M. Locati, A. Mantovani, F.O. Martinez, J.L. Mege, D.M. Mosser, G. Natoli, J.P. Saeij, J.L. Schultze, K.A. Shirey, A. Sica, J. Suttles, I. Udalova, J.A. van Ginderachter, S.N. Vogel and T.A. Wynn, *Macrophage activation and polarization: nomenclature and experimental guidelines.* Immunity, 2014. **41**(1): p. 14-20.
28. Benoit, M., B. Desnues and J.L. Mege, *Macrophage polarization in bacterial infections.* J Immunol, 2008. **181**(6): p. 3733-9.
29. Mantovani, A., A. Sica, S. Sozzani, P. Allavena, A. Vecchi and M. Locati, *The chemokine system in diverse forms of macrophage activation and polarization.* Trends Immunol, 2004. **25**(12): p. 677-86.
30. Gordon, S., *Alternative activation of macrophages.* Nat Rev Immunol, 2003. **3**(1): p. 23-35.
31. Gordon, S. and F.O. Martinez, *Alternative activation of macrophages: mechanism and functions.* Immunity, 2010. **32**(5): p. 593-604.
32. Weisberg, S.P., D. Hunter, R. Huber, J. Lemieux, S. Slaymaker, K. Vaddi, I. Charo, R.L. Leibel and A.W. Ferrante, Jr., *CCR2 modulates inflammatory and metabolic effects of high-fat feeding.* J Clin Invest, 2006. **116**(1): p. 115-24.

33. Kanda, H., S. Tateya, Y. Tamori, K. Kotani, K. Hiasa, R. Kitazawa, S. Kitazawa, H. Miyachi, S. Maeda, K. Egashira and M. Kasuga, *MCP-1 contributes to macrophage infiltration into adipose tissue, insulin resistance, and hepatic steatosis in obesity.* J Clin Invest, 2006. **116**(6): p. 1494-505.
34. Lumeng, C.N., J.L. Bodzin and A.R. Saltiel, *Obesity induces a phenotypic switch in adipose tissue macrophage polarization.* J Clin Invest, 2007. **117**(1): p. 175-84.
35. Martinez, F.O., L. Helming and S. Gordon, *Alternative activation of macrophages: an immunologic functional perspective.* Annu Rev Immunol, 2009. **27**: p. 451-83.
36. Zeyda, M. and T.M. Stulnig, *Adipose tissue macrophages.* Immunol Lett, 2007. **112**(2): p. 61-7.
37. Ferrante, C.J. and S.J. Leibovich, *Regulation of Macrophage Polarization and Wound Healing.* Adv Wound Care (New Rochelle), 2012. **1**(1): p. 10-16.
38. Pollard, J.W., *Trophic macrophages in development and disease.* Nat Rev Immunol, 2009. **9**(4): p. 259-70.
39. Forbes, S.J. and N. Rosenthal, *Preparing the ground for tissue regeneration: from mechanism to therapy.* Nat Med, 2014. **20**(8): p. 857-69.
40. Muraille, E., O. Leo and M. Moser, *TH1/TH2 paradigm extended: macrophage polarization as an unappreciated pathogen-driven escape mechanism?* Front Immunol, 2014. **5**: p. 603.
41. Glass, C.K. and J.M. Olefsky, *Inflammation and lipid signaling in the etiology of insulin resistance.* Cell Metab, 2012. **15**(5): p. 635-45.
42. Rosen, E.D. and B.M. Spiegelman, *What we talk about when we talk about fat.* Cell, 2014. **156**(1-2): p. 20-44.
43. Porcheray, F., S. Viaud, A.C. Rimaniol, C. Leone, B. Samah, N. Dereuddre-Bosquet, D. Dormont and G. Gras, *Macrophage activation switching: an asset for the resolution of inflammation.* Clin Exp Immunol, 2005. **142**(3): p. 481-9.
44. Zeyda, M., D. Farmer, J. Todoric, O. Aszmann, M. Speiser, G. Gyori, G.J. Zlabinger and T.M. Stulnig, *Human adipose tissue macrophages are of an anti-inflammatory phenotype but capable of excessive pro-inflammatory mediator production.* Int J Obes (Lond), 2007. **31**(9): p. 1420-8.
45. Aron-Wisnewsky, J., J. Tordjman, C. Poitou, F. Darakhshan, D. Hugol, A. Basdevant, A. Aissat, M. Guerre-Millo and K. Clement, *Human adipose tissue macrophages: m1 and m2 cell surface markers in subcutaneous and omental depots and after weight loss.* J Clin Endocrinol Metab, 2009. **94**(11): p. 4619-23.
46. Haase, J., U. Weyer, K. Immig, N. Kloting, M. Bluher, J. Eilers, I. Bechmann and M. Gericke, *Local proliferation of macrophages in adipose tissue during obesity-induced inflammation.* Diabetologia, 2004. **57**(3): p. 562-71.
47. Titos, E., B. Rius, A. Gonzalez-Periz, C. Lopez-Vicario, E. Moran-Salvador, M. Martinez-Clemente, V. Arroyo and J. Claria, *Resolvin D1 and its precursor docosahexaenoic acid promote resolution of adipose tissue inflammation by eliciting macrophage polarization toward an M2-like phenotype.* J Immunol, 2011. **187**(10): p. 5408-18.
48. Svensson-Arvelund, J., R.B. Mehta, R. Lindau, E. Mirrasekhian, H. Rodriguez-Martinez, G. Berg, G.E. Lash, M.C. Jenmalm and J. Ernerudh, *The human fetal placenta promotes tolerance against the semiallogeneic fetus by inducing regulatory T cells and homeostatic M2 macrophages.* J Immunol, 2015. **194**(4): p. 1534-44.

49. Dupasquier, M., P. Stoitzner, H. Wan, D. Cerqueira, A. van Oudenaren, J.S. Voerman, K. Denda-Nagai, T. Irimura, G. Raes, N. Romani and P.J. Leenen, *The dermal microenvironment induces the expression of the alternative activation marker CD301/mMGL in mononuclear phagocytes, independent of IL-4/IL-13 signaling.* J Leukoc Biol, 2006. **80**(4): p. 838-49.
50. Kambara, K., W. Ohashi, K. Tomita, M. Takashina, S. Fujisaka, R. Hayashi, H. Mori, K. Tobe and Y. Hattori, *In vivo depletion of CD206+ M2 macrophages exaggerates lung injury in endotoxemic mice.* Am J Pathol, 2015. **185**(1): p. 162-71.
51. Lee, S.J., S. Evers, D. Roeder, A.F. Parlow, J. Risteli, L. Risteli, Y.C. Lee, T. Feizi, H. Langen and M.C. Nussenzweig, *Mannose receptor-mediated regulation of serum glycoprotein homeostasis.* Science, 2002. **295**(5561): p. 1898-901.
52. Tang, Z., T. Niven-Fairchild, S. Tadesse, E.R. Norwitz, C.S. Buhimschi, I.A. Buhimschi and S. Guller, *Glucocorticoids enhance CD163 expression in placental Hofbauer cells.* Endocrinology, 2013. **154**(1): p. 471-82.
53. Shaul, M.E., G. Bennett, K.J. Strissel, A.S. Greenberg and M.S. Obin, *Dynamic, M2-like remodeling phenotypes of CD11c+ adipose tissue macrophages during high-fat diet--induced obesity in mice.* Diabetes, 2010. **59**(5): p. 1171-81.
54. Svensson, J., M.C. Jenmalm, A. Matussek, R. Geffers, G. Berg and J. Ernerudh, *Macrophages at the fetal-maternal interface express markers of alternative activation and are induced by M-CSF and IL-10.* J Immunol, 2011. **187**(7): p. 3671-82.
55. Ritter, M., C. Buechler, T. Langmann, E. Orso, J. Klucken and G. Schmitz, *The scavenger receptor CD163: regulation, promoter structure and genomic organization.* Pathobiology, 1999. **67**(5-6): p. 257-61.
56. Van den Heuvel, M.M., C.P. Tensen, J.H. van As, T.K. Van den Berg, D.M. Fluitsma, C.D. Dijkstra, E.A. Dopp, A. Droste, F.A. Van Gaalen, C. Sorg, P. Hogger and R.H. Beelen, *Regulation of CD 163 on human macrophages: cross-linking of CD163 induces signaling and activation.* J Leukoc Biol, 1999. **66**(5): p. 858-66.
57. Lumeng, C.N., S.M. Deyoung, J.L. Bodzin and A.R. Saltiel, *Increased inflammatory properties of adipose tissue macrophages recruited during diet-induced obesity.* Diabetes, 2007. **56**(1): p. 16-23.
58. Fujisaka, S., I. Usui, A. Bukhari, M. Ikutani, T. Oya, Y. Kanatani, K. Tsuneyama, Y. Nagai, K. Takatsu, M. Urakaze, M. Kobayashi and K. Tobe, *Regulatory mechanisms for adipose tissue M1 and M2 macrophages in diet-induced obese mice.* Diabetes, 2009. **58**(11): p. 2574-82.
59. Osborn, O. and J.M. Olefsky, *The cellular and signaling networks linking the immune system and metabolism in disease.* Nat Med, 2012. **18**(3): p. 363-74.
60. Vance, D.E., Z. Li and R.L. Jacobs, *Hepatic phosphatidylethanolamine N-methyltransferase, unexpected roles in animal biochemistry and physiology.* J Biol Chem, 2007. **282**(46): p. 33237-41.
61. DeLong, C.J., Y.J. Shen, M.J. Thomas and Z. Cui, *Molecular distinction of phosphatidylcholine synthesis between the CDP-choline pathway and phosphatidylethanolamine methylation pathway.* J Biol Chem, 1999. **274**(42): p. 29683-8.
62. Quehenberger, O., A.M. Armando, A.H. Brown, S.B. Milne, D.S. Myers, A.H. Merrill, S. Bandyopadhyay, K.N. Jones, S. Kelly, R.L. Shaner, C.M. Sullards, E. Wang, R.C. Murphy, R.M. Barkley, T.J. Leiker, C.R. Raetz, Z. Guan, G.M.

Laird, D.A. Six, D.W. Russell, J.G. McDonald, S. Subramaniam, E. Fahy and E.A. Dennis, *Lipidomics reveals a remarkable diversity of lipids in human plasma.* J Lipid Res, 2010. **51**(11): p. 3299-305.

63. Cole, L.K., J.E. Vance and D.E. Vance, *Phosphatidylcholine biosynthesis and lipoprotein metabolism.* Biochim Biophys Acta, 2012. **1821**(5): p. 754-61.
64. Walkey, C.J., L.R. Donohue, R. Bronson, L.B. Agellon and D.E. Vance, *Disruption of the murine gene encoding phosphatidylethanolamine N-methyltransferase.* Proc Natl Acad Sci U S A, 1997. **94**(24): p. 12880-5.
65. Pilgeram, L.O. and D.M. Greenberg, *Susceptibility to experimental atherosclerosis and the methylation of ethanolamine 1,2-C14 to phosphatidyl choline.* Science, 1954. **120**(3123): p. 760-1.
66. Zhao, Y., B. Su, R.L. Jacobs, B. Kennedy, G.A. Francis, E. Waddington, J.T. Brosnan, J.E. Vance and D.E. Vance, *Lack of phosphatidylethanolamine N-methyltransferase alters plasma VLDL phospholipids and attenuates atherosclerosis in mice.* Arterioscler Thromb Vasc Biol, 2009. **29**(9): p. 1349-55.
67. Noga, A.A., L.M. Stead, Y. Zhao, M.E. Brosnan, J.T. Brosnan and D.E. Vance, *Plasma homocysteine is regulated by phospholipid methylation.* J Biol Chem, 2003. **278**(8): p. 5952-5.
68. Jacobs, R.L., Y. Zhao, D.P. Koonen, T. Sletten, B. Su, S. Lingrell, G. Cao, D.A. Peake, M.S. Kuo, S.D. Proctor, B.P. Kennedy, J.R. Dyck and D.E. Vance, *Impaired de novo choline synthesis explains why phosphatidylethanolamine N-methyltransferase-deficient mice are protected from diet-induced obesity.* J Biol Chem, 2010. **285**(29): p. 22403-13.
69. Vance, D.E., *Physiological roles of phosphatidylethanolamine N-methyltransferase.* Biochim Biophys Acta, 2013. **1831**(3): p. 626-32.
70. Horl, G., A. Wagner, L.K. Cole, R. Malli, H. Reicher, P. Kotzbeck, H. Kofeler, G. Hofler, S. Frank, J.G. Bogner-Strauss, W. Sattler, D.E. Vance and E. Steyrer, *Sequential synthesis and methylation of phosphatidylethanolamine promote lipid droplet biosynthesis and stability in tissue culture and in vivo.* J Biol Chem, 2011. **286**(19): p. 17338-50.
71. Hotamisligil, G.S., N.S. Shargill and B.M. Spiegelman, *Adipose expression of tumor necrosis factor-alpha: direct role in obesity-linked insulin resistance.* Science, 1993. **259**(5091): p. 87-91.
72. Gao, X., J.N. van der Veen, M. Hermansson, M. Ordonez, A. Gomez-Munoz, D.E. Vance and R.L. Jacobs, *Decreased lipogenesis in white adipose tissue contributes to the resistance to high fat diet-induced obesity in phosphatidylethanolamine N-methyltransferase-deficient mice.* Biochim Biophys Acta, 2015. **1851**(2): p. 152-62.
73. Hotamisligil, G.S. and E. Erbay, *Nutrient sensing and inflammation in metabolic diseases.* Nat Rev Immunol, 2008. **8**(12): p. 923-34.
74. Lumeng, C.N. and A.R. Saltiel, *Inflammatory links between obesity and metabolic disease.* J Clin Invest, 2011. **121**(6): p. 2111-7.
75. Nguyen, M.T., S. Favelyukis, A.K. Nguyen, D. Reichart, P.A. Scott, A. Jenn, R. Liu-Bryan, C.K. Glass, J.G. Neels and J.M. Olefsky, *A subpopulation of macrophages infiltrates hypertrophic adipose tissue and is activated by free fatty acids via Toll-like receptors 2 and 4 and JNK-dependent pathways.* J Biol Chem, 2007. **282**(48): p. 35279-92.
76. Savage, D.B., K.F. Petersen and G.I. Shulman, *Disordered lipid metabolism and the pathogenesis of insulin resistance.* Physiol Rev, 2007. **87**(2): p. 507-20.

77. Itani, S.I., N.B. Ruderman, F. Schmieder and G. Boden, *Lipid-induced insulin resistance in human muscle is associated with changes in diacylglycerol, protein kinase C, and IkappaB-alpha.* Diabetes, 2002. **51**(7): p. 2005-11.
78. Sharma, N.K., K.A. Langberg, A.K. Mondal and S.K. Das, *Phospholipid biosynthesis genes and susceptibility to obesity: analysis of expression and polymorphisms.* PLoS One, 2013. **8**(5): p. e65303.
79. Waki, H. and P. Tontonoz, *Endocrine functions of adipose tissue.* Annu Rev Pathol, 2007. **2**: p. 31-56.
80. Lumeng, C.N., J.B. DelProposto, D.J. Westcott and A.R. Saltiel, *Phenotypic switching of adipose tissue macrophages with obesity is generated by spatiotemporal differences in macrophage subtypes.* Diabetes, 2008. **57**(12): p. 3239-46.
81. Pettersen, J.S., J. Fuentes-Duculan, M. Suarez-Farinas, K.C. Pierson, A. Pitts-Kiefer, L. Fan, D.A. Belkin, C.Q. Wang, S. Bhuvanendran, L.M. Johnson-Huang, M.J. Bluth, J.G. Krueger, M.A. Lowes and J.A. Carucci, *Tumor-associated macrophages in the cutaneous SCC microenvironment are heterogeneously activated.* J Invest Dermatol, 2011. **131**(6): p. 1322-30.
82. Vogel, D.Y., E.J. Vereyken, J.E. Glim, P.D. Heijnen, M. Moeton, P. van der Valk, S. Amor, C.E. Teunissen, J. van Horssen and C.D. Dijkstra, *Macrophages in inflammatory multiple sclerosis lesions have an intermediate activation status.* J Neuroinflammation, 2013. **10**: p. 35.
83. Gordon, S. and P.R. Taylor, *Monocyte and macrophage heterogeneity.* Nat Rev Immunol, 2005. **5**(12): p. 953-64.
84. Biswas, S.K. and A. Mantovani, *Macrophage plasticity and interaction with lymphocyte subsets: cancer as a paradigm.* Nat Immunol, 2010. **11**(10): p. 889-96.
85. Takahashi, K., S. Mizuarai, H. Araki, S. Mashiko, A. Ishihara, A. Kanatani, H. Itadani and H. Kotani, *Adiposity elevates plasma MCP-1 levels leading to the increased CD11b-positive monocytes in mice.* J Biol Chem, 2003. **278**(47): p. 46654-60.
86. Tsou, C.L., W. Peters, Y. Si, S. Slaymaker, A.M. Aslanian, S.P. Weisberg, M. Mack and I.F. Charo, *Critical roles for CCR2 and MCP-3 in monocyte mobilization from bone marrow and recruitment to inflammatory sites.* J Clin Invest, 2007. **117**(4): p. 902-9.
87. Zou, W., Z.Y. Li, Y.L. Li, K.L. Ma and Z.C. Tsui, *Overexpression of PEMT2 downregulates the PI3K/Akt signaling pathway in rat hepatoma cells.* Biochim Biophys Acta, 2002. **1581**(1-2): p. 49-56.

Conclusions

9. CONCLUSIONS

From the results obtained in this thesis, the following conclusions may be drawn.

1. C1P induces activation of MMPs and promotes actin polymerization, which are important processes in C1P-induced macrophage migration. These actions require activation of the PI3K and ERK pathways.

2. Ceramide kinase (CerK) participates in adipocyte cell differentiation.

3. C1P attenuates adipogenesis through a mechanism involving activation of ERK1/2 kinases.

4. *Pemt* knock-out mice are protected against obesity-induced inflammation through processes involving the reduction of leptin adipokine, downregulation of pro-inflammatory cytokines TNFα, IL-4, MCP-1, RANTES and upregulation of anti-inflammatory IL-10.

5. PEMT deficiency reduces M1 “pro-inflammatory” macrophage markers in mice fed a HFD for 10 weeks.

6. Overexpression of PEMT in J774A.1 macrophages induces cell migration. This action involves activation of the PI3K/Akt/mTOR pathway.

Appendix

PUBLICATIONS:

1. Arana L, Gangoiti P, Ouro A, Rivera IG, **Ordoñez M**, Trueba M, Lankalapalli RS, Bittman R, Gomez-Muñoz A. Generation of reactive oxygen species (ROS) is a key factor for stimulation of macrophage proliferation by ceramide 1-phosphate. Exp Cell Res. 2012 Feb 15; 318(4):350-60. **ISI: 3.372**
2. Gomez-Muñoz A., Trueba M., Gangoiti A., Arana L., Rivera I.G., **Ordoñez M.**, Ouro A. Control of arachidonic acid levels by ceramide 1-phosphate and its impact in cell biology. Ch.5, Nova Science Publishers, New York. 2012
3. Gomez-Muñoz A, Gangoiti P, Arana L, Ouro A, Rivera IG, **Ordoñez M,** Trueba M. New insights on the role of ceramide 1-phosphate in inflammation. Biochim Biophys Acta, 2013 Feb 11, 1831(6):1060-1066 **ISI: 3.829**
4. Ouro A, Arana L, Gangoiti P, Rivera IG, **Ordoñez M**, Trueba M, Lankalapalli RS, Bittman R, Gomez-Muñoz A. Ceramide 1-phosphate stimulates glucose uptake in macrophages. Cell Signal, 2013 Apr 25, (4):786-95 **ISI: 4.471**
5. Arana L, **Ordoñez M**, Ouro A, Rivera IG, Gangoiti P, Trueba M, Gomez-Munoz A. Ceramide 1-phosphate (C1P) induces macrophage chemoattractant protein-1 release: involvement in C1P-stimulated cell migration. Am J Physiol Endocrinol Metab, 2013 Jun 1; 304(11) E1213-26. **ISI: 4.088**
6. Ouro A, Arana L, Rivera IG, **Ordoñez M**, Gomez-Larrauri A, Presa N, Simón J, Trueba M, Gangoiti P, Bittman R, Gomez-Muñoz A. Phosphatidic acid inhibits ceramide 1-phosphate-stimulated macrophage migration. Biochem Pharmacol, 2014 Dec 15;92(4):642-50 **ISI: 4.65**
7. Gao X, van der Veen JN, Hermansson M, **Ordoñez M**, Gomez-Muñoz A, Vance DE, Jacobs RL. Decreased lipogenesis in white adipose tissue contributes to the resistance to high fat diet-induced obesity in phosphatidylethanolamine N-methyltransferase-deficient mice. Biochim Biophys Acta. 2015 Feb;1851(2):152-62. **ISI: 3.829**
8. Gao X, van der Veen JN, Zhu L, Chaba T, **Ordoñez M**, Lingrell S, Koonen DP, Dyck JR, Gomez-Muñoz A, Vance DE, Jacobs RL. Vagus nerve contributes to the development of steatohepatitis and obesity in phosphatidylethanolamine N-methyltransferase deficient mice. J Hepatol. 2015 Apr;62(4):913-20 **ISI: 10.401**

CONTRIBUTION TO CONFERENCES:

"22nd IUBMB & 37th FEBS Congress: From Simple Molecules to Systems Biology" September 2012. Sevilla, Spain.

Ceramide-1-phosphate stimulates carbohydrate metabolism

Ordoñez M, Ouro A, Arana L, Rivera IG, Gangoiti P, Trueba M, Gómez-Muñoz A

Ceramide 1-phosphate induces cd69 expression in immune cells through a mechanism involving ERK1-2 activation

Arana L, Ouro A, Rivera IG, Ordoñez M, Gangoiti P, Gomez-Muñoz A, Vannucci L

"2nd International Conference on Translational Medicine" June 2013. Chicago, US

Ceramide 1-phosphate is a novel regulator of cell migration: Implication in inflammatory responses

Gomez-Munoz A, Arana L, M. Ordonez, A. Ouro, I.G. Rivera, and A. Gomez-Larrauri

"7th International Ceramide Conference" Oct 2013. Montauk, Long Island, US

Ceramide-1-phosphate promotes cell migration through stimulation of MCP-1 release

Arana L, Ordoñez M, Gangoiti P, Ouro A, Rivera IG, Gomez-Larrauri A, Trueba M, Gomez-Muñoz A

"Integrating Metabolism and Tumor Biology" Vancouver, British Columbia, Canada

VEGF mediates the stimulation of cell proliferation by ceramide 1-phosphate

Gomez-muñoz A, Arana L, Riazy M, Ordoñez M, Rivera IG, Gomez-Larrauri A, Trueba M, Trueba M, Duronio V

"40th FEBS Congress" July, 2015. Berlin, Germany

Activation of gelatinases plays a key role in C1P-induced macrophage migration

M. Ordoñez, L . Arana, I.G. Rivera, N. Presa, J. Simón, A. Gomez- Larrauri, M. Trueba, A. Gomez- Muñoz